SURFACE FLASHOVER STUDIES OF DIELECTRIC POLYMER NANOCOMPOSITES UNDER KHZ UNIPOLAR PULSED FIELDS IN PARTIAL VACUUM ENVIRONMENT

by

Fang Li

A thesis submitted to the Graduate Faculty of
Auburn University
in partial fulfillment of the
requirements for the Degree of
Master of Science

Auburn, Alabama
May 07, 2012

Approved by

Dr. Hulya Kirkici, Chair, Professor of Electrical and Computer Engineering
Dr. Michael Baginski, Professor of Electrical and Computer Engineering
Dr. Robert Nelms, Professor of Electrical and Computer Engineering

SURFACE FLASHOVER STUDIES OF DIELECTRIC POLYMER NANOCOMPOSITES UNDER KHZ UNIPOLAR PULSED FIELDS IN PARTIAL VACUUM ENVIRONMENT

Fang Li

_____

Signature of Author

_____

Date of Graduation

Abstract

Insulating materials play a significant role in high voltage power systems. In general, the high performance electrical insulation materials and structures must be free from unwanted and unpredictable dielectric breakdown through the insulator as well as over the surface. Over the years, surface flashover in partial vacuum conditions under repetitive pulsed or ac applied fields became important for aerospace applications. Furthermore, new nanodielectric materials are also being considered as insulating media for many applications. This thesis presents the studies of the surface flashover characteristics of nano-composites at partial pressure. The nano-composite samples used in the experiments are prepared using electrically insulating two-part epoxy filled with 2%, 6%, and 15% Al_2O_3 and TiO_2 particles. Different substrates are used to cast the nanodielectric and the performances of nanodielectric composites are studied. The plasma characteristics under DC and unipolar signal, such as voltage of breakdown events are collected and analyzed; breakdown characteristics under changing frequency and duty cycle are also studied.

Acknowledgments

I would like to thank my advisor, Dr. Hulya Kirkici for giving me an opportunity to join this enthusiastic group, her never ending patience and assistance guide me through my years at Auburn. I would like to thank Dr. Baginski and Dr. Nelsm for serving as the committee members. Also thanks to the faculty and staff in Electrical and Computer Engineering Department, they have made my work a lot easier. Thanks are also due to all the members of our group for helping me around the lab and making the place fun to work. Especially to Huirong Li, Haitao Zhao, Zhenhong Li and Ramesh Bokka, they have been very helpful in conducting experiments again and again. Thanks are also due to my parents for understanding, always believing in me and supporting my decisions.

Style manual or journal used Graduate School's Thesis and Dissertation Guide

Computer software used Microsoft Office 2007

Table of Contents

List of Tables

List of Figures

List of Abbreviations

E	Electric field
D	Electric flux density
P	Electric polarization
ε_0	Permittivity in free space
ε	Dielectric constant or complex permittivity
ε'	Real part of complex permittivity
ε''	Imaginary part of complex permittivity
$tan\delta$	Loss tangent
ω	Angular frequency
torr	1 torr = 1333.2 Pascals (760 Torr = 1atm)
millitorr	1 millitorr = 10^{-3} torr
kHz	kilohertz
cm	centimeter
DC	direct current

CHAPTER I

BACKGROUND

1.1 Introduction

Insulating materials play a significant role in the design of high voltage power systems, where they can be used as charge storage and for mechanical support, in addition to serving as an electrical insulating media. When using dielectric materials as insulator, there are several issues that need to be addresses. Surface flashover is one of the major issues in electrical insulation of power systems operating both in vacuum and atmospheric pressure, thus has been a topic of interest in the area of power systems [1, 2]. In recent years, surface flashover studies in sub-atmospheric pressure have also became important for aerospace power systems operating in this pressure regime [3].

There are many traditional dielectric materials being utilized in the design and construction of aerospace power systems. However, there are also many new and electrically, mechanically, chemically improved materials being developed. Therefore, research in breakdown and surface flashover characteristics of these materials are needed and are being investigated [4]. Polymeric and ceramic composites consisting of dispersed nano-particles, cross-linked agents, specially functionalized molecules, and other fillers are being used as advanced dielectric materials in applications and research [4]. Nano-dielectrics are a group of filled-polymers where sub-micrometer or nanometer sized ceramic or metal-oxide insulating particles added to the

polymeric dielectric materials. Although the physical and chemical properties are still not completely understood, it has already been confirmed by several research groups worldwide that nano dielectric composite is a promising "new" insulating material [4]. The advantages of this material came from the fact that the dramatic increase of interface between polymer and nano-particles, when nano-sized dielectric incorporated into a polymer matrix. This thesis is a study of surface flashover characteristic of in-house fabricated nano-dielectric materials under DC and kHz frequency, repetitive pulsed applied fields in sub-atmospheric pressures.

1.2 High Voltage Breakdown in Partial Vacuum

1.2.1 Gas Discharge

A gas can exhibit conductivity when it possesses free charged particles (ions and electrons). Even in the absence of an electric field, a small amount of ions and electrons exist in the gas as background ionization, and the rate of ionization balances the rate of deionization because the rate of the ionization is extremely small. Therefore equilibrium is reached and the gas is "charge-neutral". However, when an external field is applied, charged particles are produced by ionization process, by liberating negatively charged electrons from atoms or molecules when they absorb enough energy, and the positively charged particles are left behind. In addition to the external field, this absorbed energy is also provided by collisions through other moving particles in the gas, or by radiation in a gas.

Plasma can be found in nature or generated in a laboratory through gas discharges. Most laboratory plasma are produced between two metal electrodes placed in a containing gas vessel, where electrons leaving the metallic surface of the cathode, gain enough energy from the external field collide with the background gas and cause the ionization of the gaseous medium

which increases the number of charged particles. There are also deionization processes such as gas diffusion and electron-ion recombination, accounts for the loss of ions and electrons in gas. All those processes affect the total number of charge particles and finally the development of the discharge.

1.2.2 Breakdown Development

To explain the development of a gas discharge or gas breakdown, a simple electrode configuration is used and shown in Figure 1.1: two metal plates are placed at a close distance and a DC voltage is applied between the plates. The development characteristics are monitored by the change of discharge current as a function of applied electric field (or the ratio of E/p precisely, where E is the electric field and p is pressure). The energy is provided by electric field E and the corresponding voltage. The quantity 1/p is proportional to the mean free path, which is defined as the distance that a particle traverses between two successive collisions. This distance is a random quantity and depends on the concentration of the atoms or the density of the gas, therefore the "mean" value is more useful.

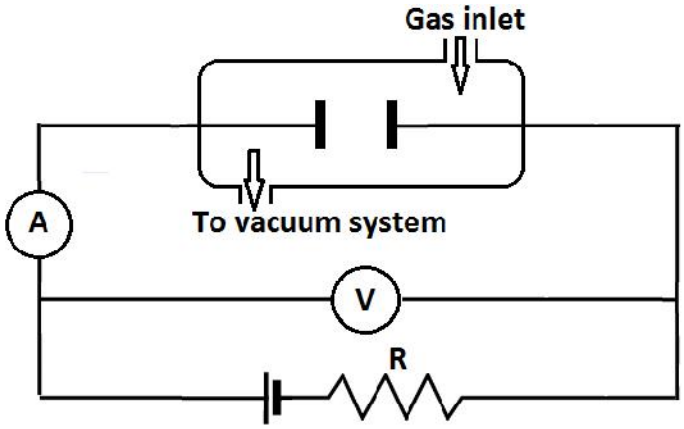

Figure 1.1 Schematic diagram of the circuit the gas breakdown.

This behavior of the gas discharge is shown in Figure 1.2 [5]. Initially, the magnitude of the applied voltage contributes little to the increase of current, until the Townsend discharge criteria of breakdown is reached, where it is characterized by an exponential increase of current from point A to B. Further increase of the applied voltage leads to an overexponential increase of current and then an abrupt drop of voltage across the gap is observed from C to D. This voltage collapse across the electrodes is known as the gas-breakdown, and the voltage at which occur is called the breakdown voltage of the gas. At this stage the current becomes independent of the external ionizing source but relies on the series resistance of the outer circuit. If the current is allowed to increase further, the voltage across the discharge will keep dropping until it reaches the glow discharge regions between D and E, and the abnormal glow discharge is reached from E to F. At abnormal glow region, the plasma starts to cover the entire cathode and requires a considerable increase in applied voltage. Finally, as the current is increased even further, the discharge undergoes an irreversible transition down into an arc discharge from F to G.

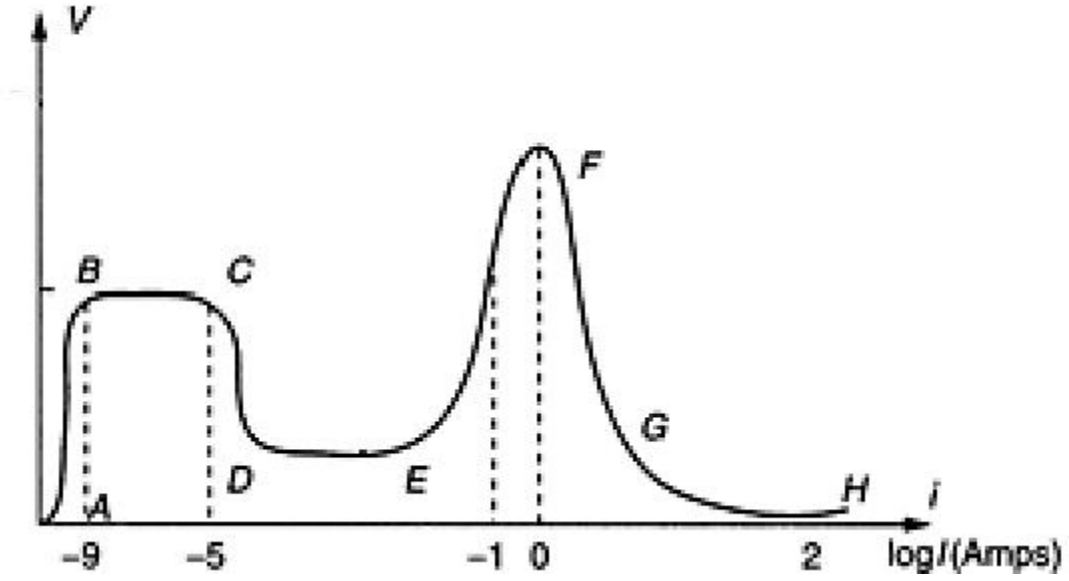

Figure 1.2 Voltage-current relationship for gaseous discharge [5].

1.2.3 Low Pressure DC Glow Discharge

Glow discharge is one of the discharge stages where the discharge voltage is constant while the current increases with the increase of applied voltage between electrodes. This is the regions marked as D to E in Figure 1.2. The appearance of the glow discharge can be separated into various dark and luminous regions from cathode to anode as shown in Figure 1.3. The luminous regions are the reason this stage is named the "glow" discharge. The dark regions are named individually by their positions between the electrodes or by the discoverers. Glow discharges have wide range of applications in lighting industry, such as fluorescence lamps and neon light advertisement displays due to their light emitting characteristics. The most important application of the UV emitting glows discharge lights is in the microelectronics industry for surface treatment or fabrication of integrated circuits.

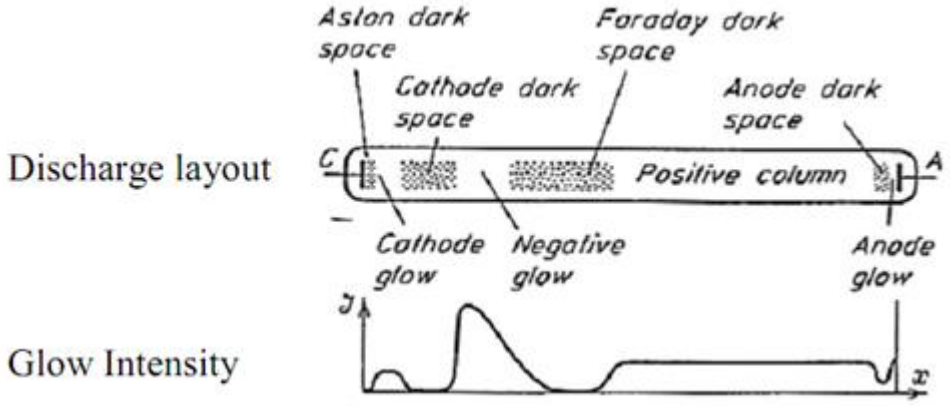

Figure 1.3 Glow discharge layout and light intensity [6].

The bright regions present different color for different gas and negative glow is the brightest region of the entire discharge. The next bright region is the positive column and has the appearance of a long, uniform and steady glow. For nitrogen, negative glow is blue and positive column is red. Figure 1.4 shows the plasma we produced in the partial vacuum nitrogen

environment (800 millitorr); cathode is on the left and presents blue color, anode is on the right and emits red light. In partial vacuum circumstance, the negative glow region shrink into a smaller volume and move closer to the cathode. The positive column is contracted and only fills a small part of the gap, therefore some discharge regions as shown in Figure 1.3 may be hard to identify or separated from each other for this electrode configuration.

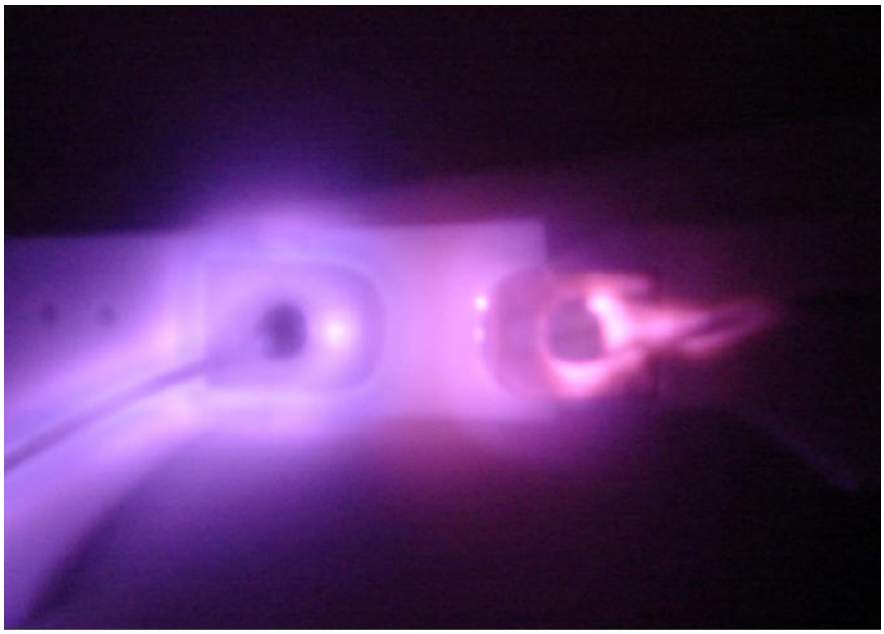

Figure 1.4 Plasma produced in the partial vacuum, nitrogen environment in our experiments.

1.3 Paschen's Law

As discussed previously, the development of discharge is a function of electric field and the pressure. The pressure is set constant to view the effect of electric field (voltage) only, as shown in Figure 1.2. At breakdown, the applied field exceeds a certain value, and is followed by glow discharge. On the other hand, it is also known that breakdown voltage is a function of the product of pressure p and distance d between electrodes and this variation is referred as Paschen's law.

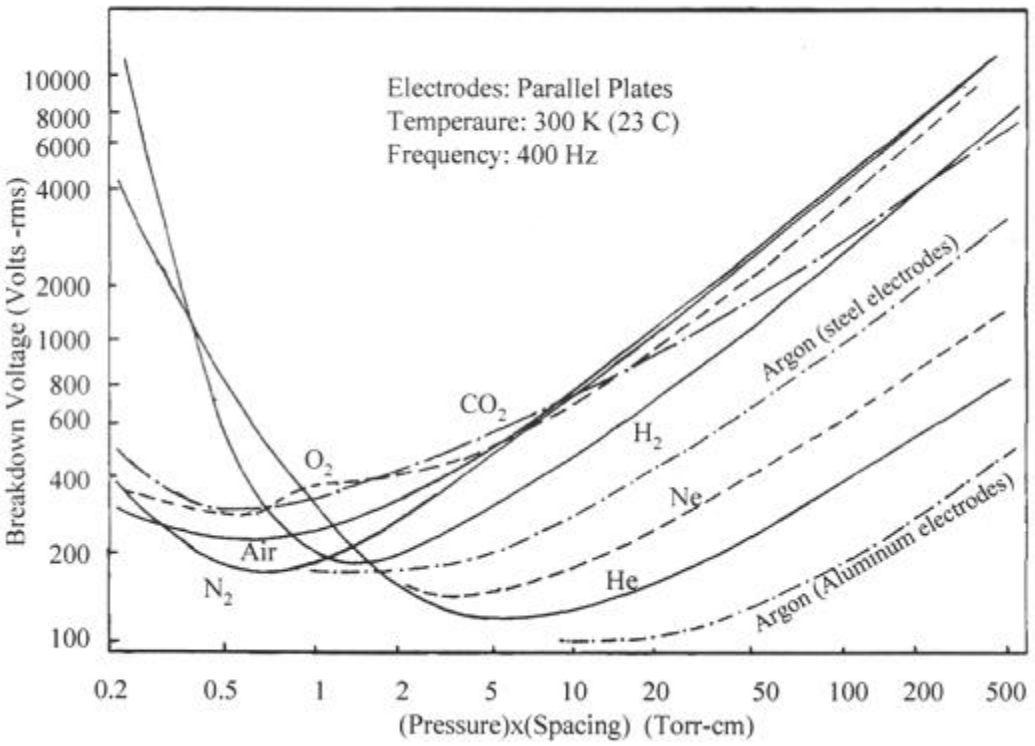

Figure 1.5 Paschen curves for various gases [7].

Paschen's law states that the breakdown voltages of a gaseous medium is a function of pd (pressure × spacing), and varies for each different gas. When the breakdown voltage is plotted as a function of pd, the curves are referred as the Paschen curves and is displaced in Figure 1.5. Paschen curves feature a minimum breakdown voltage at a specific pd value for a given gas and it increases for values of $pd < pd_{min}$ and $pd > pd_{min}$. This is because at relatively low pressures, there are very few particles in the gas and the mean free path is large, so the electron collisions are relatively infrequent, making it harder for an electron avalanche process to occur. Therefore, the applied voltage must be very high to form a conducting channel, thus for a breakdown. Increasing pressure on the left side of pd_{min} while keeping the electrode gap constant, the breakdown voltage decrease until a point where the minimum breakdown voltage occurs. As the pressure is further increased, the breakdown voltage starts to increase again. In this case there are

so many particles in the gas that the charge particles travel only a small distance before colliding with other particles. During this short distance they cannot gain enough energy from the electric field to ionize any atoms or molecules in the collision, so the increased breakdown voltage is observed, as the pressure is increased to the right side of the pd_{min}.

1.4 Unipolar Pulsed Breakdown

Other than DC field, signals with time varying waveform are also used to study the breakdown mechanism. If the direction of electric field between the electrodes alternates, the electrons/ions will experience opposing forces and the breakdown mechanism could be much different than when the applied field is DC. However, in the case of slowly varying ac electric fields such as the utility power frequency of 50/60Hz, the breakdown mechanism is essentially the same as under the steady field (or DC field), because it takes relatively long time for the field to reverse from (+) to (-). As the frequency of alternating field increased, charge particles with different motilities are affected differently. First heavy, slowly moving ions, then light, fast moving electrons are affected by the change of field direction, therefore the breakdown characteristics are significantly different in high frequency fields as discussed in [8]. The high frequency effect on the breakdown seems to start at around 20 kHz for both polar sinusoidal or unipolar fields [6].

For unipolar pulsed signal with 50% duty cycle, the electric force moves charged particles in one direction for half of the cycle and exerts no net force in the other half cycle. During the "on" cycle of the field the charges gain energy from the field and drift to the opposite electrode, while during the "off" cycle of the field they do not gain any energy and may diffuse (drift to the walls). Therefore, the breakdown voltage of a gas under unipolar fields is different than the ones

observed for DC or AC field. The breakdown of gases under kHz frequency, unipolar fields have been observed to be typically less than the corresponding dc fields, as reported in [9]. Breakdown under impulse voltage is reported in [8]. As reported, a single impulse voltage with short duration, approximately 1 μs or less, there may not be an initiatory "seed" electron available to start the avalanche process. Therefore a higher voltage than the dc breakdown voltage is required to start the breakdown process when impulse voltage is applied.

1.5 Vacuum Surface Flashover

In practice, the surface of an insulator fails before the bulk, and the phenomenon is called the "surface flashover". The physical mechanism responsible of this flashover of solid insulator has been studied for years [2]. Surface flashover usually occurs under Metal Insulator Metal (MIM) gap configurations, in which two metal electrodes are bridged by a solid insulator. The MIM gap features a triple junction (that is the interface of the insulator, metal electrode, and vacuum) as shown in Figure 1.6, and this cathode triple junction plays an important role in the surface flashover (surface breakdown) process.

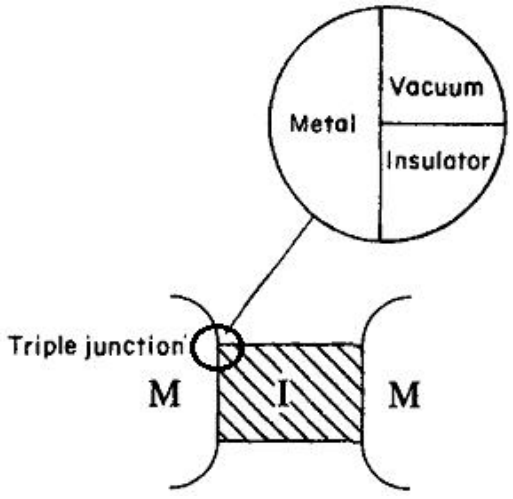

Figure 1.6 Schematic illustrations of bridged MIM vacuum gap and triple junction [2].

There is a general agreement that the initiation of a surface flashover in vacuum is due to the emission of electrons from the triple junction, and the surface flashover ends when emitted electrons generate ionization on the surface of the dielectric due to the presence of the gas desorbed from the surface of the dielectric or vaporized insulator [2], forming the background gas for the ionization.

There have been variety of theories presented to model the development or the intermediate stage of the surface flashover events and the generally accepted mechanism for the intermediate stage is believed to be due to the secondary electron emission avalanche process (SEEA) [2] in vacuum. In this process, the seed or the primary electrons are field emitted from the triple junction and move towards the anode. As shown in Figure 1.7, primary electrons on their propagation to the anode, strike the surface of the insulator producing secondary emitted electrons leaving positively charged surface behind. Some of these secondary electrons are lost by attaching to the surface, but others collide with the insulator surface again. Continuation of this process results in a cascade along the surface and develops into SEEA, which leads to a complete breakdown on the surface of the insulator.

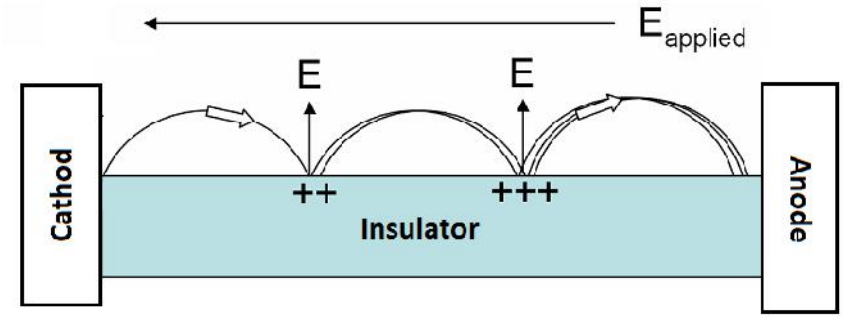

Figure 1.7 Schematic illustration of secondary electron emission avalanche process.

In this model, desorption of adsorbed surface gas (or vaporized insulator material for organic insulators such as PMMA-polymethylmethacrylte) is expected to help the completion of the surface flashover [2].

Most of the surface flashover studies are done in vacuum environment; there are also studies of the surface flashover in atmosphere pressure [10]. Atmosphere pressure surface flashover studies are done for utility power systems and lines [1]. One research group has been studying the partial vacuum surface flashover since 1999 [3]. In these studies it is shown that emitted electrons may also collide with the background gas near the surface during the intermediate processes. Therefore, ionization also should be considered for discharge development in conjunction with vacuum flashover. In addition, since the number of gas molecule is proportional to the pressure, breakdown voltage as a function of pressure is also conducted in these studies [11]. For both vacuum and partial vacuum, some of the positive ions drift towards the cathode and enhance the electric field at the triple junction. This then results in an increased electron emission from the triple junction and thus increases the current along the surface [2].

CHAPTER II

DIELECTRIC POLYMER NANOCOMPOSITE

2.1 Background of Dielectrics

Dielectrics, also known as insulators, are an important class of materials in electrical, electronic device and systems. Electrons in a dielectric material are strongly bound to their atoms and they cannot move freely in the bulk material. Under low electric field, they can be displaced from bound state to form what is called polarization state. When high enough electric field is applied across a dielectric material, some of these electrons become free and electrical breakdown of the bulk material is observed.

Derived from Coulomb's law, for time independent electric field **E,** in vacuum environment, electric flux density **D** is defined as

$$\boldsymbol{D} = \varepsilon_0 \boldsymbol{E}\,, \qquad (2.1)$$

where $\varepsilon_0 = 8.85 \times 10^{-12}\ F/m$ is the permittivity in free space (used to measure material's ability to transmit or "permit" an electric field). This simple equation holds only for ideal medium, i.e. vacuum, this means not only the medium is linear, homogeneous, and isotropic but also responses to the changes of electric field immediately. For "real" dielectrics there will be a polarization process term in the equation. In general, materials are categorized as polar or nonpolar materials based on the existence of permanent dipoles in them. For the atoms in nonpolar materials, when an externally electric field $\boldsymbol{E}$ applied, the center of the electron cloud is

displaced from the center of the atom by a distance d; positive (the nucleus) and negative center are no longer located in the same point. Such process caused by the external field is called polarization and electric dipoles are formed. However for polar material, composed of permanent dipoles already in the material, the external field will try to align the originally randomly oriented dipoles into the field direction. To take accounts of the polarization properties, the previous equation is modified as

$$\boldsymbol{D} = \varepsilon_0 \boldsymbol{E} + \boldsymbol{P}, \qquad (2.2)$$

$$\boldsymbol{P} = \varepsilon_0 \chi \boldsymbol{E}, \qquad (2.3)$$

where **P** is called electric polarization field and is proportional the electric field **E**, χ is electric susceptibility of the material and is the measure of how easily a dielectric material is polarized by electric field. Inserting Eq. (2.3) to Eq. (2.2), we have

$$\boldsymbol{D} = \varepsilon_0 \boldsymbol{E} + \varepsilon_0 \chi \boldsymbol{E} = \varepsilon_0 (1 + \chi) \boldsymbol{E} = \varepsilon \boldsymbol{E}, \qquad (2.4)$$

where $\varepsilon = \varepsilon_r \varepsilon_0 = \varepsilon_0 (1 + \chi)$ is defined as permittivity of the material which directly related to electric susceptibility, and ε_r is the relative permittivity. The electric flux density $\boldsymbol{D}$ is also known as the electric displacement vector and stands for "displacement," of the electrons in the presence of external field that will create or align dipoles; displace them from their original position.

There are no free electrons in the dielectric as long as the applied electric field is lower than a critical value. This limiting value is known as dielectric strength. If the applied electric field is larger than the dielectric strength, ions and free electrons are generated inside the material resulting in electron flow, and loss of insulation properties of dielectric. This process is called the dielectric breakdown. For time varying electric field, with an angular frequency ω, the permittivity becomes a frequency dependent quantity [12]. This frequency dependence of

permittivity reflects that the polarization of real dielectric cannot change instantaneously by applied field and will lead to energy loss. Permittivity is usually given in complex form

$$\varepsilon = \varepsilon' - j\varepsilon'' \qquad (2.5)$$

where ε' is the real part of the complex dielectric constant and used to measure the "perfect" behavior of the dielectric, ε'' is the imaginary part of the complex dielectric constant and used to measure the energy loss. It should be pointed out that the real and imaginary parts of the permittivity are not necessarily related. The complex value means that the dipoles in dielectrics try to orient themselves in the direction of the alternating electric field. At relatively high frequency, orientation will lag behind E because the direction of the field changes very rapidly and more energy will be lost as heat. Therefore, the complex expression of permittivity is used to obtain a very useful quantity, the loss tangent, defined as

$$tan\delta = \frac{\varepsilon''}{\varepsilon'} \qquad (2.6)$$

Loss tangent, also called the dissipation factor, is a ratio of loss power over available power of the electric field. Another term $sin\delta$, is a measure of the heat dissipated or electrical power absorbed in dielectrics, because for dielectrics $tan\delta$ is less than 0.5 [13], and approximately $sin\delta = tan\delta$, therefore the energy absorbed is proportional to $tan\delta$, or $sin\delta$.

There are different types of polarization mechanisms in a dielectric, based on the scale of the dipoles. They are electronic polarization, ionic polarization, dipolar polarization, and interfacial polarization.

Electronic polarization exhibits the smallest polarization vector $\vec{p}$, and defined as $\vec{p} = \vec{d}Ne$, where d is the distance between positive and negative charges, N is the number of charges, [14] and e is the electron charges. As shown in Figure 2.1 (a) and (b), without external field, the center of electron cloud coincides with the nucleus, when field is applied, the center of the

electron cloud is displaced relative to the nucleus at a distance of *d*, but electrons are still attached to the nucleus.

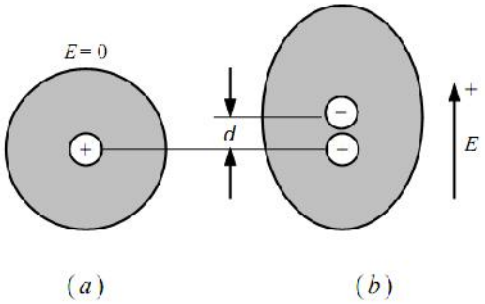

Figure 2.1 Schematic illustration of electronic polarization (a) in the absence of an external electric field, (b) in the presence of an external electric field [15].

Ionic polarization requires the material to have ionic structure examples of such material will be NaCl or KCl. As shown in Figure 2.2, each pair of oppositely charged ions can be considered as a dipole, but can only move slightly around its rest position and are unable to rotate. The distance between them is much longer than electronic dipoles, and also the forces involved are more complicated [16].

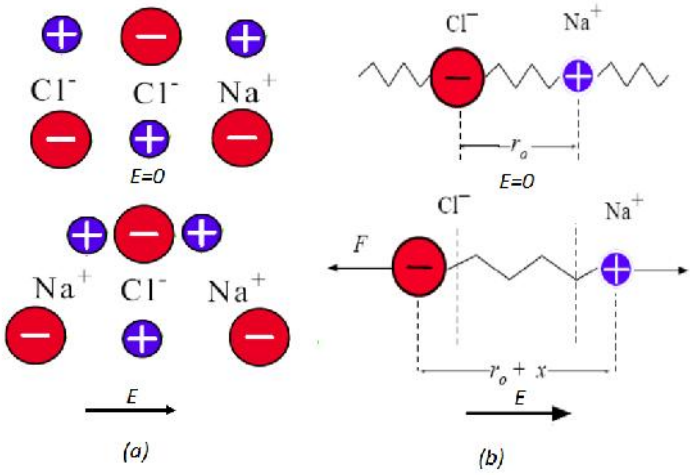

Figure 2.2 Schematic illustration of ionic polarization [16].

Orientation polarization also known as dipole relaxation requires material to have permanent dipoles, contrast to ionic polarization, these dipoles are independent of each other and can rotate easily as shown in Figure 2.3. In the absence of an E field, the thermal agitation of the molecules results dipoles to be aligned randomly, in the presence of *E*, the electric field try to rotate the dipoles and then align them along the field direction, against the thermal agitation [16].

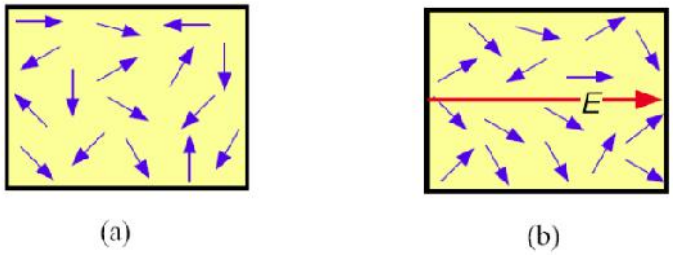

Figure 2.3 Schematic illustration of dipole relaxation [16].

Interfacial polarization is the most common form of polarization in low frequency, and happens when charges tend to pile up at electrode/dielectric interface or intercrystalline boundaries of a sample under the applied electric field as shown in Figure 2.4. In both cases the separation distance of positive and negative charges are significant large compare to other polarization mechanism.

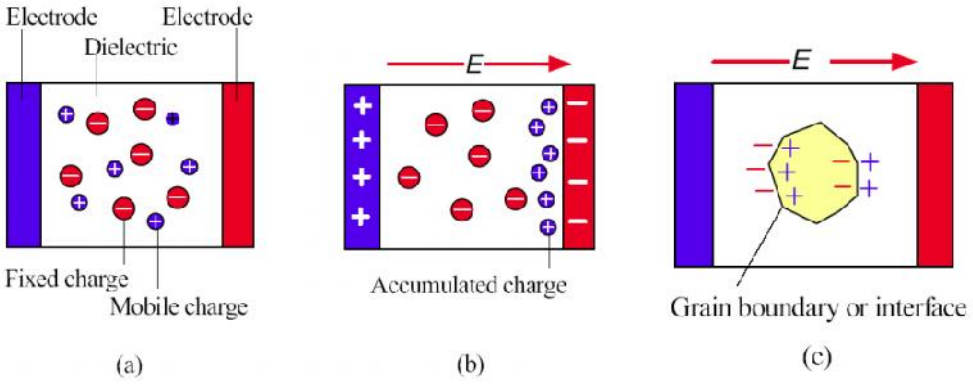

Figure 2.4 Schematic illustration interfacial polarization [16].

Different frequency works on different dipole models; the connection structure between charges have different length, (the separation distance between the opposite charges) i.e. from atomic level to beyond molecule level, also the connection material and structure are different. Know from Debye equation [13] given in Equation (2.7) and Equation (2.8), the values of ε' and ε'' depend on the frequency ω, of the applied field and can be displayed by plotting ε' and ε'' as a function of frequency as shown in Figure 3.5.

$$\varepsilon' = \varepsilon_\infty + \frac{(\varepsilon_s - \varepsilon_\infty)}{1+\omega^2\tau^2} \qquad (2.7)$$

and

$$\varepsilon'' = \frac{(\varepsilon_s - \varepsilon_\infty)\omega\tau}{1+\omega^2\tau^2} \qquad (2.8)$$

where ε_∞ is the permittivity at infinity (i.e. $\omega \rightarrow \infty$) and ε_s is the permittivity at zero frequency (i.e. $\omega \rightarrow 0$), and τ is a time constant. Plotting ε' and ε'' as function of frequency gives dielectric spectroscopy and determined by performing several isothermal scans of the dielectric as a function of frequency.

Each dielectric polarization mechanism discussed earlier, is centered on its characteristic frequency. The energy absorbed by these polarizing species maximum at the characteristic frequencies and $\varepsilon''$is a measure of this. The enhancement of complex permittivity of the material is only at the characteristic frequency and all lower frequencies. At high frequency the large species cannot move quickly enough to have any effect.

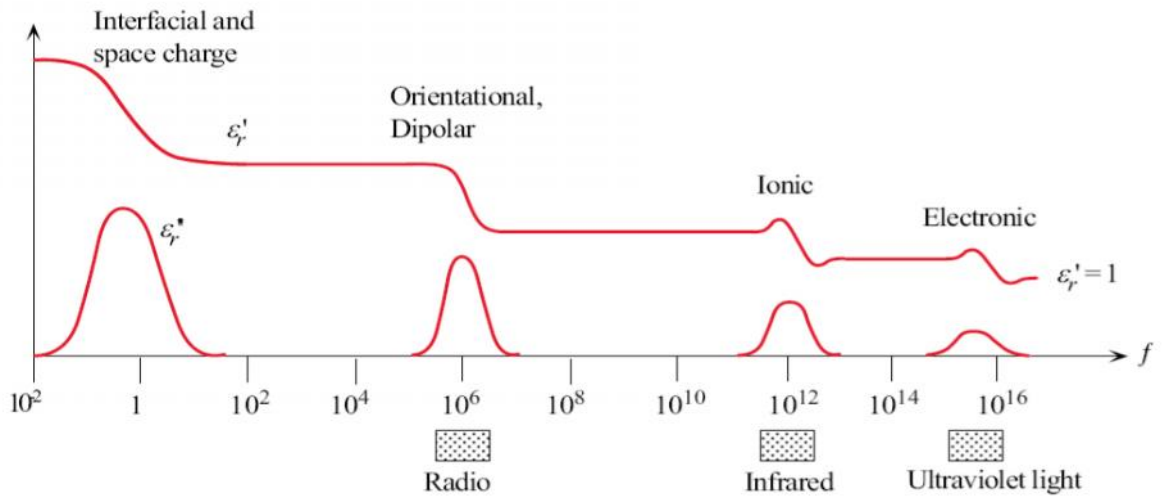

Figure 2.5 Frequency dependence of the dielectric constant [16].

2.2 Polymers

Polymers, a major part of the modern plastics industry, are made of large molecule chains, which are composed of repetition of small and relatively simple chemical units. Molecule chains can be linear or branched and interconnected to form three dimensional networks. The repeated units of the polymer are usually equivalent or nearly equivalent to monomer. For example, in polyethylene, the repeated unit is $-CH_2-CH_2-$ which form monomer $CH_2=CH_2$. Polymers that composed of single type of repeated units are homopolymers, while polymers containing more than two types of repeated units are known as copolymers. The most significant feature distinguish polymers from other materials is the existence of large molecules considered in both length and weight. The length of molecule could be represented by how many times chain unit repeats and the weight is represented by molecular weight. The molecular weight of polymer is distributed in various ranges and average value is needed to represent the sample.

Epoxy resins, are used widely as insulator in electrical systems and electronics/micro-electronics. Epoxy is in the polymer family and usually contains two liquid parts: resin and hardener.

Hardener is added into resin for curing. As the name implies liquid epoxy resins change from fusible and soluble material into infusible and insoluble material and form a covalently crosslinked, thermally stable network, during the curing process. [17].

2.3 Dielectric Polymer Nanocomposites

Many polymers are used as base material and are blended with particulate solid powder such as alumina, magnesia, and zinc oxide to form composite materials. Wide varieties of inorganic and organic materials are added into plastic to change the refractive index and this lead to colored "plastic" products. These additive materials can also greatly enhance other properties of polymer such as dimensional stability, tensile, and compressive strength.

Recently, nano-fillers are added to polymers to form nano-composites, and these nano-composites have shown improved electrical properties as discussed in [4]. An earlier work on nano-composites served as a theoretical paper was proposed by Lewis [18] in1994. In this paper, it is expected that the final composite presents new properties when the size of additive particles reaches nanometer scale (<100nm) and was first documented experimentally in 2002 [19]. It was believed that the principal reason for the changes in properties is related to that the nano-particles introduce more interface zones between the additive materials and the base polymers as shown in Figure 2.6. This interface zone is responsible for the new properties of nano-composites which is better than either the original polymer or additives alone [4].

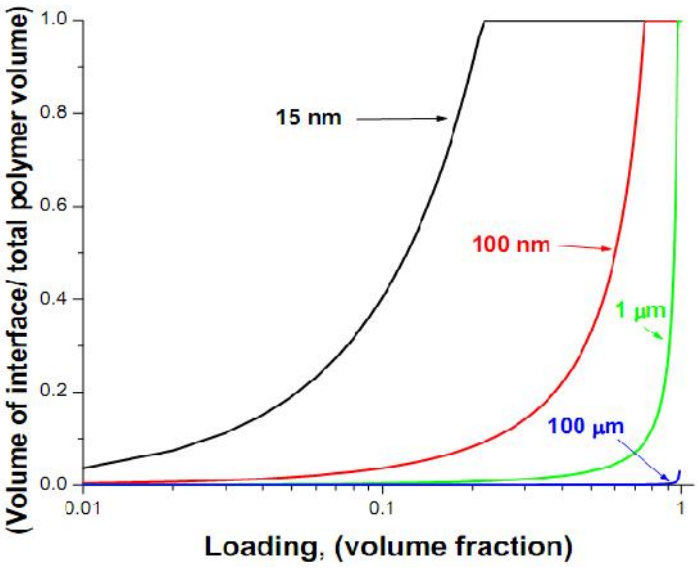

Figure 2.6 Surface-to-volume ratios of nanocomposites as a function of nano-particle loading [4].

As shown in Figure 2.6, for quite modest loadings, the surface area associated with the internal interfaces is very large for nano-additive. In this way, properties associated with the interface may become dominant so that the "new" material can then display properties which are not necessarily provided by either of the phases from which it is derived. The inclusion of nano-particles in an insulator could change the properties of the material surrounding the particle substantially and it is difficult yet important to classify the electrical properties of this "interaction zone" through large amount of fundamental experiments.

Based on the previous discussion, we know the properties of nanocomposite are the result of dominant polymer-additive interface zone in the bulk material. It is also very important to point out that the interface is directly related to the compounding process. When producing nano-composites, nano-particles should be properly dispersed and be distributed inside the host polymer. Nanoparticles should also be well dispersed instead of aggregating together. One

should also make sure that the nanoparticles are well distributed inside, and they are evenly distributed in the bulk and on the surface of the base material, when mixing.

In this thesis, two metallic oxides, namely aluminum oxide (Al_2O_3, also referred as alumina) and titanium oxide (TiO_2, also referred as Tatiana) are used to make nano-dielectric materiel from the base polymer (epoxy).

Similar to conductor and semiconductor, the electrical properties of insulator is also based on the analysis of charge storage and transport behavior inside the material, but the situation is much more complicated for polymer as well as nano-composites The process used to make the nanodielectric samples used in this study is given in the following Chapter.

CHAPTER III

SAMPLE PREPARATION AND EXPERIMENTAL SET UP

3.1 Sample Preparation

The nano-dielectric samples are prepared in-house [20] using commercially available two-part epoxy resin (EPO-TEK301-1, from Epoxy Technology) with relative permittivity of 4.26 (at 1 kHz). Al_2O_3 and TiO_2 powders are used as the nano-particles and both obtained from AlfaAesar. Al_2O_3 powder is 99.98% pure with 0.85 to 1 micrometer size and TiO_2 powder is 99.9 % pure with average size of 32 nm. Sample preparation scheme is depicted in Figure 3.1. Epoxy resin is first pour into a container, and then particles are added. When these two mixed thoroughly, hardener is added and mixes again. Finally the mixture is poured onto different substrates and cured for more than 24 hours in room temperature as instructed by the manufacture manual.

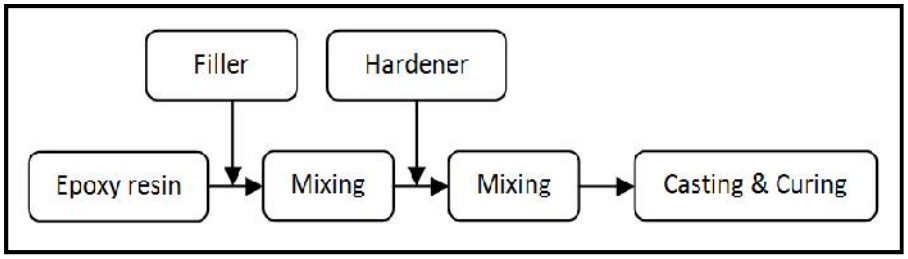

Figure 3.1 Dielectric nanocomposite preparation schematic.

Preparing the epoxy/powder mixture, 50:1, 50:3 and 50:7 weight ratios (2%, 6% and 15% loaded samples respectively) are used as summarized in Table 3.1. The substrates are 2.5cm by 2cm sized, with two different types, namely Teflon and Alumina. Control samples of pure epoxy

without nano-particles and heavily loaded samples are also prepared and used in the experiments. Once the samples are prepared, experiments are conducted for each sample.

	Al2O3 on Tefon	Al2O3 on Alumina	TiO2 on Tefon	TiO2 on Alumina
2%	3 Samples	2 Samples	2 Samples	2 Samples
6%	3 Samples	2 Samples	2 Samples	2 Samples
15%	3 Samples	2 Samples	2 Samples	2 Samples

Table 3.1 Sample list.

3.2 Experimental Set Up

The experimental setup contains a vacuum chamber, power supply, and data acquisition system, as shown in Figure 3.2, and similar to the one described in [21].

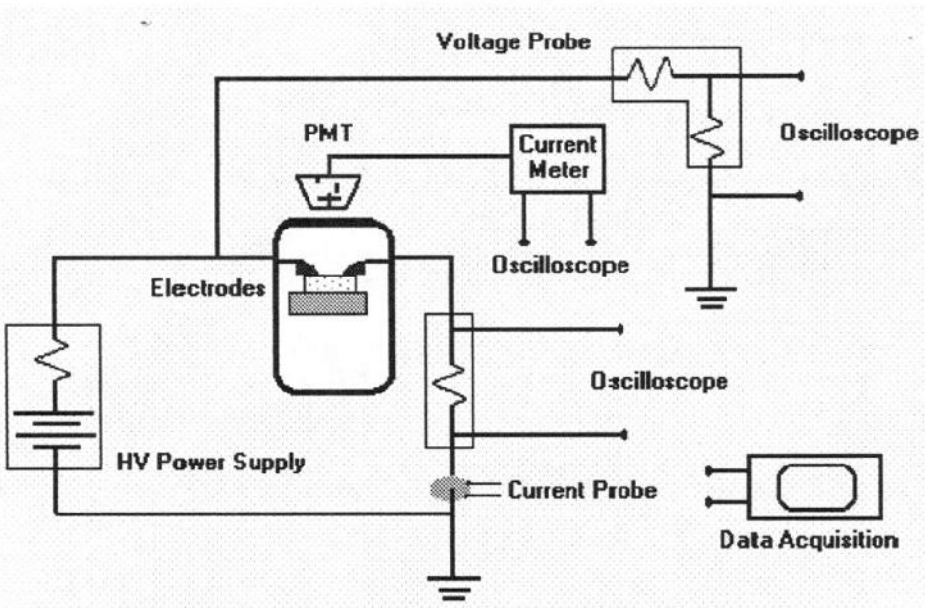

Figure 3.2 Surface flashover experiment system setup [21].

Nitrogen with ultra high purity level is chosen as operating gas. High voltage power supply is feed through well insulated ports. The electrode setup consists of two tapered copper electrodes firmly attached 1 cm apart from each other on top of the sample as shown in Figure 3.3.

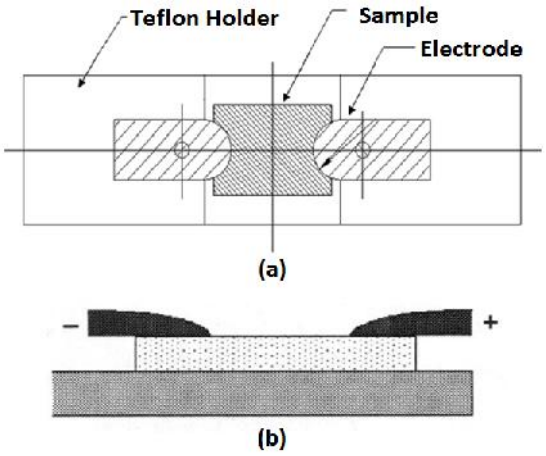

Figure 3.3 Schematic of final sample and electrode setup, (a) Top, (b) Cross section view [22].

Acquisition system is triggered by the light emission from the plasma generated during the breakdown initiation. This emission is monitored by a Photomultiplier Tube (PMT) manufactured by Hamamatsu that is mounted on to an optical port of the chamber. PMT operates based on photoelectric effect which converts photo absorption into electron emission and the corresponding current is the output. This current is then converted to voltage through an electrometer and fed to a digital oscilloscope for recording. Breakdown voltage is monitored using a Tektronix p6015 high voltage probe and breakdown current which flow to the ground is monitored using a Pearson coil. A Tektronix TDS 2024 digital oscilloscope is used to capture the voltage, current, and the optical signals data simultaneously.

Surface breakdown characteristic is studied under DC and unipolar pulsed applied fields. The DC voltage is generated by CVC SDC-100 High voltage dc power supply which has a build in maximum current protection. Unipolar Pulsed waveform is generated by a DEI PVX-4150 pulse generator which is designed to drive capacitive loads, and generated square pulsed waveform with rise times less than 20ns. A BK Precision-4040 20 MHz function generator is fed to the pulse generator, and used to control the width, duty cycle, and frequency of the pulsed

waveform. The CVC SDC-100 high voltage dc power supply is also fed to pulse generator to control the amplitude of the pulse. The maximum output pulse voltage differential (V_{low} to V_{high}) is between 0 and1500V.

3.3 Experimental Procedure

Surface flashover characteristics are recorded under varying pressure, frequency, and duty cycle. First, the samples with different loading ratio are tested under a pressure range from 0.2 to 3.0 torr (26.6 to 400 Pa) for both DC signal and pulsed unipolar signal. This is called the pressure sweep tests. The unipolar pulse frequency is set at 20 kHz at 50% duty cycle for these experiments. For both the DC and pulsed experiments, the voltage is gradually increased from zero at a rate of about 100 V/s until the breakdown event is initiated. The light emission at breakdown triggered the data acquisition system. At each constant pressure point, the voltage, current and light emission waveforms of the events are collected. This is repeated at least 3 times for each pressure value and averaged to form one data point for that pressure. This procedure is repeated until the breakdown events for the entire pressure range are recorded. Final curve of breakdown as a function of pressure is plotted for each sample. For comparison, the experiments are also conducted using one pure epoxy sample and several heavily filled (15%) samples.

Second, the pressure is set at a constant value and the pulse parameters such as the frequency and duty cycle are changed. This is called the frequency test and only a few specific samples are tested. For these experiments, first the pressure is set at 0.8 torr, and then the frequency of applied signal changed from 20 kHz to 220 kHz with an increment of 20 kHz. Then the pressure is set at 1.2 torr and pulse frequency is reset to 20 kHz, and then increase to 220 kHz again same as the 0.8 torr test. The specific samples used in these experiments are the Al_2O_3 filled nano

dielectrics on Teflon substrate. There is also a test conducted under different duty cycle from 20% to 80% with 20% incremental steps. Samples under duty cycle test are 2% Al_2O_3 on Teflon Sample #2. These tests were conducted at 20 kHz frequency for 0.8 and 1.2 torr.

Every new sample, once placed in the chamber, was left in the chamber over 12 hours. During this time; the chamber is pumped under millitorr range as the first step of the preparation stage. Detailed procedure of one complete pressure test is shown in Figure 3.4. Chamber is always flushed with the nitrogen before every experiment. At the fourth step of the preparation, plasma is generated using DC voltage for 15 to 20 times to clean the surface of the sample, this is defined as the conditioning step of the test and no data is recorded for conditioning. Since the current limiting of the power supply, only glow discharge is allowed to develop across the electrodes.

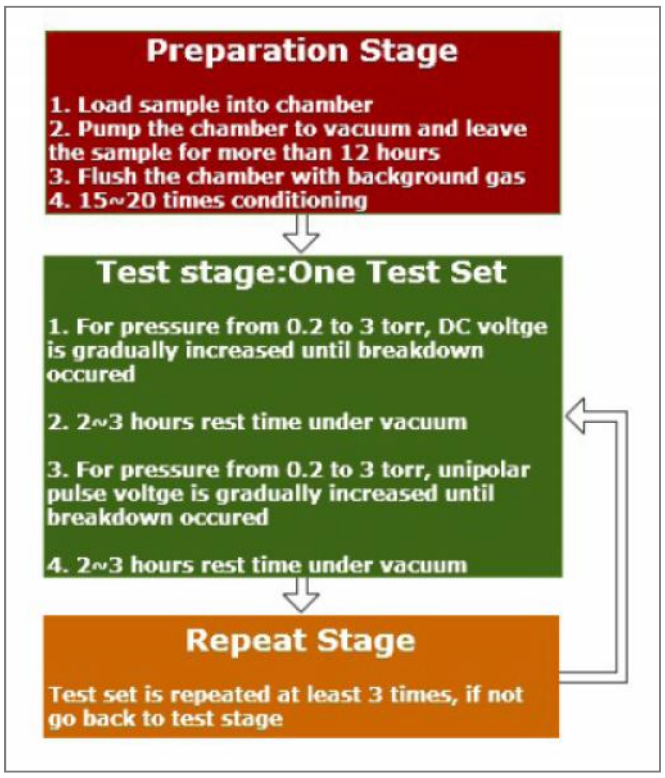

Figure 3.4 Pressure test procedure details.

A pair of DC and pulse data is defined as one "test set" in this thesis. These test sets are repeated for another two times and there are totally 3 test sets for each sample. For explanation convenience, Table 3.2 shows the list of the test-sets. The detailed list of the samples and the experiments conducted on them are given in Table 3.3. The name of the sample such as "2%s1-Al_T" indicates that this is first 2% Al_2O_3 loaded, nano-dielectric on Teflon sample and we prepared totally three such samples with labels from number 1 to 3. Totally there are 27 samples tested under different text conditions and then test data is analyzed.

	Number of tests for each different signal			Number of tests for each different signal	
Sample Name	**DC**	**Pulse(20kHz)**	**Sample Name**	**DC**	**Pulse(20kHz)**
2%s1-Al_T	3	3	2%s1-Ti_T	3	3
2%s2-Al_T	4	4	2%s2-Ti_T	3	3
2%s3-Al_T	3	3	6%s1-Ti_T	3	3
6%s1-Al_T	3	3	6%s2-Ti_T	3	3
6%s2-Al_T	3	3	15%s1-Ti_T	3	3
6%s3-Al_T	3	3	15%s2-Ti_T	3	3
15%s1-Al_T	3	3	2%s1-Ti_A	3	3
15%s2-Al_T	3	3	2%s2-Ti_A	3	3
15%s3-Al_T	3	3	6%s1-Ti_A	3	3
2%s1-Al_A	3	3	6%s2-Ti_A	3	3
2%s2-Al_A	3	3	15%s1-Ti_A	3	3
6%s1-Al_A	3	3	15%s2-Ti_A	3	3
6%s2-Al_A	3	3			
15%s1-Al_A	3	3			
15%s2-Al_A	3	3			

Table 3.2 Test details list

CHAPTER IV

RESULTS AND DISCUSSION

4.1 Surface Flashover as a Function of Pressure

4.1.1 DC and Pulse Surface Flashover Comparison

The surface flashover tests are conducted under DC voltage first then under and pulse voltages. After the DC test conducted, we let the sample rest in vacuum chamber for more than two hours before the pulse voltage is applied. Representative voltage, current and light emission waveforms recorded at breakdown for DC signal are shown in Figure 4.1 for pure epoxy. A similar data for pulsed applied field is shown in Figure 4.2.

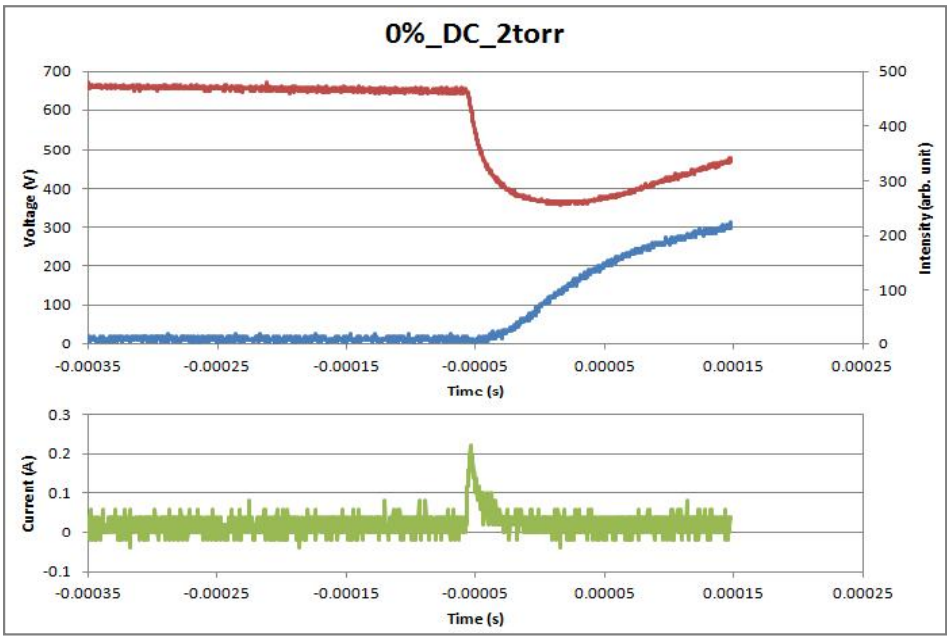

Figure 4.1 Voltage, current and light emission waveforms for pure epoxy at 2 torr for DC signal during the surface flashover [21].

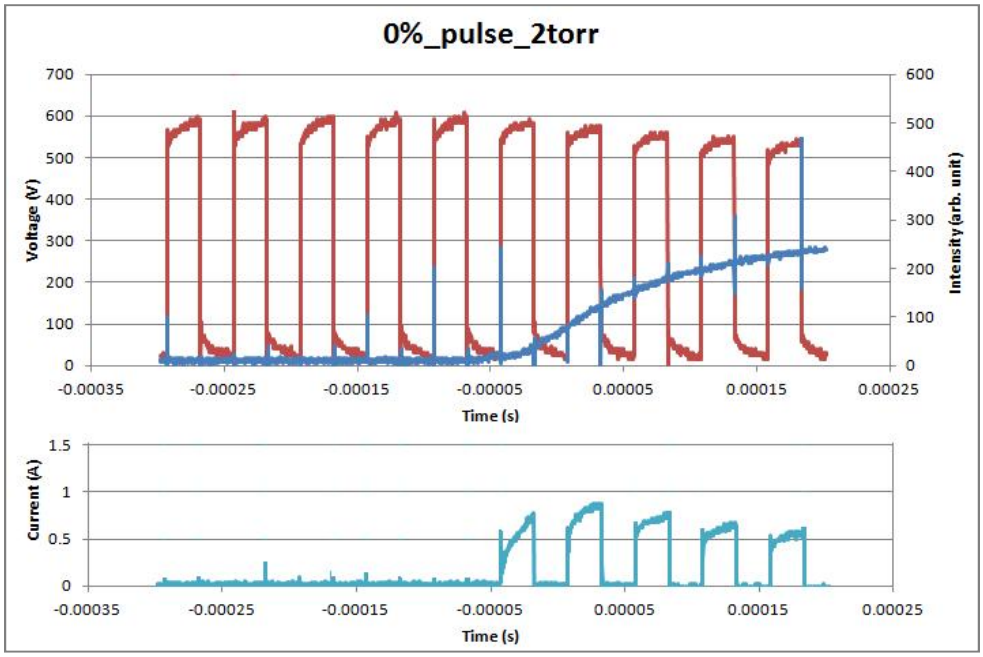

Figure 4.2 Voltage, current and light emission waveforms for pure epoxy at 2 torr for unipolar pulse signal during the surface flashover [21].

From these voltage waveform data, the breakdown voltage for each pressure is studied. A pair of DC and pulse data is compared together and defined as one "test set". Once the entire pressure range is swept, for both the DC and pulsed signals, the data is plotted. Figure 4.3 show such plots for 2% loaded Al_2O_3 on Teflon sample (in this case, it is the sample 2 of 2% Al_2O_3 loaded nano-dielectric sample on Teflon substrate). To plot the data in Figure 4.3, at least 3 to 5 surface flashover events like shown in Figure 4.1 or Figure 4.2 are acquired for each fixed pressure and then these breakdown voltages are averaged to get one breakdown voltage data point. Then these points are plotted with the corresponding pressure [20]. Also notice in Figure 4.3, the last part of the Figure title "re#3" indicating that this is the third repeated test for this particular sample.

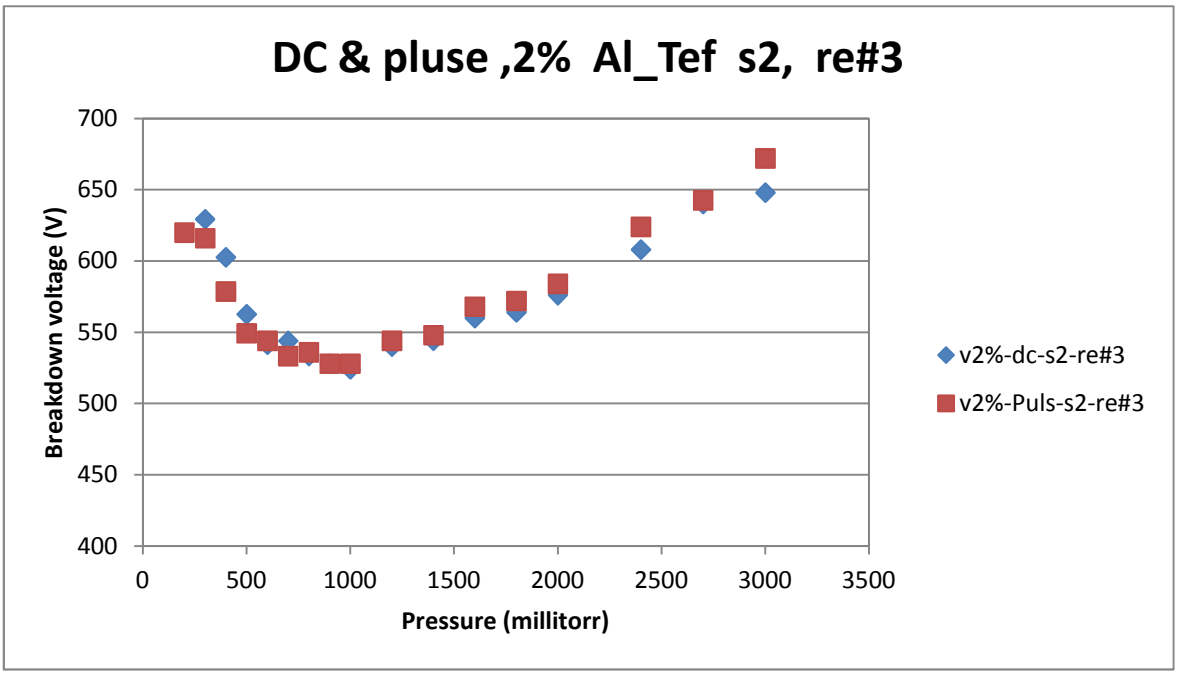

Figure 4.3 Representative "test set" plot. DC and pulse breakdown voltage curves of 2% Al_2O_3 on Teflon Sample 2, repeat #3.

From these plots, the minimum breakdown voltage is found to be at around 0.8 torr for all the samples tested. The plots presenting the complete data for all of the samples with different loading on different substrate are listed in Appendix A. Form these curves, the minimum surface flashover breakdown voltage for every test is determined. These values are summarized as shown in Table 4.3.

#	Smaple name	Filler type	Substrate Type	Loading Ratio	DC minimum Breakdown Voltage(V)				Pulse (20kHz) minimum BK Voltage(V)			
					1st run	2nd run	3rd run	4th run	1st run	2nd run	3rd run	4th run
	0% Al_T	None	Teflon	0%	564				512			
1	2%s1-Al_T	Al2O3	Teflon	2%	661	568	550		592	576	572	
2	2%s2-Al_T			2%	600	552	536	528	550	544	532	533
3	2%s3-Al_T			2%	544	540	530		533	536	536	
4	6%s1-Al_T			6%	538	538	538		536	536	540	
5	6%s2-Al_T			6%	520	538	538		533	538	538	
6	6%s3-Al_T			6%	520	528	532		536	540	544	
7	15%s1-Al_T			15%	544	552	552		572	552	552	
8	15%s2-Al_T			15%	512	520	536		508	532	532	
9	15%s3-Al_T			15%	525	546	522		532	550	530	
10	2%s1-Al_A	Al2O3	Alumina	2%	526	476	500		530	512	508	
11	2%s2-Al_A			2%	488	500	500		500	500	500	
12	6%s1-Al_A			6%	490	466	474		496	490	488	
13	6%s2-Al_A			6%	456	472	488		490	500	500	
14	15%s1-Al_A			15%	472	480	480		490	504	490	
15	15%s2-Al_A			15%	480	480	480		498	490	490	
16	2%s1-Ti_T	TiO2	Teflon	2%	461	477	477		490	484	484	
17	2%s2-Ti_T			2%	474	464	466		480	476	472	
18	6%s1-Ti_T			6%	484	488	498		515	514	512	
19	6%s2-Ti_T			6%	488	484	498		515	512	514	
20	15%s1-Ti_T			15%	490	506	501		522	522	516	
21	15%s2-Ti_T			15%	477	498	498		512	506	506	
22	2%s1-Ti_A	TiO2	Alumina	2%	485	510	510		512	514	512	
23	2%s2-Ti_A			2%	468	504	500		514	516	514	
24	6%s1-Ti_A			6%	608	554	544		562	549	546	
25	6%s2-Ti_A			6%	528	541	536		538	538	538	
26	15%s1-Ti_A			15%	515	530	532		525	525	525	
27	15%s2-Ti_A			15%	512	533	533		522	522	522	

Table 4.1 Minimum breakdown voltage summary of all the samples tested.

As mentioned in Chapter III, the pressure range of the test is from 200 millitorr to 3000 millitorr, and separated into low pressure range (200-500 millitorr), moderate pressure range (600-1200millitorr) and high pressure range (1400-3000 millitorr) for explanation convenience. Also

note that, “nano-sized particle” is loosely defined as those particles smaller than a few 100 nanometers. The smallest Al_2O_3 particle commercially available is around 0.8 micro meters, which is larger than TiO_2 particles that we have used to prepare the nano-dielectric samples.

As Figure 4.2 indicates, both the DC and pulse breakdown voltages fit the Paschen curve which is a function of the product of electrode separation distance (d) and pressure (p). Since we use the same electrode gap distance for all tests and kept at d=1.0 cm, breakdown voltage is shown as a function of pressure only, in the Figure 4.3and all other Figures.

Exploring the detail of Figure 4.3, both DC and 20 kHz pulse breakdown curves have a high surface flashover voltage value at the pressure close to vacuum (200 millitorr), then decrease rapidly as the pressure increased in the low pressure range. The flashover with lowest voltage happens at moderate pressure range, generally between 700 millitorr and 1000 millitorr. The breakdown voltage increases with a small slope when the pressure extends to 3000 millitorr, from about 1000 millitorr. Such features are also found in a typical Paschen curve. In general, the pressure range where the minimum breakdown occurs could shift to higher or lower pressure and also the breakdown voltage would be different for different sample and different test (or electrode) set up. This behavior is also observed in our experiments as expected. Also notice, in Figure 4.3, the DC breakdown voltage has no significant difference compare with pulse signal, which is different result than the ones obtained in previous studies shown in [21]. Figure 4.4 and Figure 4.5 are the “test set” plots for 2% and 15% loaded Al_2O_3 on Alumina substrate samples first test set data respectively. For these samples, again, the surface flashover voltage as a function of pressure presents features similar to Paschen curve.

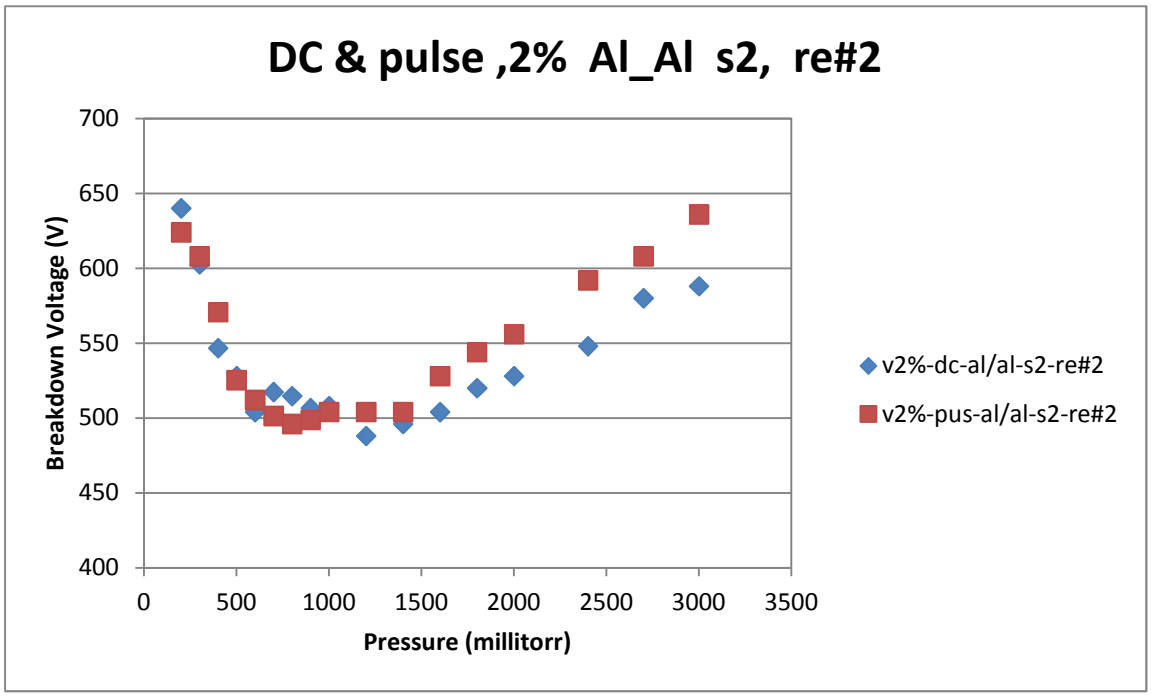

Figure 4.4 DC and pulse breakdown voltage curves of 2% Al_2O_3 on Alumina, sample #2.

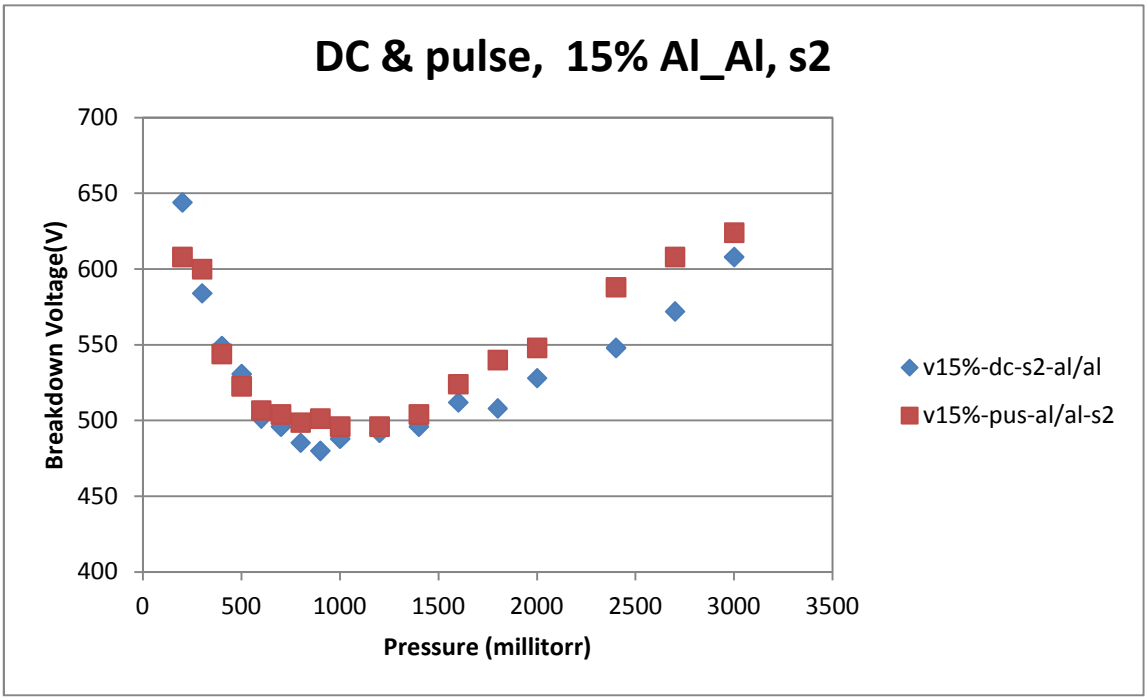

Figure 4.5 DC and pulse breakdown voltage curves of 15% Al_2O_3 on Alumina, sample #2.

The difference of Al_2O_3 on Alumina substrate compare to the Al_2O_3 on Teflon substrate samples is: the pulse breakdown is clearly higher than the DC when the pressure higher than 1500 millitorr range. This observation is the same for all Al_2O_3 on Alumina substrate samples; and the difference is about 20 to 30 volts for 2% and 15% loaded samples as show in Figure 4.4 and Figure 4.5. On the other hand, for the 6% loaded Al_2O_3 on Alumina substrate samples, the situation is the same; except the voltage difference is about 30 to 40 volts in the moderate as well as high pressure range as show in Figure 4.6.

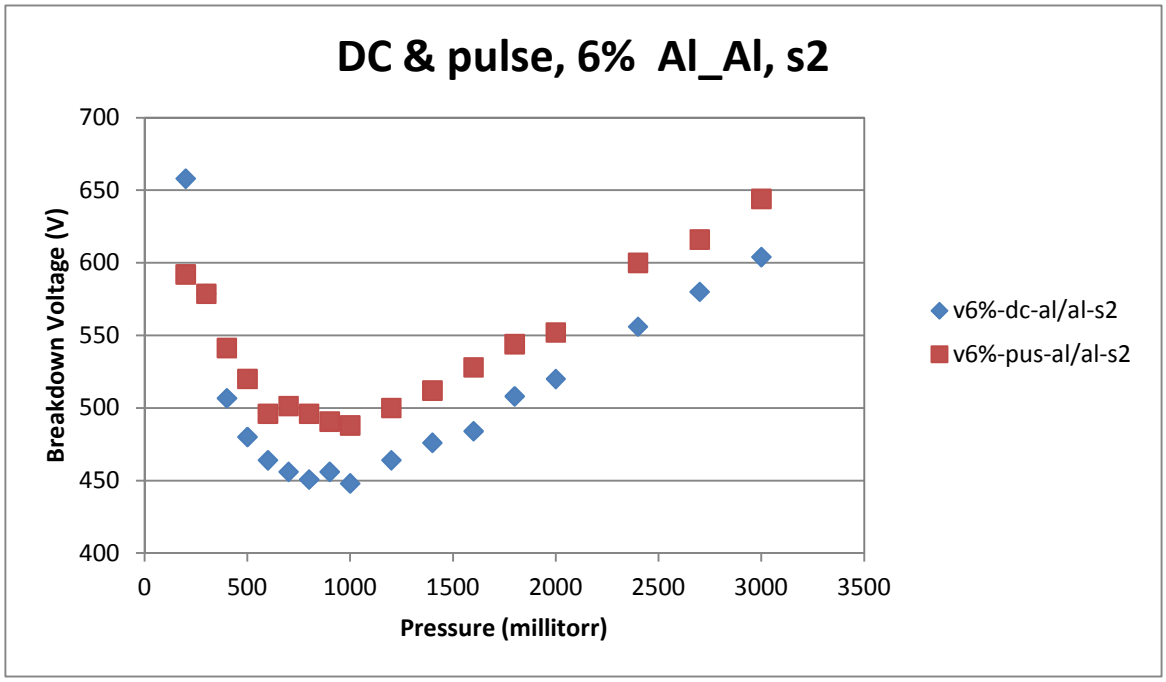

Figure 4.6 DC and pulse breakdown voltage curves of 6% Al_2O_3 on Alumina, sample #2.

As mentioned earlier, the Al_2O_3 samples are relatively larger than nano-meter scale, and the TiO_2 particles are the only nano particles that are used to prepare the test samples. Similarly, Figure 4.7, Figure 4.8, and Figure 4.9 show the surface flashover voltage as a function of pressure for TiO_2 nano dielectric on Teflon substrate with different loading ratio. In these figures, it is shown that for the TiO_2 nano-dielectrics on Teflon substrate samples, the data is not consistent. The

pulse breakdown voltage is higher than the DC in different pressure ranges for samples with different loading ratios. For the 2% loaded samples, voltage difference starts at moderate pressure range where pressure larger than 1000 millitorr, and increases about 30 to 40 V as the pressure increases. As the loading ratio of the sample increased to 6% and 15%, the breakdown voltage difference between pulse and DC shift into lower pressure range, and is found to be 30 to 50 V for 6% sample, but 20 to 30V for 15% sample.

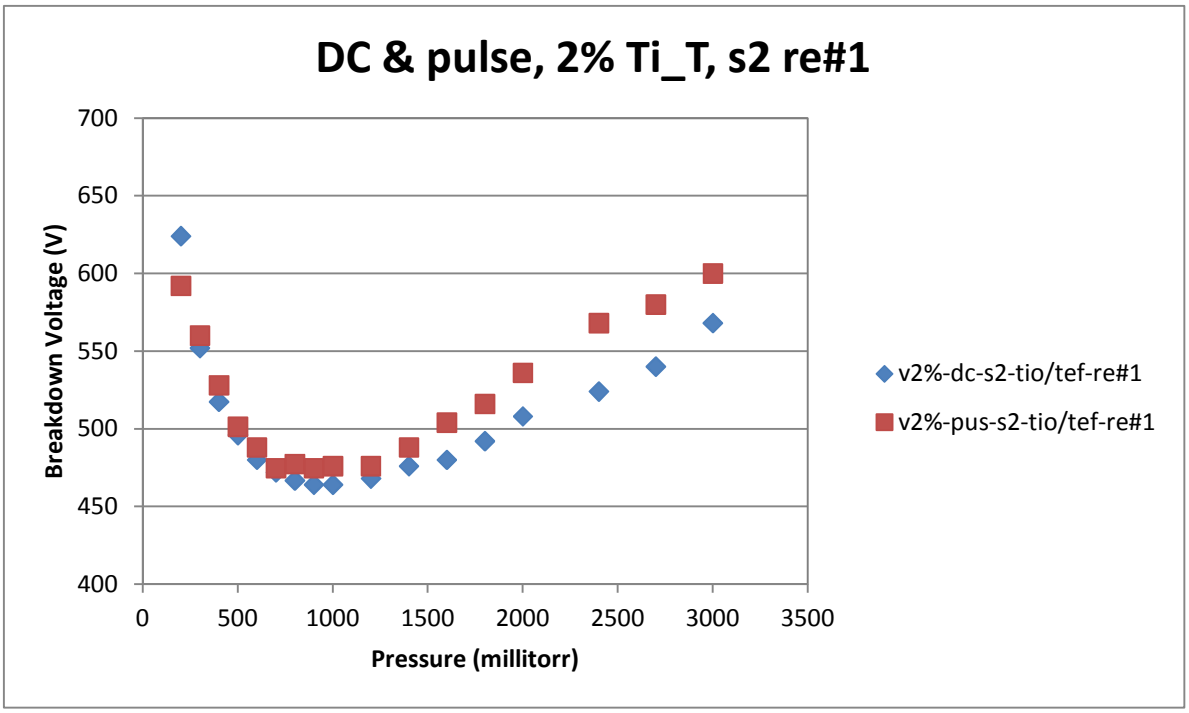

Figure 4.7 DC and pulse breakdown voltage curves of 2% TiO_2 on Teflon, sample #2.

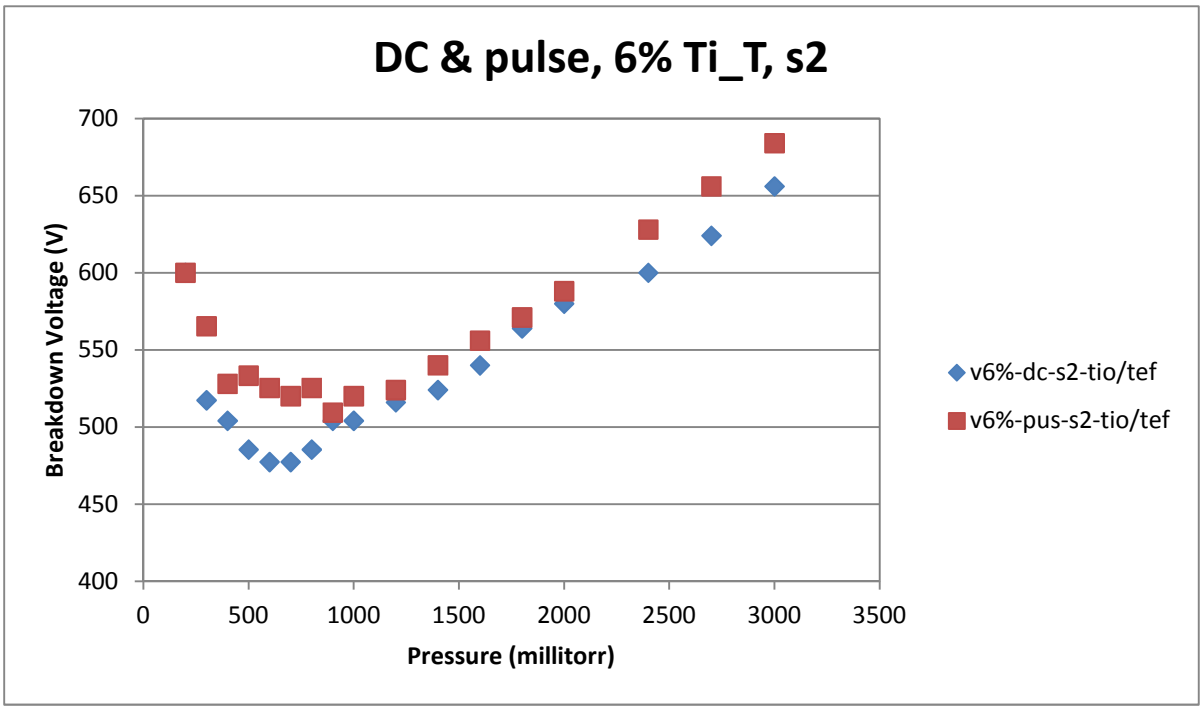

Figure 4.8 DC and pulse breakdown voltage curves of 6% TiO_2 on Teflon, sample #2.

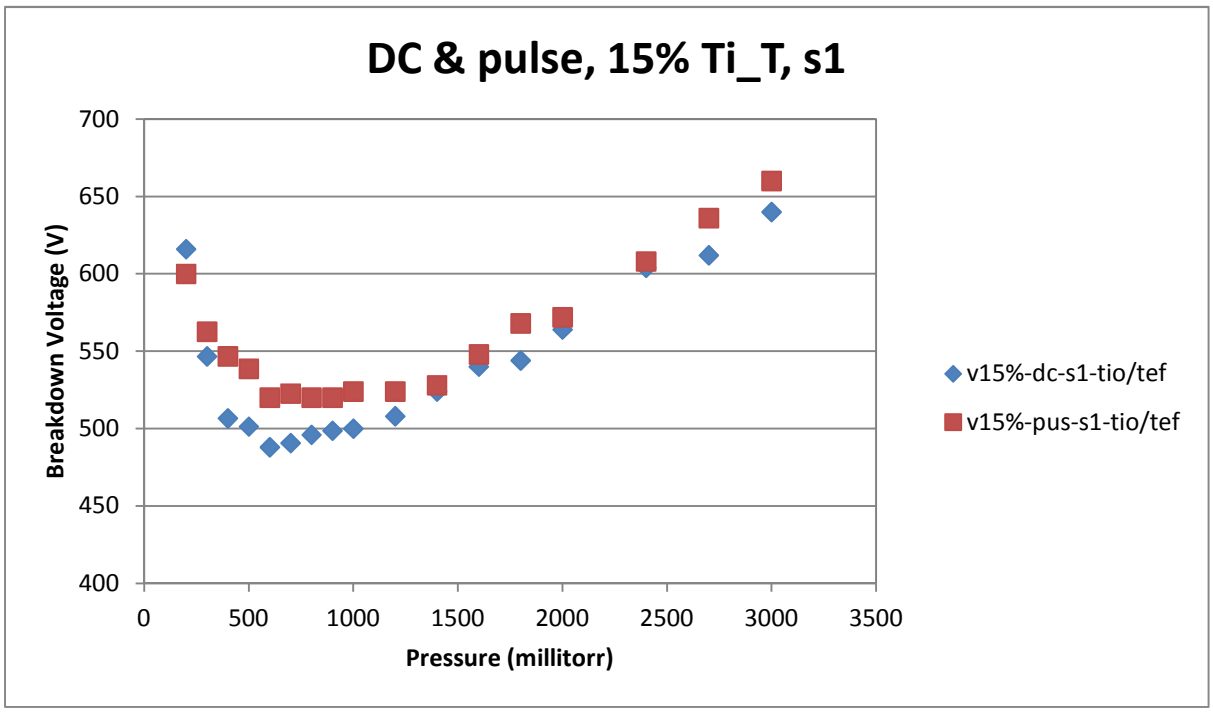

Figure 4.9 DC and pulse breakdown voltage curves of 15% TiO_2 on Teflon, sample #2.

On the contrary, for the TiO_2 loaded nano-dielectric on Alumina substrate samples, there is no significant difference observed between DC and pulsed breakdown voltage at varying pressure range. Figure 4.10 is representative of such data for 2% TiO2 loaded sample on Alumina substrate. Other data is show in Appendix A.

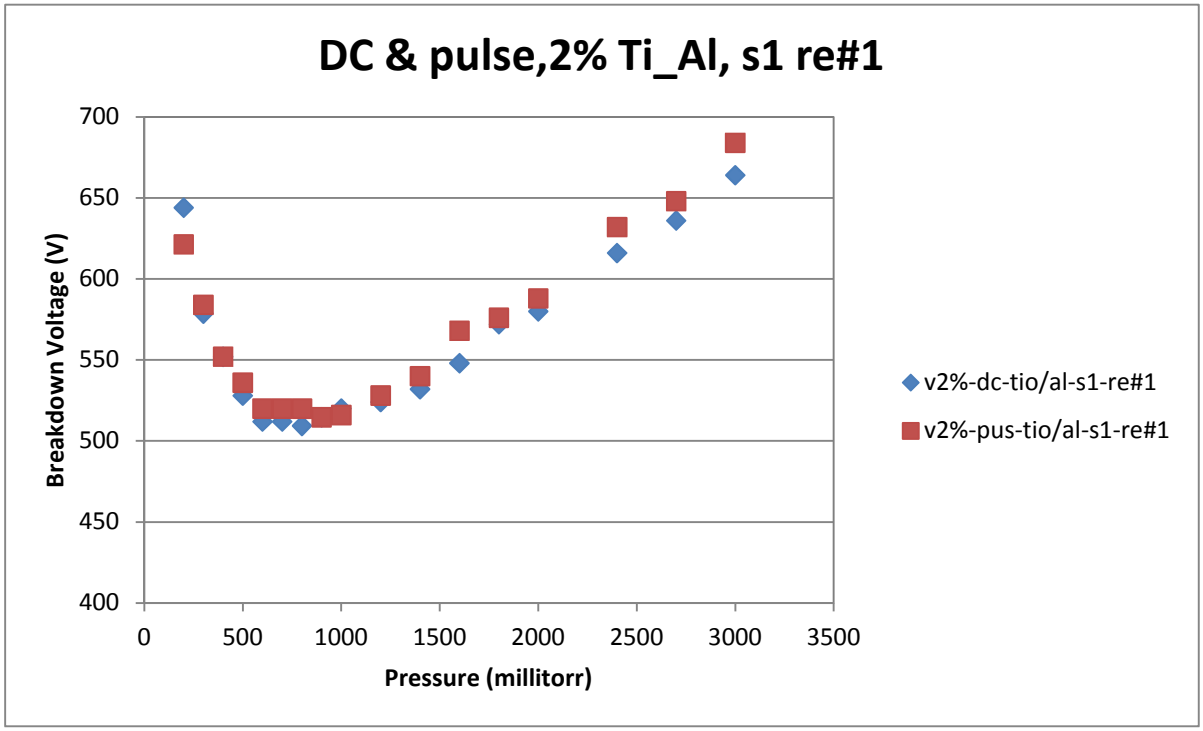

Figure 4.10 DC and pulse breakdown voltage curves of 2% TiO_2 on Alumina, sample#1.

4.1.2 Conditioning and Surface Effects on Surface Flashover

From the DC breakdown voltage curves listed in Appendix A, four different DC curves for one of the 2% Al_2O_3 loaded dielectric on Teflon substrate samples is picked and plotted in Figure 4.11. Complete set of DC comparison curves for other samples are listed in Appendix B. Although all of the DC curves exhibit similar behavior to Paschen curve and the minimum breakdown occurs at the similar pressure range, there is a significant voltage drop after the first test run. The breakdown voltage decreases as the sample is tested further. After being tested

second time, the curve starts to become predictable, as the 3rd and the 4th (re#2 and re#3) curve are almost identical with each other.

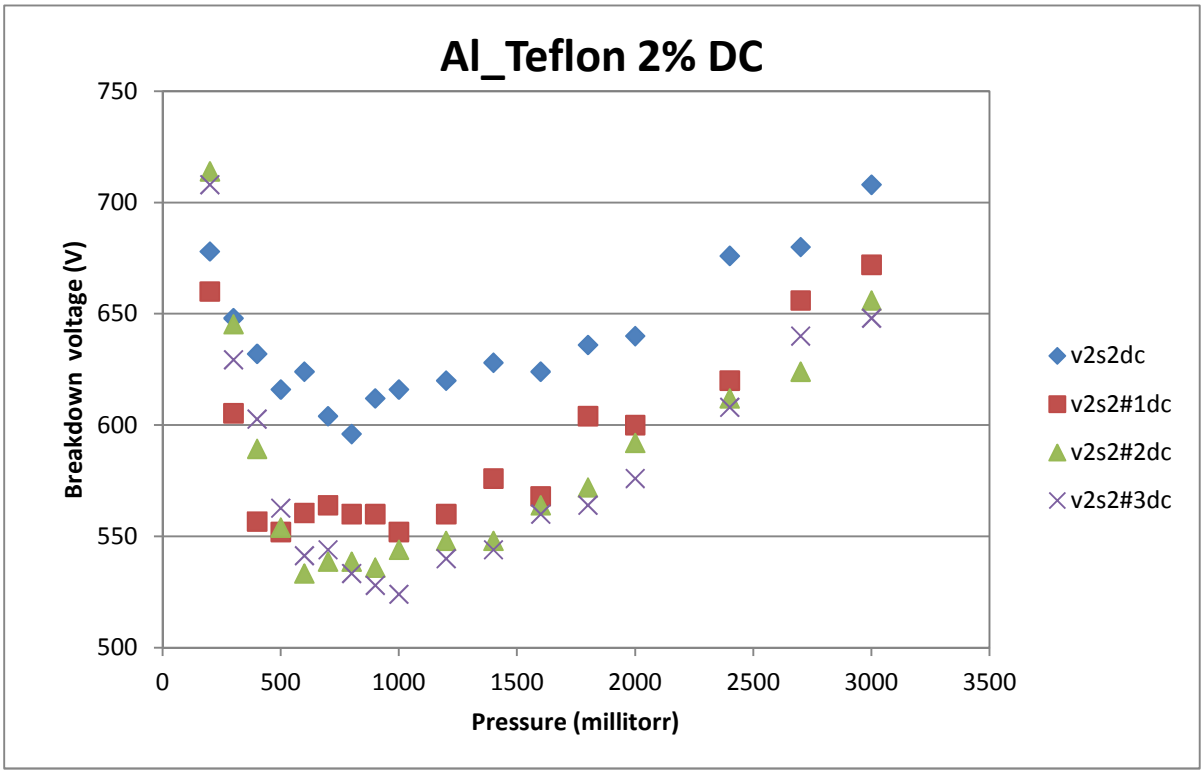

Figure 4.11 DC breakdown voltage comparison for 2% Al_2O_3 on Teflon sample #2.

The 6% loaded and 15% loaded Al_2O_3 nano-dielectric on Teflon substrate samples exhibit more predictable breakdown behavior for repeated test runs under DC fields as shown in Figure 4.12 and Figure 4.13 respectively. As seen, no significant difference between the first, second, and third curves is present.

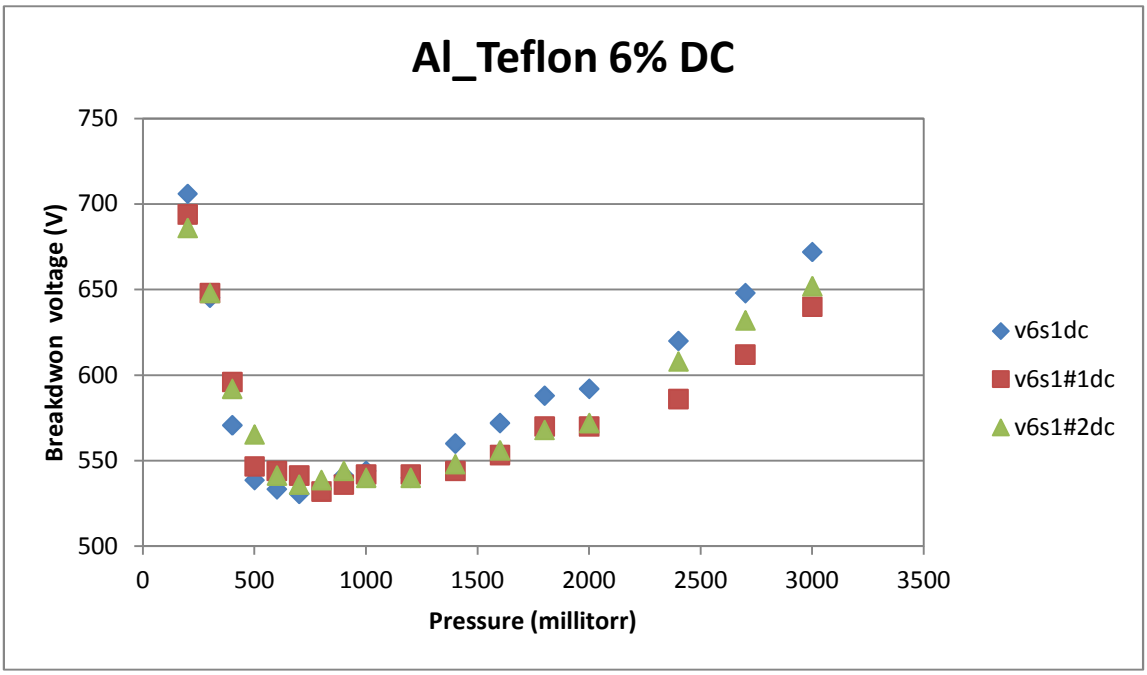

Figure 4.12 DC breakdown voltage comparison for 6% Al_2O_3 on Teflon sample #1.

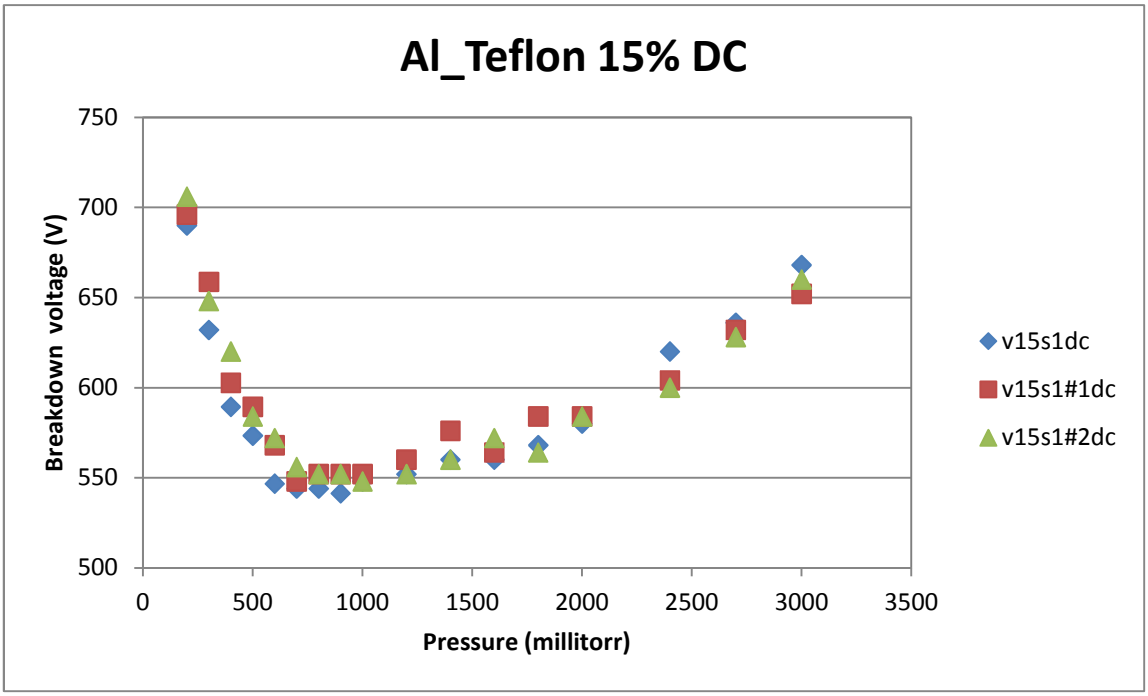

Figure 4.13 DC breakdown voltage comparison for 15% Al_2O_3 on Teflon sample #1.

In Figure 4.14, four different curves from 4 consecutive test runs are shown for the same 2% Al_2O_3 nano-dielectric on Teflon substrate sample #2. The DC data for this sample is in Figure 4.11. Complete set of pulse comparison curves for other samples are listed in Appendix B. The plots for pulse field are more consistent than the DC-case, but small voltage drop (less than 20V) between 1st and 2nd curve still exist at only in the moderate to high pressure range. Minimum pulse breakdown voltage is about 530V occurring at around 0.9 to 0.8 torr, same as in the case of DC tests, with DC minimum voltage varying from 600 to 530V.

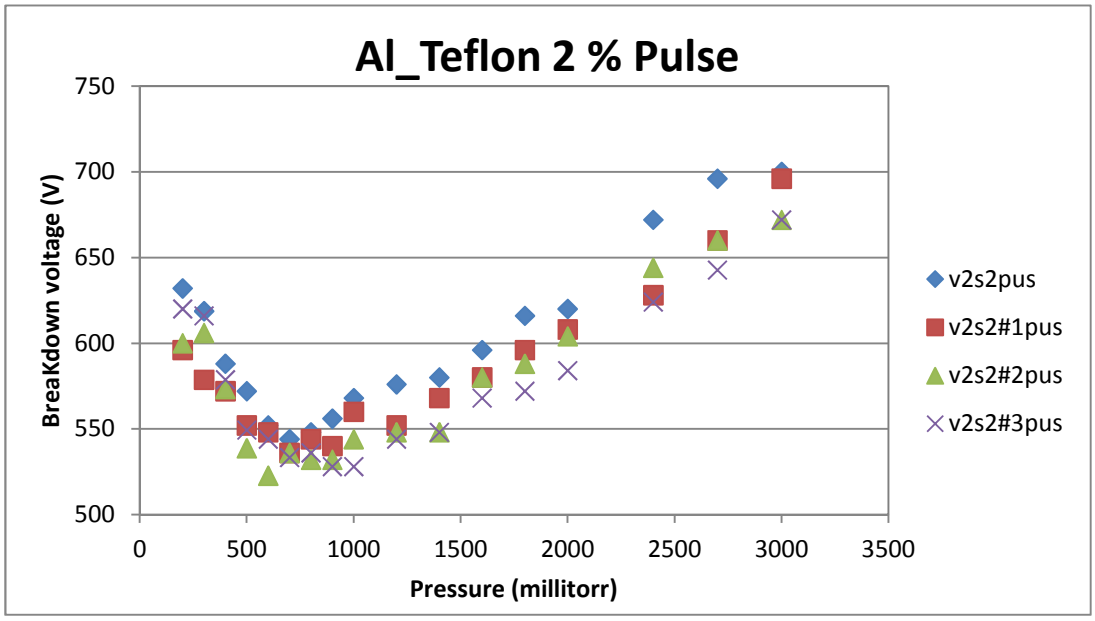

Figure 4.14 Consecutive test results of pulse breakdown voltage for 2% Al_2O_3 on Teflon sample #2, as a function of pressure.

The data for the 6% and 15% Al_2O_3 loaded dielectrics on Teflon substrate sample, using the pulsed applied field is similar to the one under DC applied field, for these 6% and 15% loaded samples. The data is consistent as the sample tested further, no significant difference between the first and second test set curves is observed. These data are shown in Figure 4.15 and Figure 4. 16 respectively.

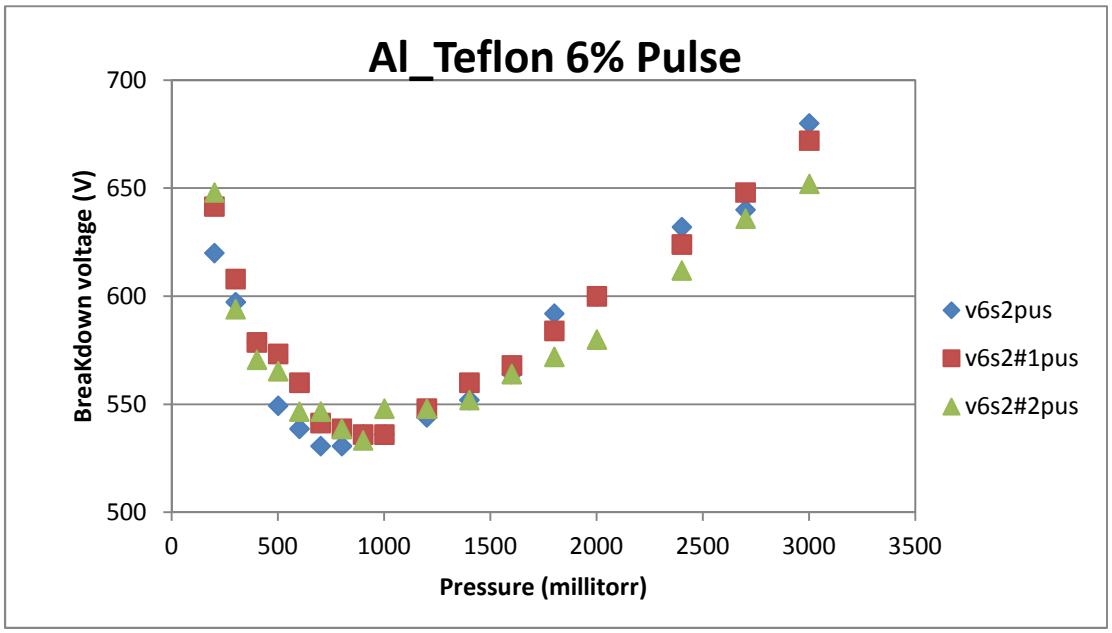

Figure 4.15 Consecutive test results of pulse breakdown voltage for 6% Al_2O_3 on Teflon sample #2, as a function of pressure.

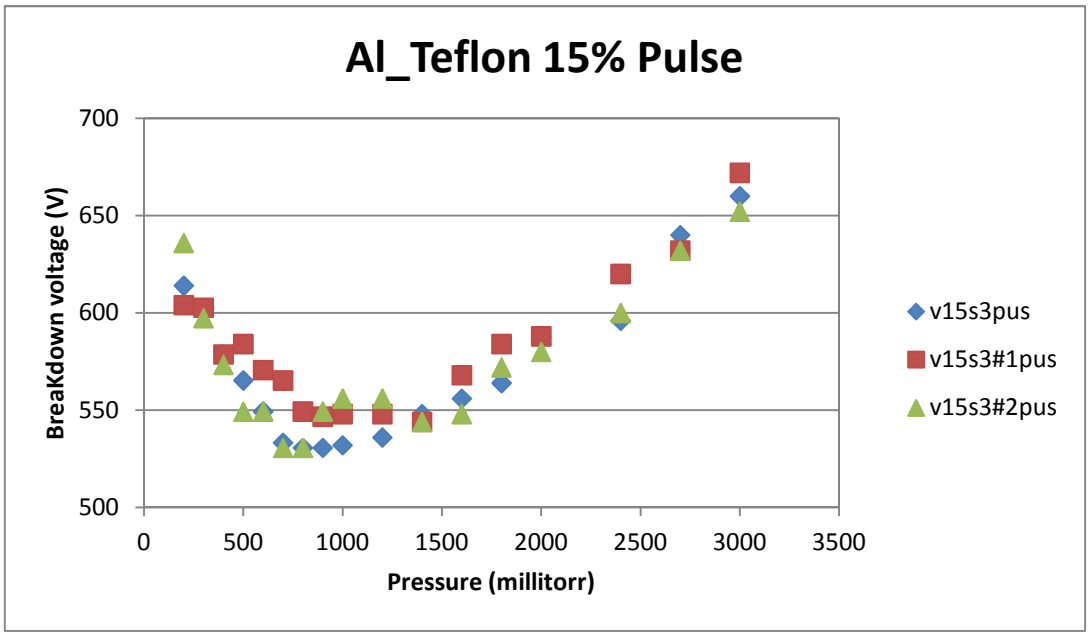

Figure 4.16 Consecutive test results of pulse breakdown voltage for 15% Al_2O_3 on Teflon sample #3, as a function of pressure.

From these data, we see that the some kind of conditioning effect may occur for the 2% sample when the applied field is DC or pulsed. The breakdown voltage as a function of pressure

decreases from its values in the 1st test-set and becomes stable as the sample tested further. This voltage drop with increased testing sequence of the sample is most significant for DC breakdown results. This may be attributed to the conditioning of the surface under the applied field as the sample is exposed to glow discharge successively. This type of conditioning has been observed in a previous work in [22], as the discharge strips away polymer on the surface, the nano-particles are exposed on the surface changing the surface characteristics of the sample. On the other hand, in this work, the progressive degradation of the surface breakdown strength of the samples is only observed for the 2% loaded sample, and the samples loaded with higher loading ratios did not exhibited as noticeable changes. Therefore, this particular observation may also be related to the loading ratio of the samples. The curves for Al_2O_3 loaded dielectric on Teflon, in Figure 4.12 and Figure 4.13 for DC field and Figure 4.15 and Figure 4 .18 for pulsed fields do not display much difference from the first set to the last set of data. For the 6% loaded sample under DC field case, only the 1st test-run is different than the others as show in Figure 4.12. Furthermore, the other curves are the same except in the high pressure range where a small difference of the breakdown voltage is present. This difference is much smaller than the 2% DC applied field case. For the 15% loaded sample, under DC and pulse applied field, there is no significant difference between the data of the consecutive test-sets, and data shown in Figure 4.13 and Figure 4.16 overlap for the entire pressure range

The situation seems to be similar for Al_2O_3 loaded nano-dielectrics on Alumina substrate samples. The 2% loaded sample exhibits "conditioning" type behavior under DC applied signal, but no change between the successive test-set data for the pulsed applied fields as in the case of the samples with Teflon substrate. Whereas the 6% and 15% loaded samples show successively consistent and repeatable behavior under both the DC and pulsed applied fields. Figure 4.17 and

4.18 are DC and pulse breakdown data for 2% loaded Al_2O_3 nano-dielectric on Alumina sample#1 respectively. Other data is shown is Appendix B.

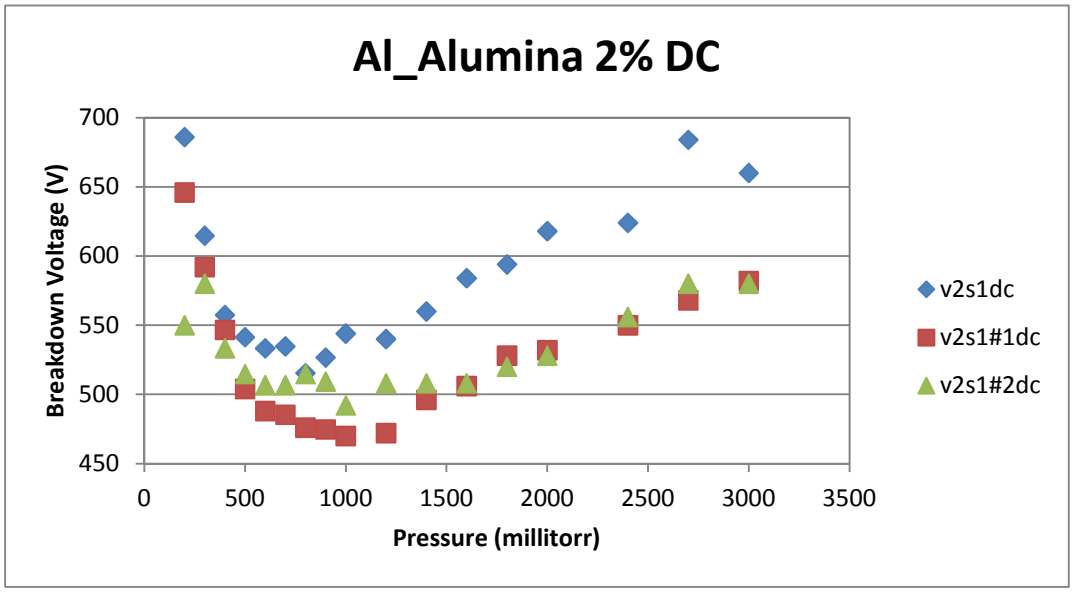

Figure 4.17 Consecutive test results of pulse breakdown voltage for 2% Al_2O_3 on Alumina sample #1.

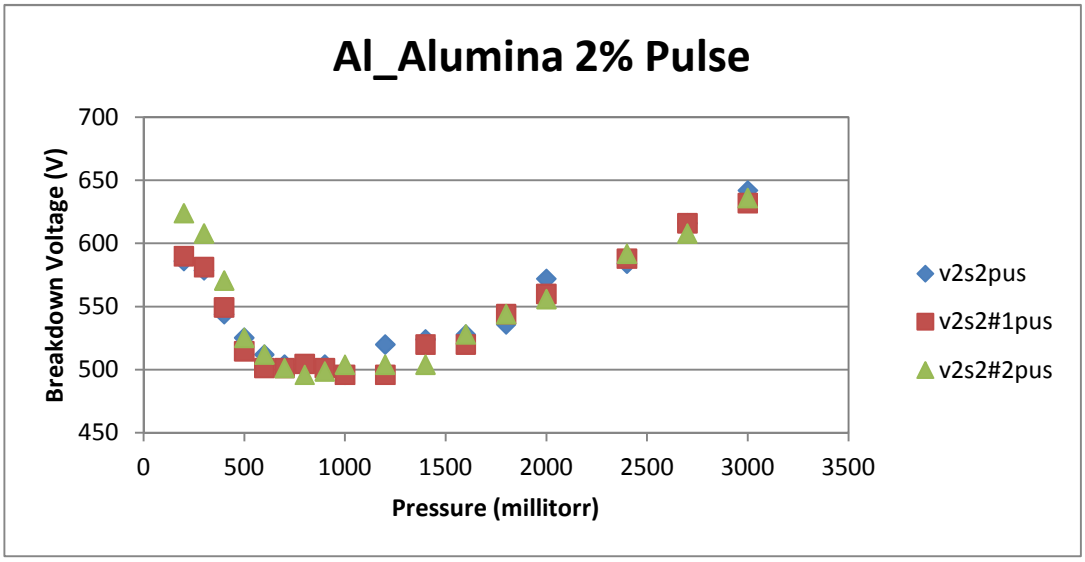

Figure 4.18 Consecutive test results of pulse breakdown voltage for 2% Al_2O_3 on Alumina sample #2.

4.1.3 Breakdown Voltage as a Function of Different Loading Ratio

As discussed in 4.1.2, DC curves show some form of conditioning effect and only the pulse breakdown voltage is unchanging between consecutive tests for the entire pressure range. Therefore, only the first pulse breakdown data of the samples with three different loading ratios is selected for comparison. Figure 4.19 is the surface flashover voltage comparison of the Al_2O_3 loaded nano-dielectric on Teflon substrate sample under pulse breakdown with different loading ratios namely, 2%, 6%, and 15%. From these data we see there is no significant breakdown voltage increase by increasing the loading ratio for pulse field for the entire pressure range the samples are tested.

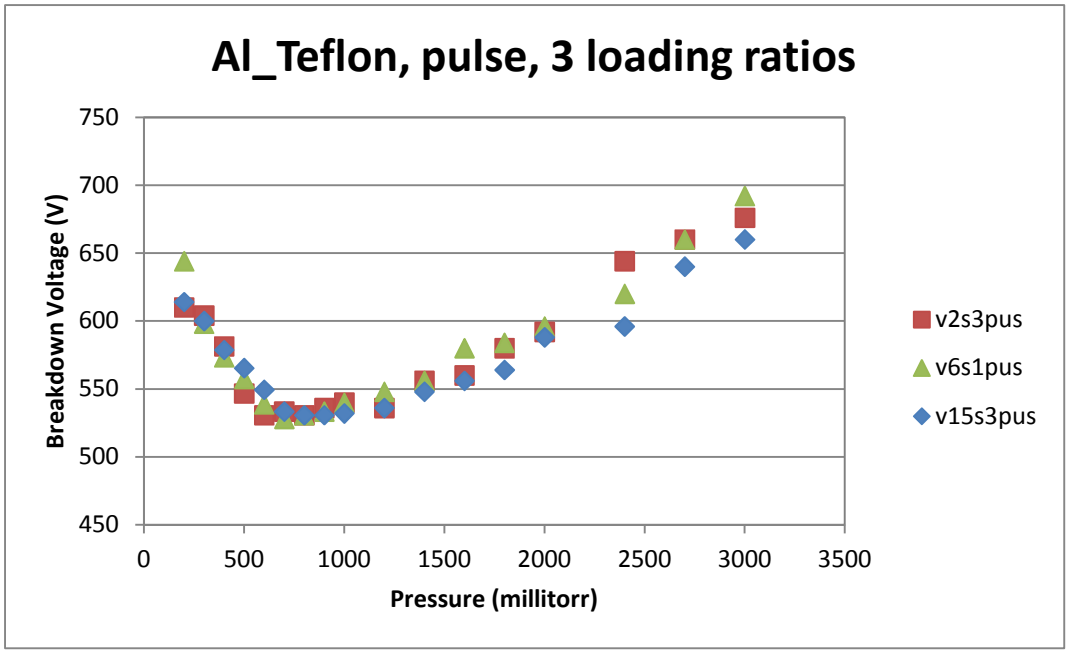

Figure 4.19 Pulse breakdown for Al_2O_3 on Teflon samples with 3 different loading ratio.

Similarly the pulse breakdown voltage as a function of pressure for the Al_2O_3 loaded nano-dielectrics on Alumina substrate with different load ratios of 2%, 6%, and 15% are ploted in Figure 4.20. Again, there is no significant voltage increase observed by increase the loading ratio for these samples on Alumina substrate. Thereore, we conclude that there is no effect of

loading ration on the surface breakdown voltage of these micro sized Al_2O_3 filled samples on two different substrates under either DC applied field or pulsed upplied fiels.

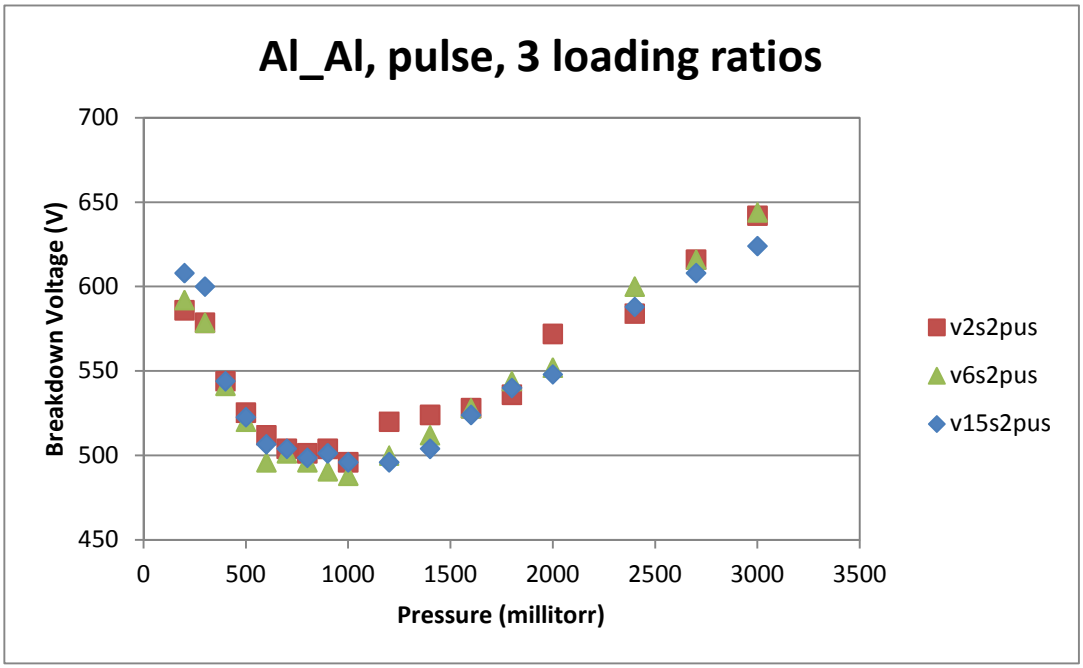

Figure 4.20 Pulse breakdown for Al_2O_3 on Alumina samples with 3 different loading ratio.

The situation is different for the nano-dielectrics samples prepared with TiO_2 particles, where these samples show a slightly different behavior than the ones with the Al_2O_3 loaded samples. The pulsed breakdown voltage data as a function of pressure for the TiO_2 on Teflon and Alumina substrates are shown in Figure 4.21 and Figure 4.22 respectively. In this case 6% loaded TiO_2 nano-dielectric on both Teflon and Alumina substrate show the highest breakdown voltage over the pressure range studied. For the TiO_2 nano-dielectric on Teflon samples, 6% results are similar to the 15% loaded sample in which, both about 20 volts higher than the breakdown voltage of the 2% loaded sample. For TiO_2 nano-dielectric on Alumina samples, again the 6% samples have the best results with a 20 volts higher breakdown voltage than the samples with other loading ratio.

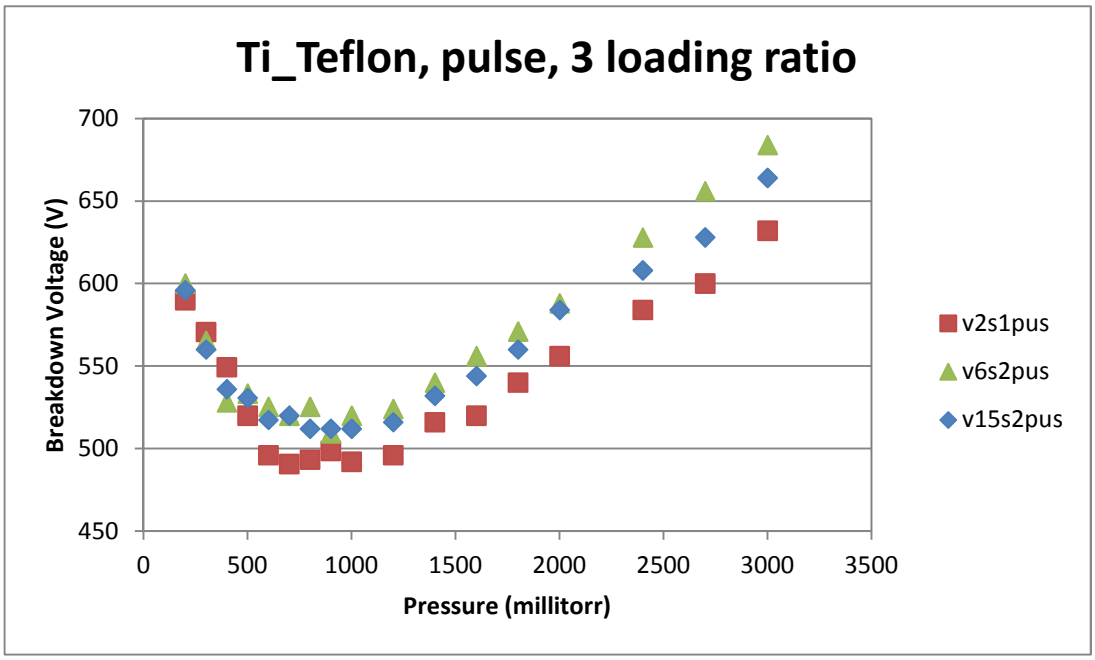

Figure 4.21 Pulse breakdown for TiO_2 on Teflon samples with 3 different loading ratio.

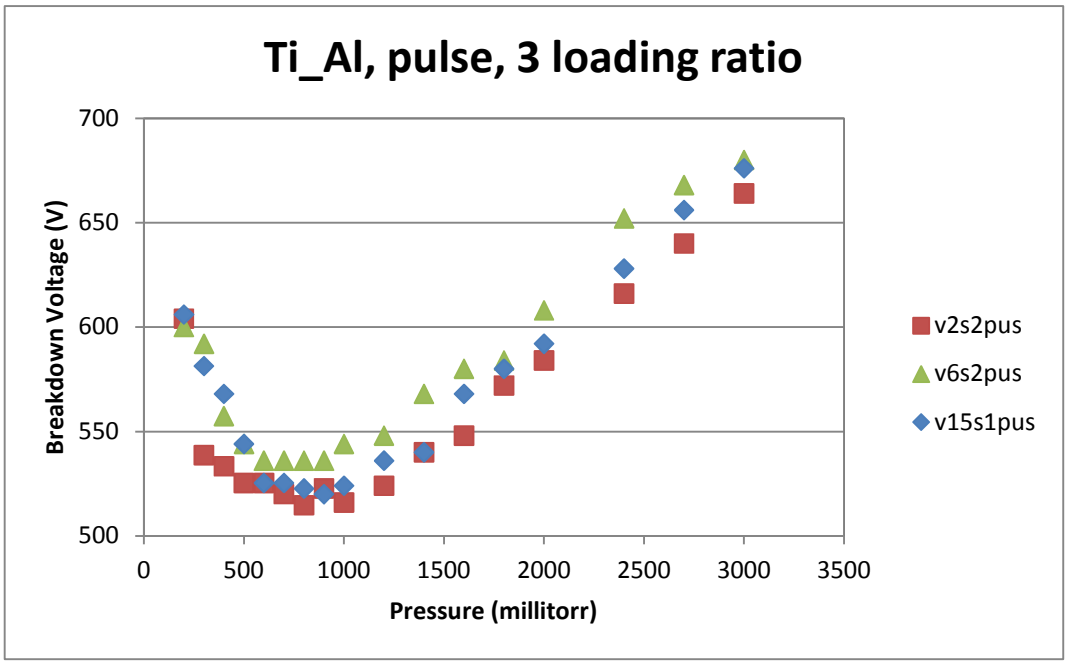

Figure 4.22 Pulse breakdown for TiO_2 on Alumina samples with 3 different loading ratio.

From these data, we can see that for the Al_2O_3 nano-dielectric samples, no significant improvement of the pulse breakdown voltage by increase the loading is observed, however for TiO_2 nano dielectrics, the 6% loading seems to be the most optimized loading ratio for both substrates used to make the test samples.

4.1.4 Optimum Substrate for Different Nano-Particles

The minimum surface breakdown voltages from repeated data are averaged and shown in Table 4.2. From this table we see that the dielectric samples made with Al_2O_3 powder give the highest DC and pulse minimum breakdown voltage when Teflon is used as the substrate. On the contrary the nano-dielectric samples made with TiO_2 nano particles give the second highest DC and pulse breakdown voltage when Alumina used as substrate. Furthermore, no significant DC and pulse breakdown voltage improvement is found by increase the loading ratio for either sample. It is also noted that the results with pulsed applied field show higher surface breakdown voltage than DC for the Al_2O_3 on Alumina, TiO_2 on Teflon and TiO_2 on Alumina configuration.

	Averaged minimum breakdown voltage (Volts)		
	2%	6%	15%
Al2O3 onTeflon dc	538	535	535.5
Al2O3 onTeflon pulse	532	537	540.3
Al2O3 on Alumina dc	496	476	478
Al2O3 on Alumina pulse	508	492	494.7
TiO2 on Teflon dc	469.83	490	495
TiO2 on Teflon pulse	481	513.67	514
TiO2 on Alumina dc	496.2	535	528
TiO2 on Alumina pulse	513	538	523.5

Table 4.2 Averaged minimum breakdown voltages.

4.2 Breakdown Voltage as a Function of Frequency

4.2.1 Tests With Varying Frequency at Constant Pressure

For a 50% duty cycle unipolar pulse, during half of the cycle, the field is zero where diffusion of the charged particles is possible in the gackground gas. It is belived that this has a large effects to the breakdown mechanism. Therefore the pulse breakdown voltage is different than the DC breakdown characteristics for gaseous medium [9]. Similalry, for the surface breakdown events, during the half cycle when the field is "off" the charges on the surface, accumulated during the "on" cycle, would have sufficient relaxation time. Therefore, it is expected that the frequency of the applied field would play a role in characteristics of the surface breakdown voltage across the dielectric surface.

The frequency sweep experiments are conducted to study the surface flashover characteristics of nano-dielectrics under high frequency applied fields to investigate the frequency effect on the surface breakdown of nano dielectrics. Only the Al_2O_3 filled nano-dielectric on Teflon substrate samples are used for the frequency sweep tests. Same testing procedure in pressure tests is used in these experiments, except, this time the pressure is kept at a predetermined value and frequency of the applied field is varied from 20 kHz to 220 kHz. For these experiments, two differenet constant pressures namely 800 & 1200milli torr are selected, which corresponds approximately where the minimum breakdown voltage occurs in Figure 4.3. Only the nano-dielectric samples made with Al_2O_3 on Teflon substrate with three different loading ratios (2%, 6%,15%) are used only in these tests. A complete set of the curves are in Appendix C.

In the previous section, all of the samples are tested under 20kHz pulse and we find out that the breakdown curve presents a relative flat bottom at 700 and 1000 millitorr pressure. In this range the breakdown voltage difference is usually less than 10 volts, and the breakdown voltage starts

to rise if the pressure is out of this range for both lower and higher ends. Therefore, 800 millitorr is chosen as the pressure corresponding to minimum breakdown voltage. We also recorded the surface breakdown voltage at 1200 millitorr as reference to test the frequency effects on the surface breakdown voltage. The pulse frequency is increased from 20kHz to 220kHz with a 20 kHz step for both 800 millitorr and 1200 millitorr pressure sets. Frequency sweep plot of surface breakdown is show in Figure 4.23 for the 2% loaded Al_2O_3 nano-dielectric on Teflon substrate sample#2. As seen, the breakdown voltage decreases as the frequency increased for both pressure. The 1200 millitorr curve has a larger decreasing slope when the frequencies is less than 100kHz in contrast the breakdown curve for of the samples in 800 millitorr decreases at a relative constant rate. The breakdown voltage curve at 1200 millitorr begins with a higher value than the one in 800 millitorr. At around 40kHz frequency of the applied field, these two curves crosses as shown in Figure 4.23 for the 2% loaded sample.

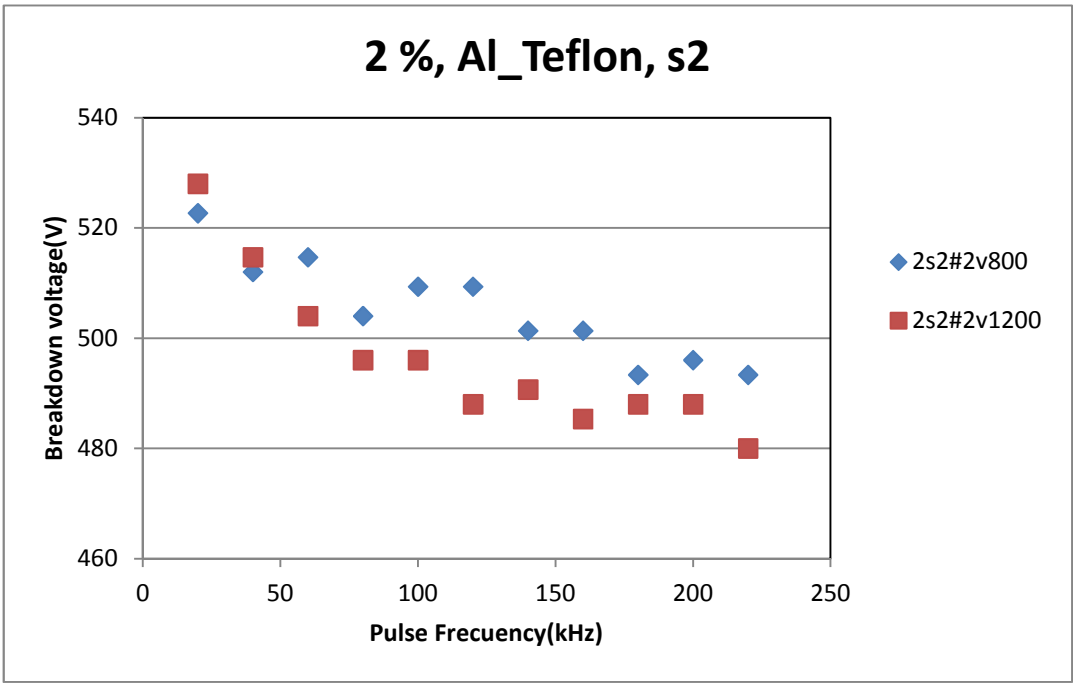

Figure 4.23 Frequency sweep test for 2% Al_2O_3 on Teflon sample2, repeat #2.

The breakdown voltage as a function of frequency test results for 6% and 15% loaded Al_2O_3 on Teflon substrate samples are shown in Figure 4.24 and Figure 4.25 respectively. Similar to the data of the 2% loaded sample, the breakdown voltage also decreases as the frequency is increased for both pressures. The surface breakdown curves for the 1200 millitorr operating pressure have a larger decreasing slope when the frequencies is less than 100kHz and it decreses as frequency increases at a relative small rate. Also the breakdwon voltage curve begins with a higher value in 1200 millitorr operating pressure than the one in 800 millitorr. At around 40kHz frequency of the applied field these two curves crosses again for both of these samples.

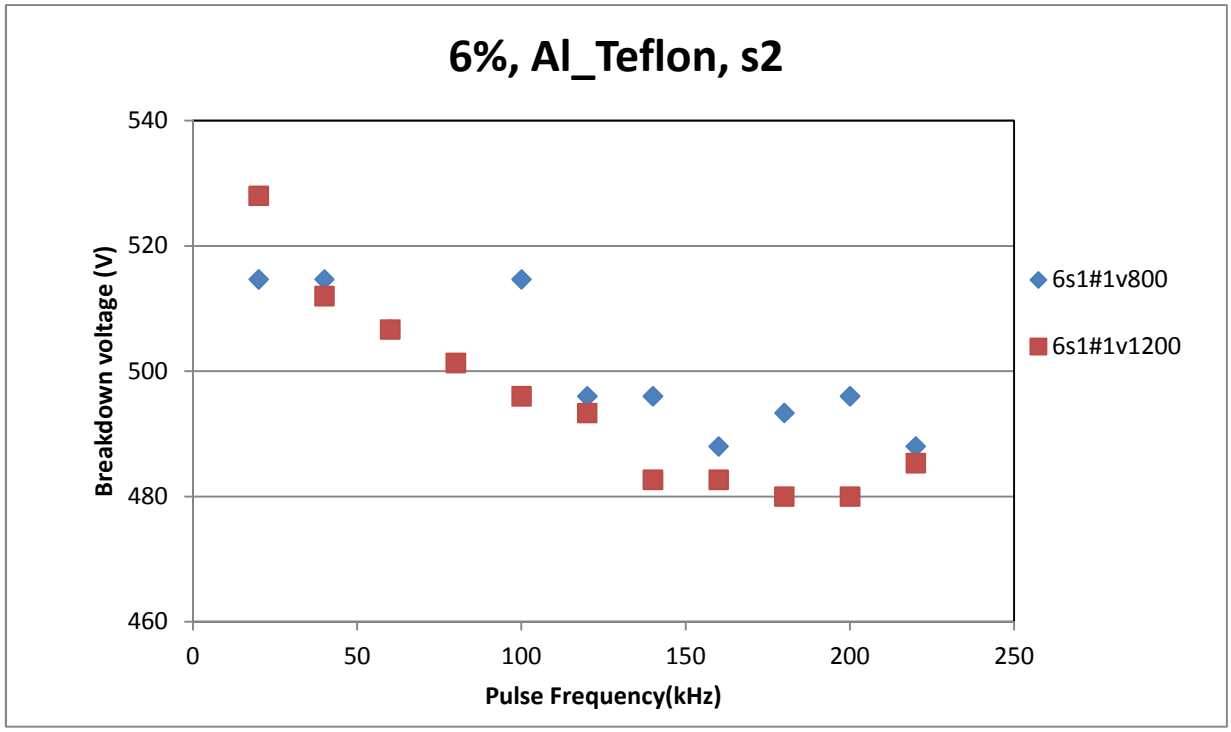

Figure 4.24 Frequency sweep test for 6% Al_2O_3 on Teflon sample1, repeat #1.

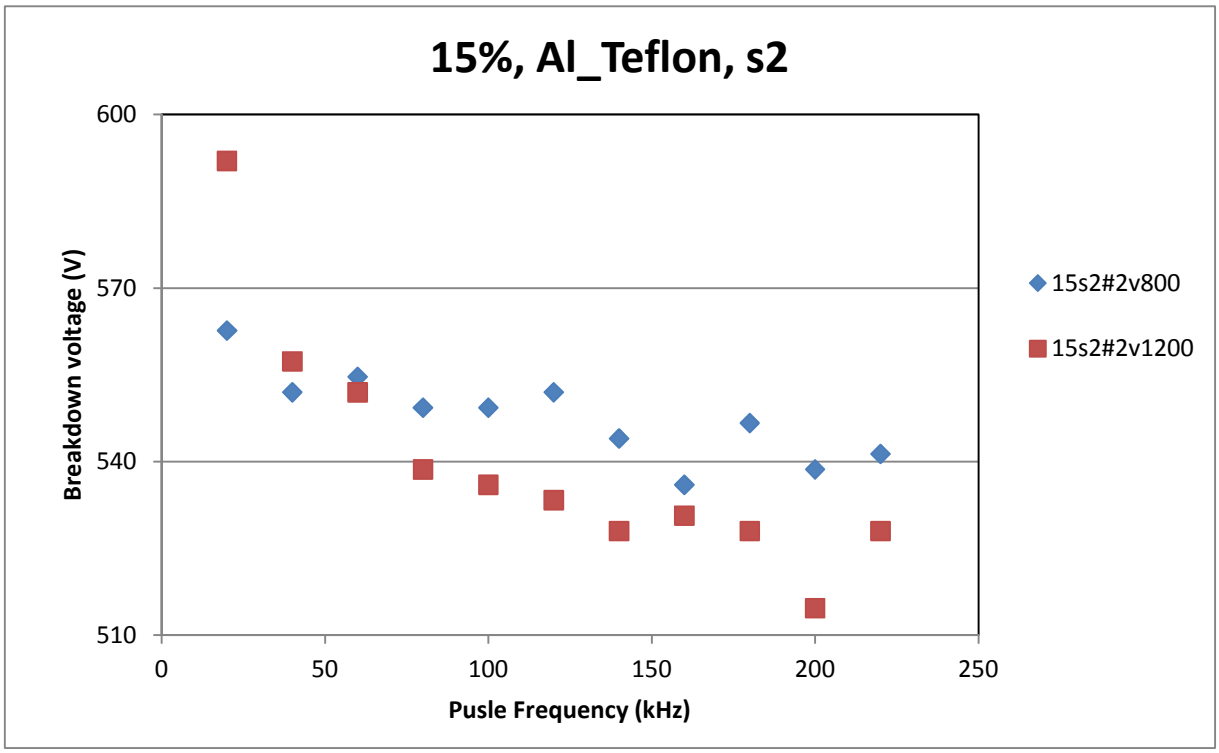

Figure 4.25 Frequency sweep test for 15% Al_2O_3 on Teflon sample1, repeat #2.

4.2.2 Duty Cycle effect on the Surface Flashover Voltage

The effect of the duty cycle of the applied field is also studied. Figure 4.26 shows the surface breakdown voltage of 2% loaded Al_2O_3 nano-dielectric on Teflon substrate sample as a function of duty cycle. The frequency of applied pulsed field is at 20 kHz and the pressure is set at 800 millitorr first, then 1200 millitorr. As seen in Figure 4.26, as the duty cycle starts from 20%, the breakdown voltage is relatively high and it starts to decrease as the duty cycle increases. This should be expected, because, when the duty cycle of the field is 20% the applied voltage is more close to an impulse waveform, which has a higher breakdown voltage as mentioned in Chapter II. When the duty increases further to 80% and over, the signal gets closer to a DC signal and the breakdown voltages is expected to be close to the one for DC fields. From Figure 4.26, it is also

observed that the breakdown at 50% duty cycle is in agreement with the data in Table 4.2 and the difference between 50% and 80% data is about 10V.

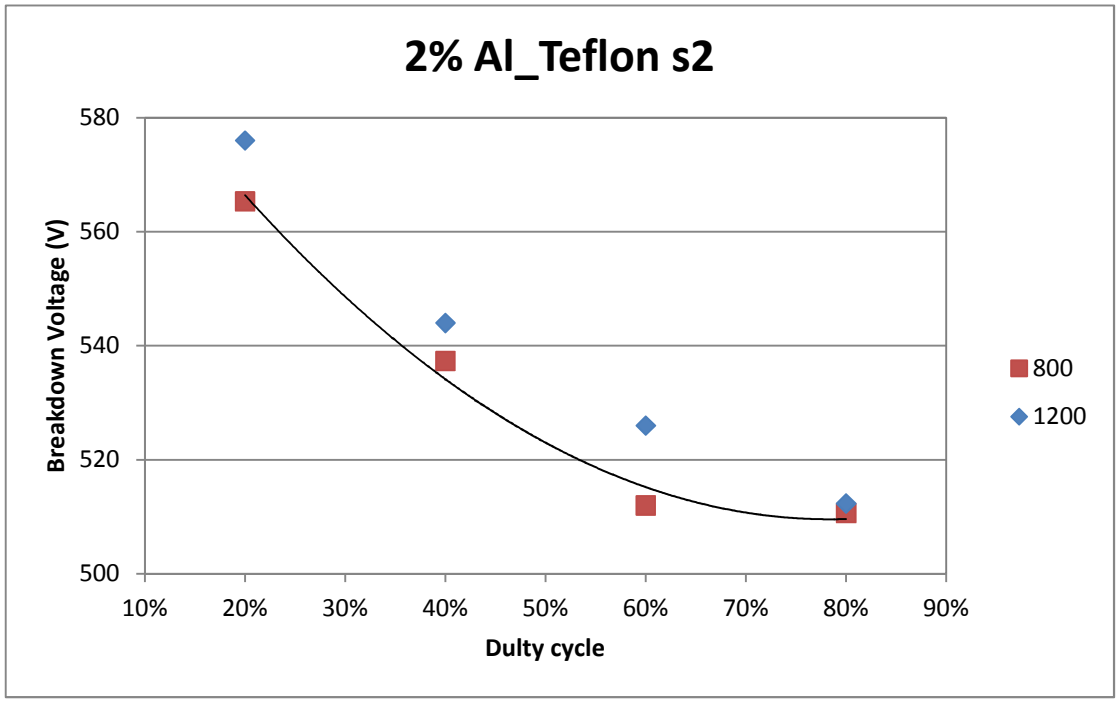

Figure 4.26 Duty cycle sweep test for 2% Al_2O_3 on Teflon sample 2.

CHAPTER V

CONCLUSION

The experimental results presented some interesting findings on surface flashover for dielectric nano-composites. All of the pressure sweep plots agree that the gas breakdown mechanism affects surface flashover in partial vacuum. For both DC and pulse signal, the surface flashover breakdown voltage curves present features similar to the Paschen curve. No consistent conclusion can be made as to which signal causes higher breakdown voltage.

When Al_2O_3 particles are used as additive to the epoxy resin, no significant minimum breakdown voltage improvement is observed for increased loading ratio, However, for TiO_2 nano particles cast in epoxy with 6% additive have the highest minimum surface flashover results compared with 2% and 15% loaded samples. Interestingly, for TiO_2 nanodielectric composite, the alumina substrate provides a higher breakdown voltage, whereas Teflon substrate is better for Al_2O_3 nanodielectric composite. Overall, Al_2O_3 nanodielectric composite with Teflon substrate provides the highest breakdown voltage.

For unipolar pulse signals, increase in frequency result in lower minimum surface flashover breakdown voltage. This reduction may be explained by a decrease in the "zero period" of the pulse signal. We observed that the "zero period" of the unipolar pulse does not seem to play an important role in the surface flashover mechanism—the longer the zero period, the higher the breakdown voltage.

The findings in these experiments bear directly on how we understand the surface flashover mechanism in partial vacuum. The performance of dielectric nanocomposite can be also optimized by using the appropriate combinations.

Reference

[1] M. Farzaneh, J. Kiernicki, “Flashover problems caused by ice build up on insulators” IEEE Electrical Insulation Magazine, Vol. 11, pp 5-15, 1995.

[2] R. Latham, *High voltage vacuum insulation: Basic concepts and technological practice*, Academic Press, pp8-11, pp 300-306, 1995.

[3] H. Kirkici, “*Surface* Flashover and Dielectric Materials for Space Environment”, Proc. Intern. Conf. on Electrical and Electronics Engineers, Turkey, pp 31-37, 1999.

[4] J. Keith, Nelson, “The Promise of Dielectric Nanocomposites”, IEEE International Symposium on Electrical Insulation, pp 452, 2006.

[5] A. A. Fridman, L. A. Kennedy, *Plasma physics and engineering*, Taylor & Francis, pp 453, 2004.

[6] K. Koppisetty, “Breakdown Studies of Helium and Nitrogen in Partial Vacuum Subject to Non-Uniform, Unipolar Fields in the 20-220 KHz Range”, Ph.D. dissertation, Auburn University, pp31, 2008.

[7] E. Hastings, G. Weyl, Guy, D. Kaufman, "Threshold voltage for arcing on negatively biased solar arrays", Journal of Spacecraft and Rockets, vol. 27, pp 539-544, 1990.

[8] E. Nasser, *Fundamentals of Gaseous Ionization and Plasma Electronics*, John Wiley & Sons Inc, pp 453, 1971.

[9] H. Kirkici and K. Koppisetty, “Breakdown Characteristics of Helium and Nitrogen at kHz Frequency Range in Partial Vacuum for Point-to-Point Electrode”, IEEE Transactions on Dielectrics and Electrical Insulation Vol. 15, pp 749 – 755, 2008.

[10] K. Morales, “Physics of pulsed unipolar dielectric surface Flashover at atmospheric conditions”, M.S. thesis, Texas Tech University, pp 2-4, 2006

[11] H. Kirkici, M. Serkan and K. Koppisetty, “Nano/Micro Dielectric Surface Flashover in Partial Vacuum”, IEEE Transactions on Dielectrics and Electrical Insulation Vol. 14, pp 790 – 795, 2007.

[12] F. T. Ulaby, *Fundamentals of applied electromagnetic*, Pearson Prentice Hall, pp 166, 2006.

[13] P. J. Harrop, *Dielectrics*, Wiley, pp 5-7, 1972.

[14] H. Bluhm, *Pulsed Power Systems: Principles and Applications*, Springer, pp 253, 2006.

[15] M. W. Barsoum, *Fundamentals of ceramics*, Taylor & Francis, pp362, 2003.

[16] S. O. Kasap, *Principles of Electronic Materials and Devices*, McGraw-Hill, 453-466, 2006.

[17] F. W. Billmeyer, Jr, *Textbook of Polymer Science*, Wiley, pp 436-452, 1984.

[18] T. J. Lewis, "Nanometric Dielectrics", IEEE Transactions on Dielectrics and Electrical Insulation, Vol. 1, pp 812-825, 1994.

[19] J. Keith Nelson, "Towards an understanding of nanometric dielectrics", 2002 Annual Report Conference on Electrical Insulation and Dielectric Phenomena, pp 295 – 298, 2002.

[20] F. Li and H. Kirkici, "Surface Flashover of Nano-composites in Partial Vacuum under kHz Pulsed Fields", 2010 IEEE International Power Modulators and High Voltage Conference, pp 453 – 456, 2010.

[21] M. Serkan, H. Kirkici and K. Koppisetty, "Surface Flashover Characteristics and Optical Emission Analysis of Nano Particle Cast Epoxy Resin", 2005 Annual Report Conference on Electrical Insulation and Dielectric Phenomena, pp 128 – 131, 2005.

[22] H. Kirkici, "Surface Flashover Characteristics of Diamond-like Carbon Thin Films in Vacuum", IEEE Transactions on Dielectrics and Electrical Insulation, Vol. 4, pp 71-78, 1997.

Appendix A

Complete set of figures for every test set, the surface flashover breakdown voltages are plotted as test pressure increased. For one test set plot, DC and unipolar pulse signal (20 kHz, 50% duty cycle) breakdown voltage are compared. Title of each figure follows the same pattern, firstly, the type of the signal used, then the loading ratio, then filler substrate configuration and sample number, lastly the repeated number.

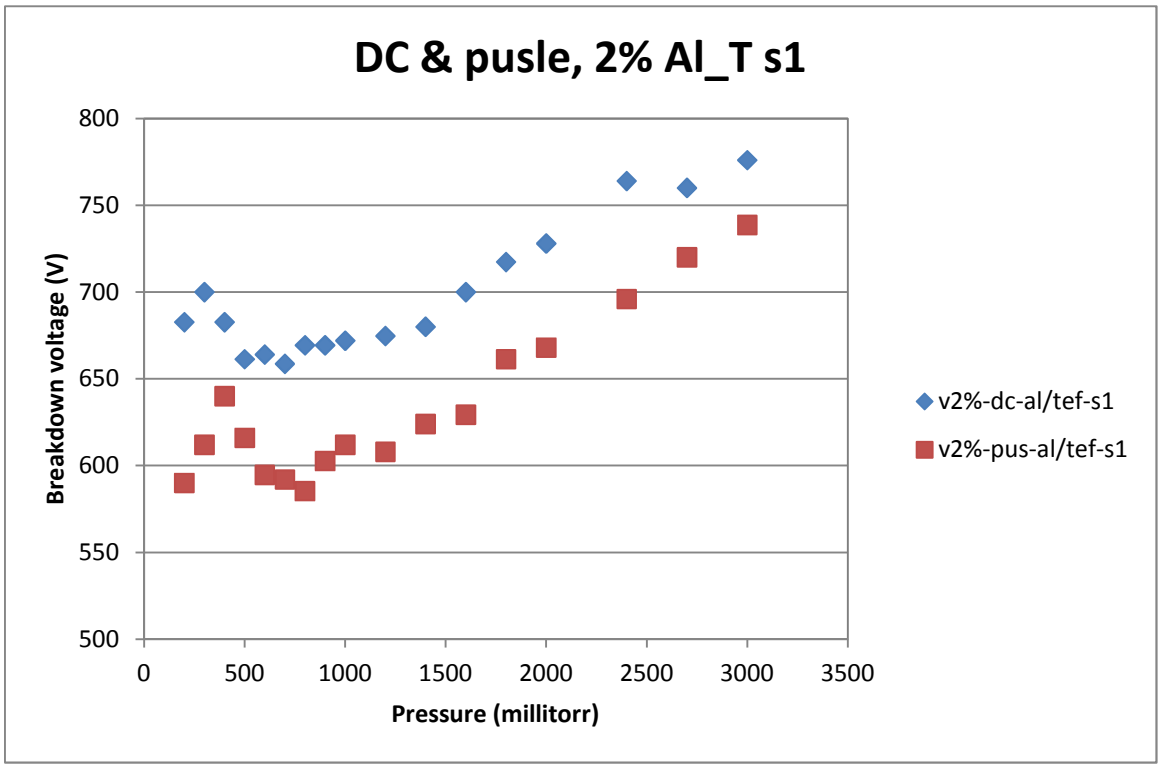

Figure A-1

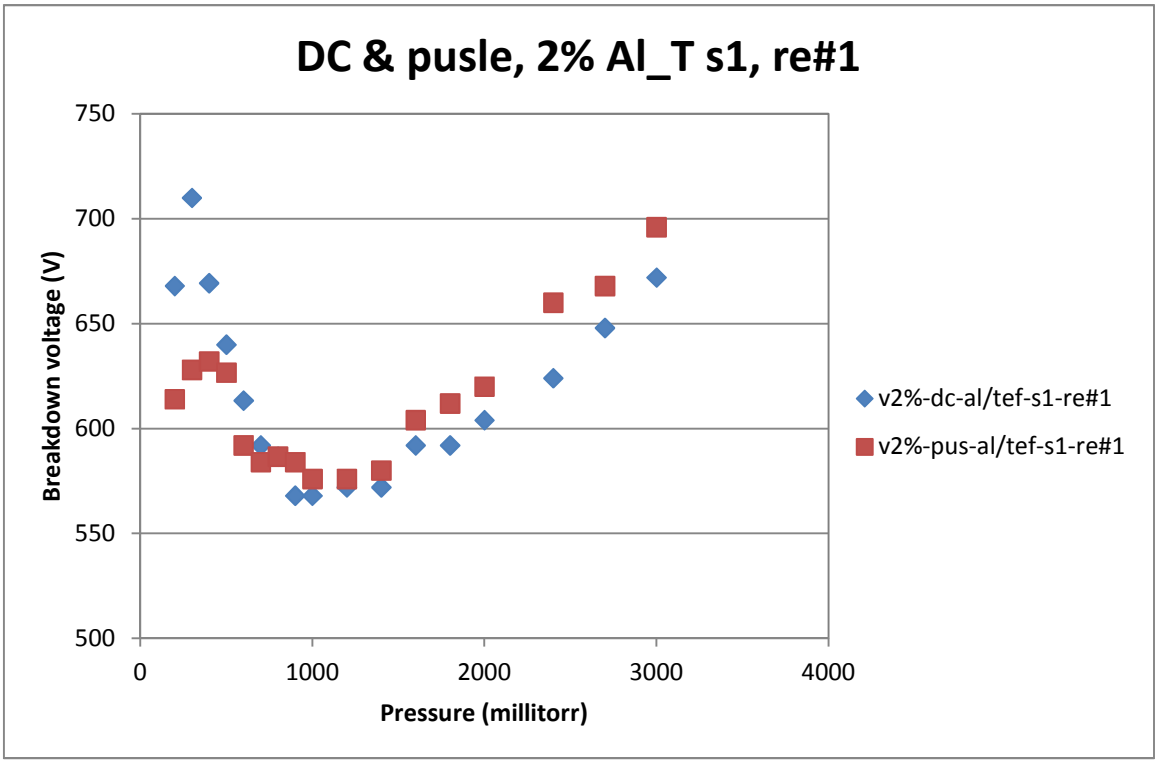

Figure A-2

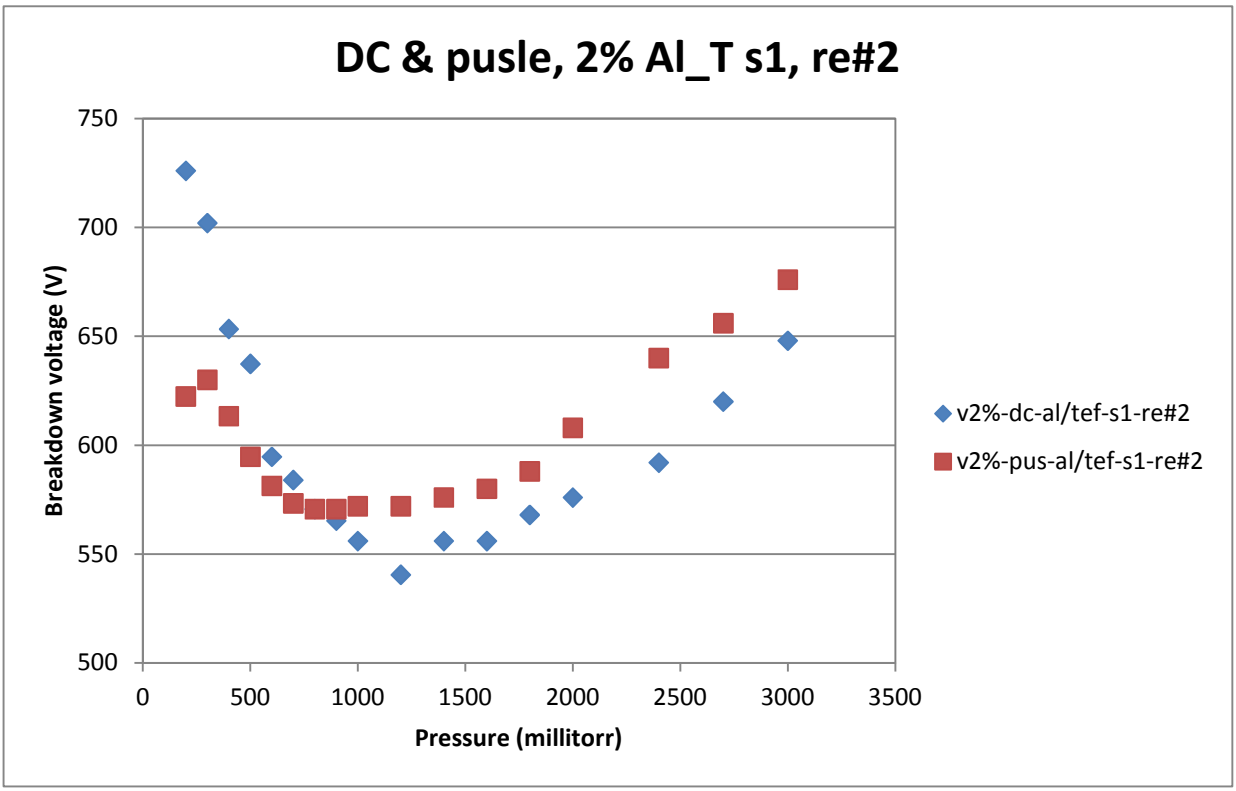

Figure A-3

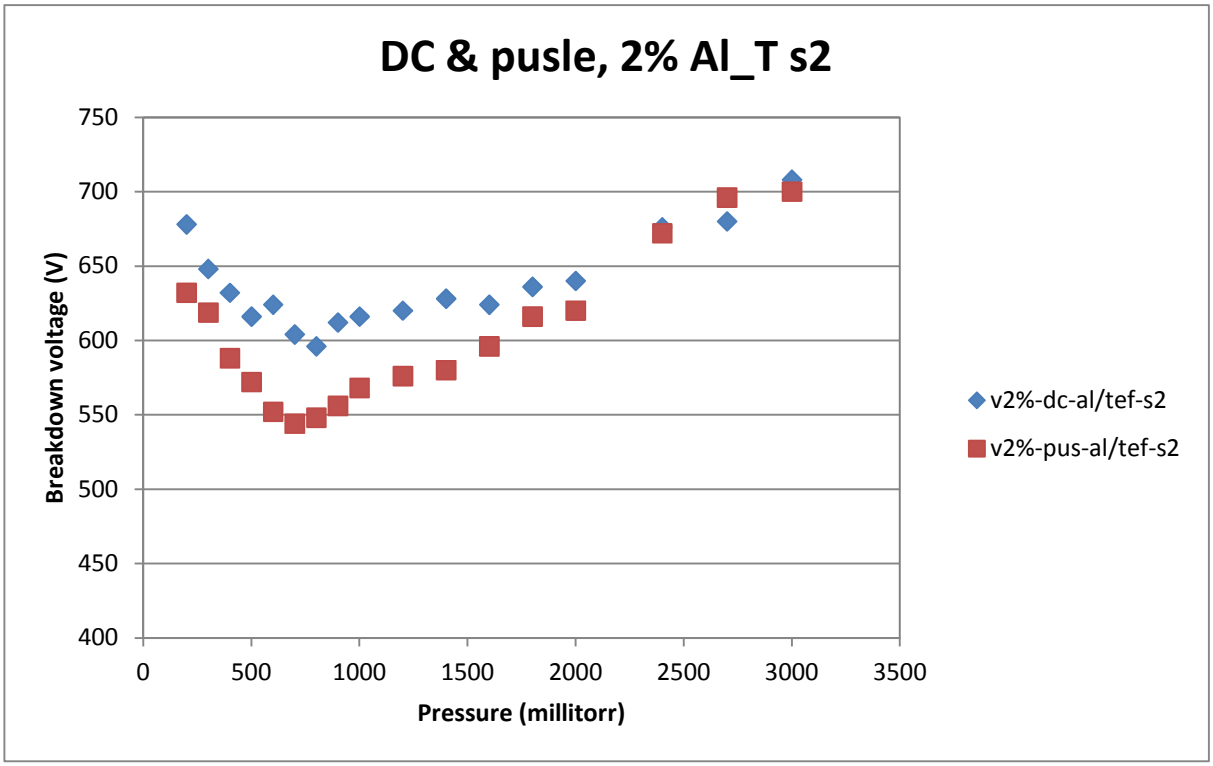

Figure A-4

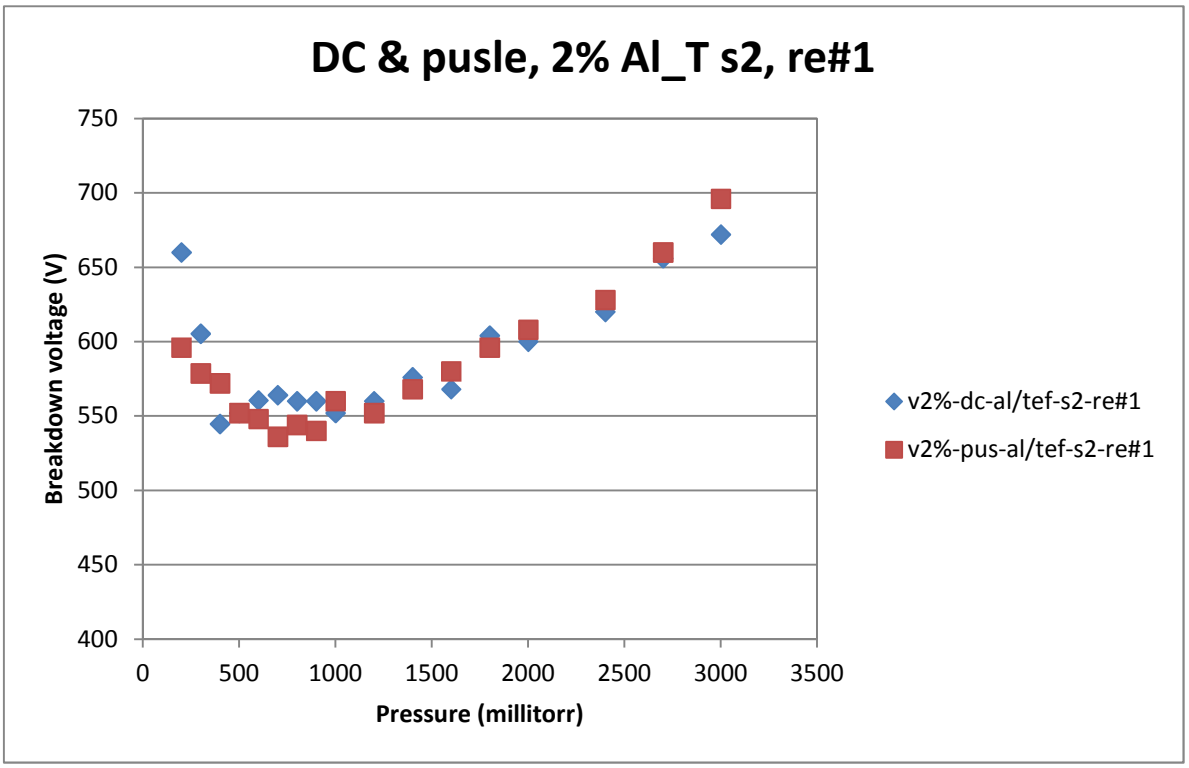

Figure A-5

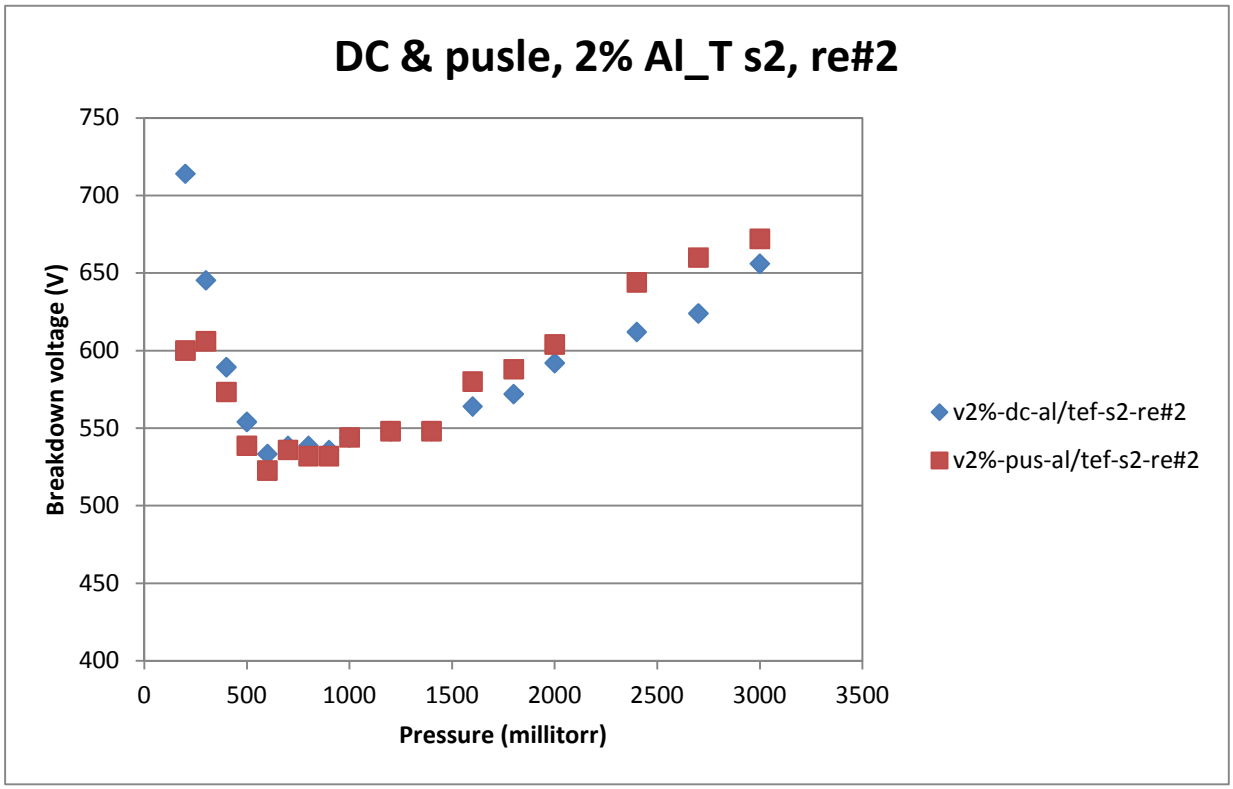

Figure A-6

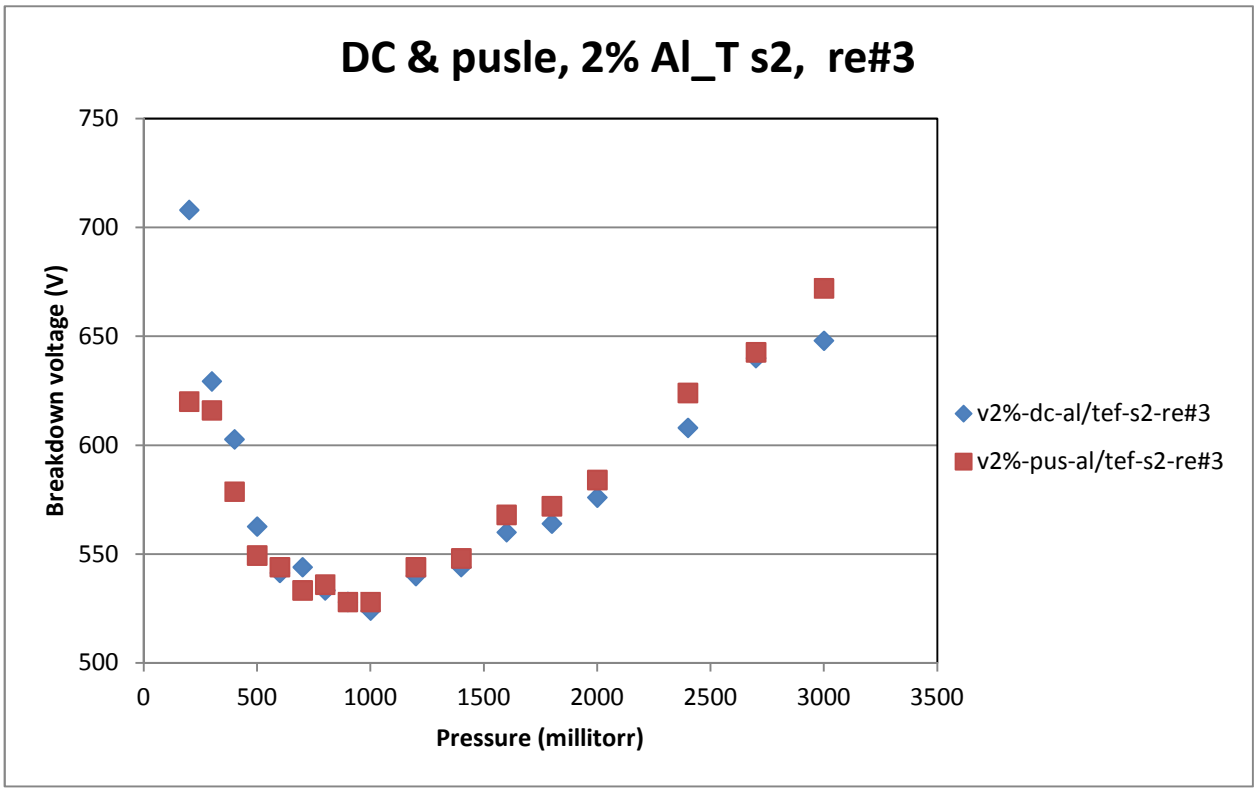

Figure A-7

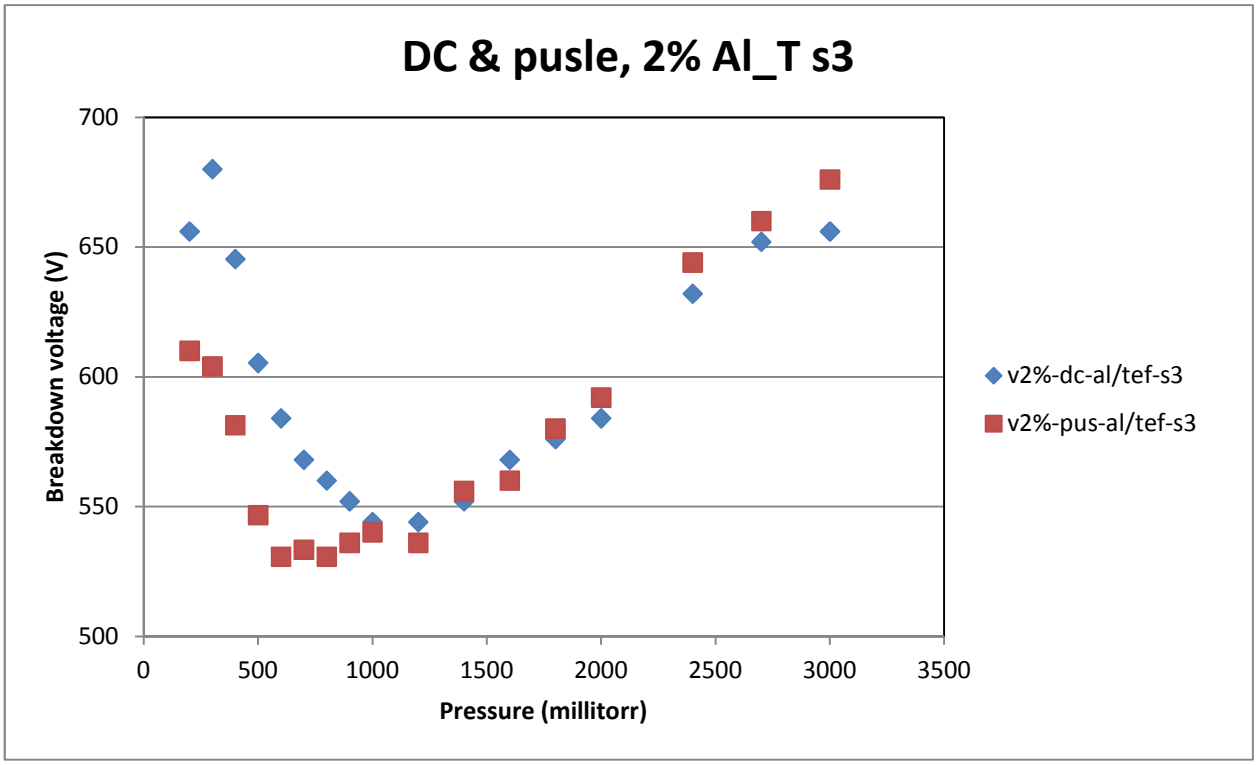

Figure A-8

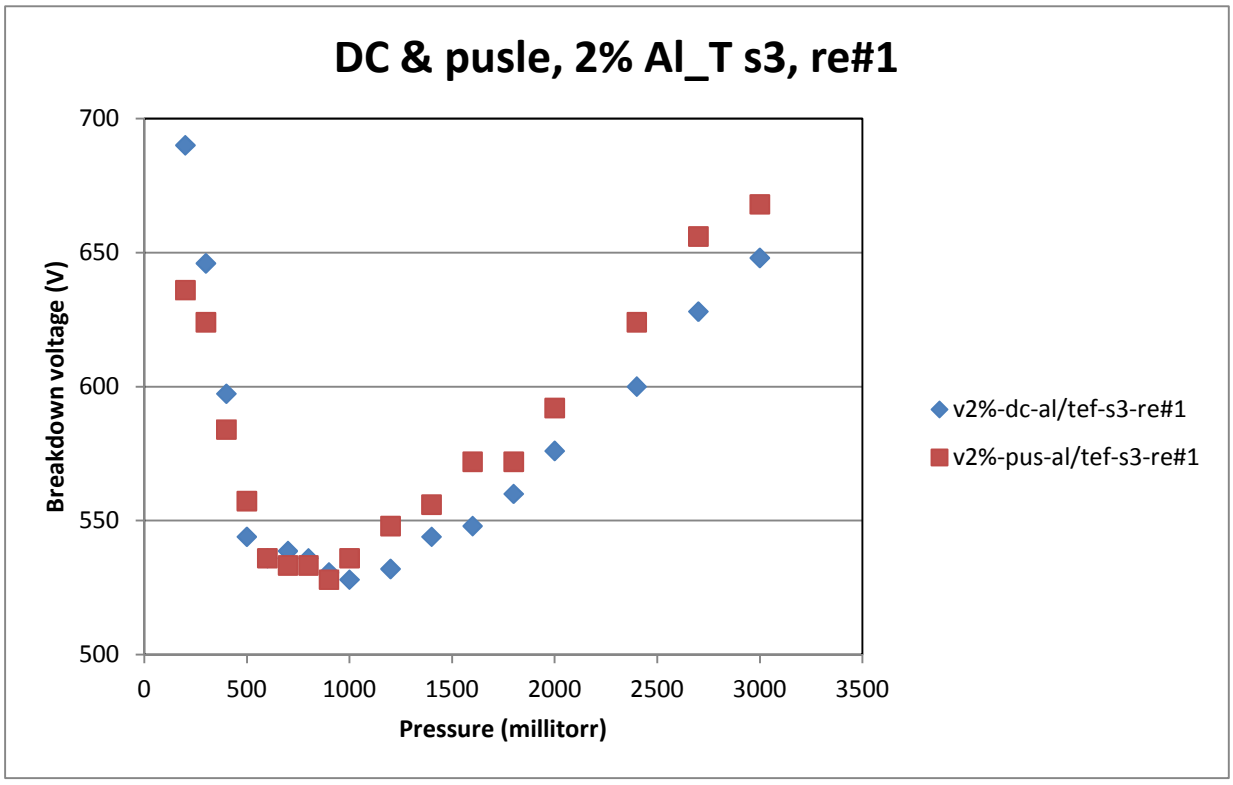

Figure A-9

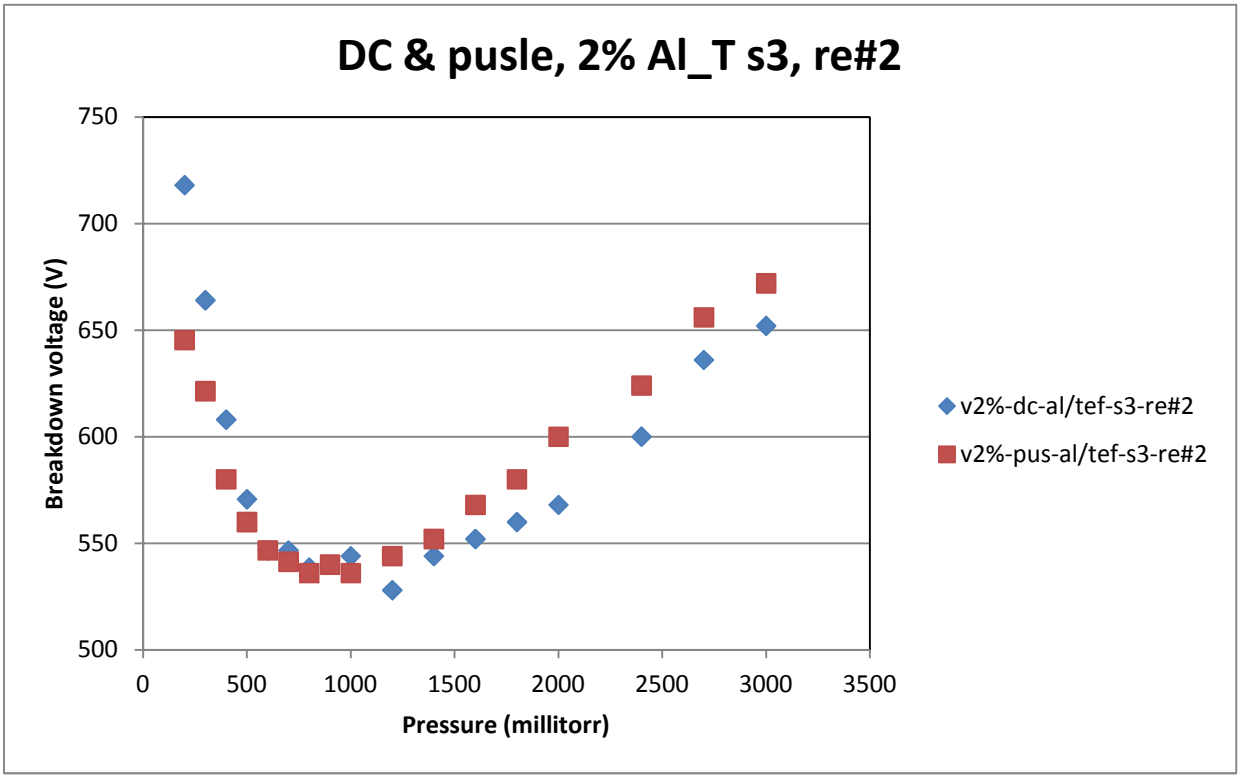

Figure A-10

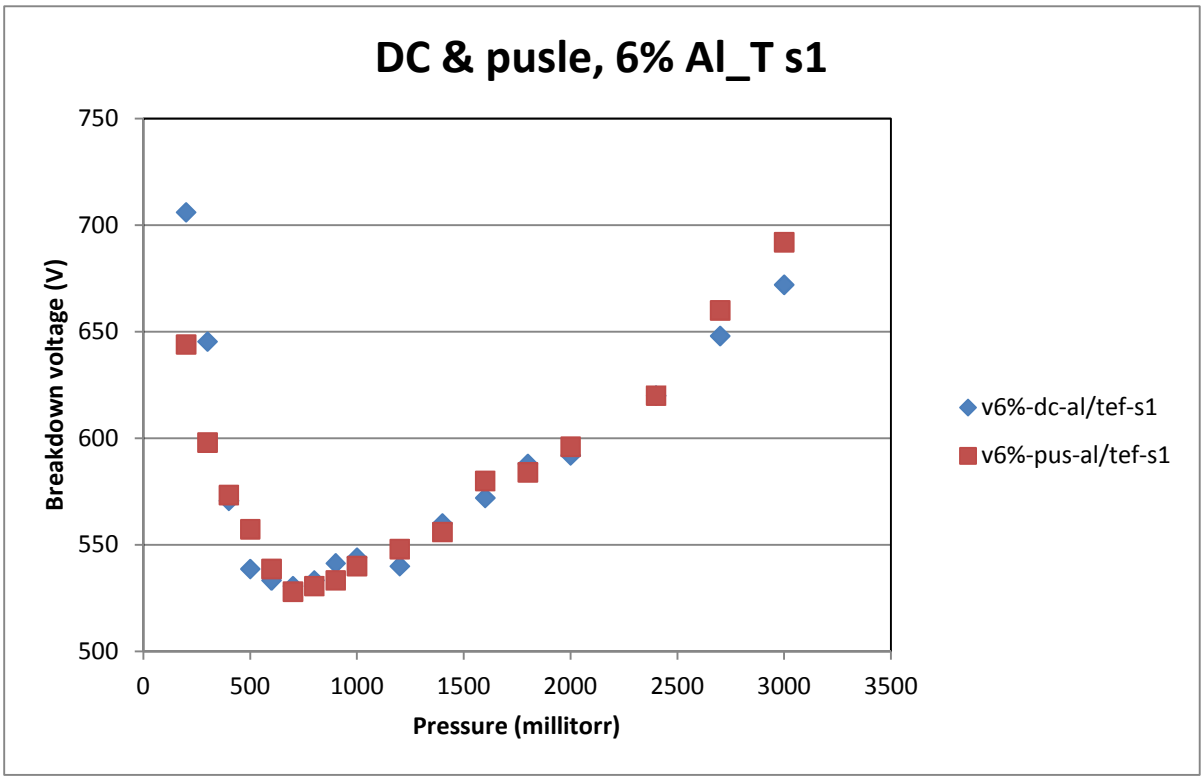

Figure A-11

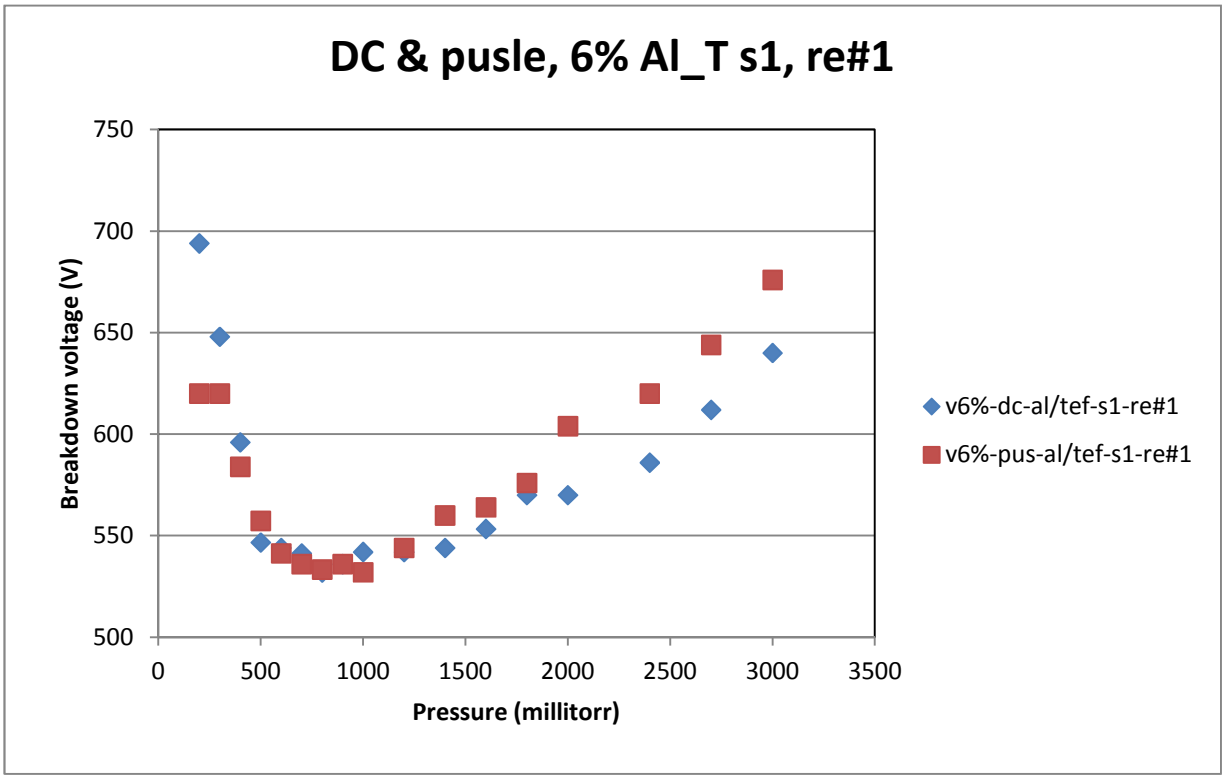

Figure A-12

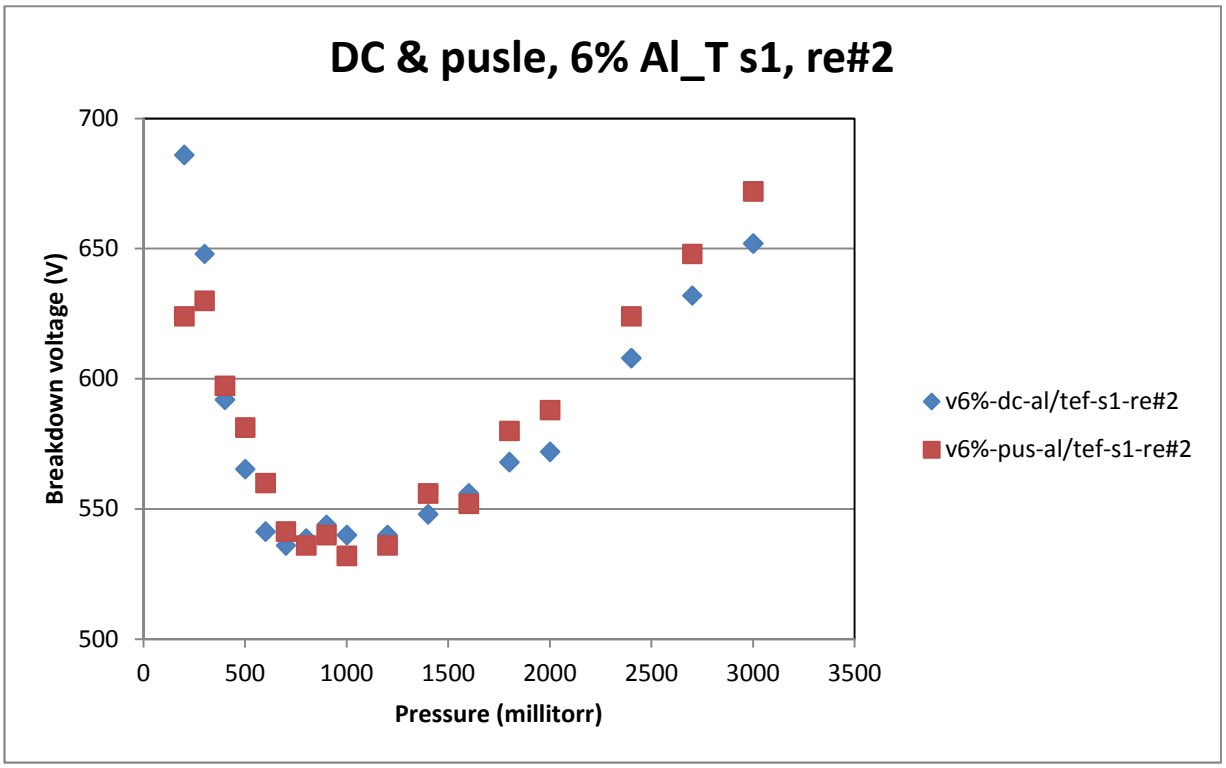

Figure A-13

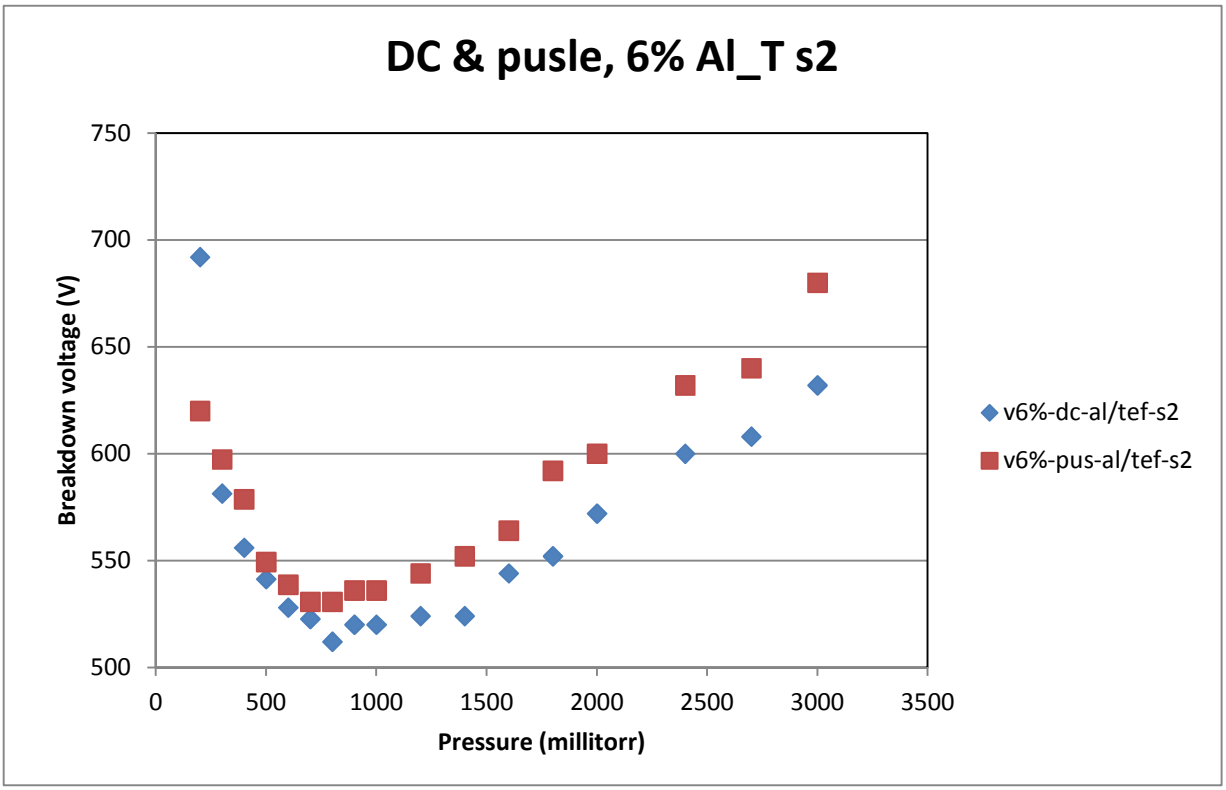

Figure A-14

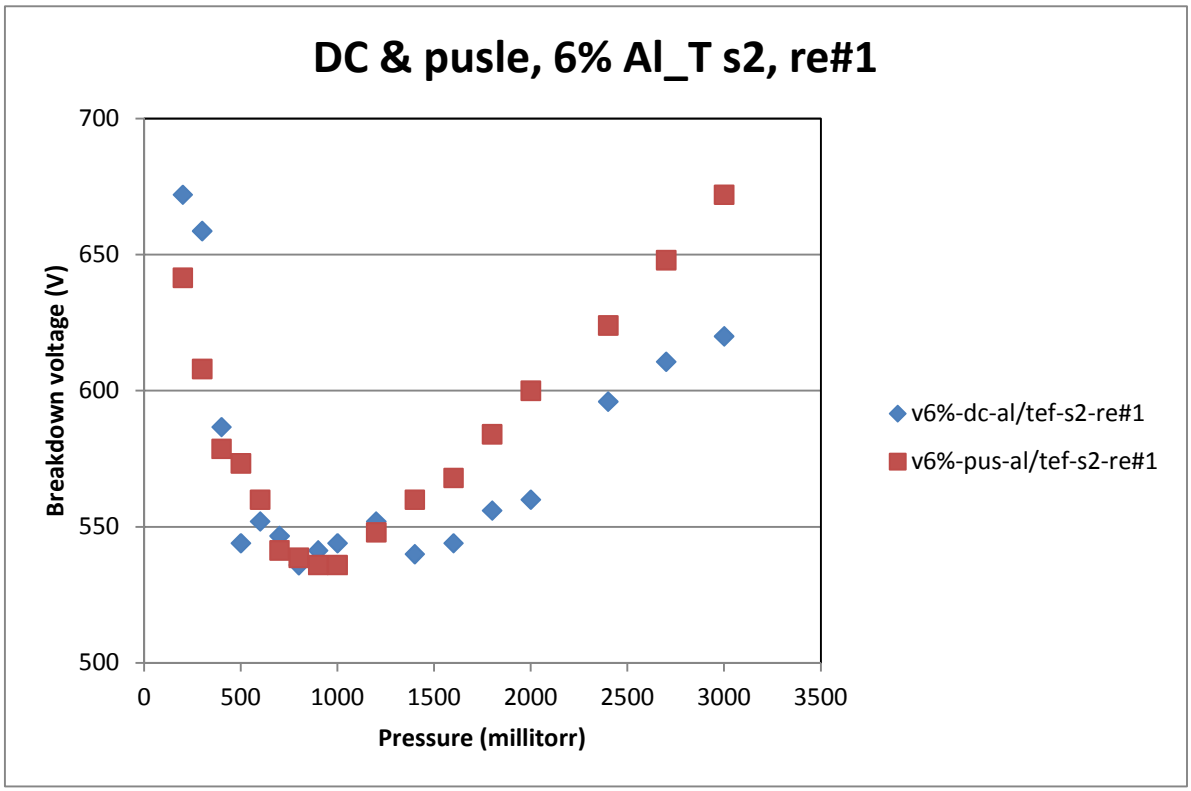

Figure A-15

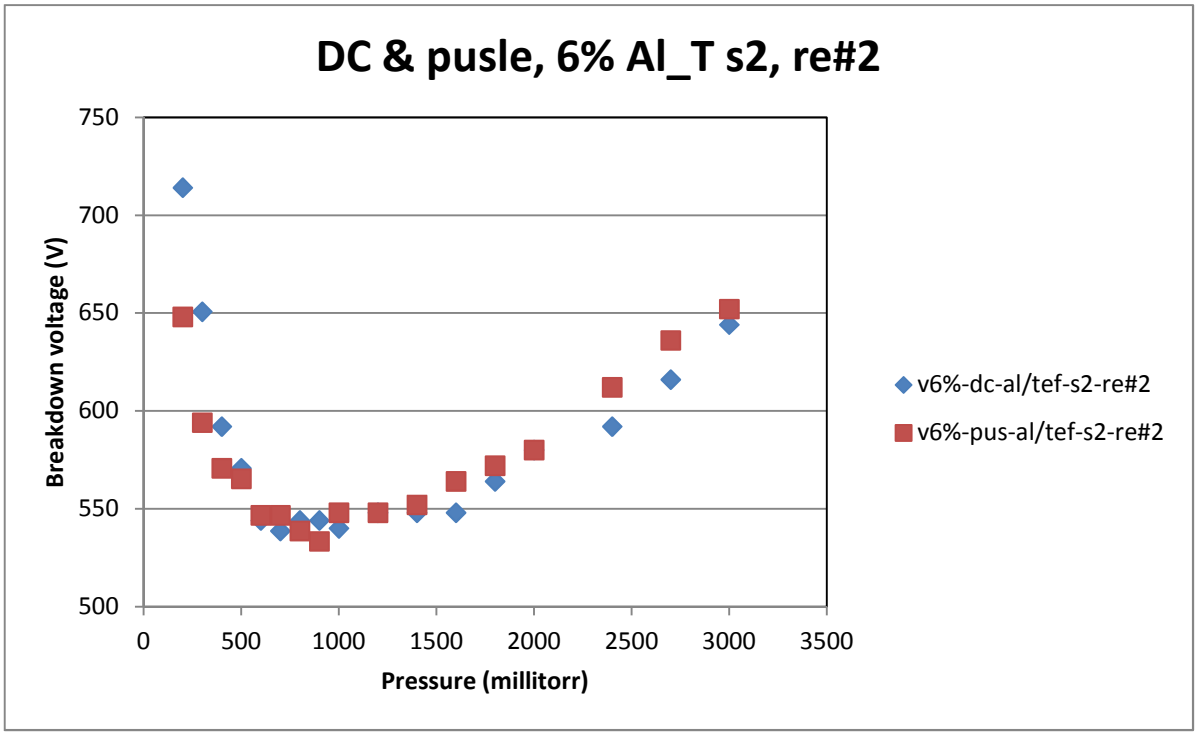

Figure A-16

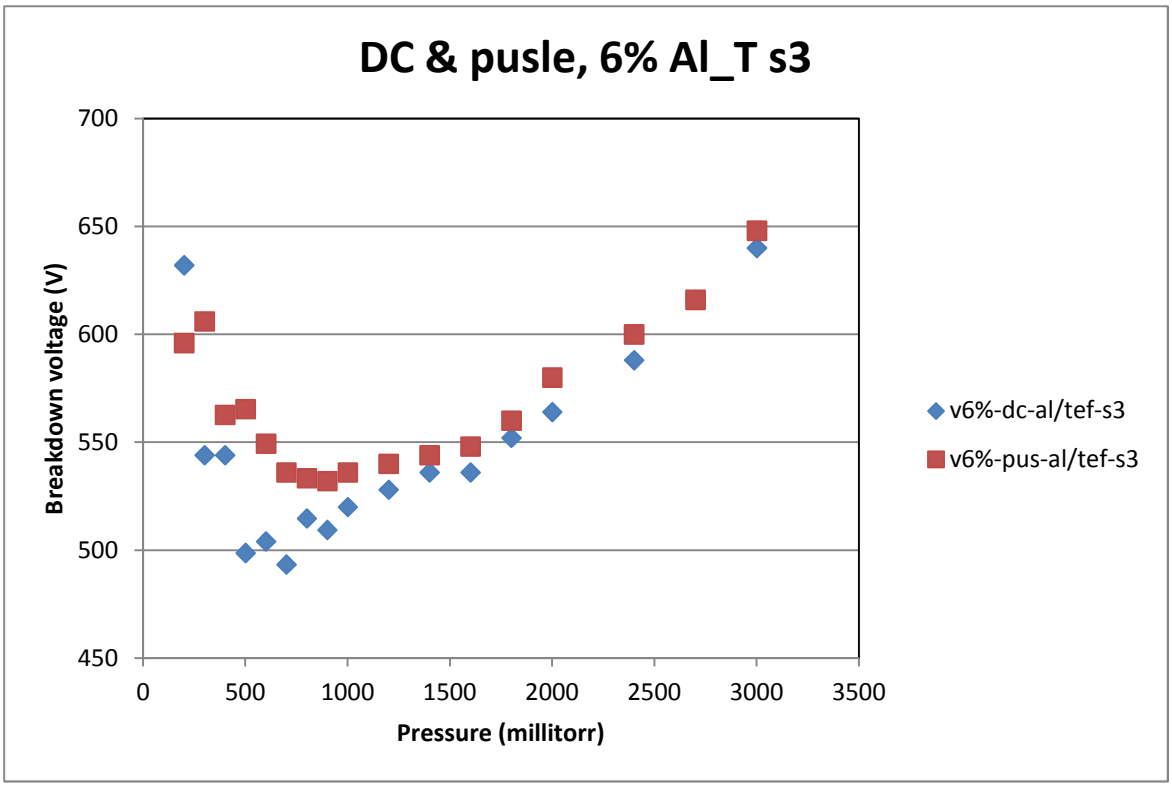

Figure A-17

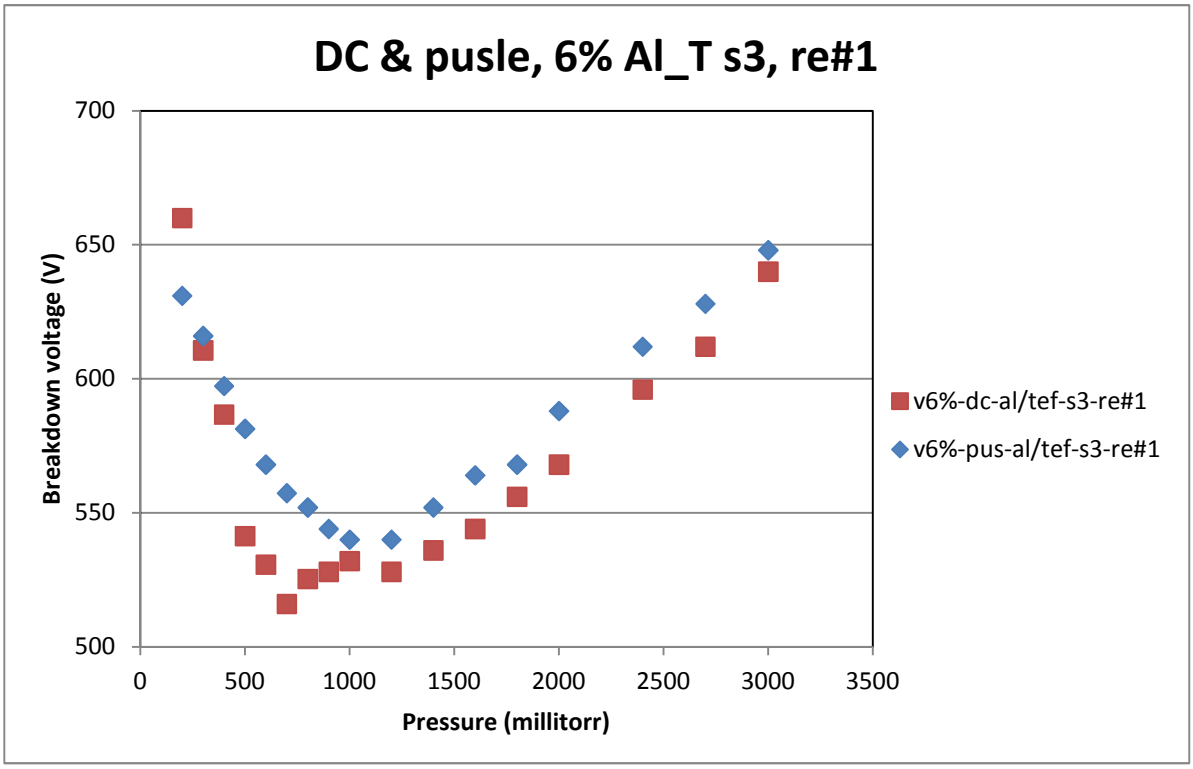

Figure A-18

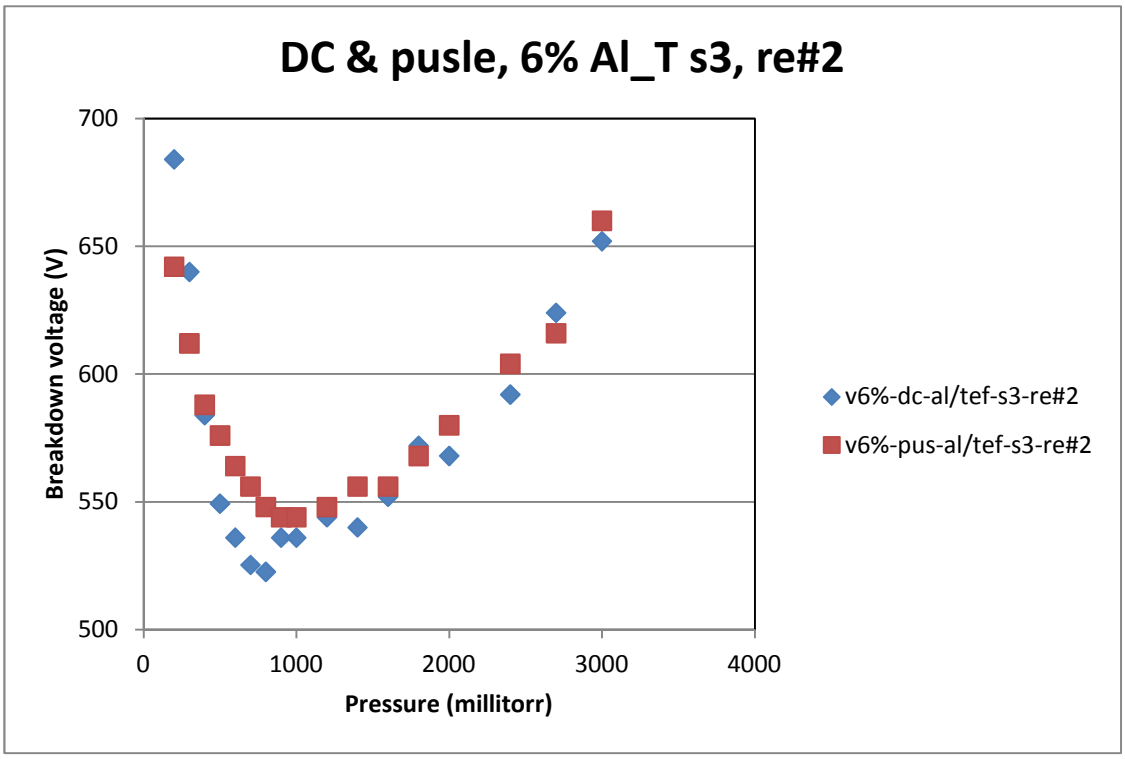

Figure A-19

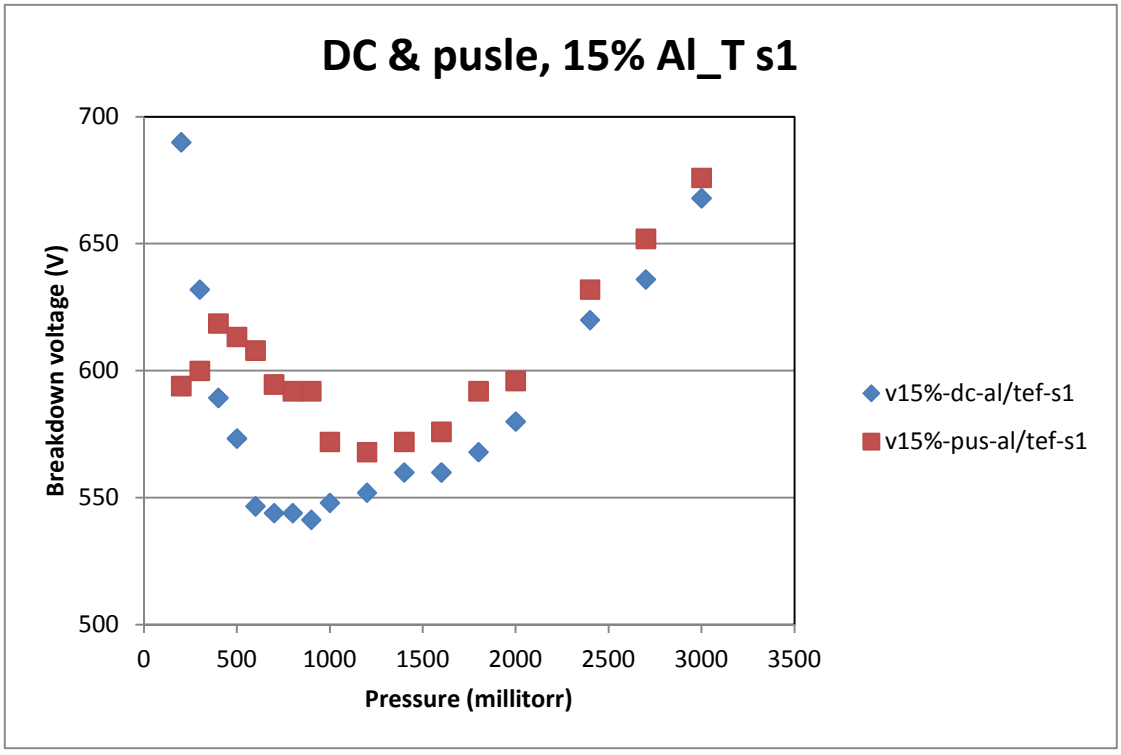

Figure A-20

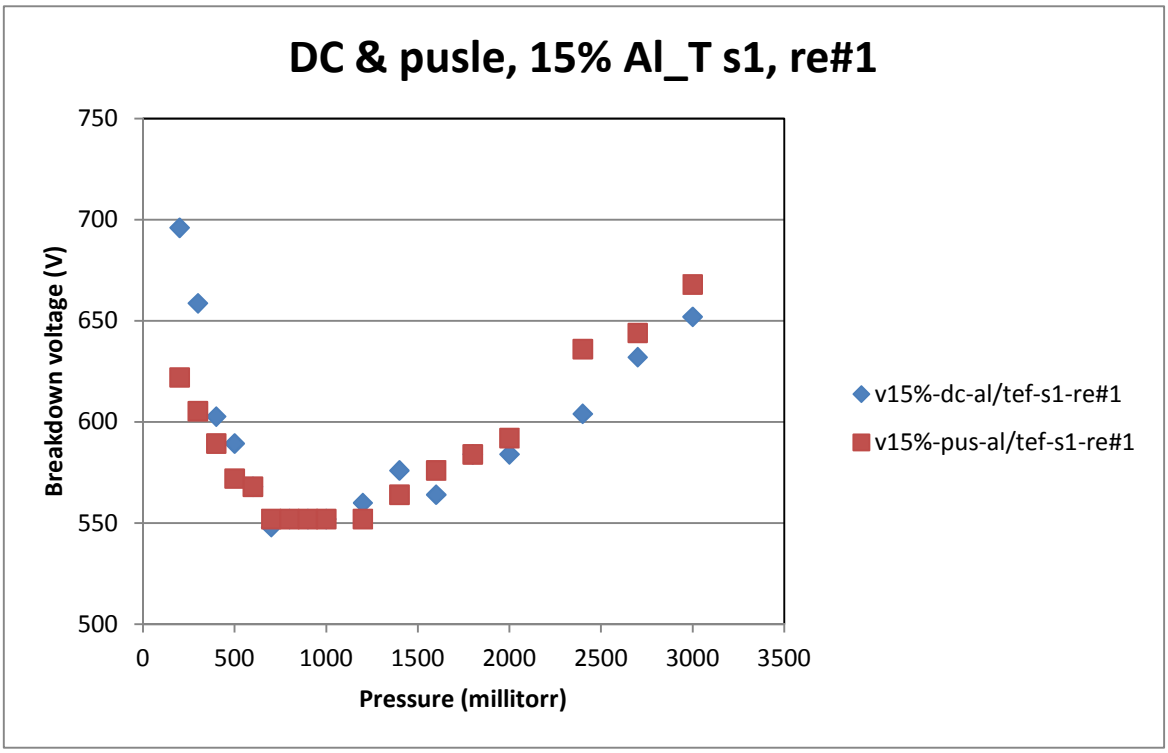

Figure A-21

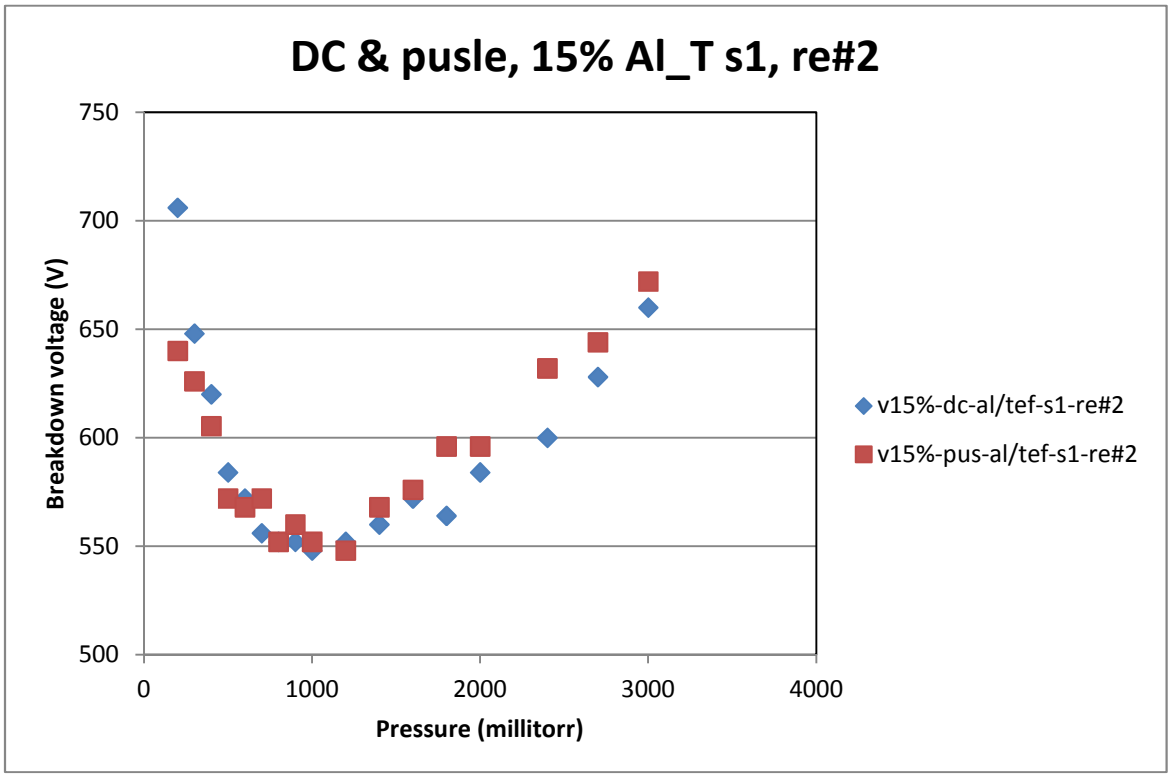

Figure A-22

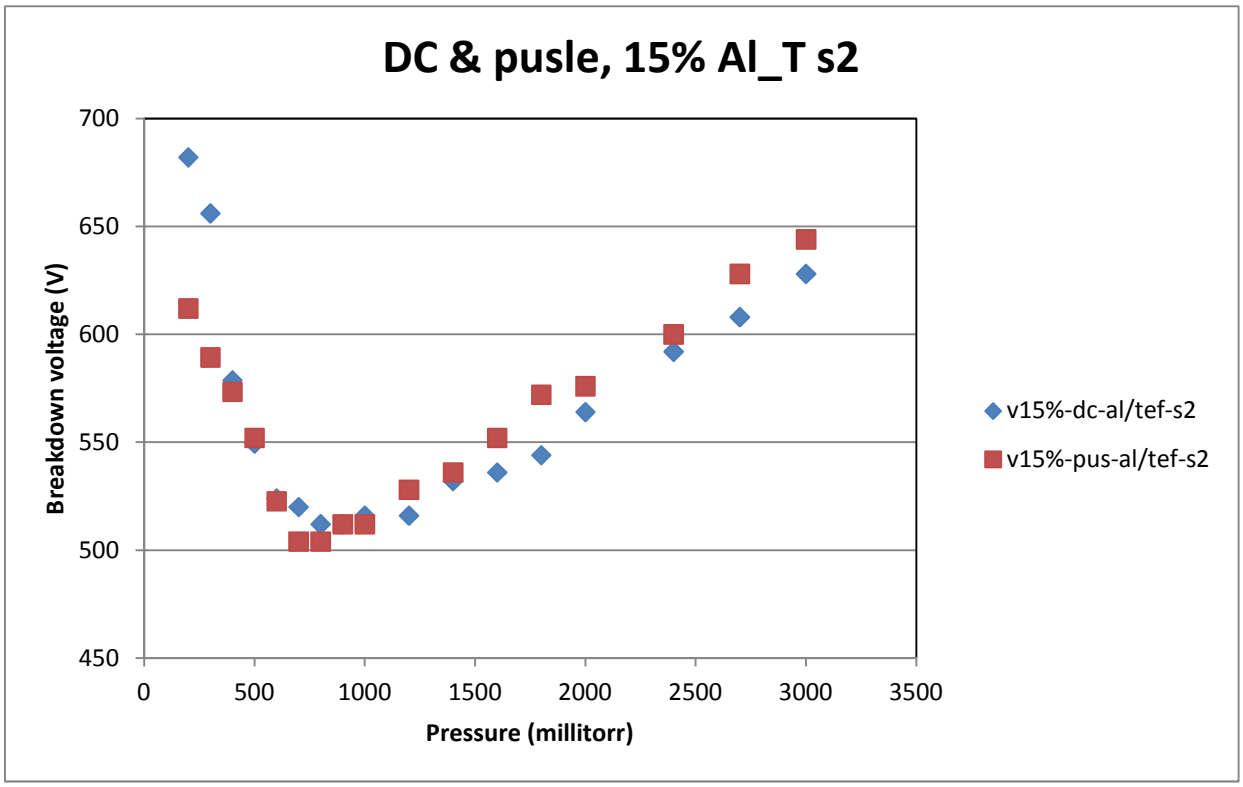

Figure A-23

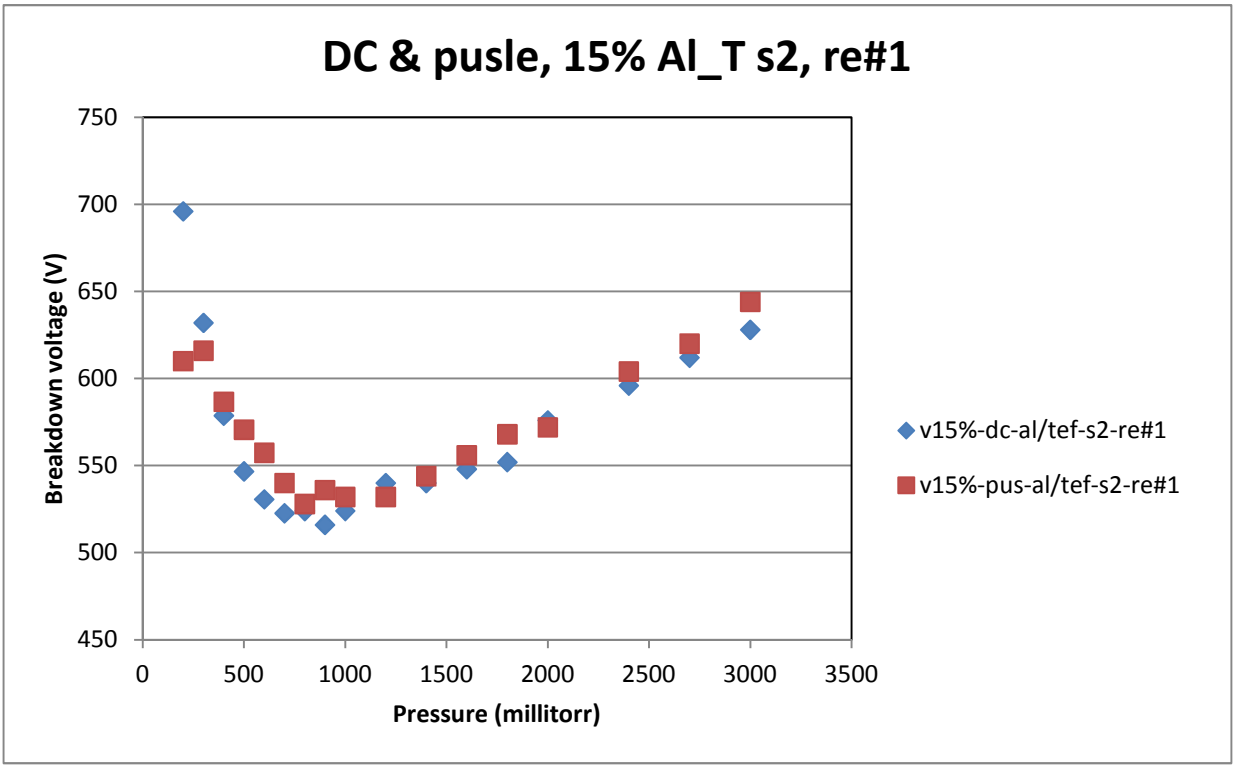

Figure A-24

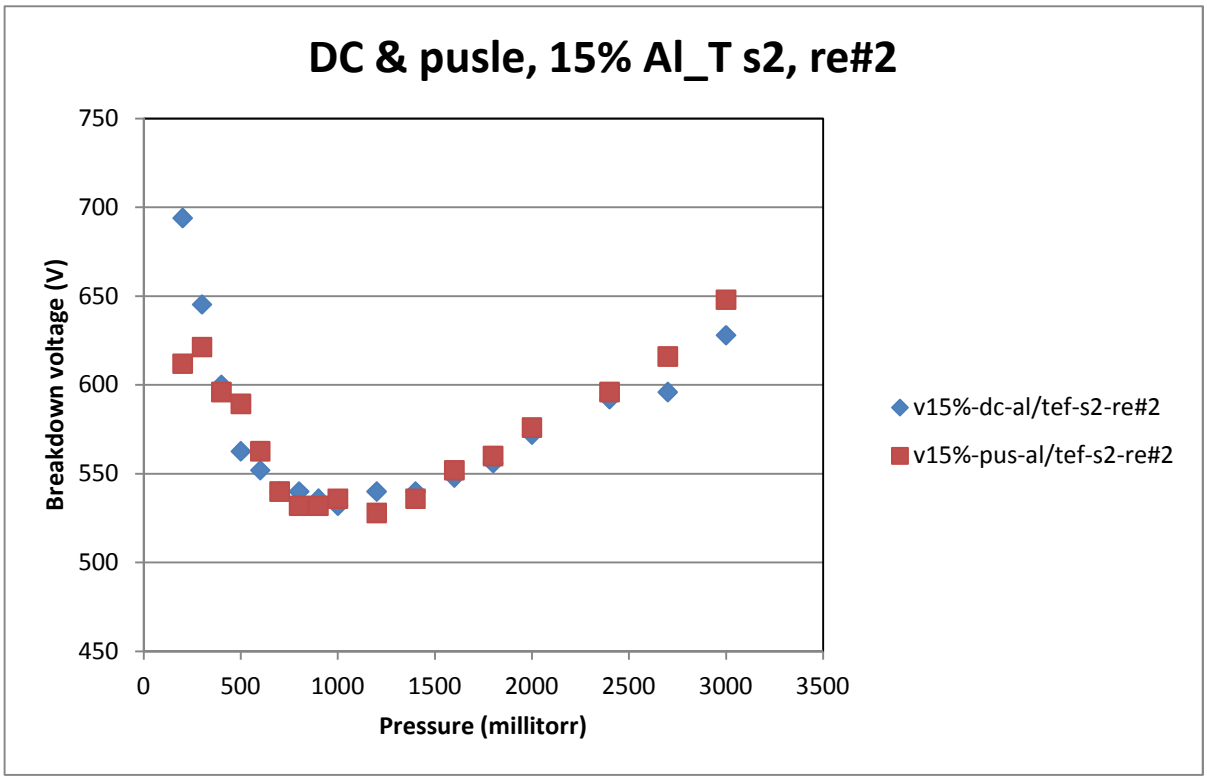

Figure A-25

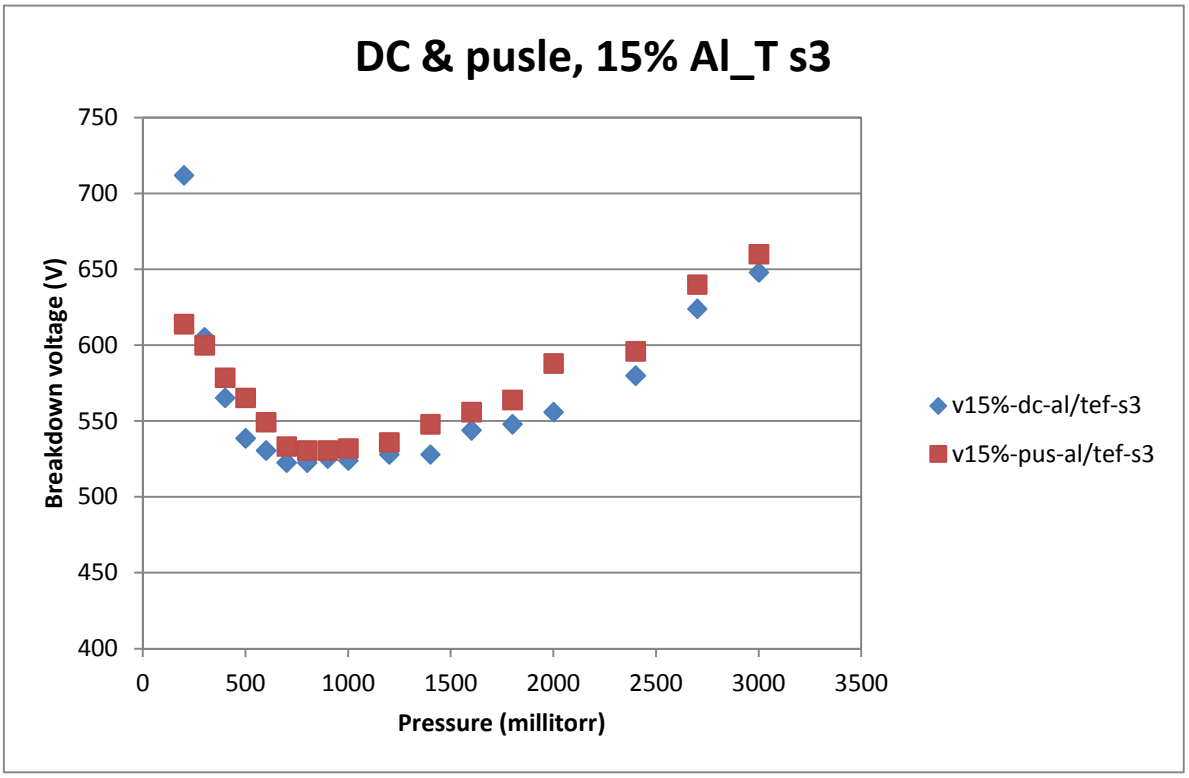

Figure A-26

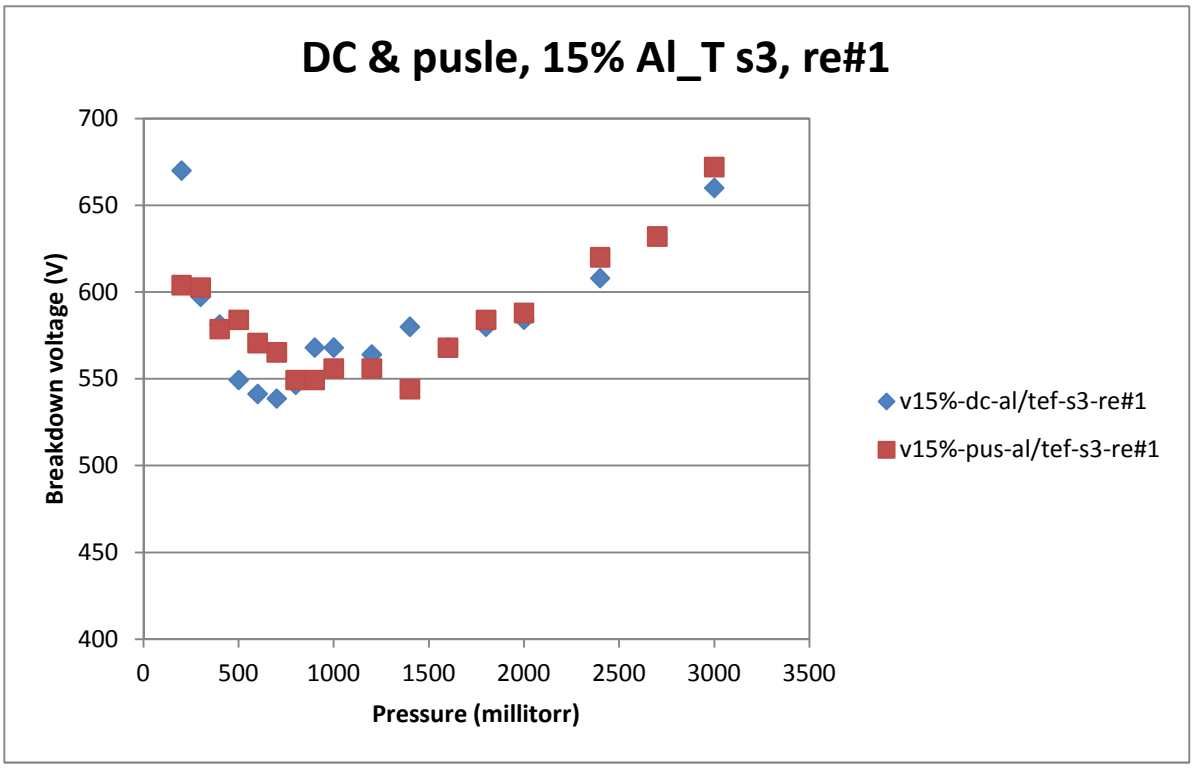

Figure A-27

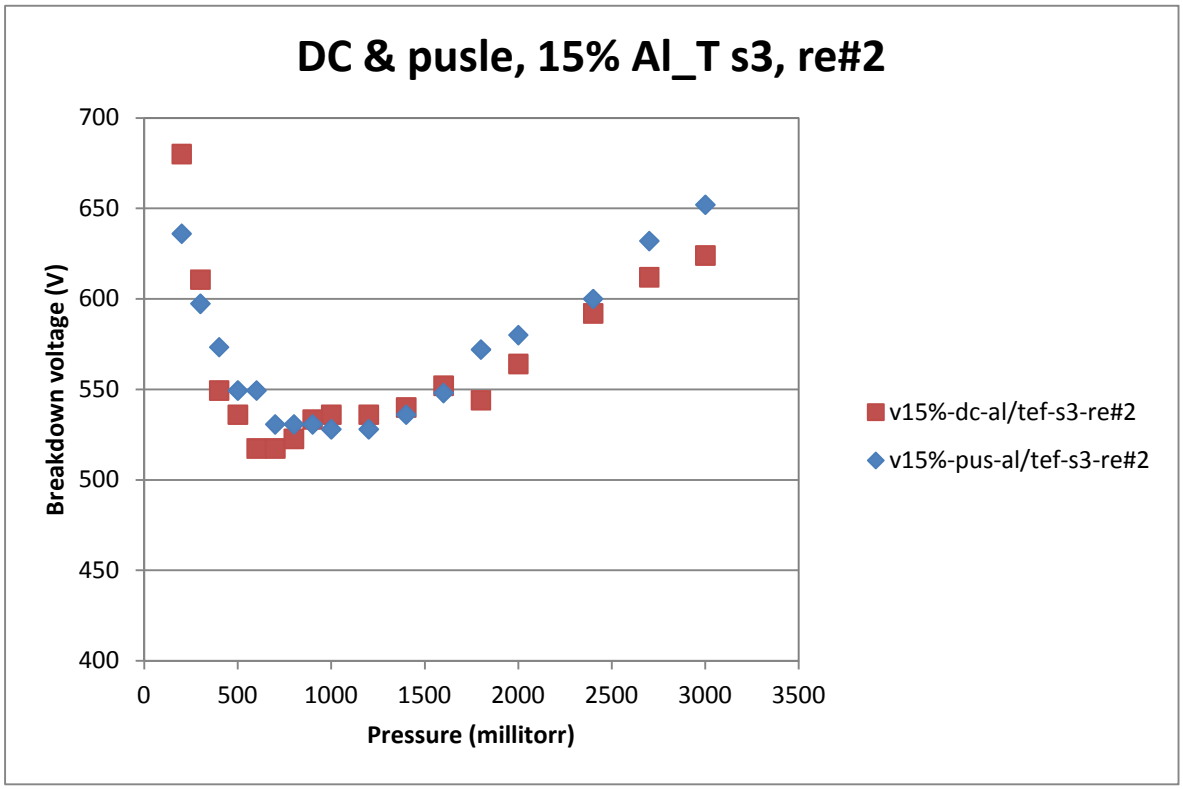

Figure A-28

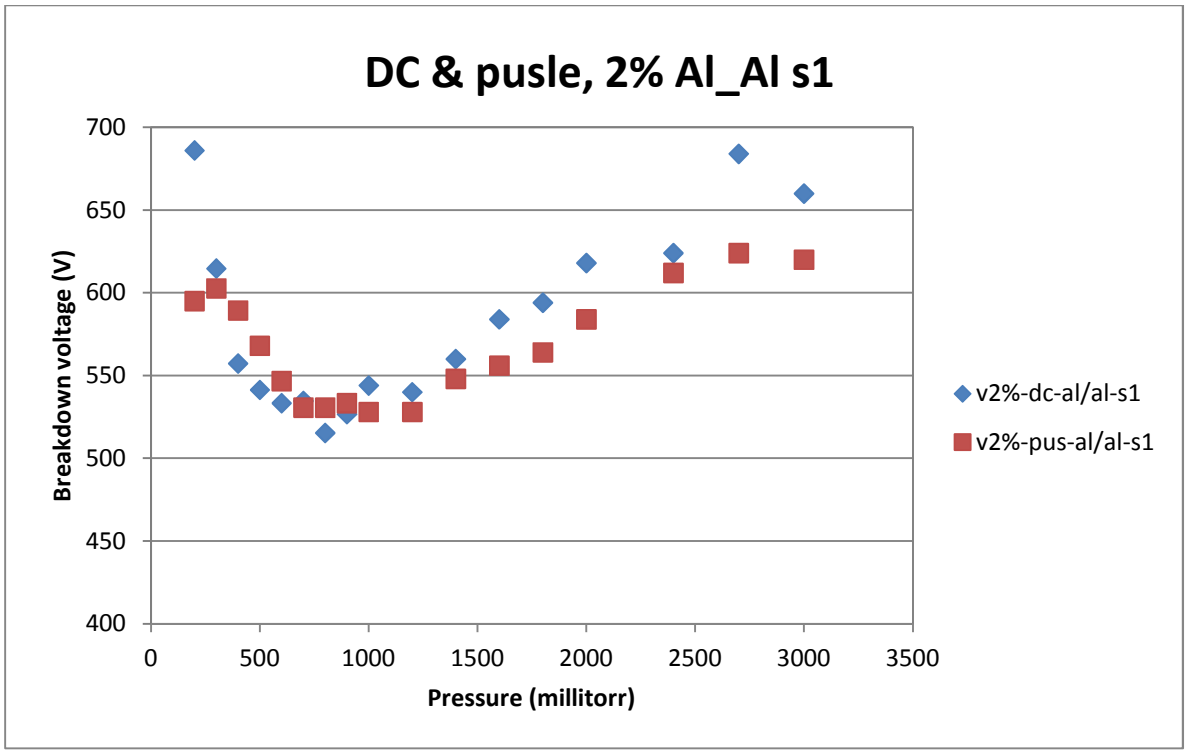

Figure A-29

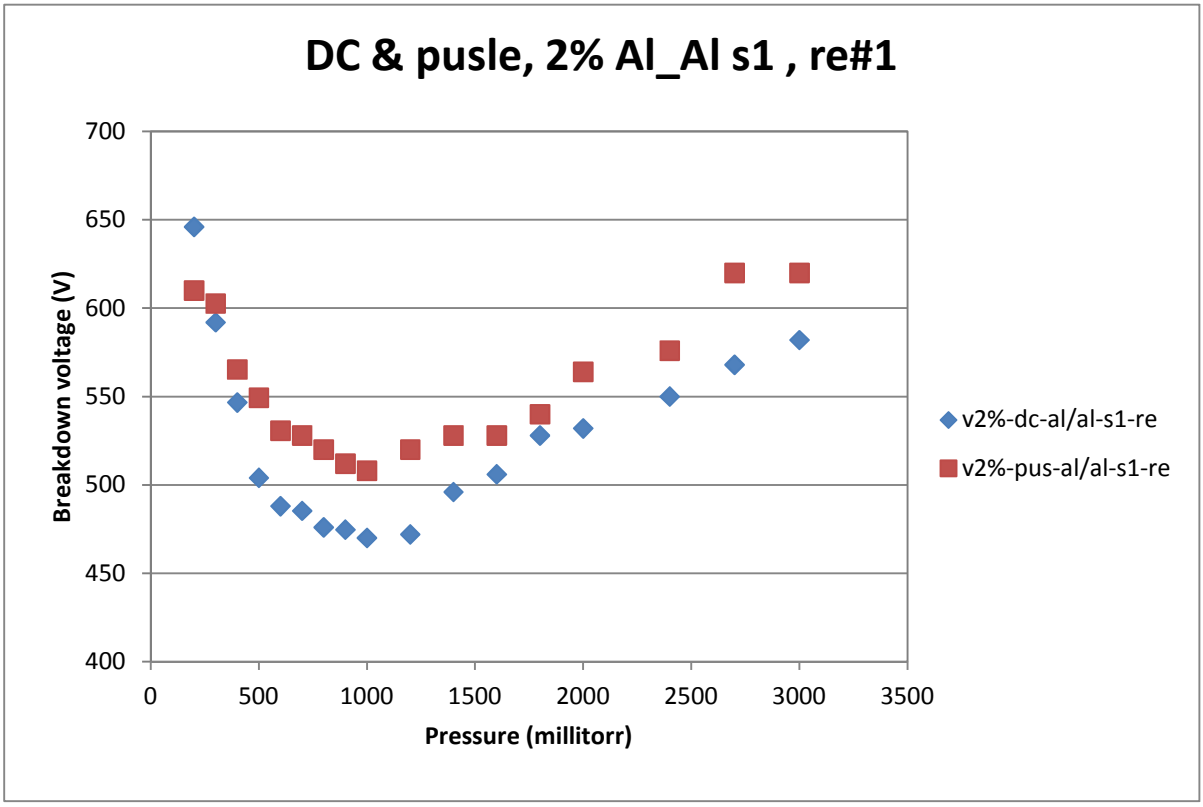

Figure A-30

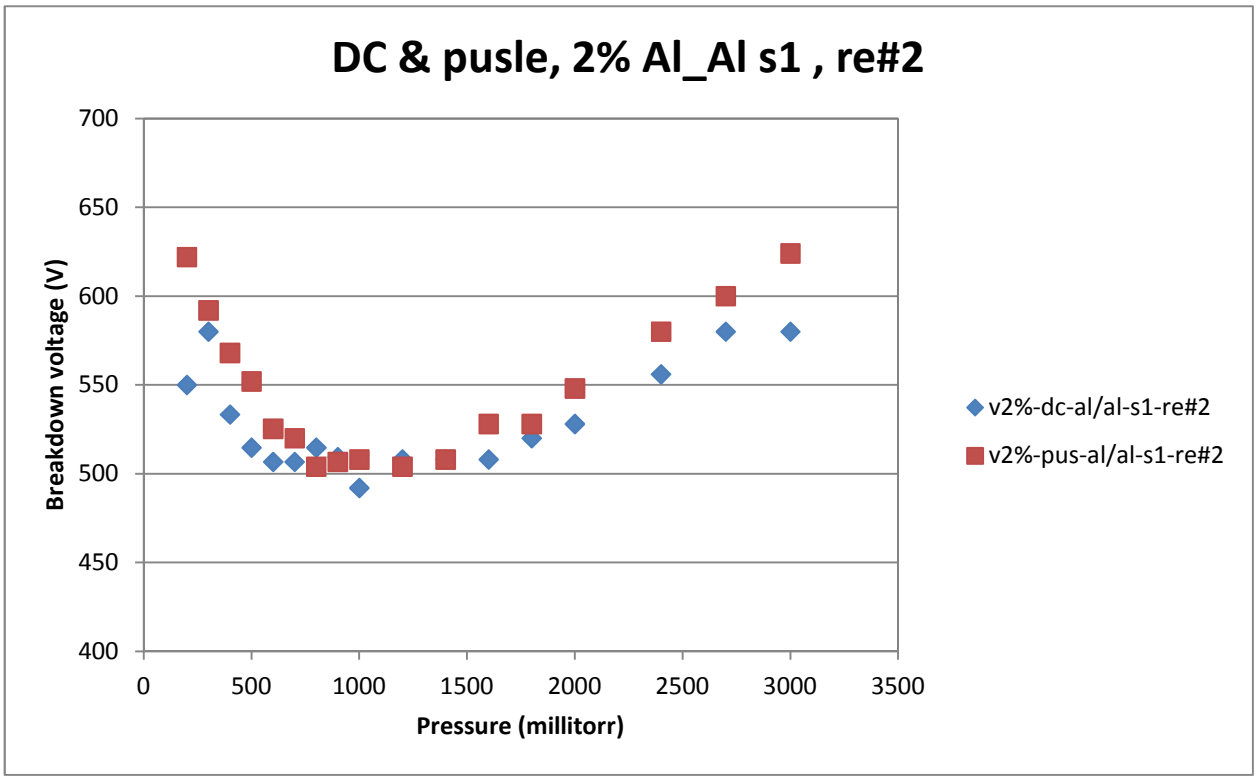

Figure A-31

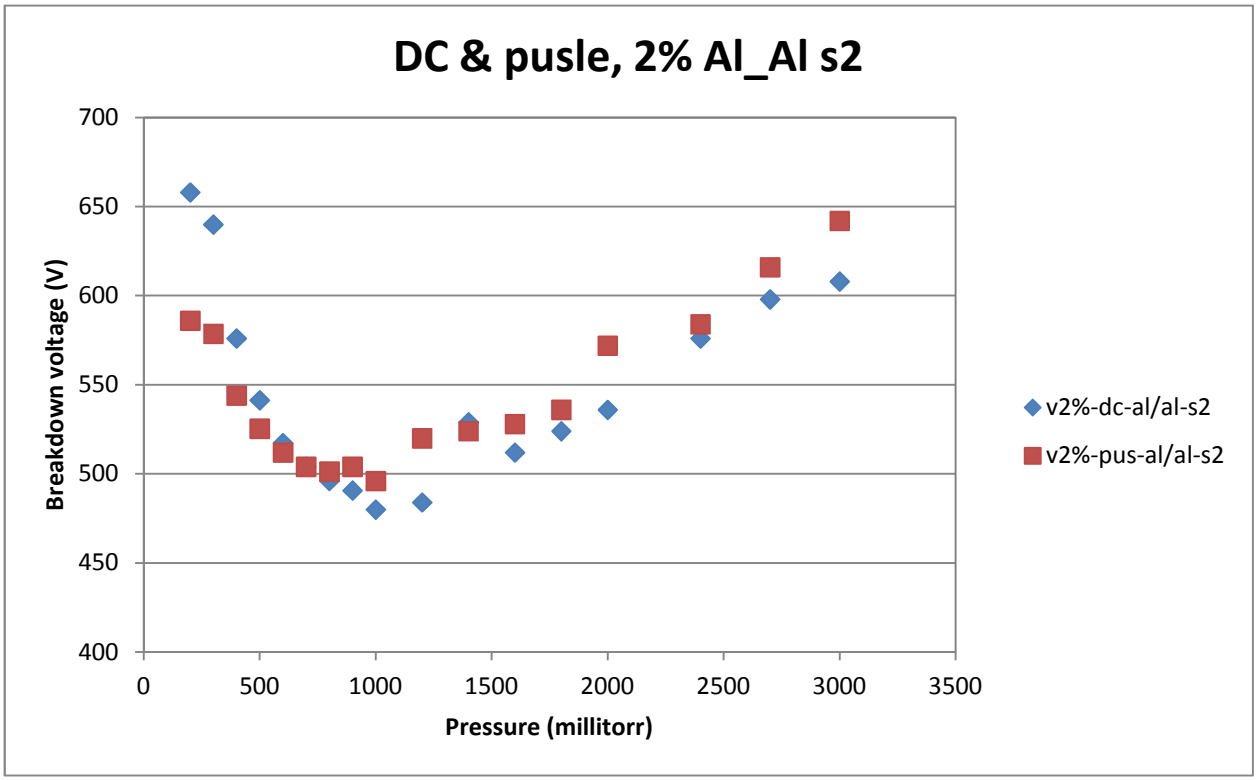

Figure A-32

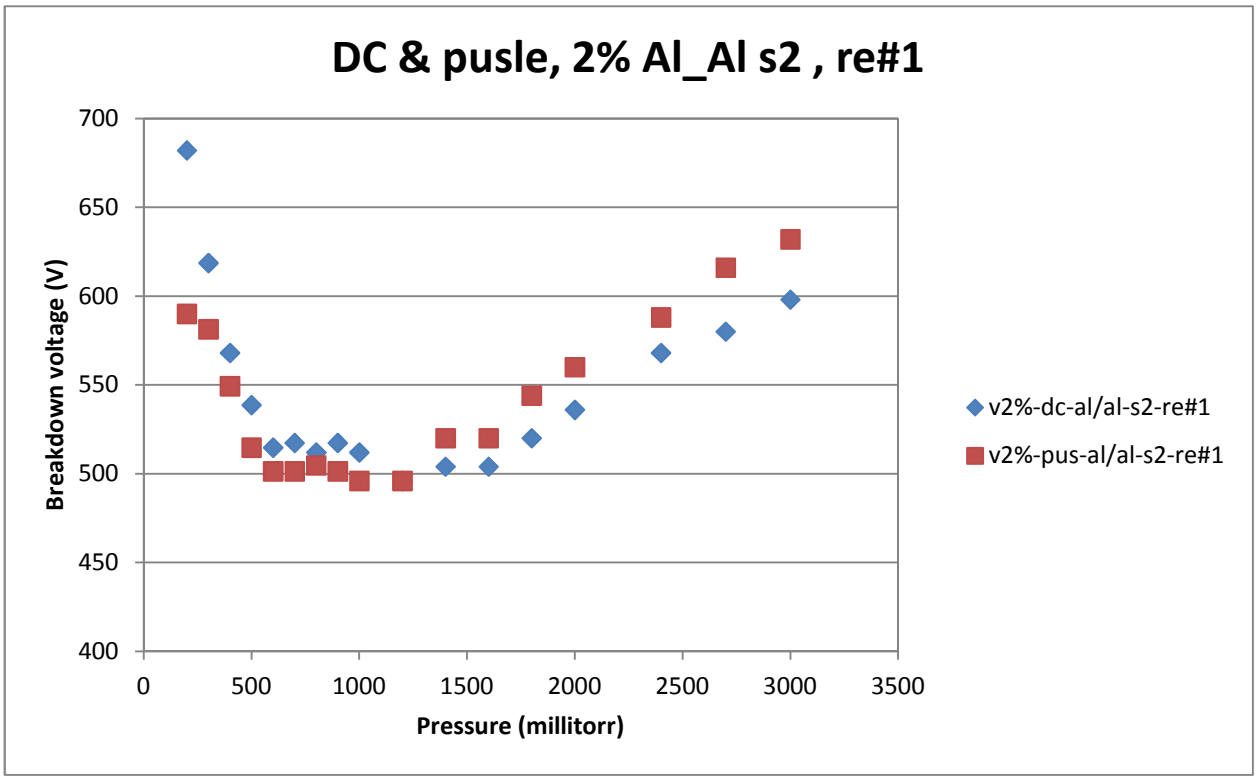

Figure A-33

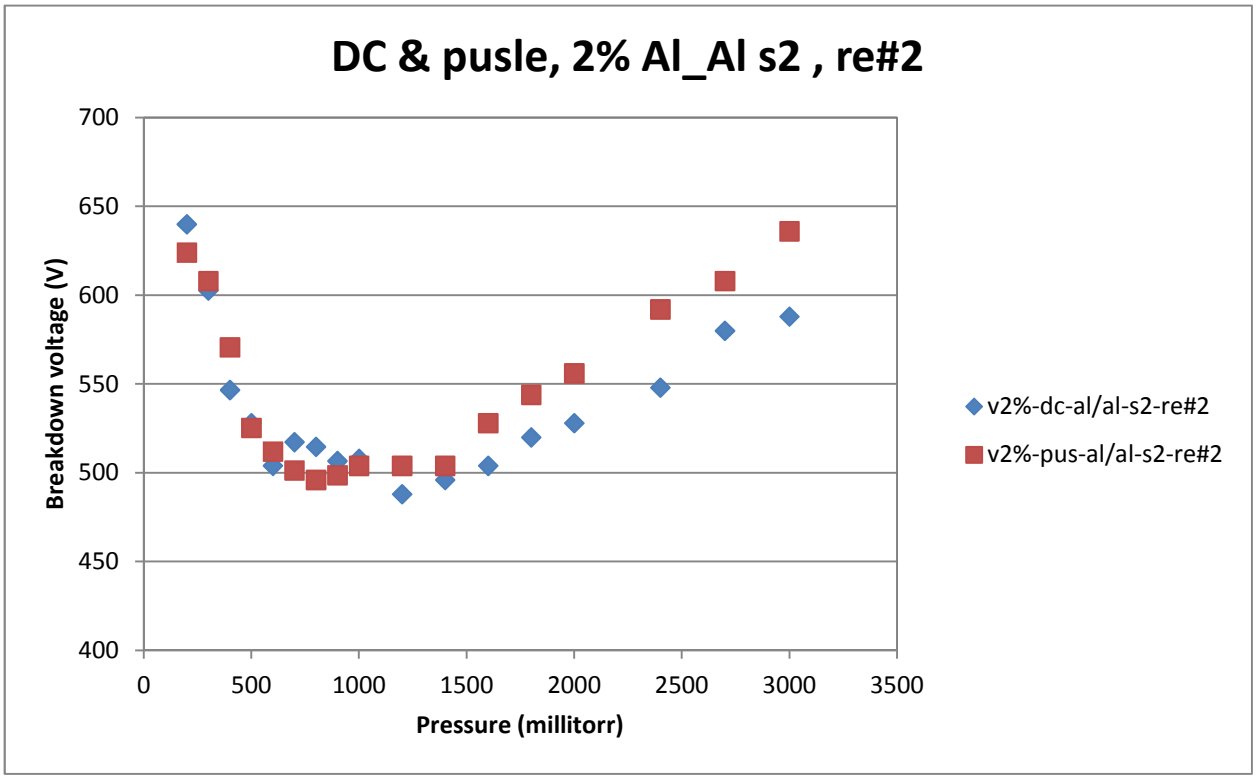

Figure A-34

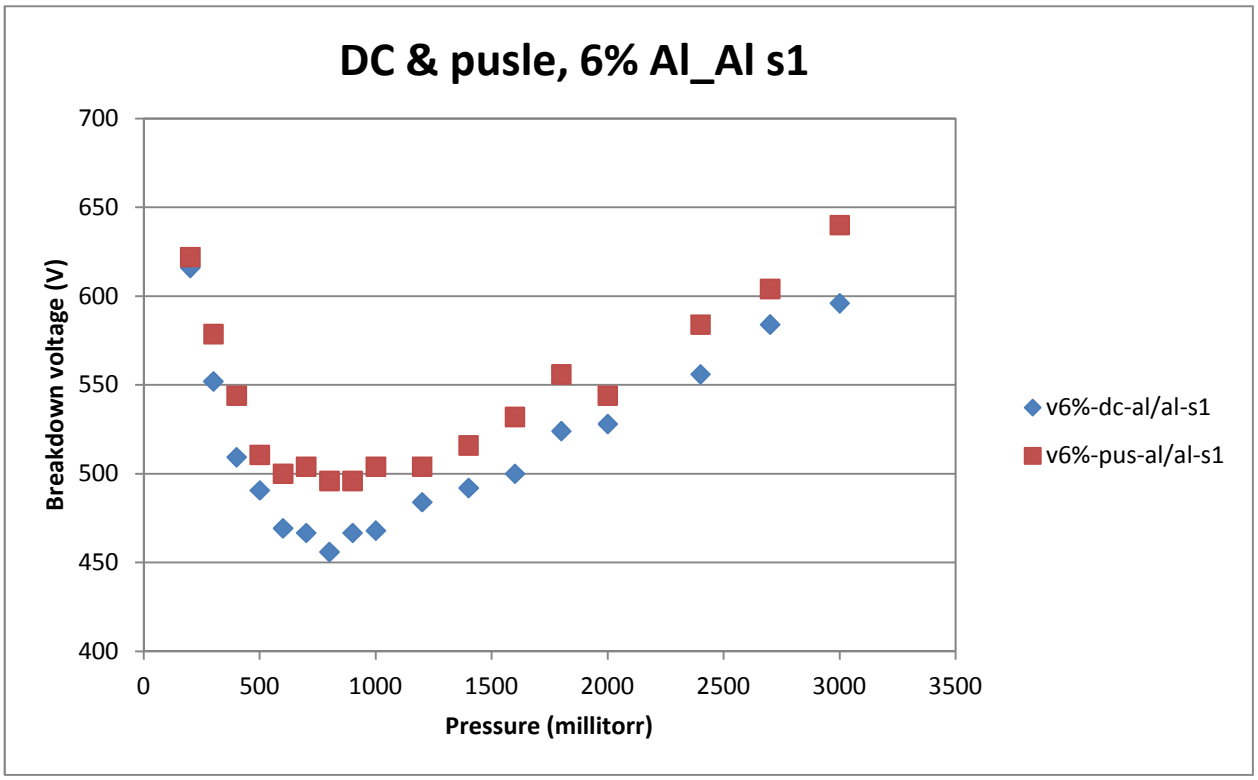

Figure A-35

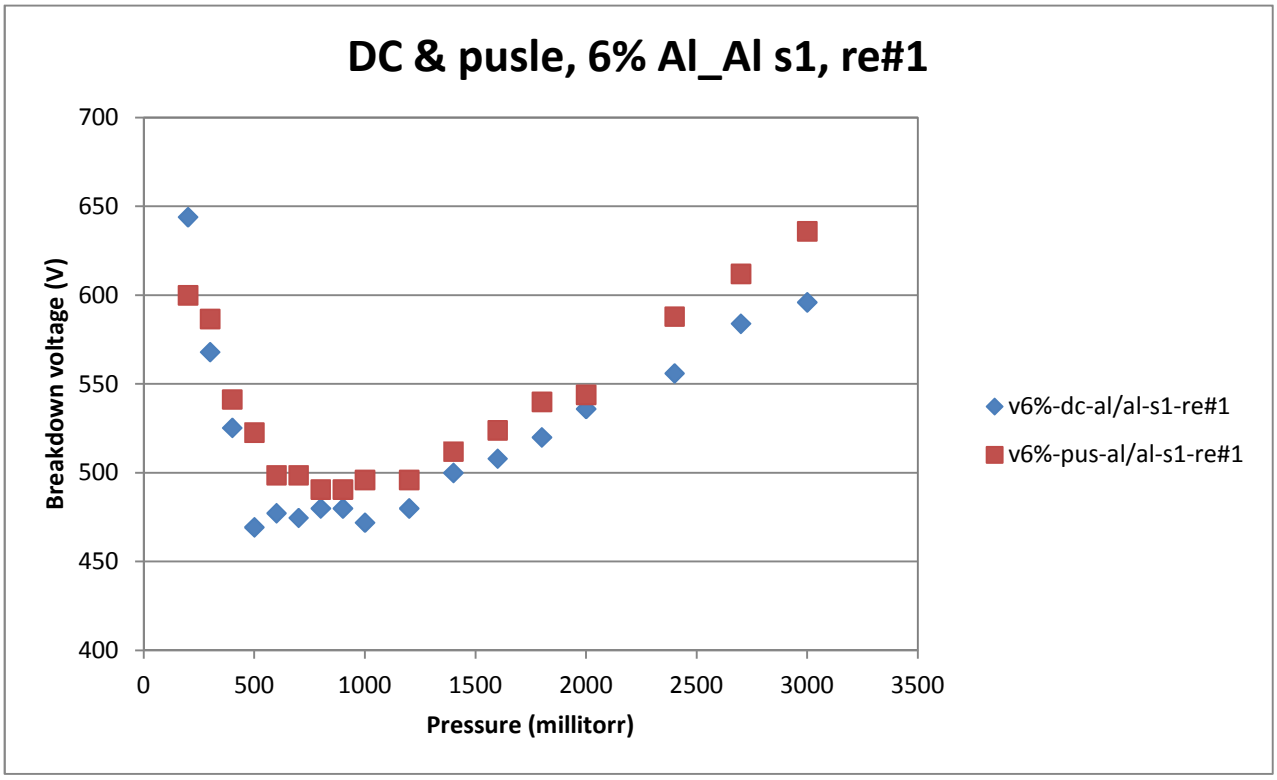

Figure A-36

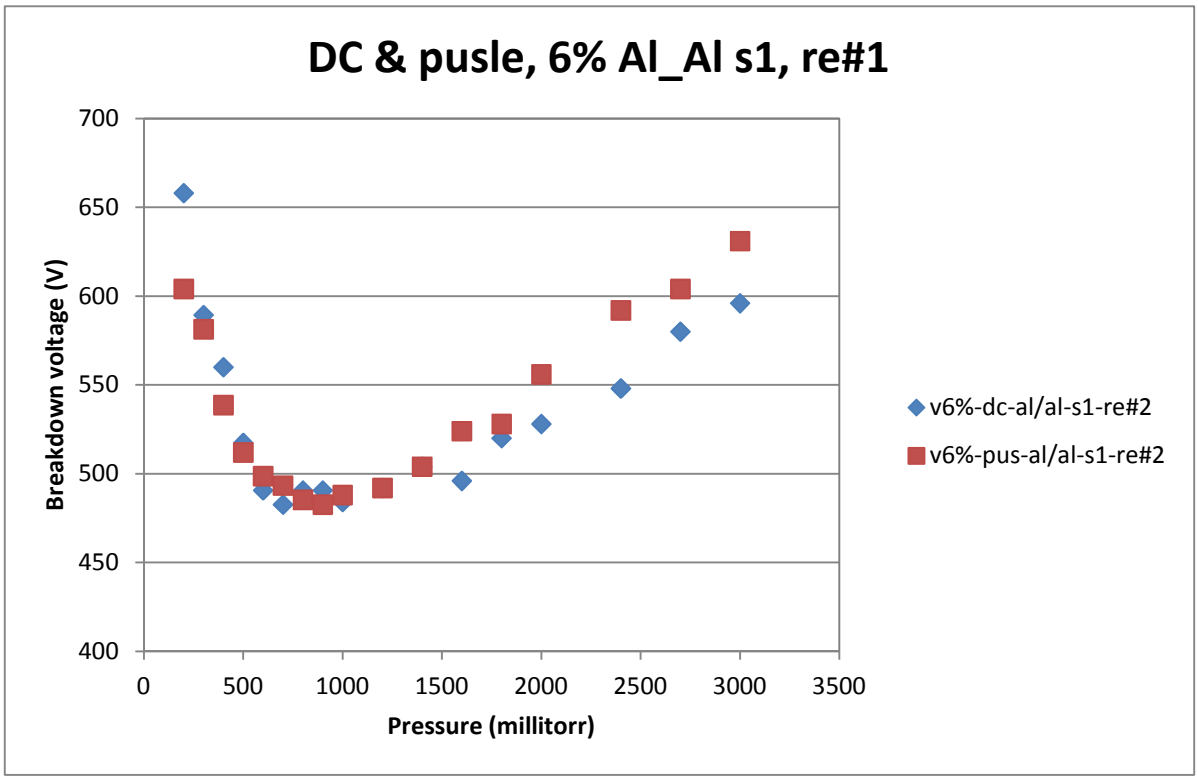

Figure A-37

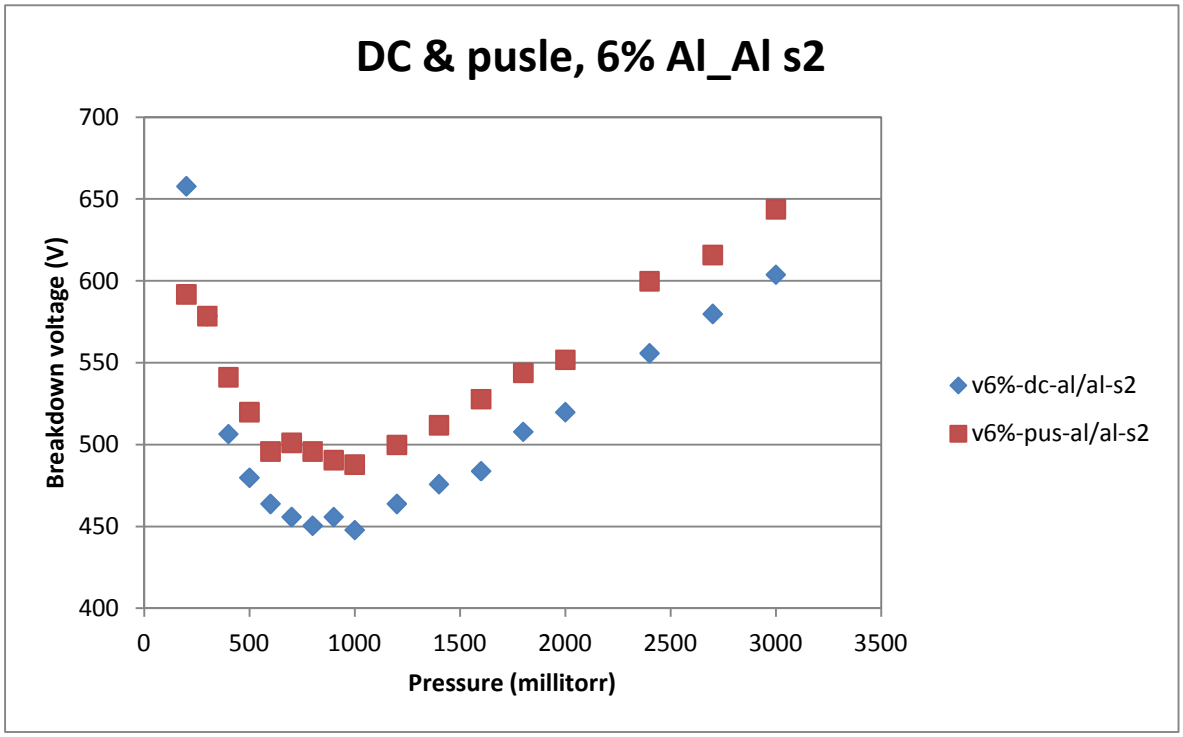

Figure A-38

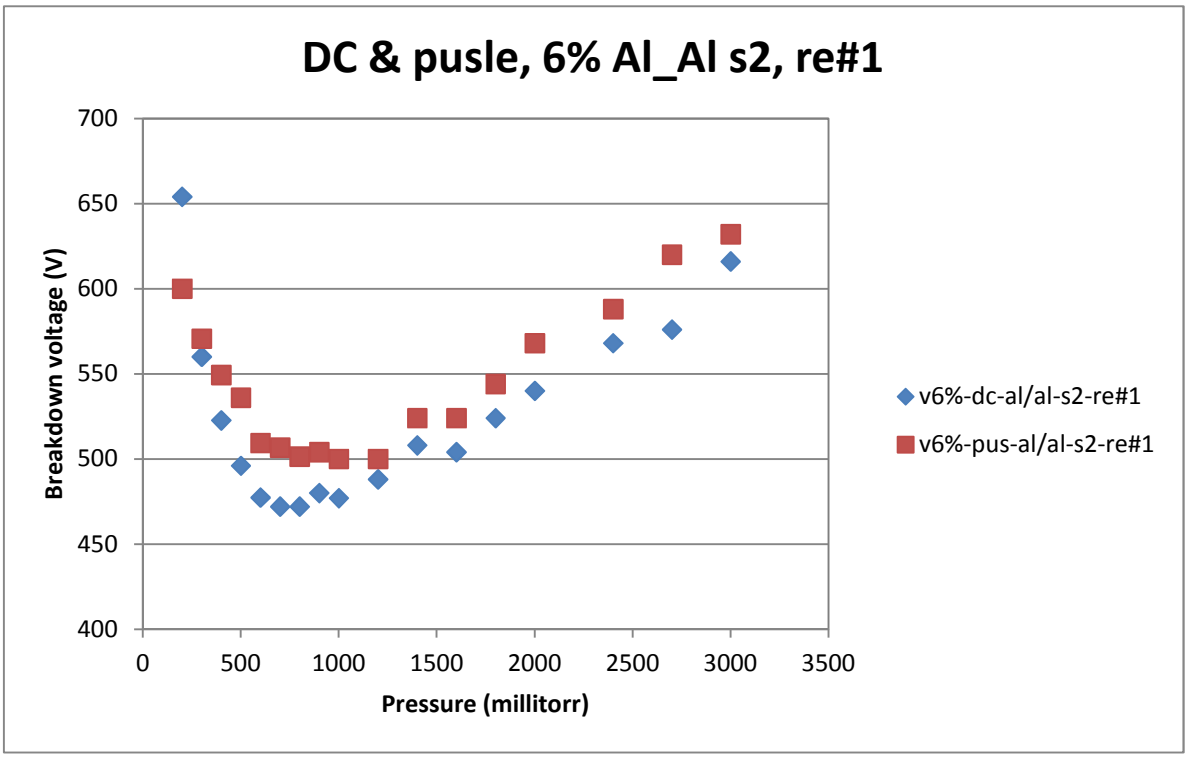

Figure A-39

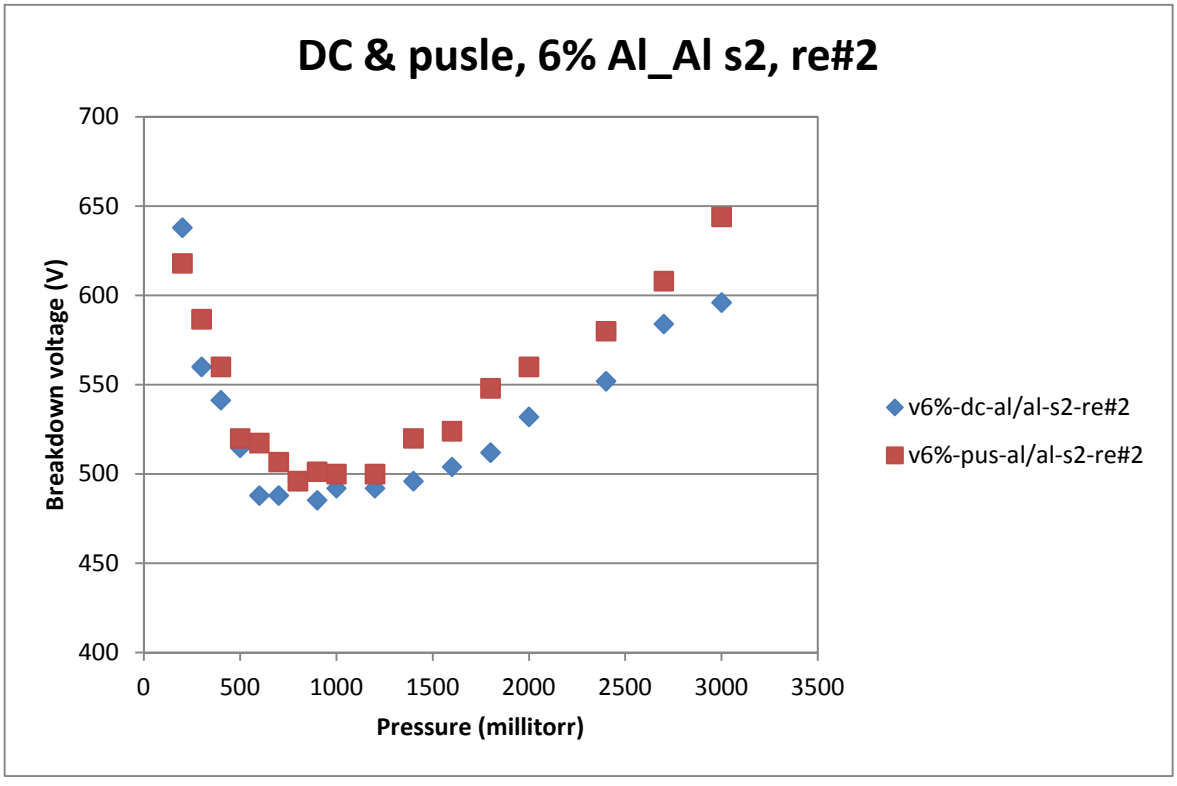

Figure A-40

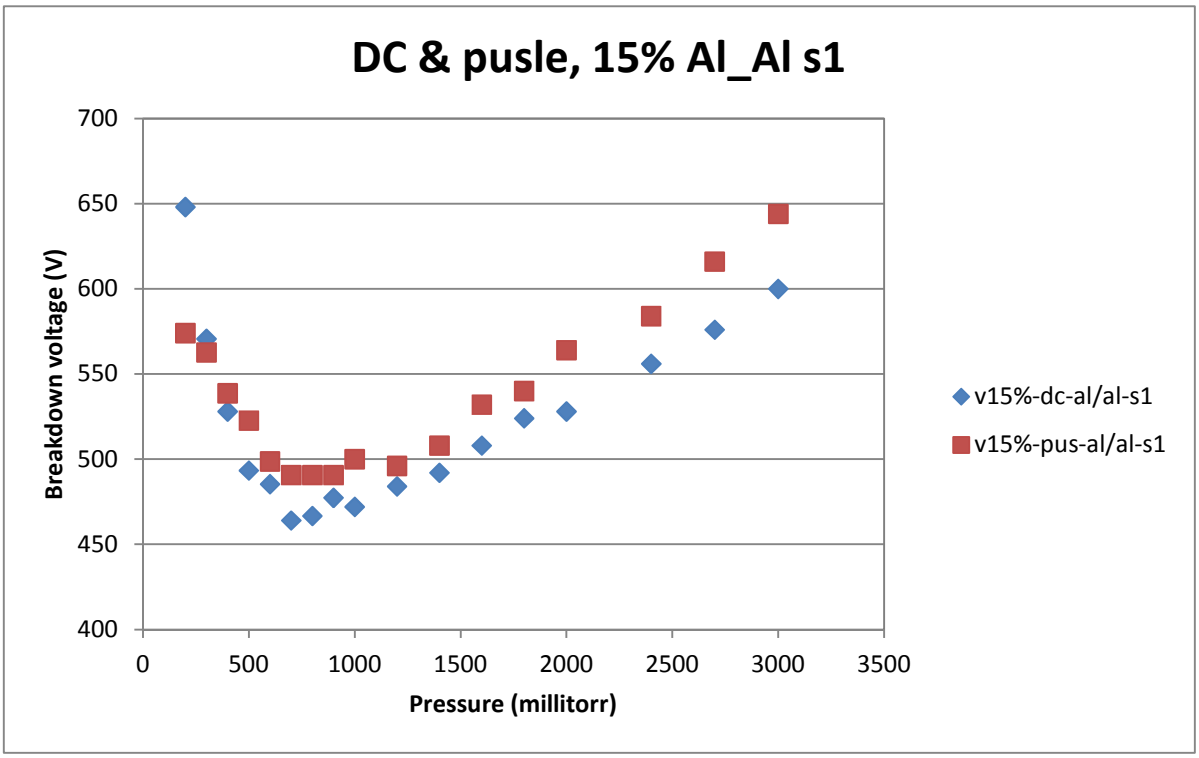

Figure A-41

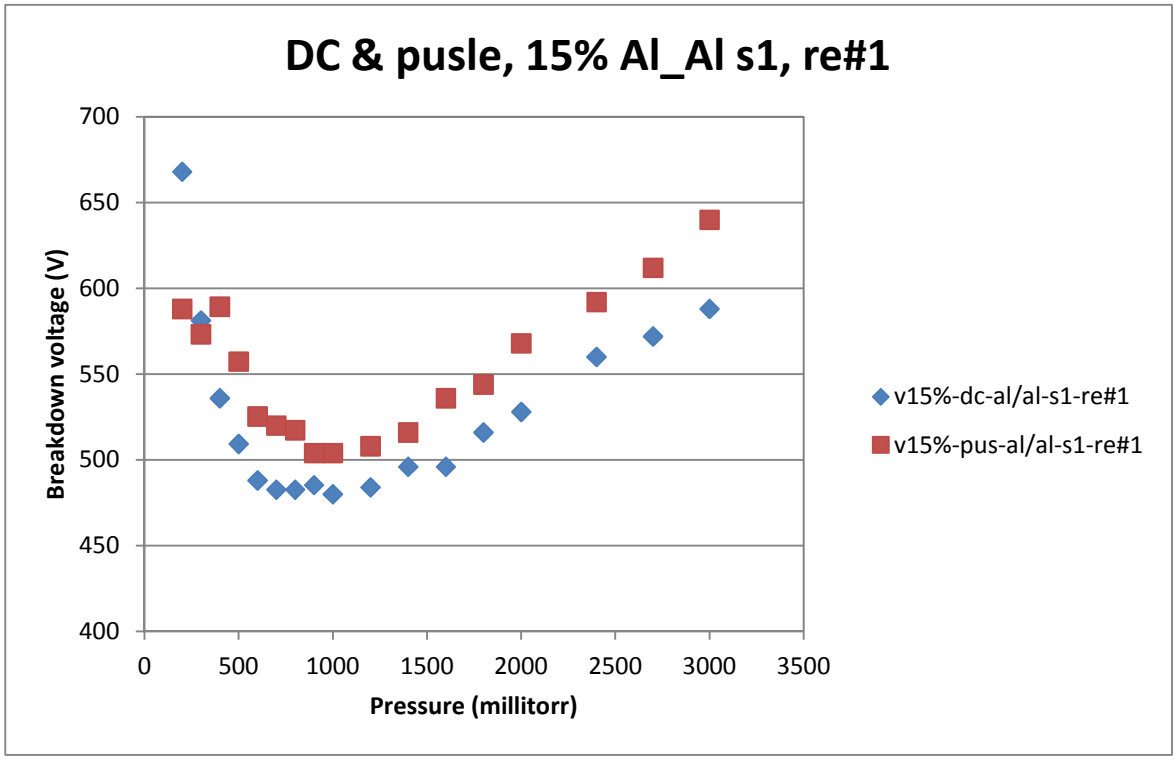

Figure A-42

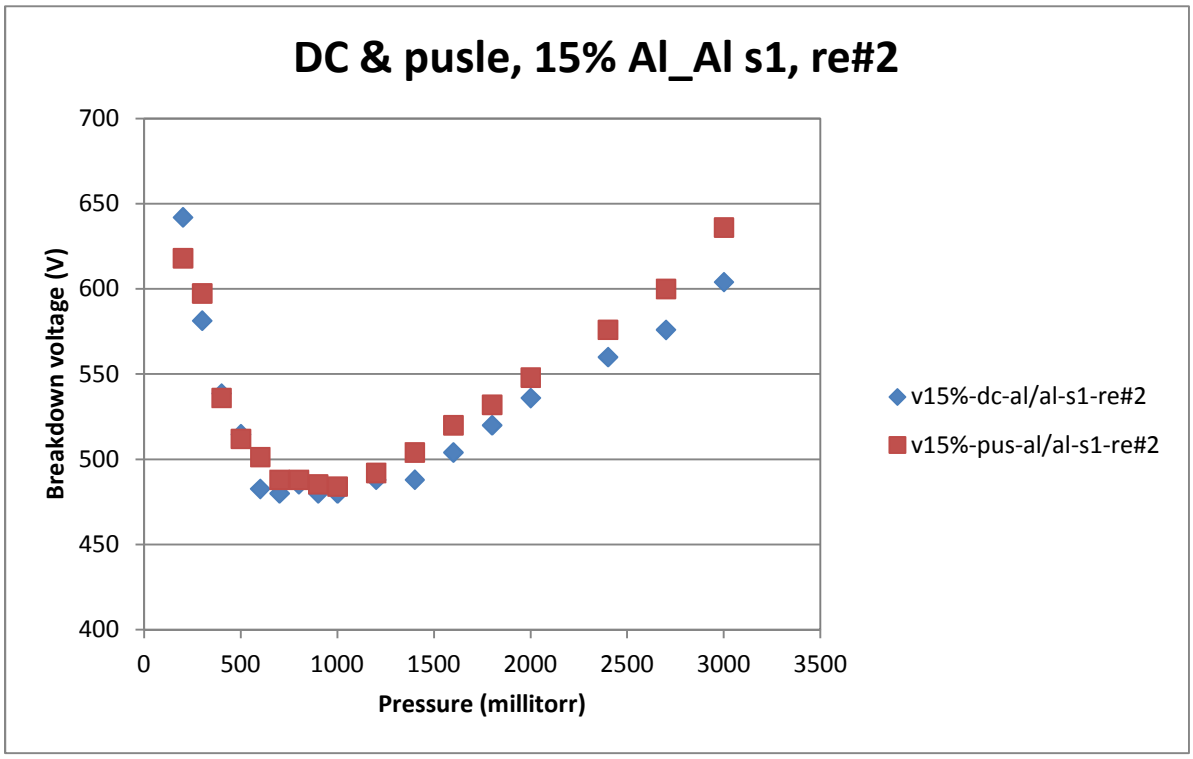

Figure A-43

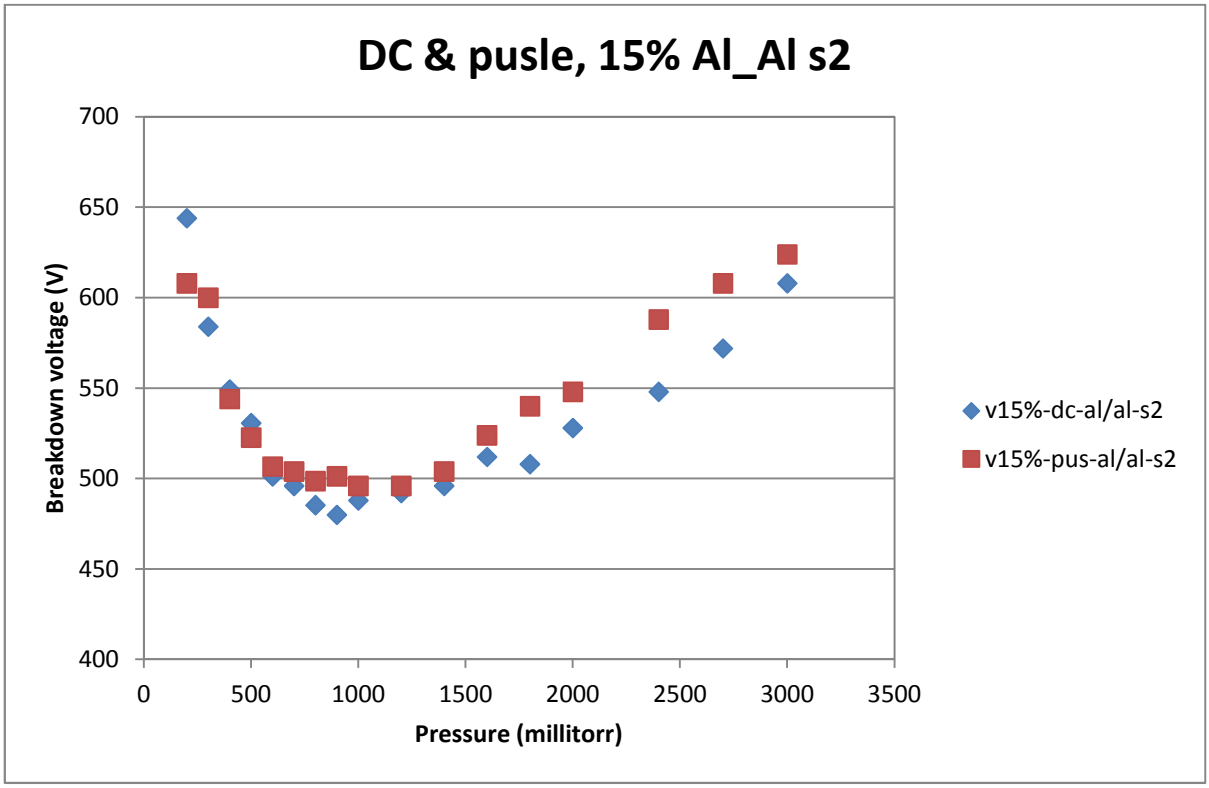

Figure A- 44

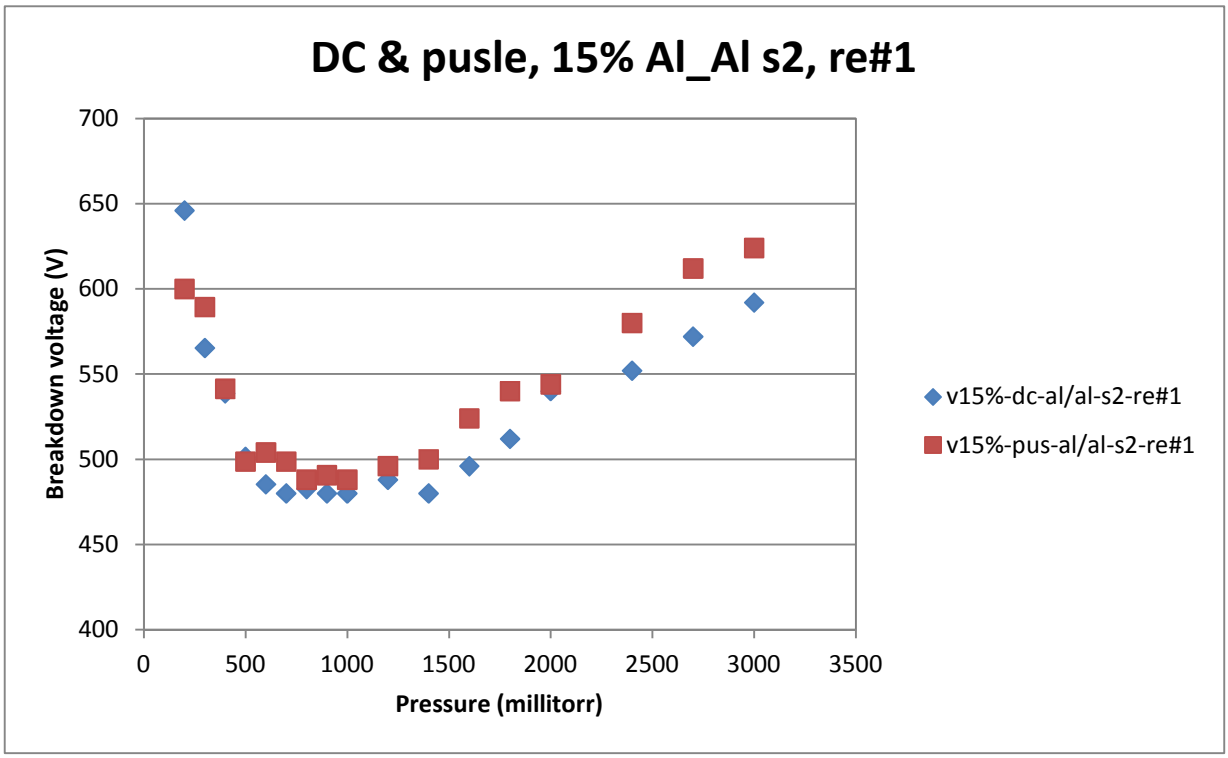

Figure A-45

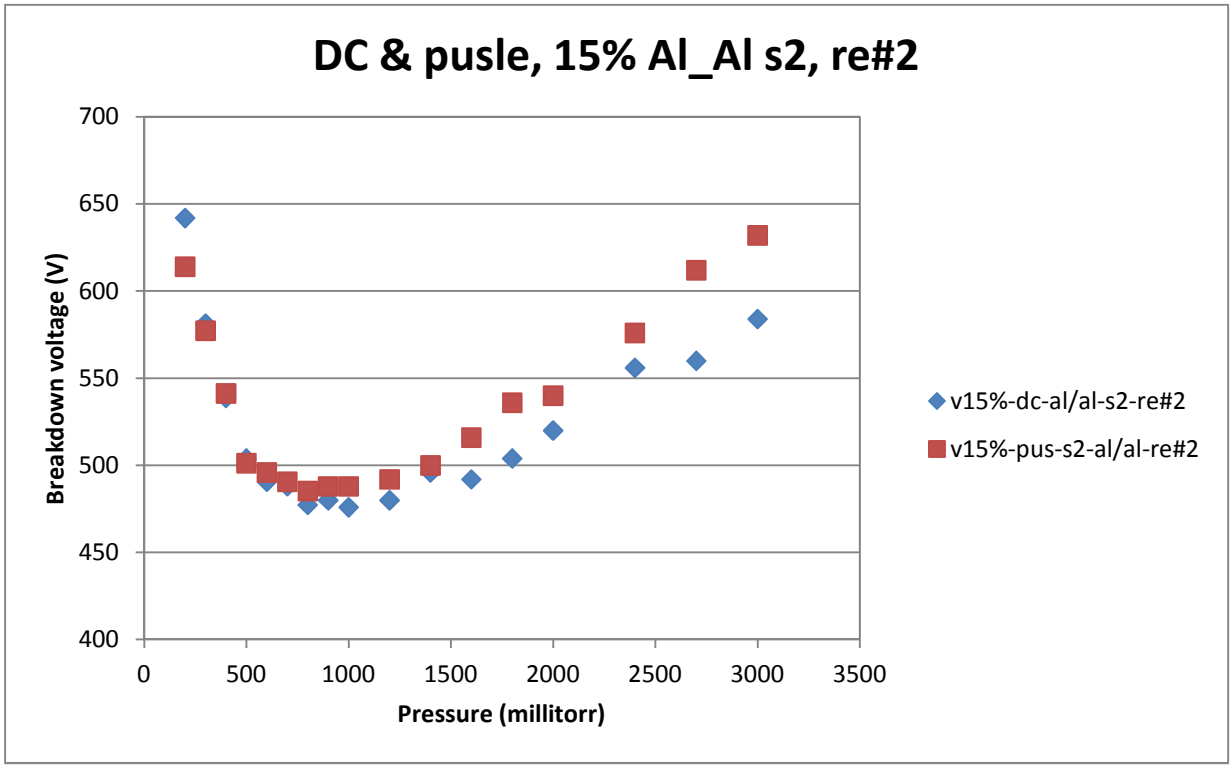

Figure A-46

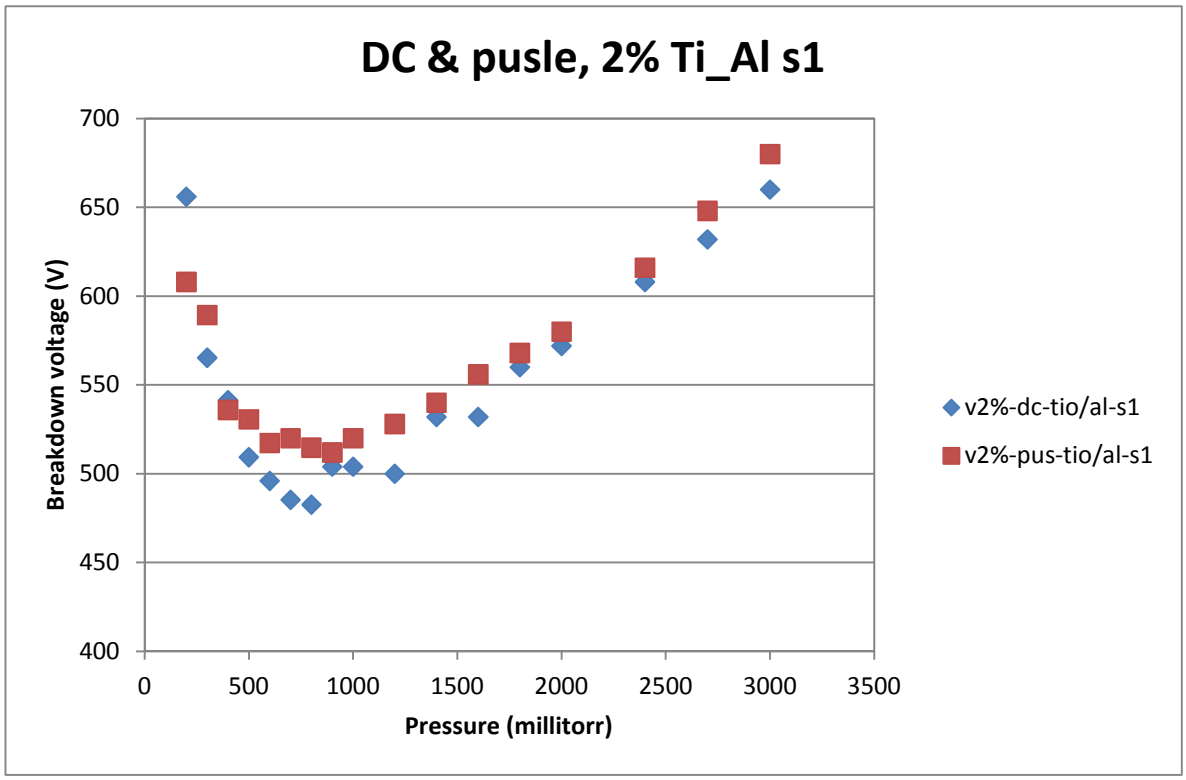

Figure A-47

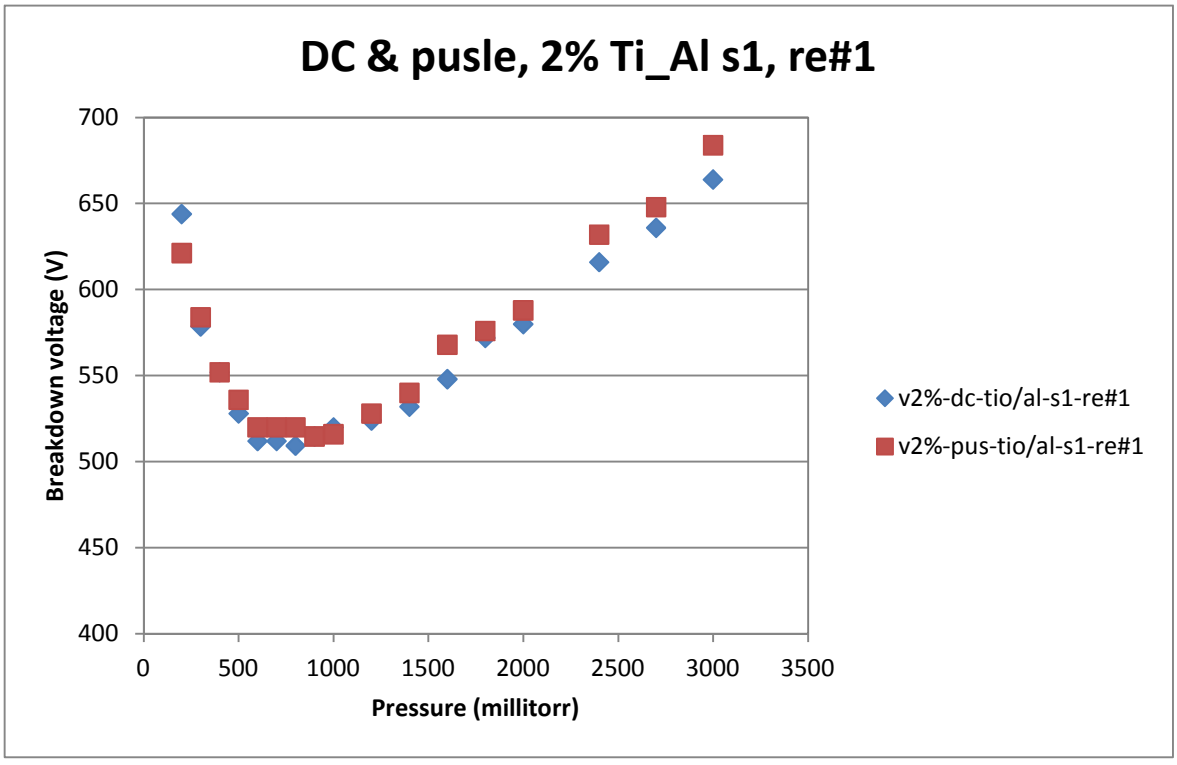

Figure A-48

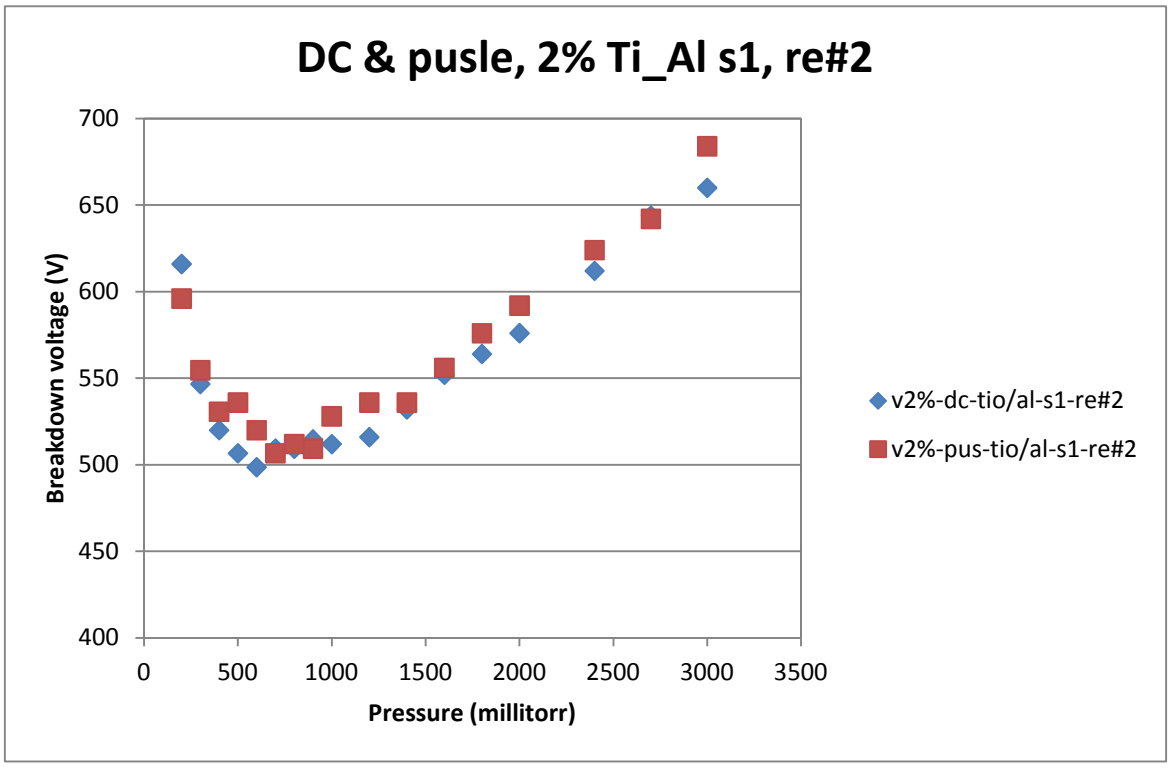

Figure A-49

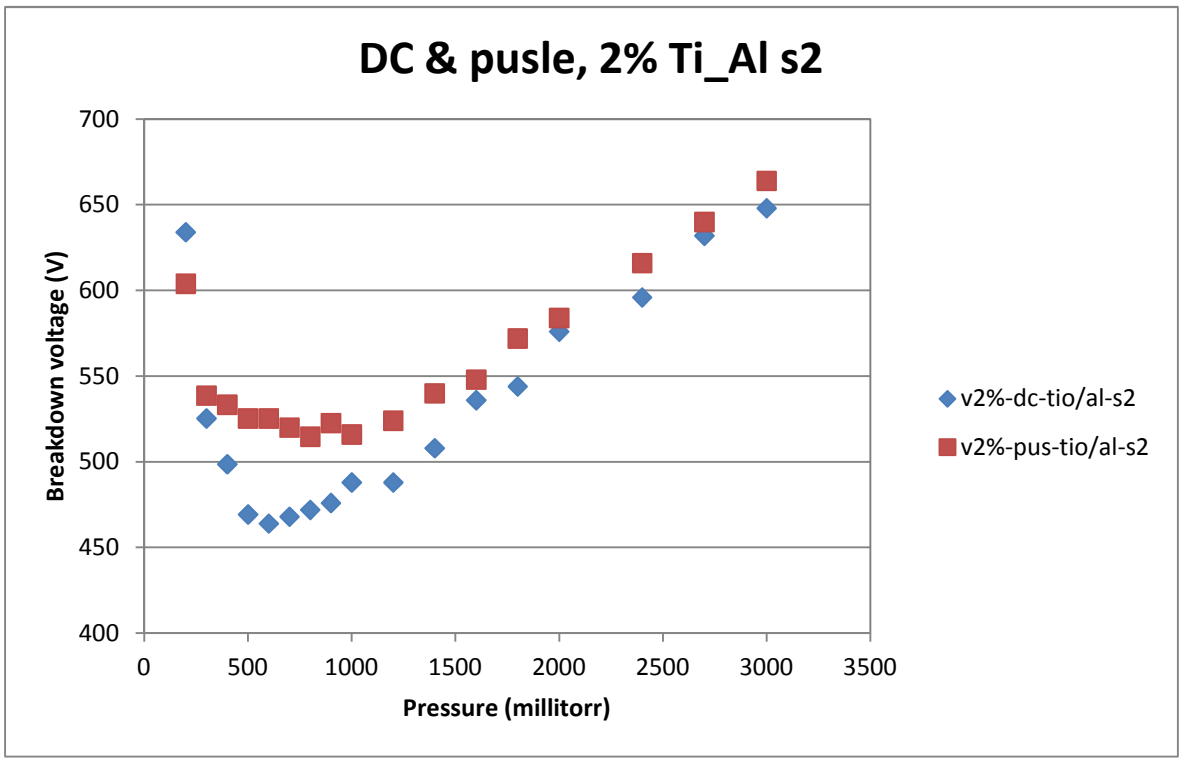

Figure A-50

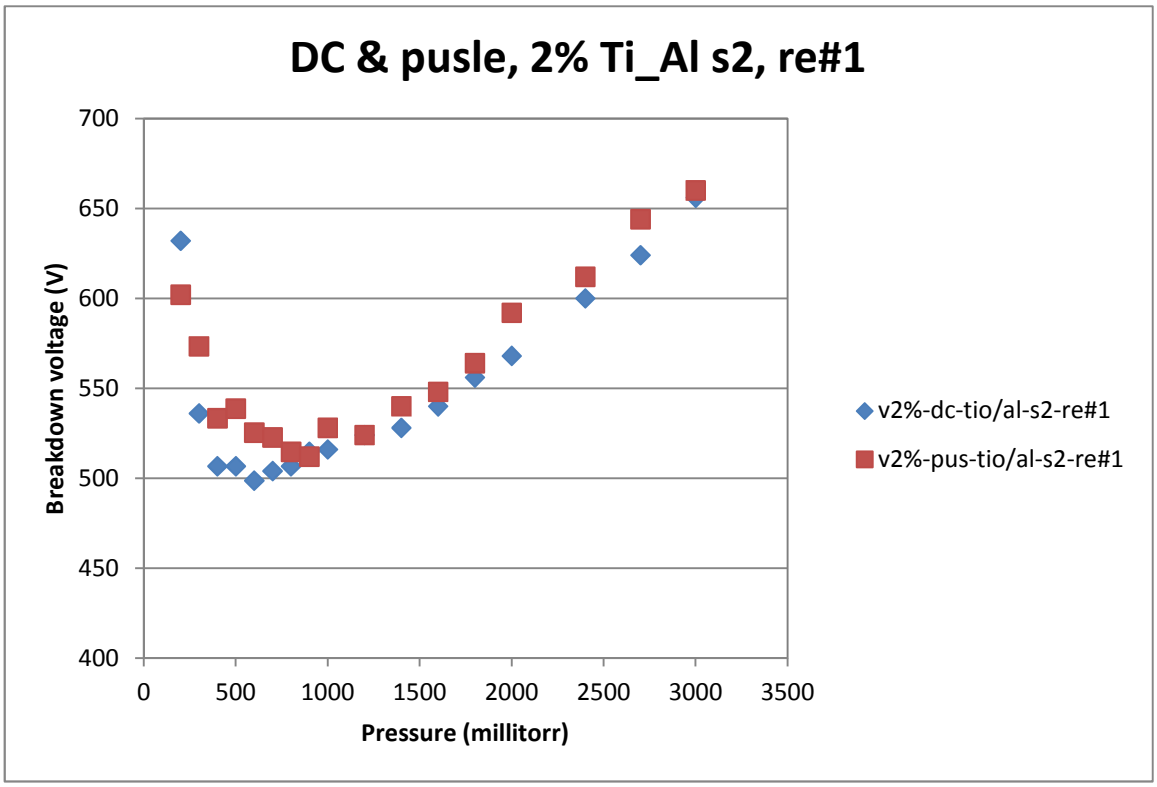

Figure A-51

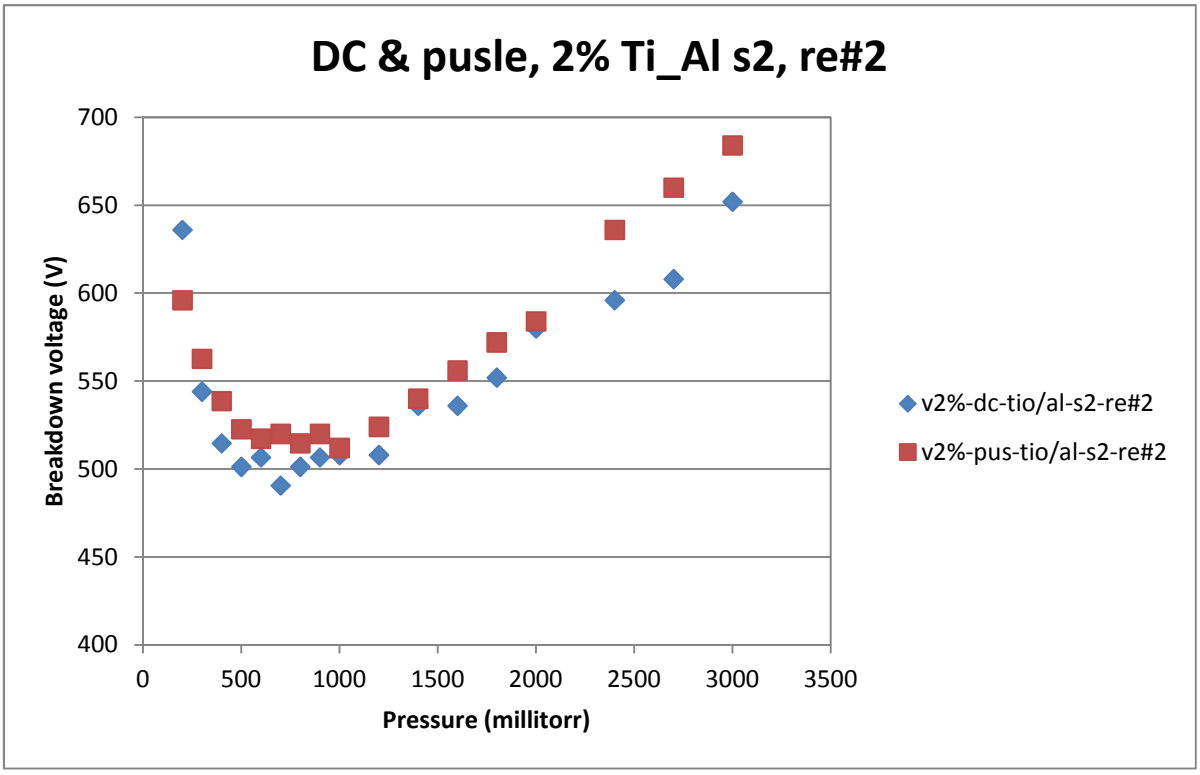

Figure A-52

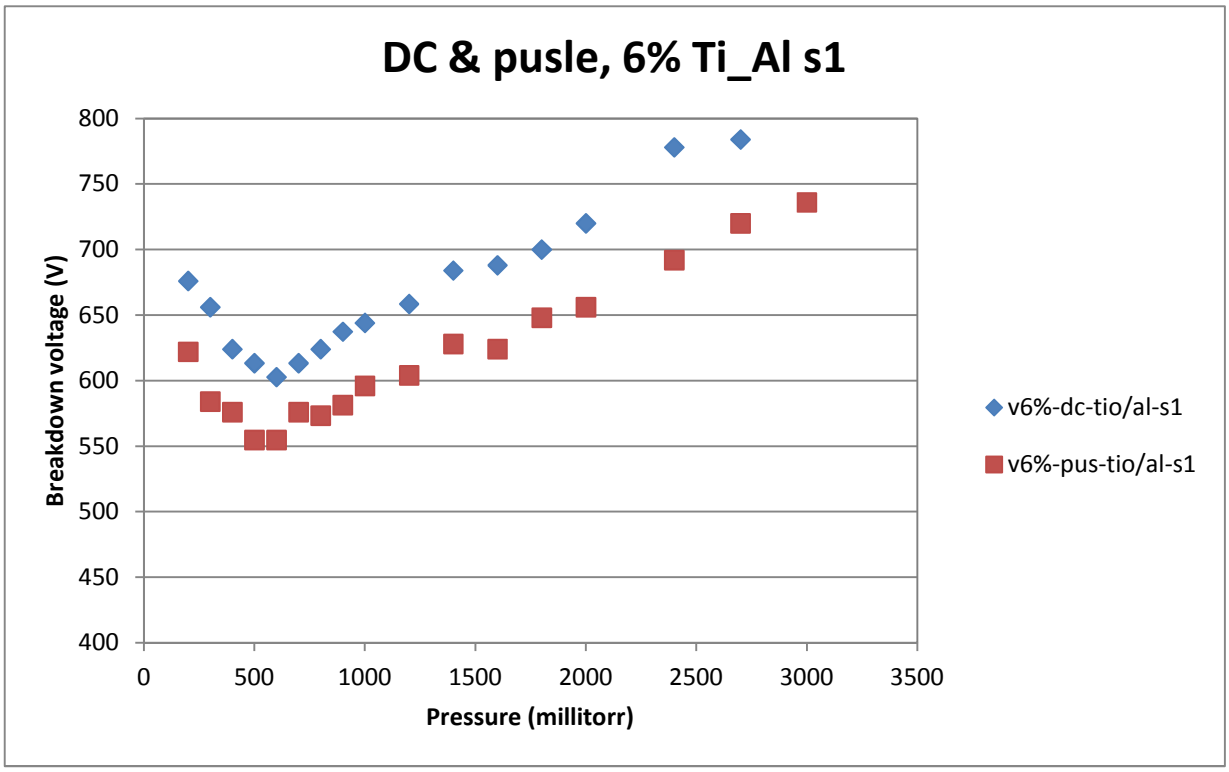

Figure A-53

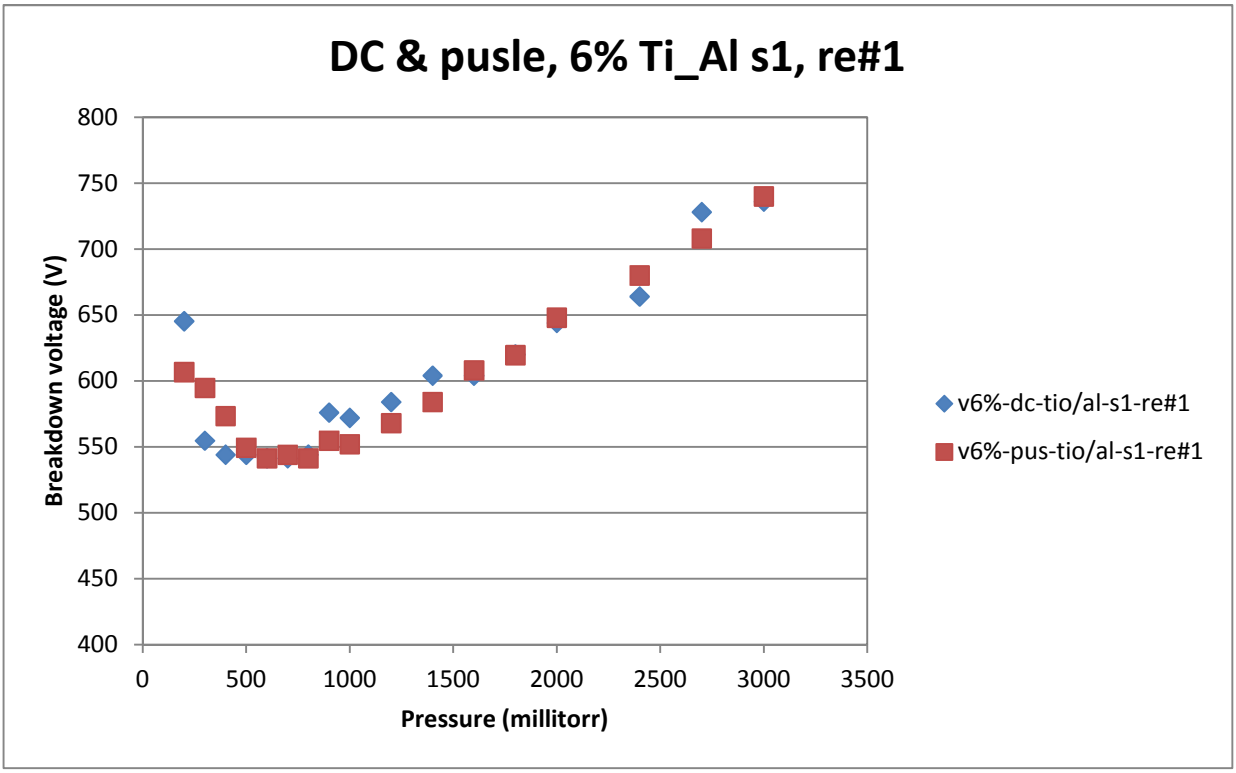

Figure A-54

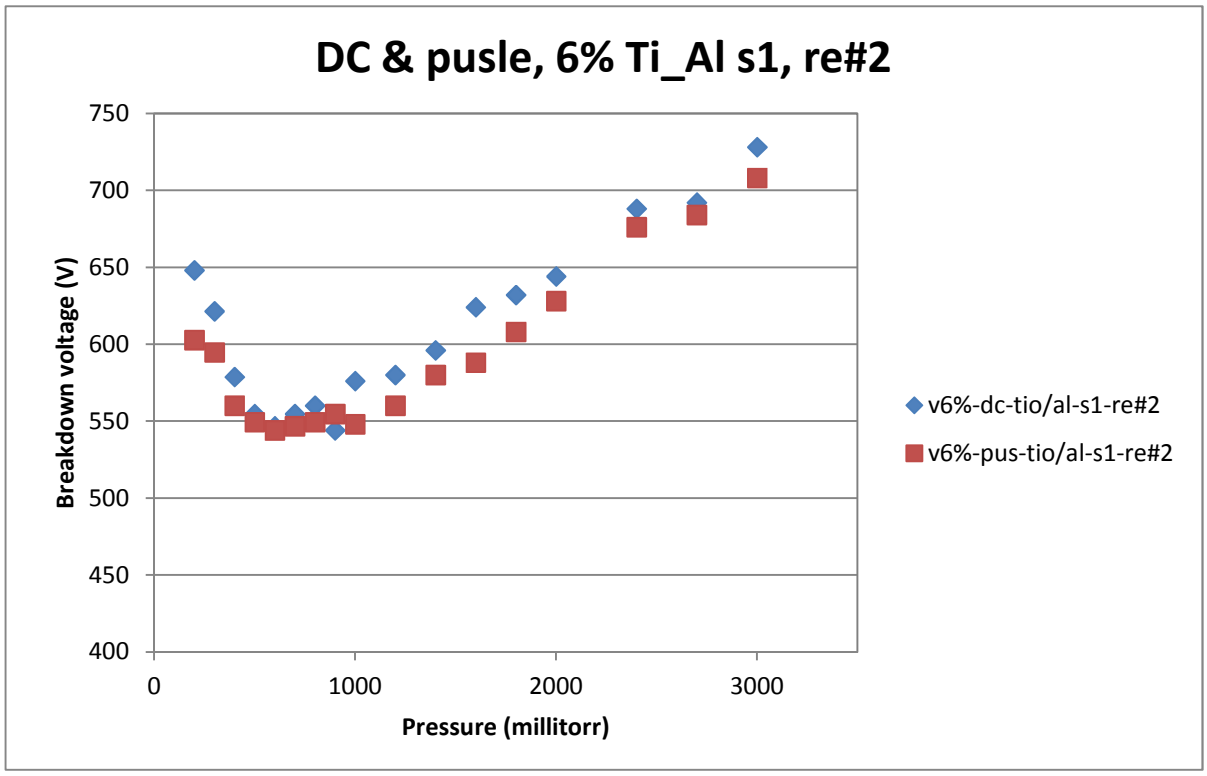

Figure A-55

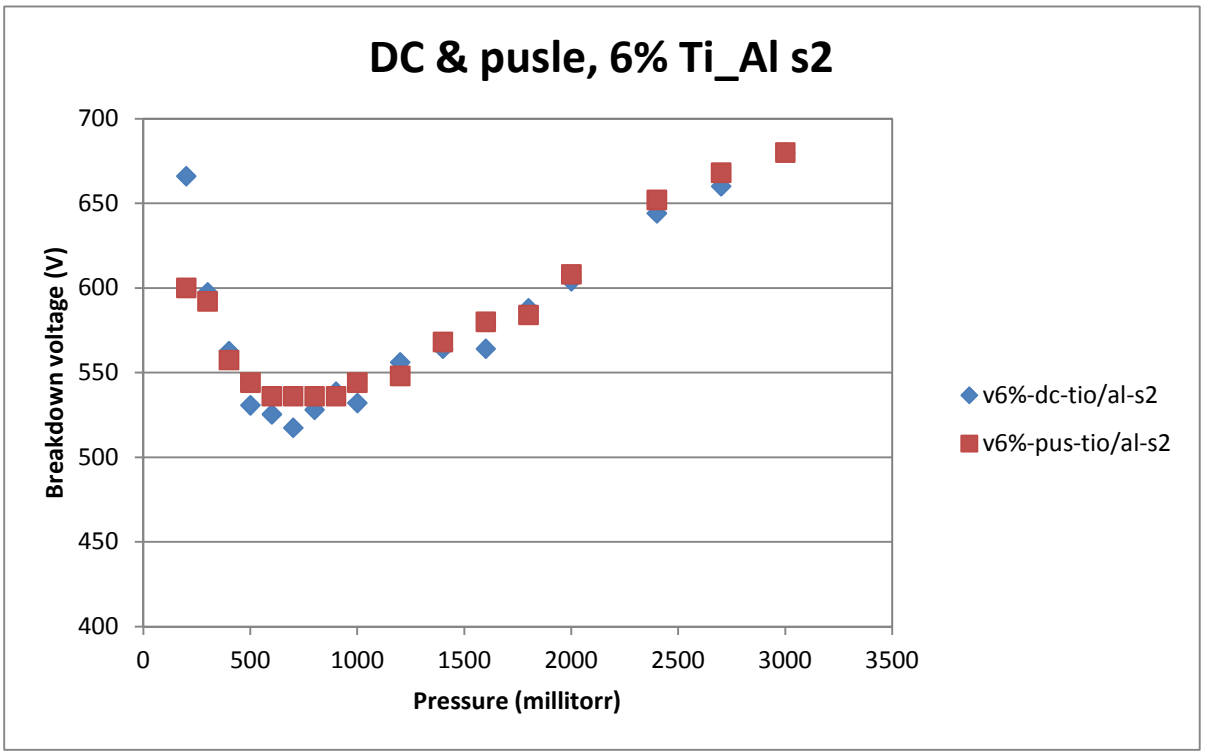

Figure A-56

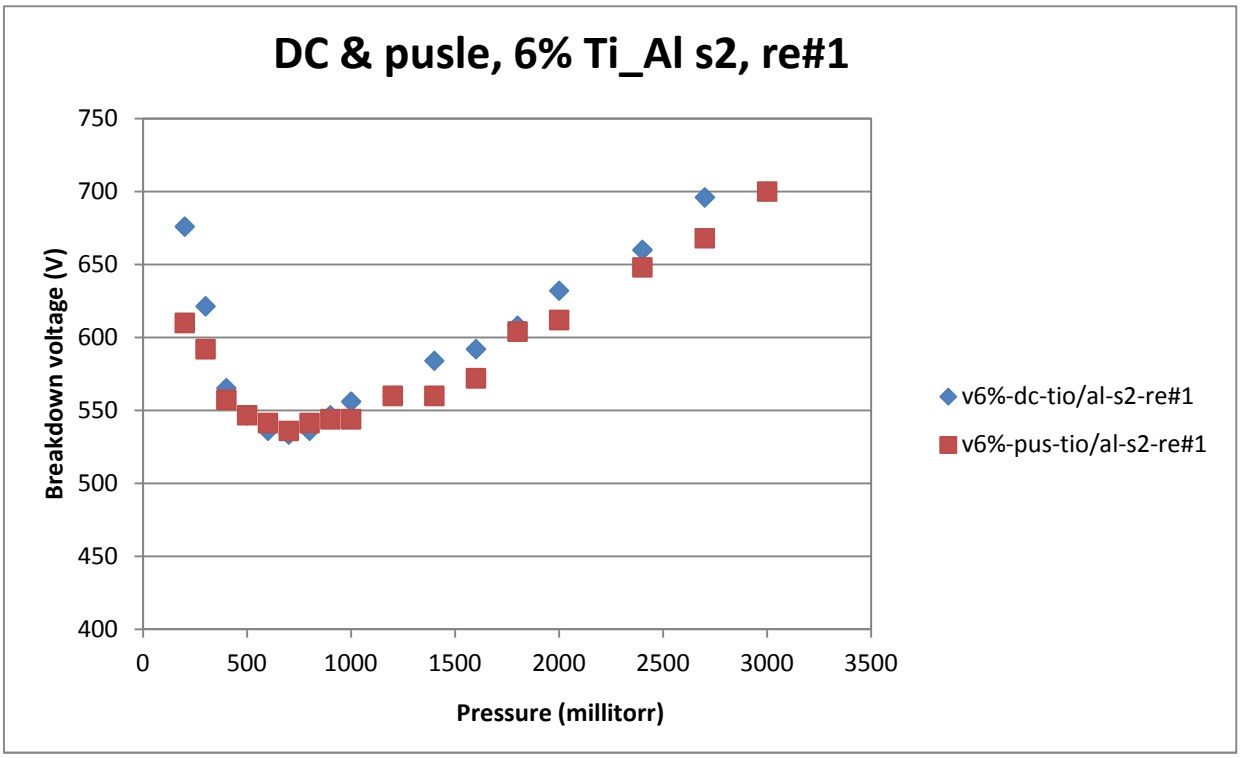

Figure A-57

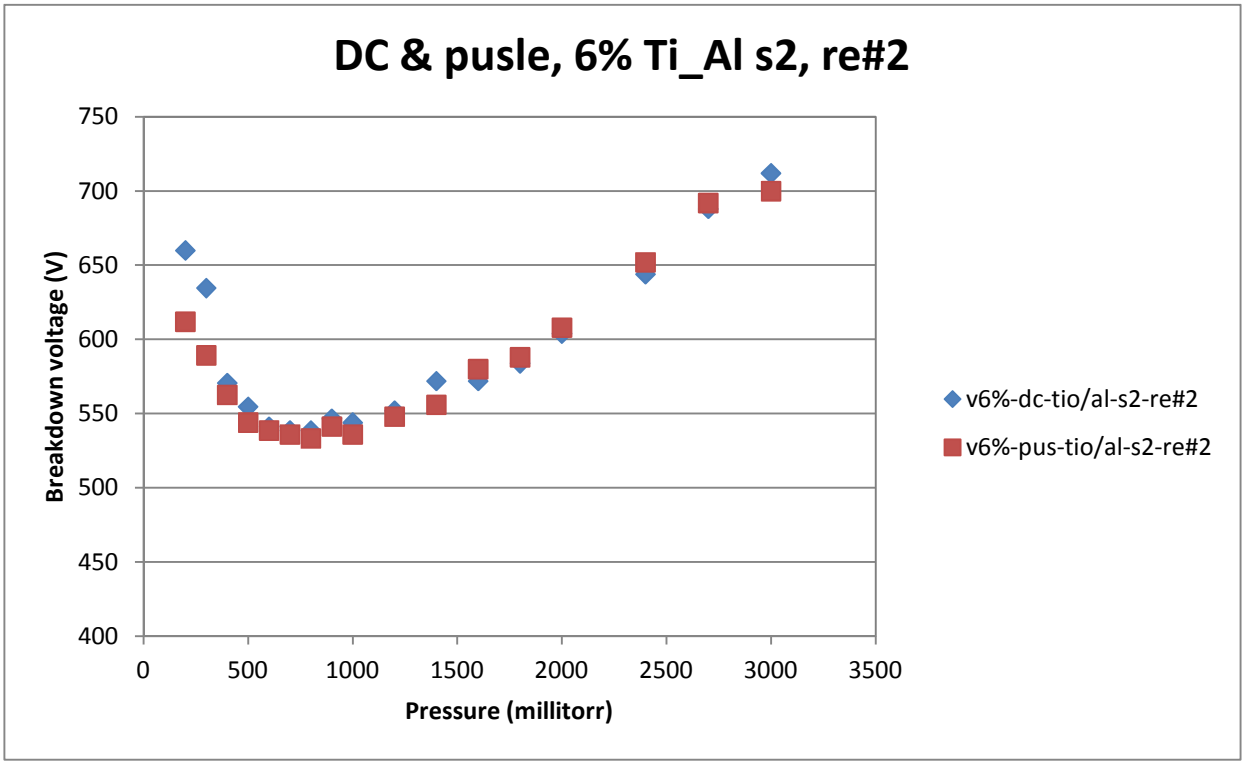

Figure A-58

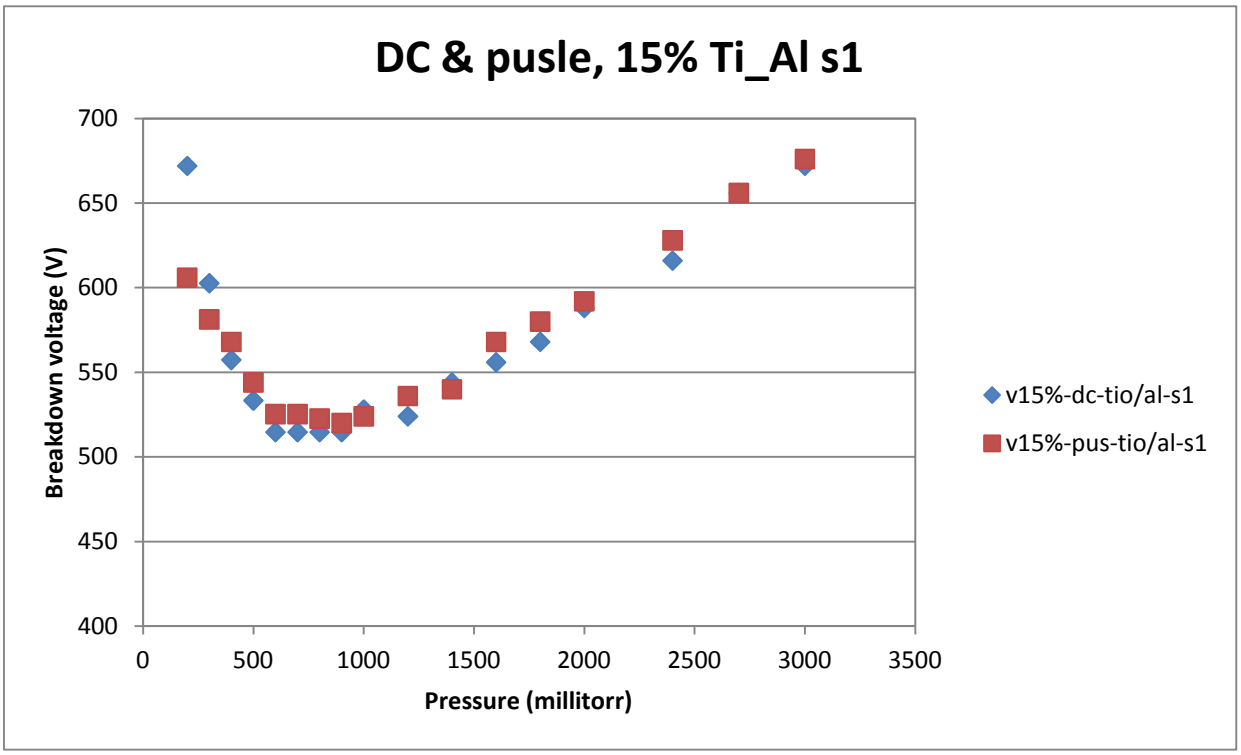

Figure A-59

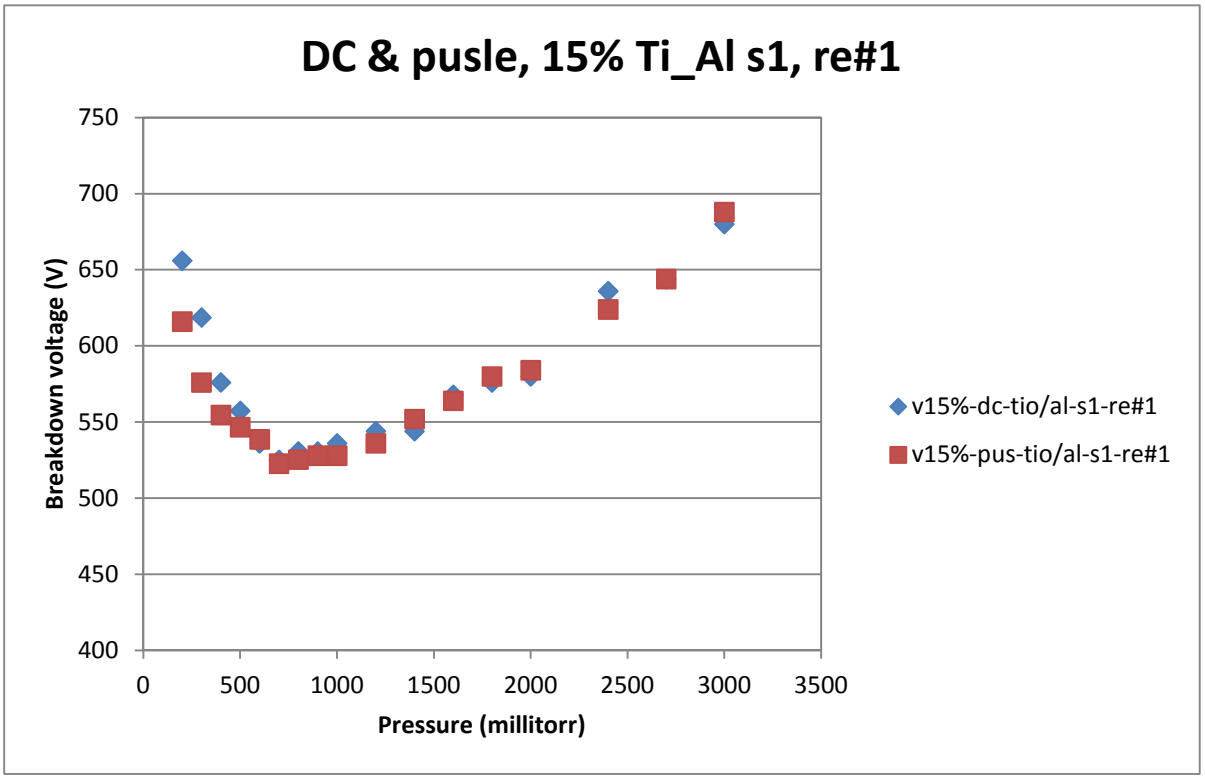

Figure A-60

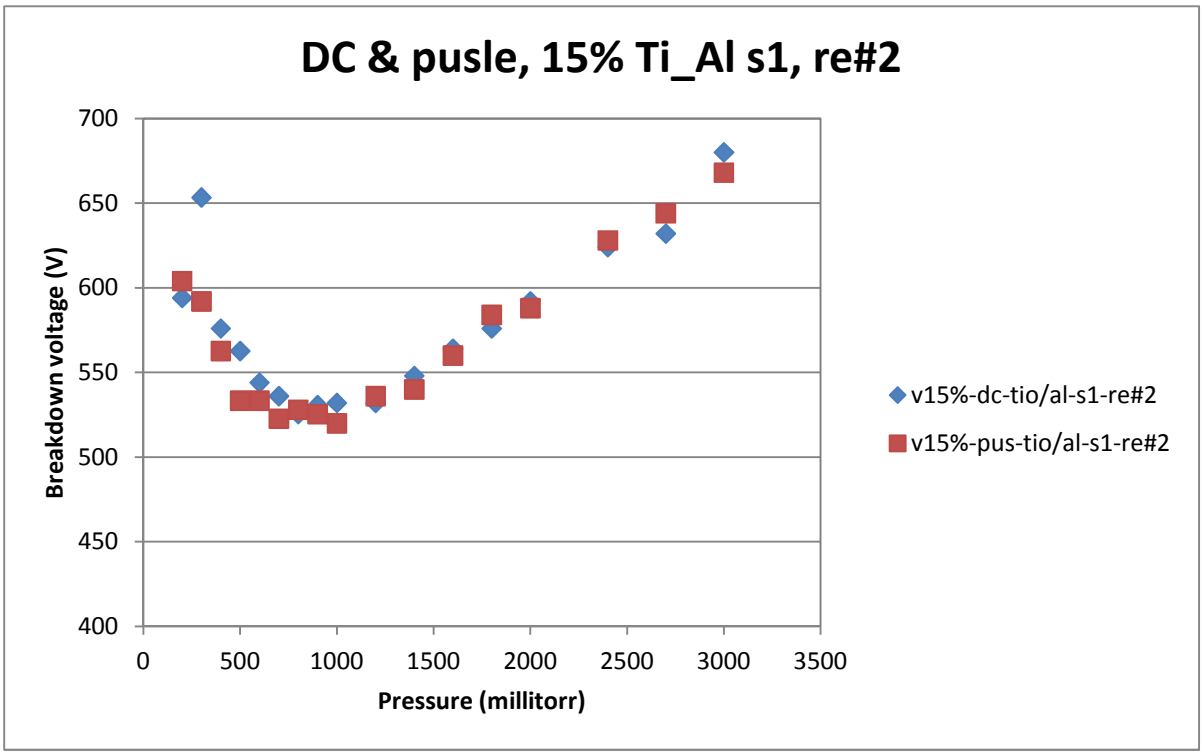

Figure A-61

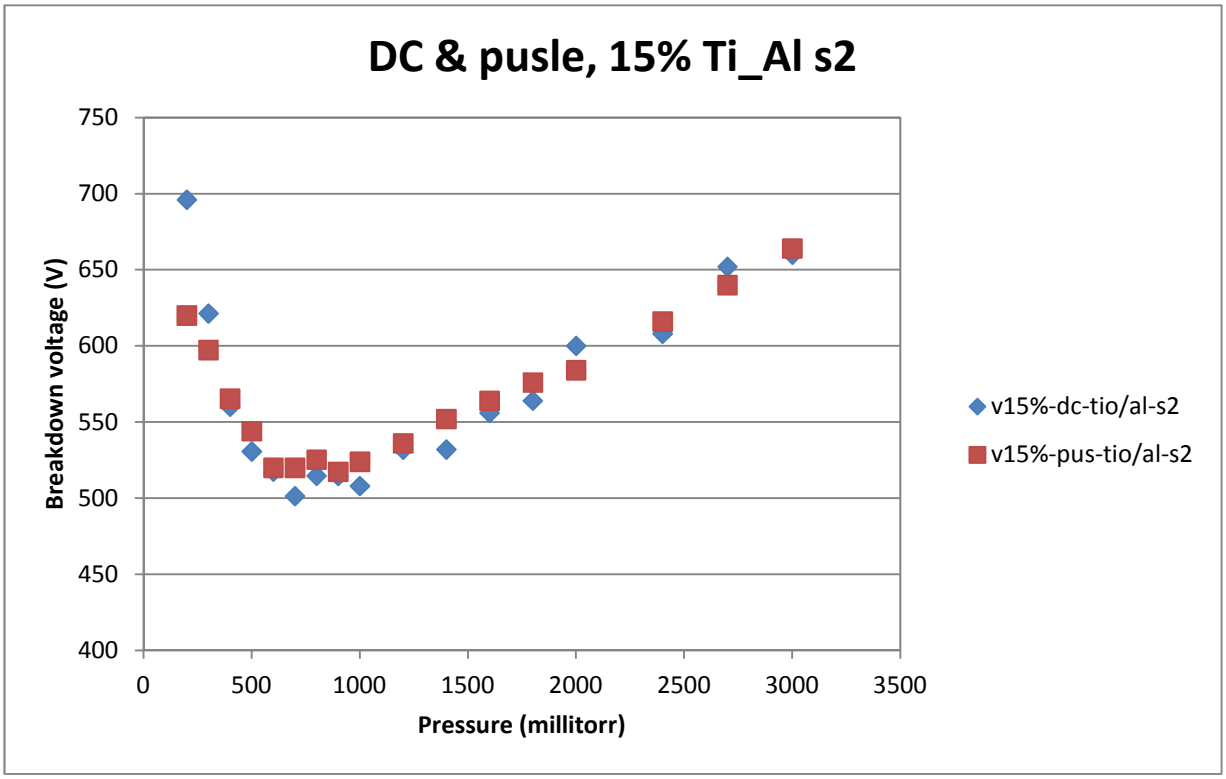

Figure A-62

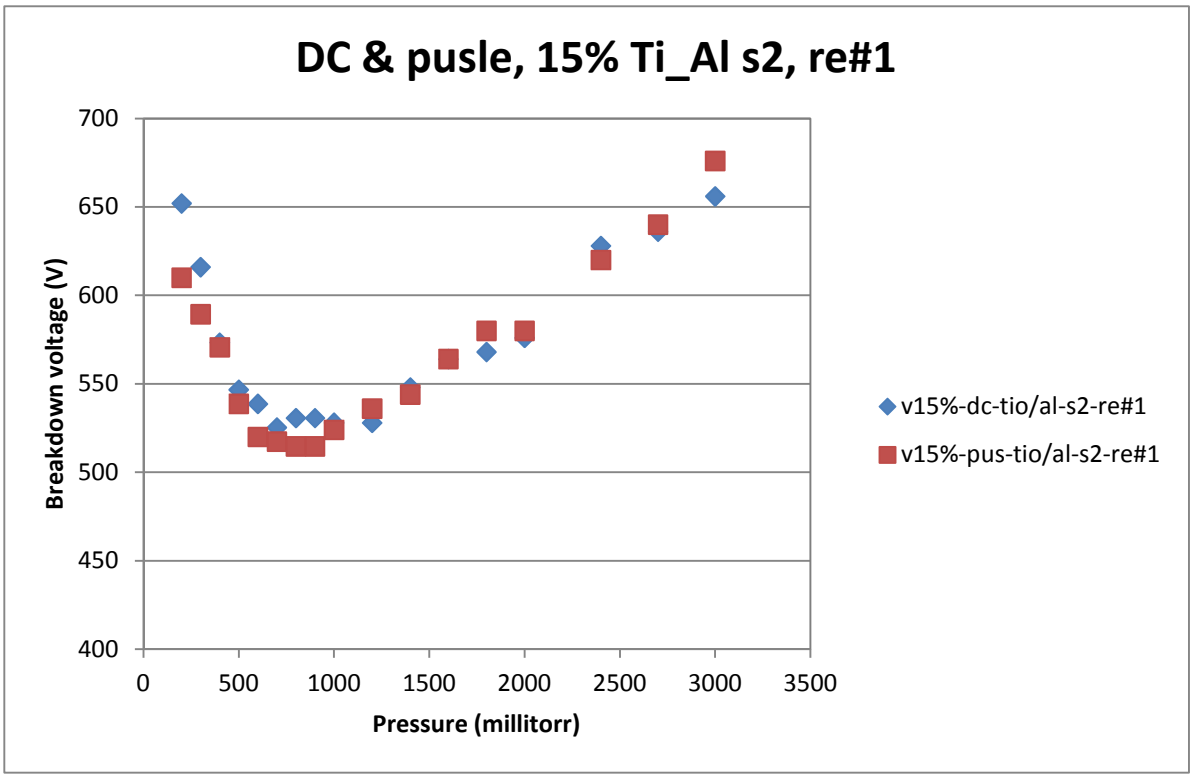

Figure A-63

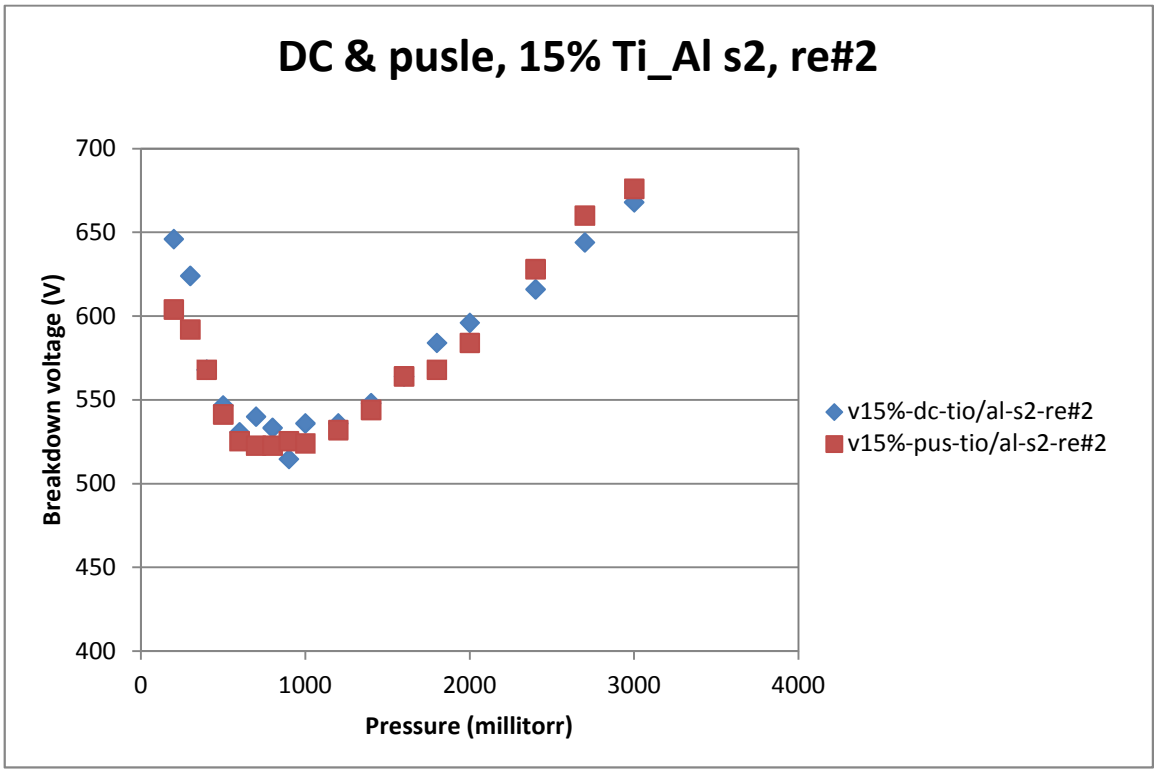

Figure A-64

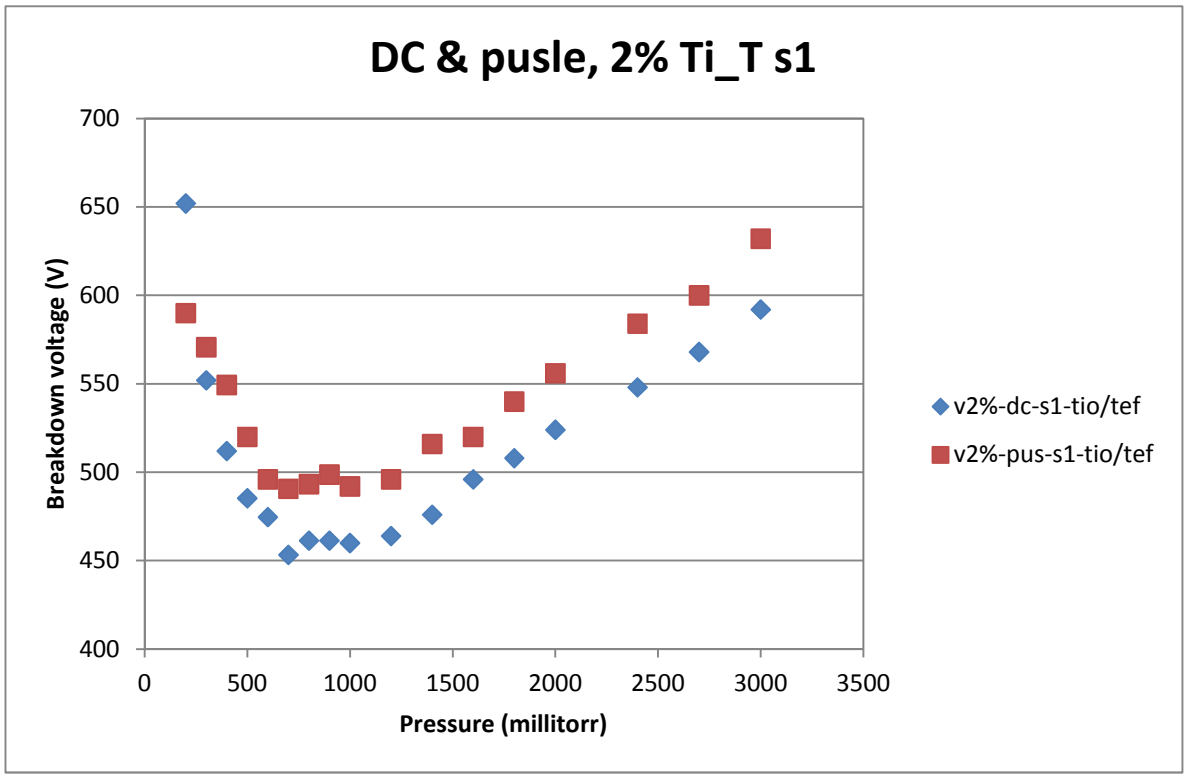

Figure A-65

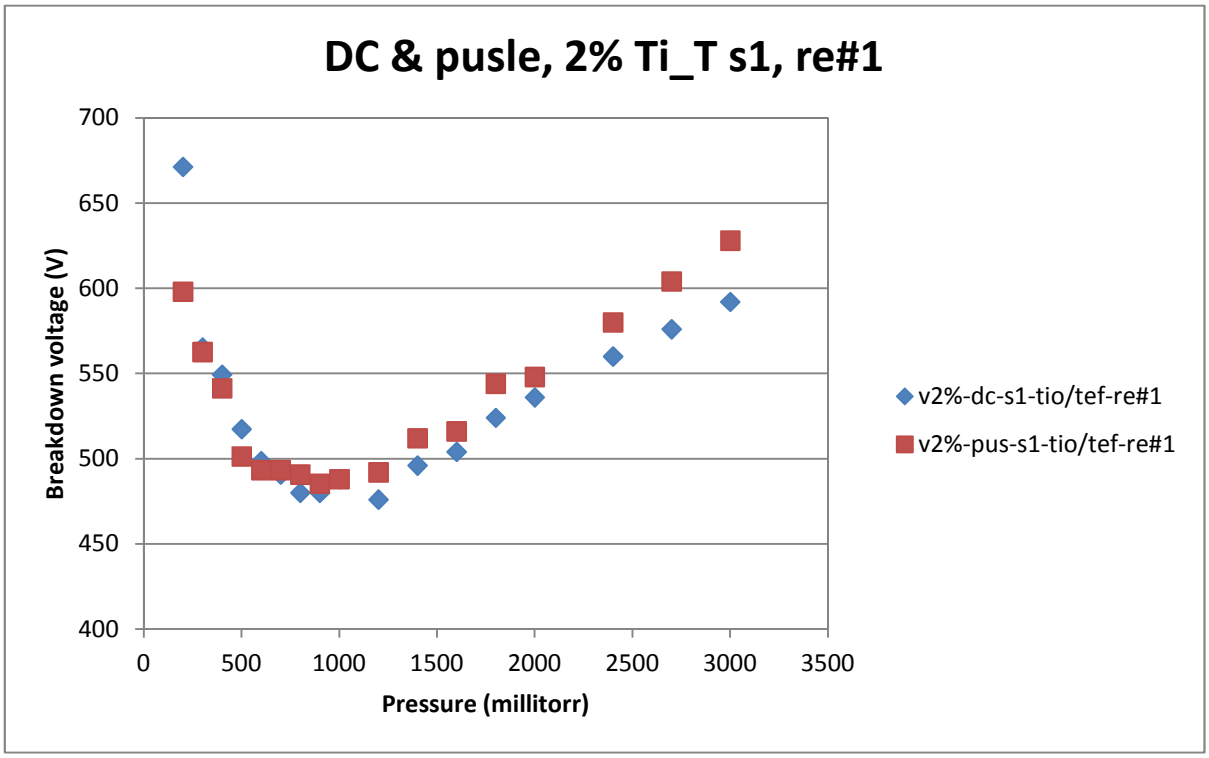

Figure A-66

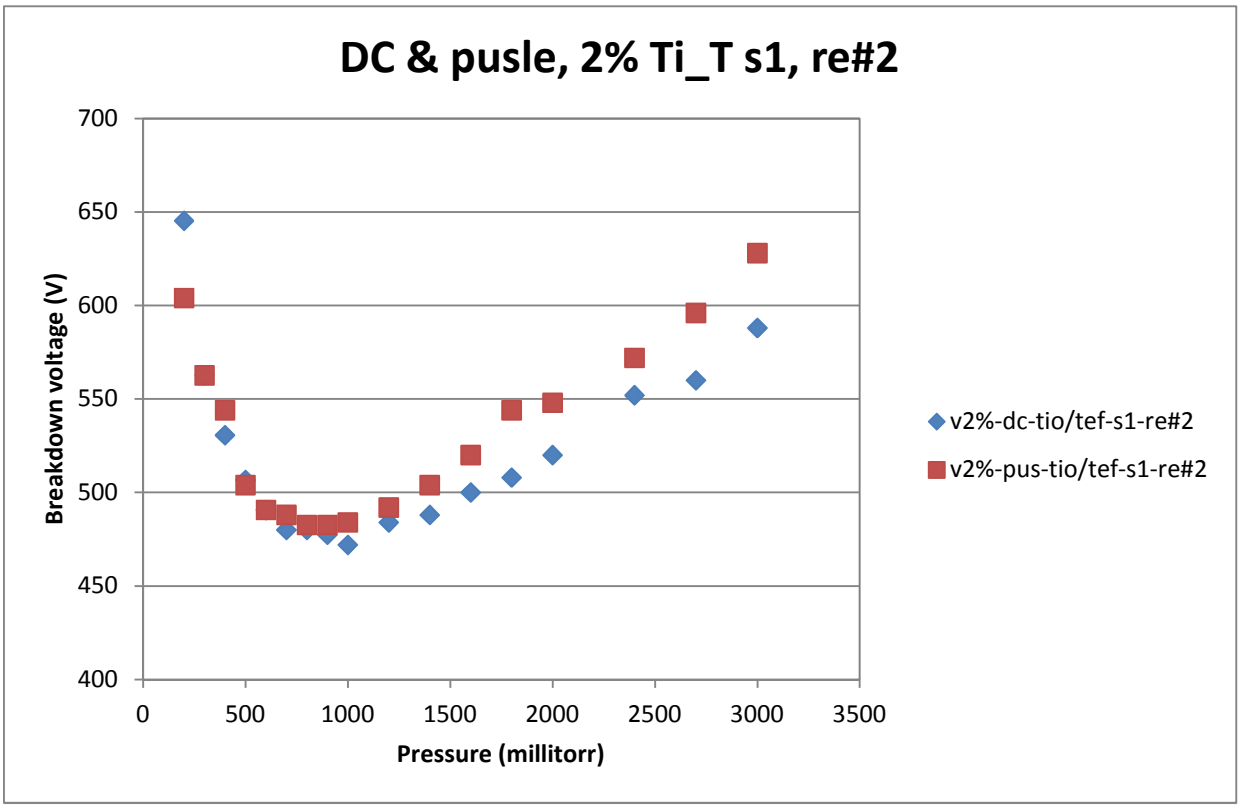

Figure A-67

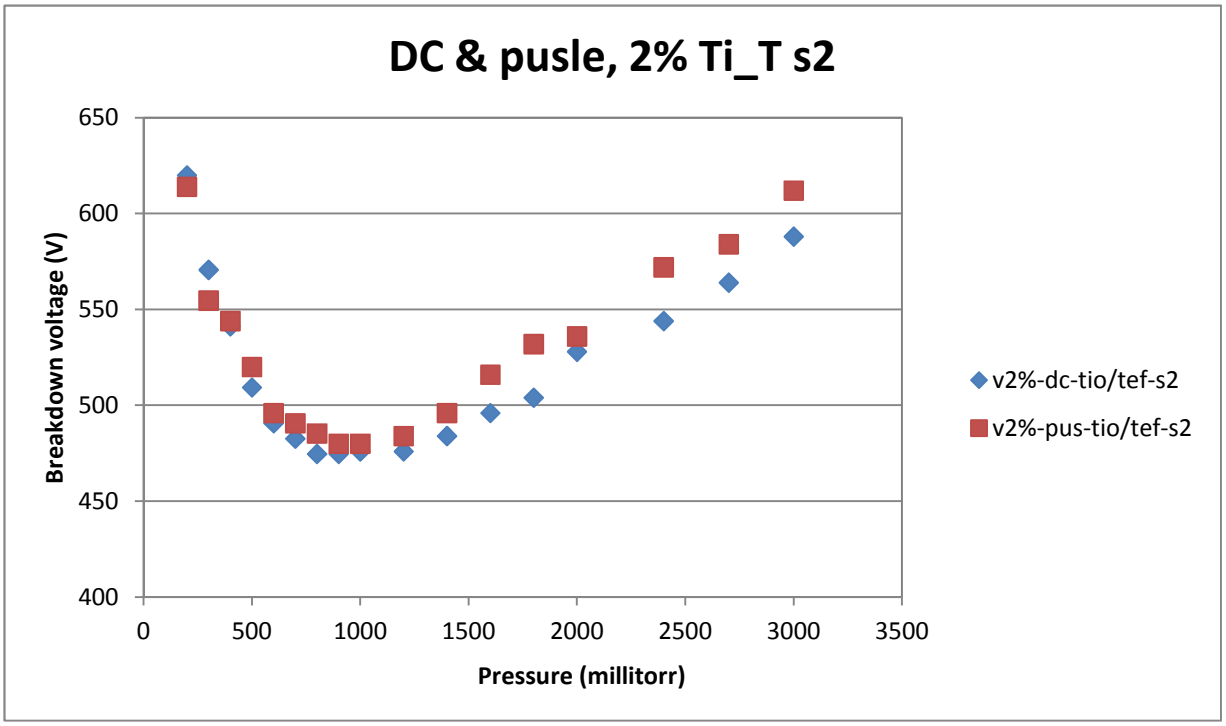

Figure A-68

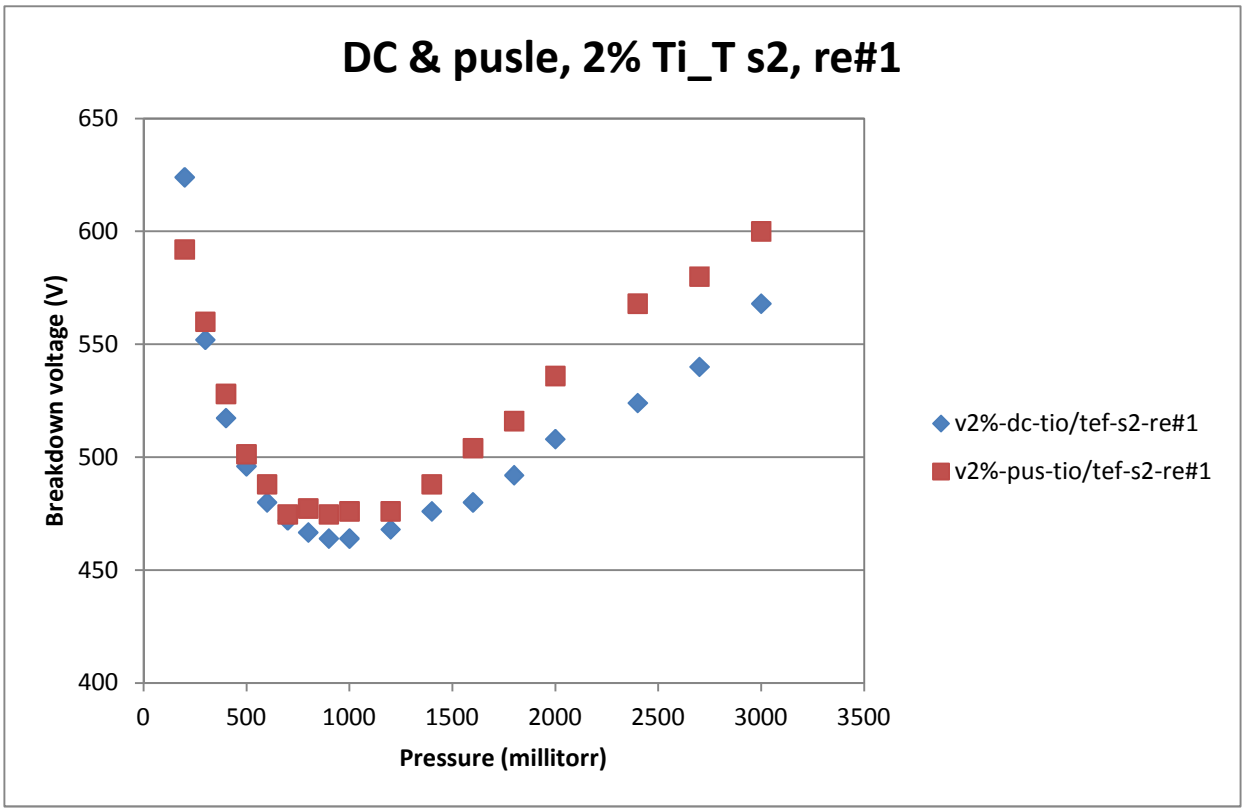

Figure A-69

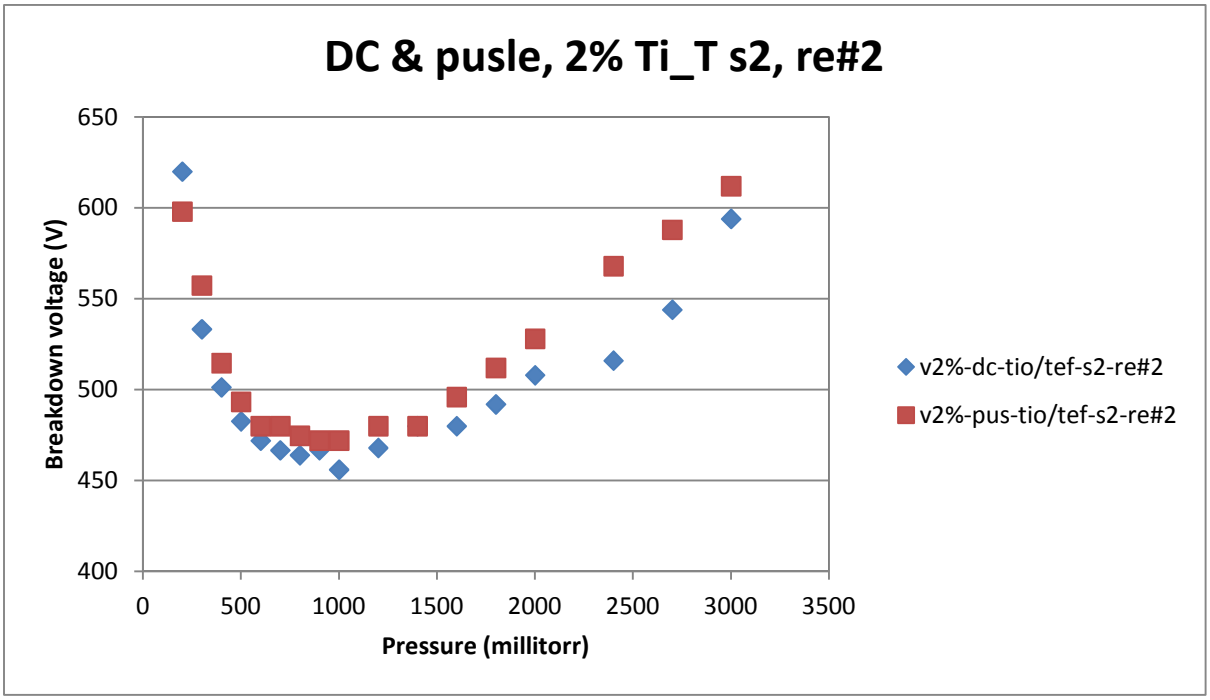

Figure A-70

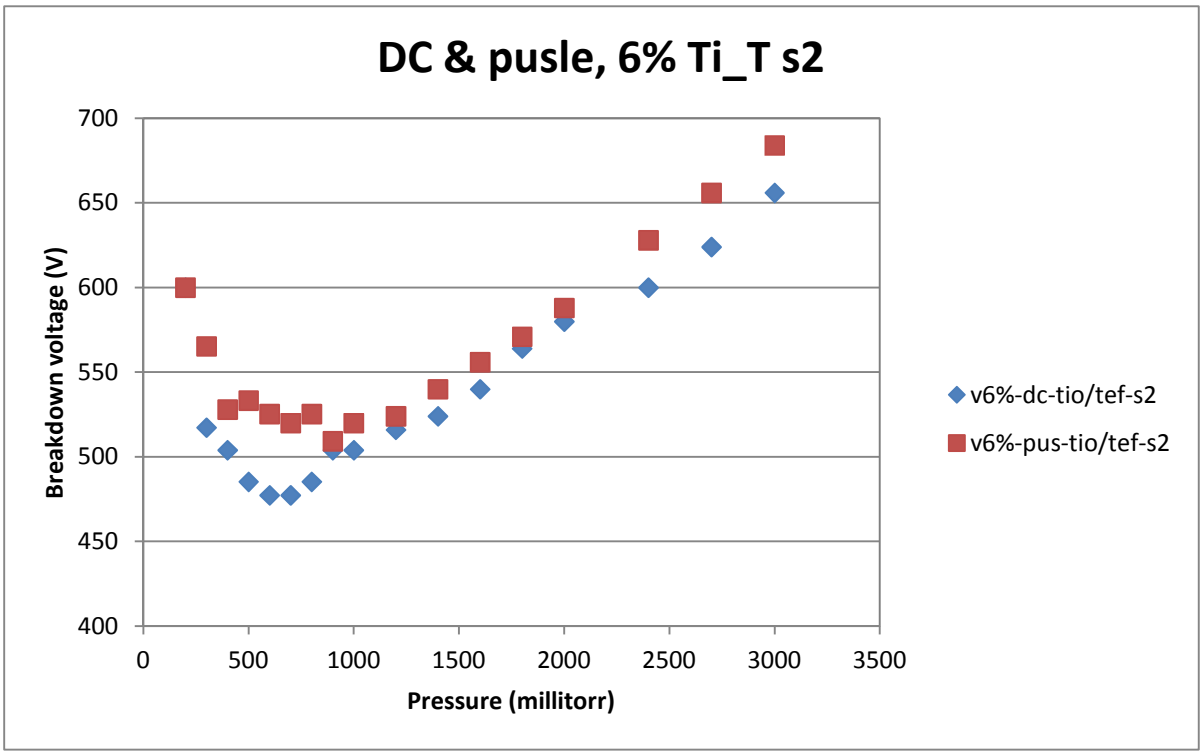

Figure A-71

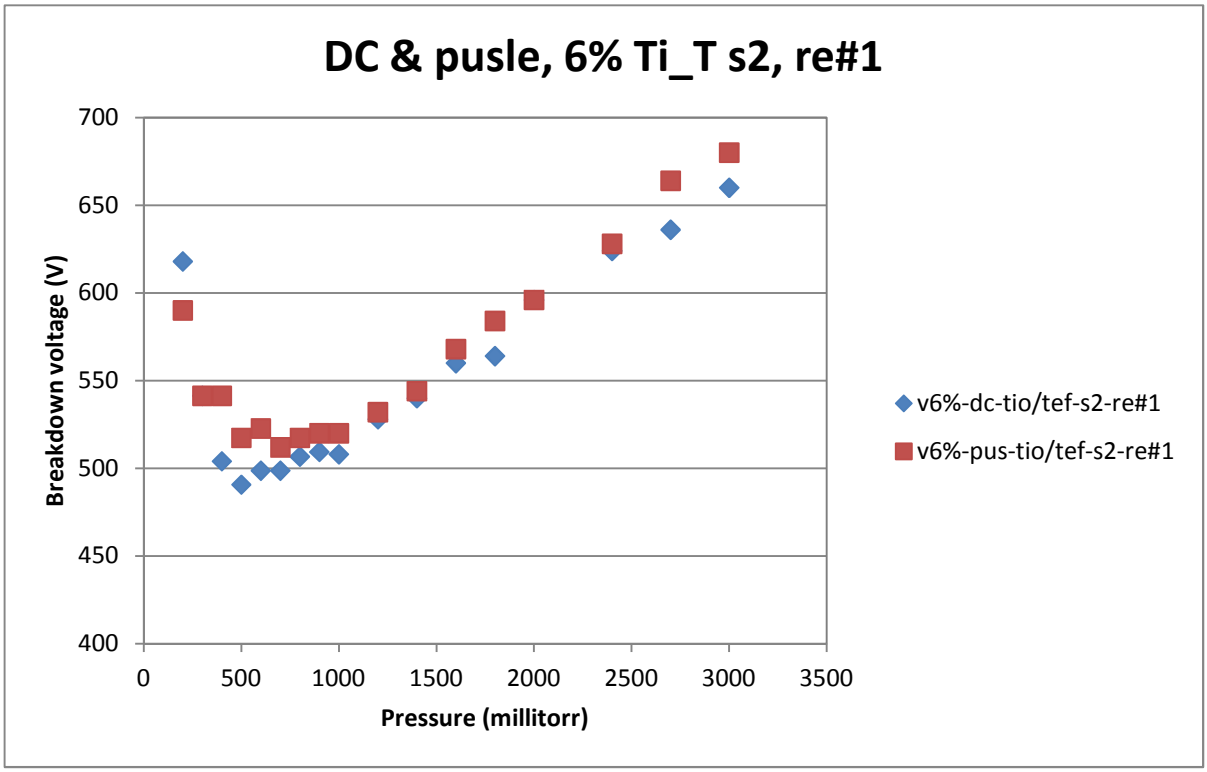

Figure A-72

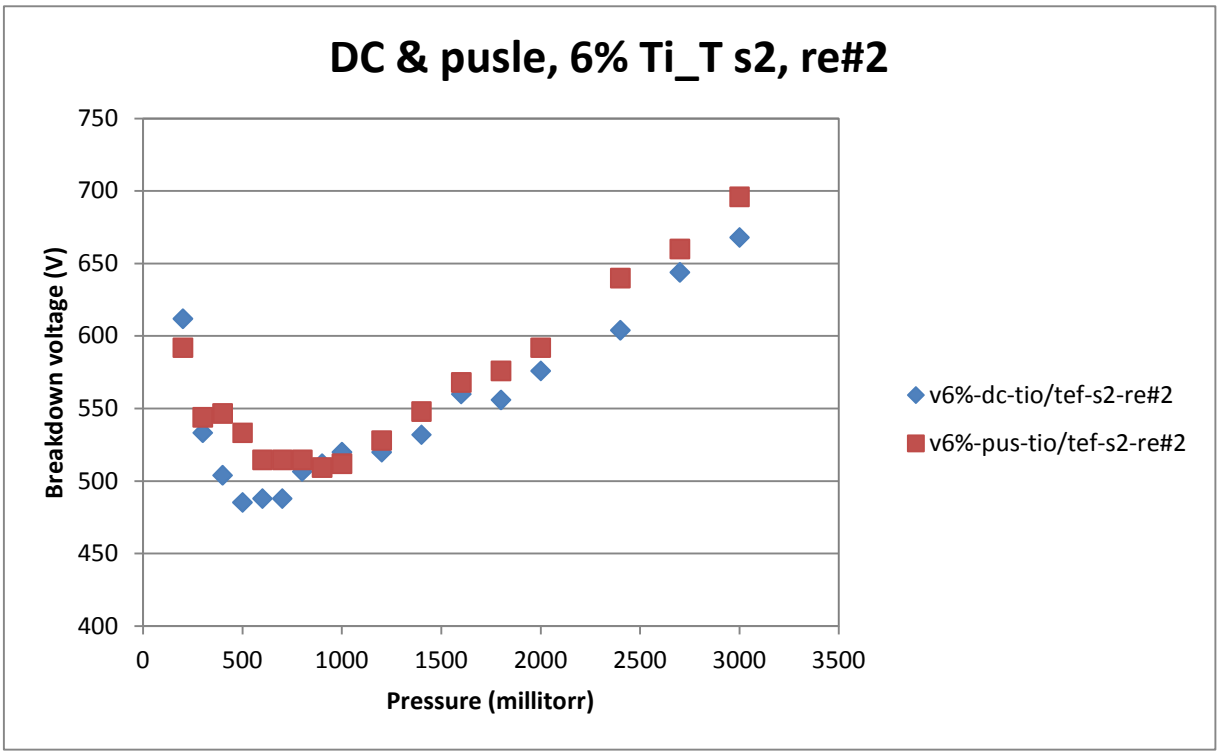

Figure A-73

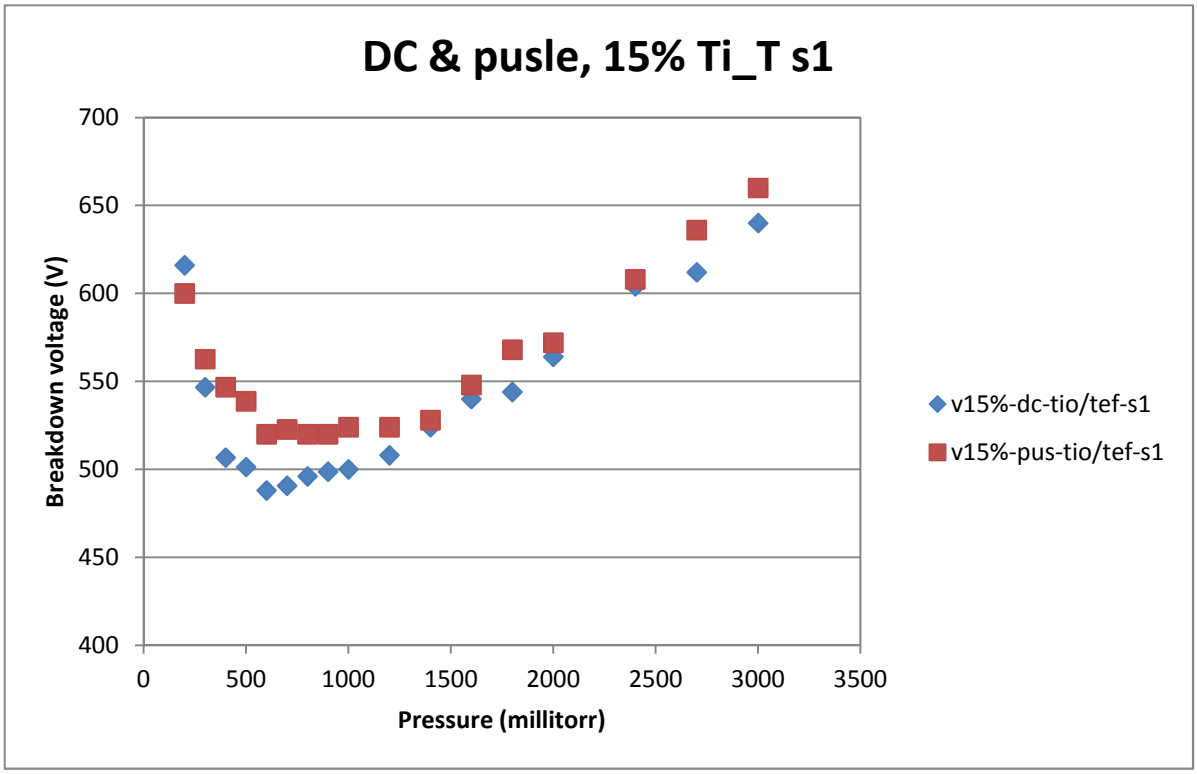

Figure A-74

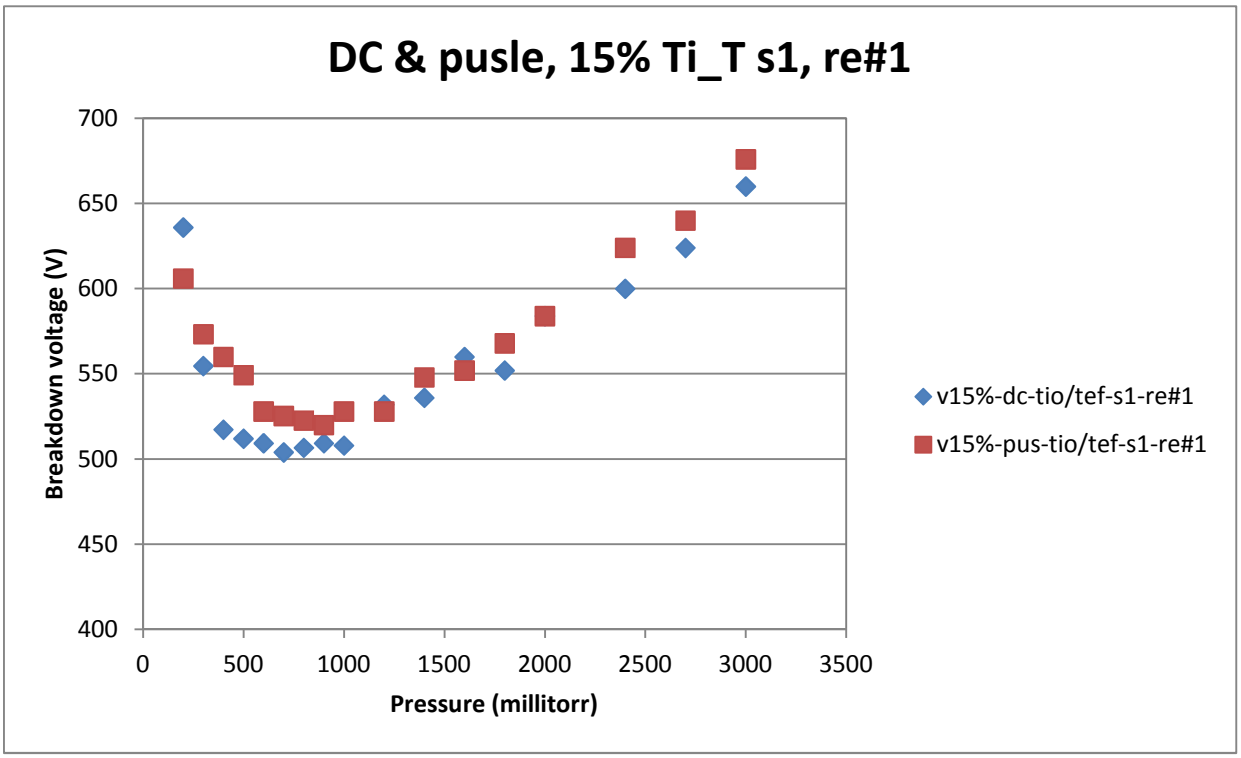

Figure A-75

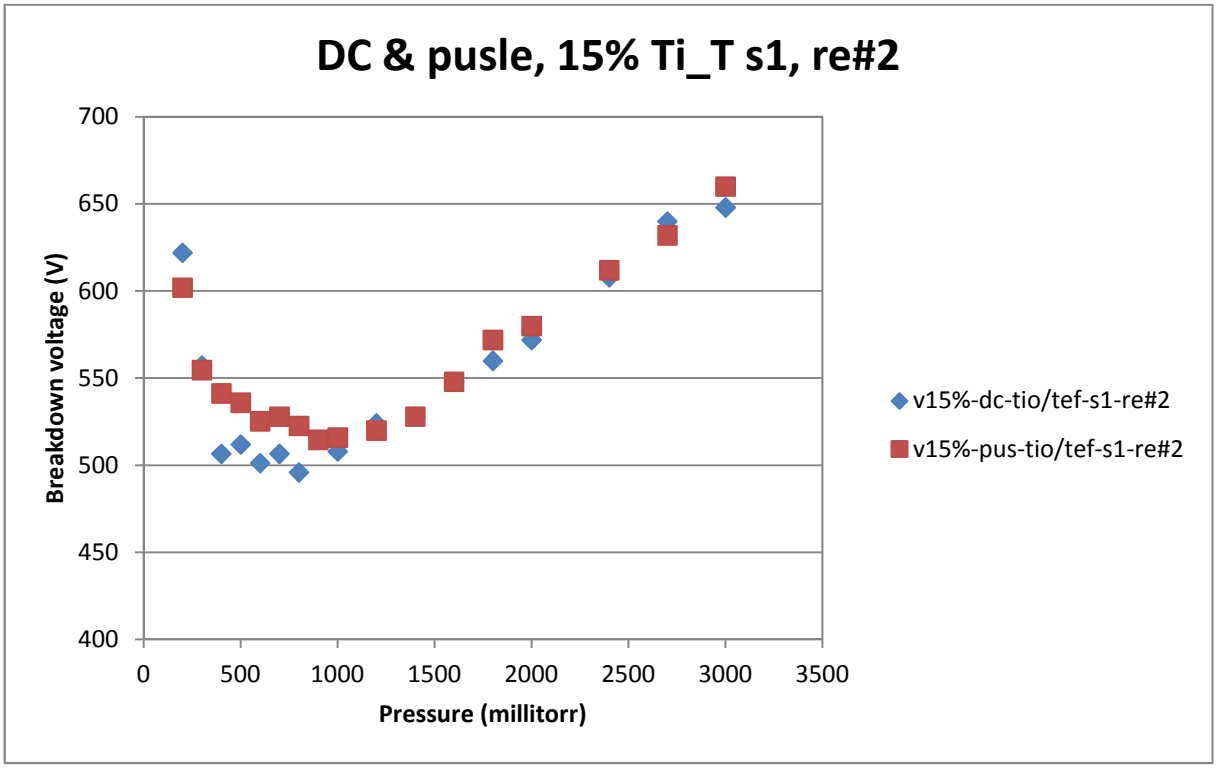

Figure A-76

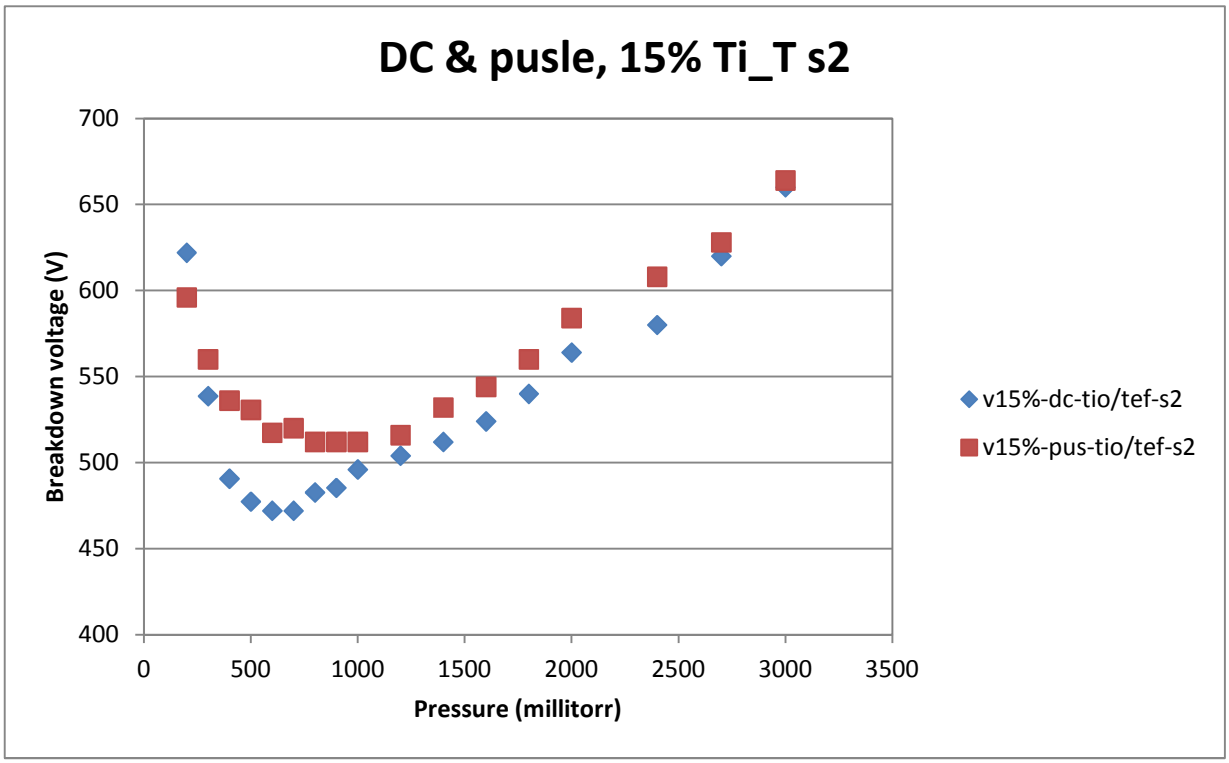

Figure A-77

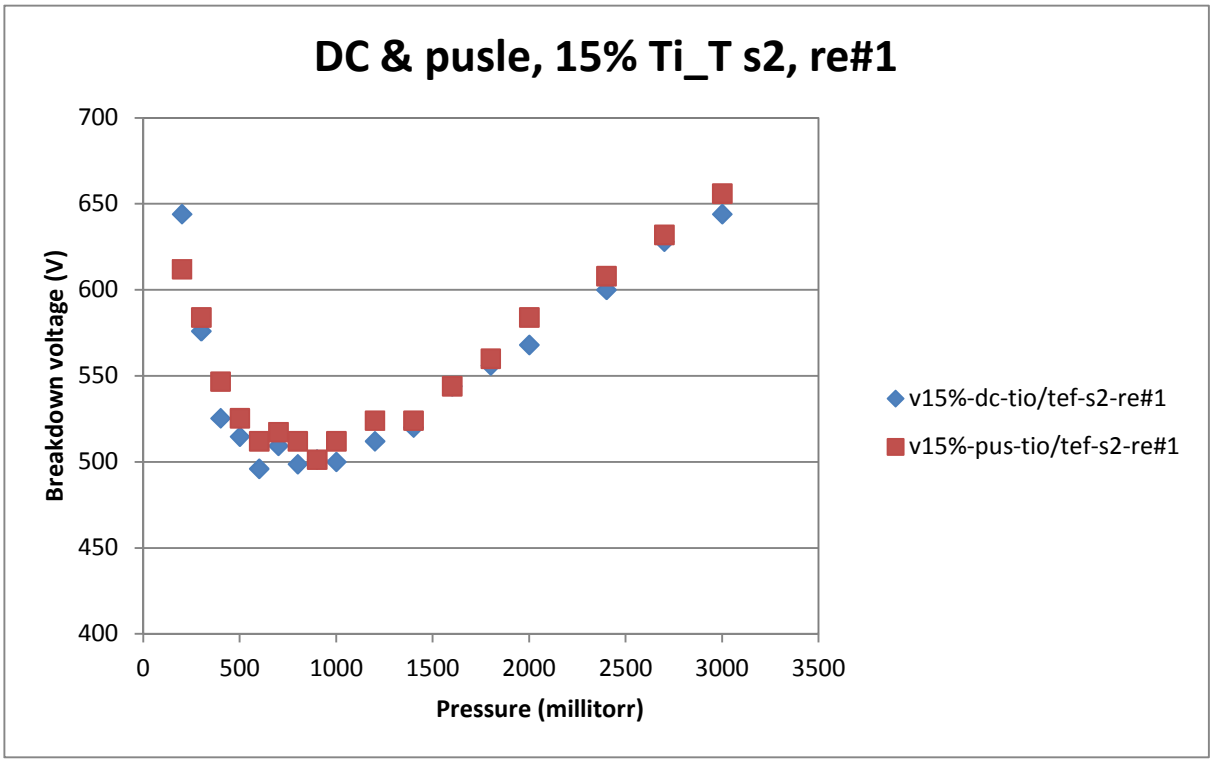

Figure A-78

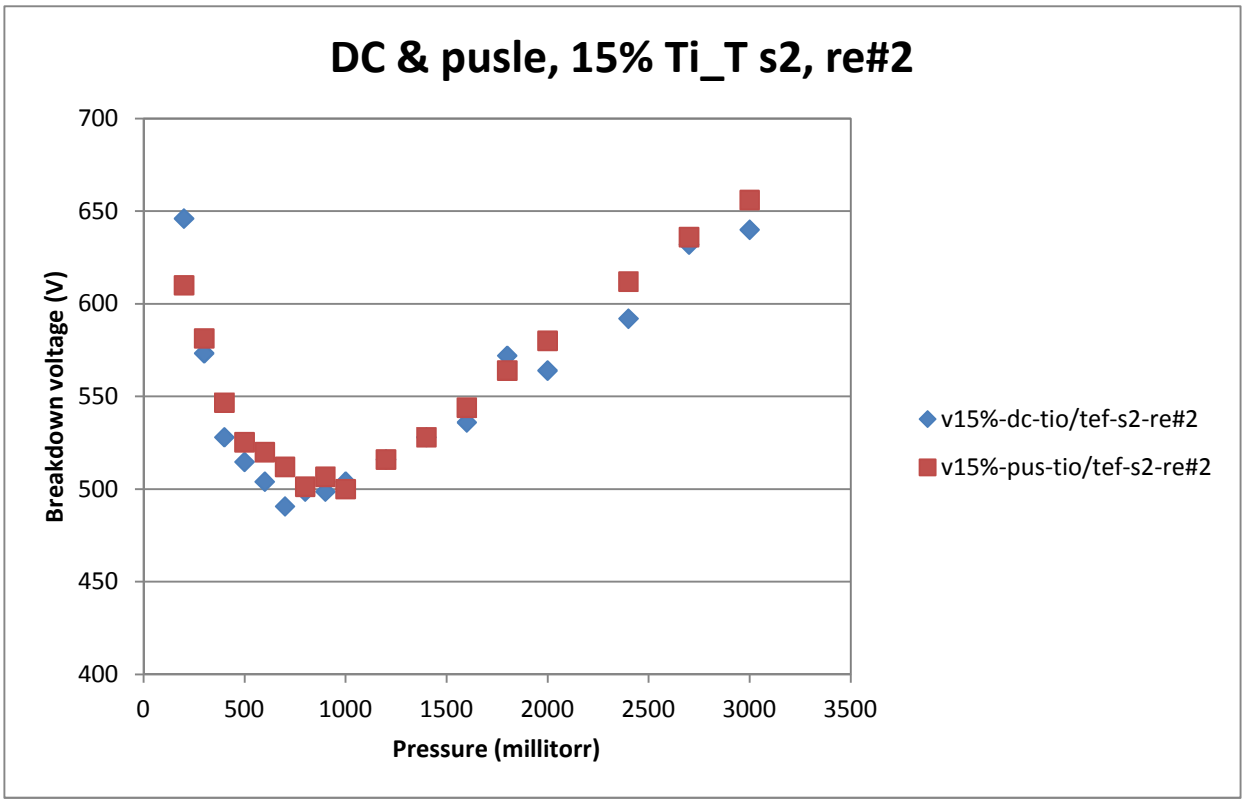
DC & pusle, 15% Ti_T s2, re#2
Breakdown voltage (V)
700
650
600
550
500
450
400
0
500
1000
1500
2000
2500
3000
3500
Pressure (millitorr)
v15%-dc-tio/tef-s2-re#2
v15%-pus-tio/tef-s2-re#2

Figure A-79

Appendix B

Complete set of figures for conditioning effect discussion. Breakdown voltages are plotted as test pressure increased. For one sample, repeated test results are compared under both DC and unipolar pulse signal (20 kHz, 50% duty cycle). Title of each Figure follows the same pattern, firstly, the type of the signal used, then the loading ratio, then sample number and lastly filler substrate configuration.

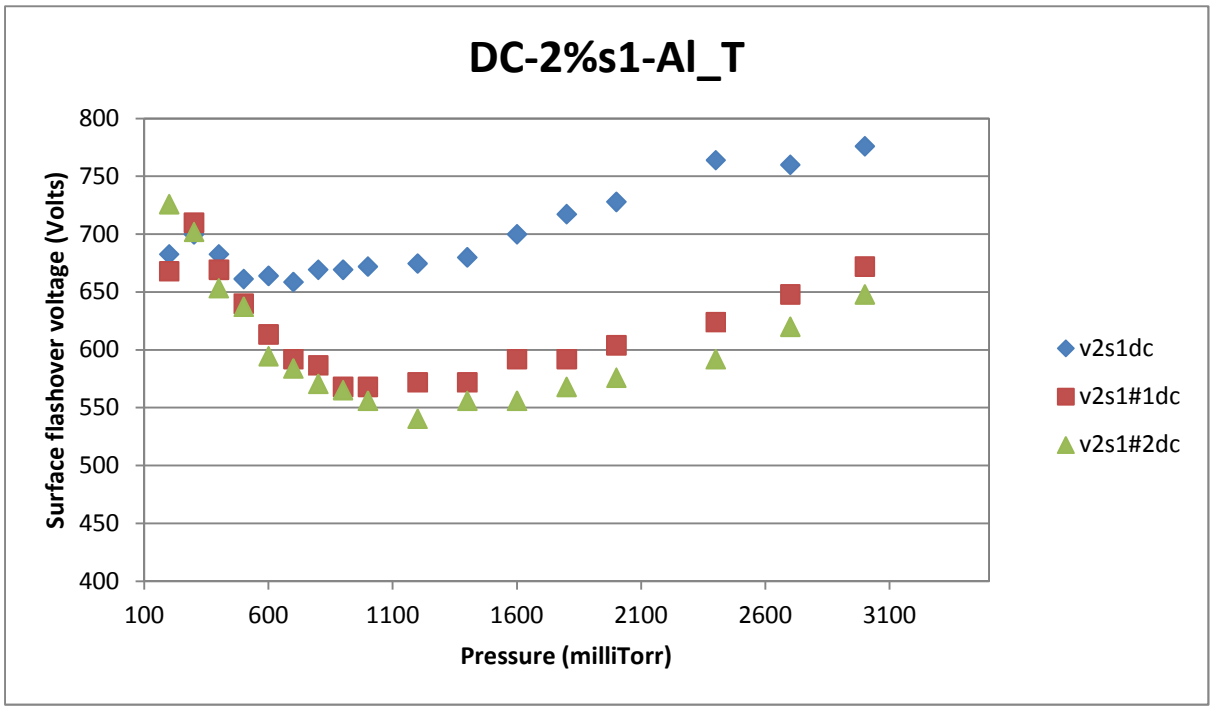

Figure B-1

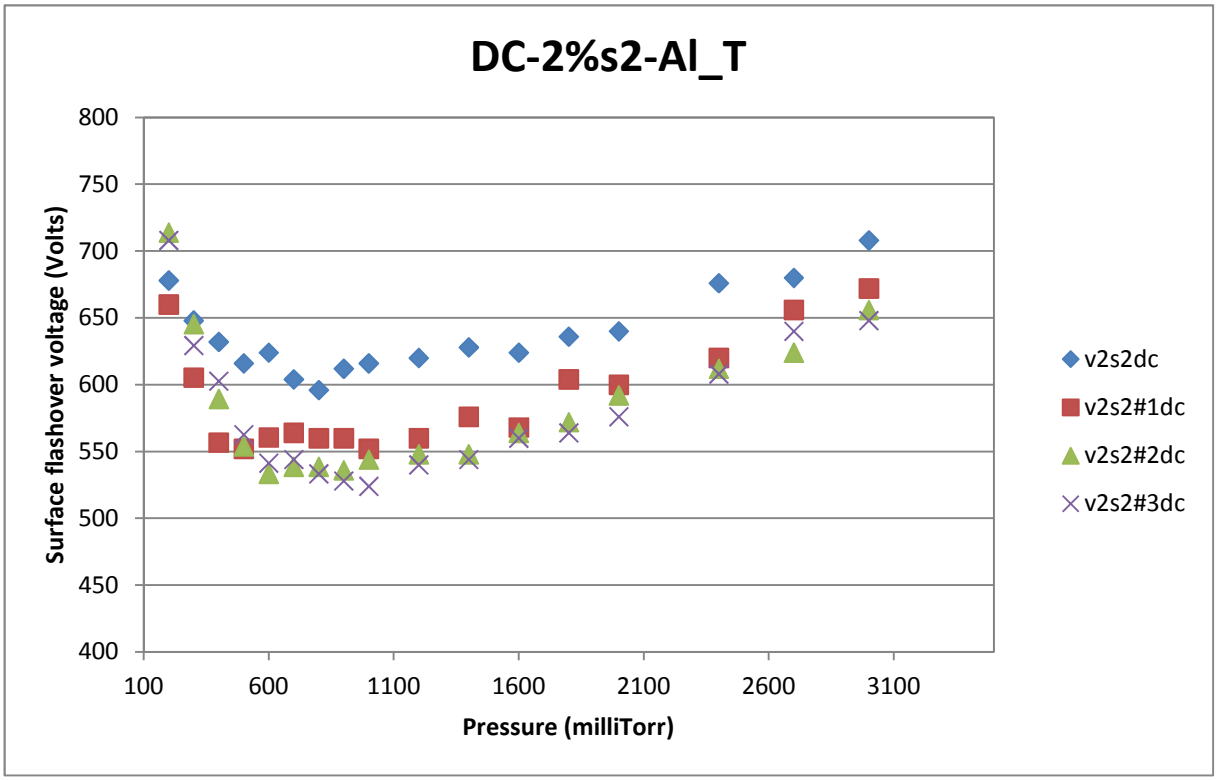

Figure B-2

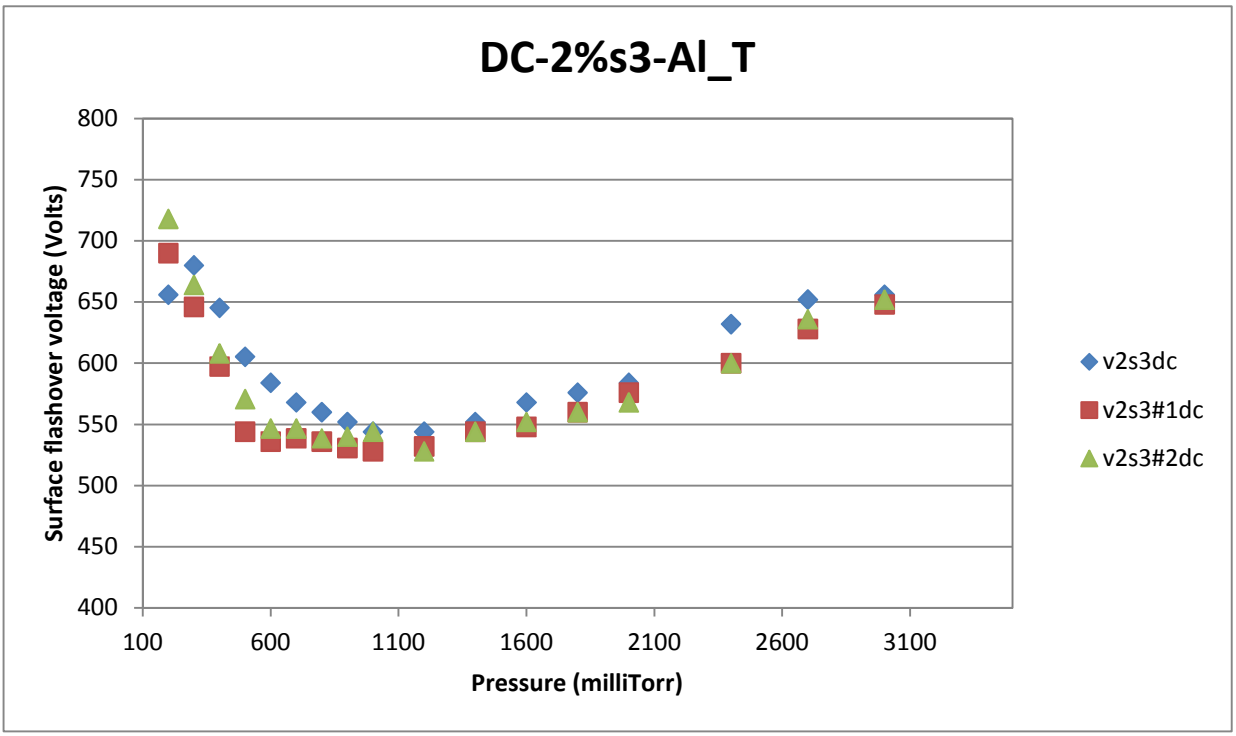

Figure B-3

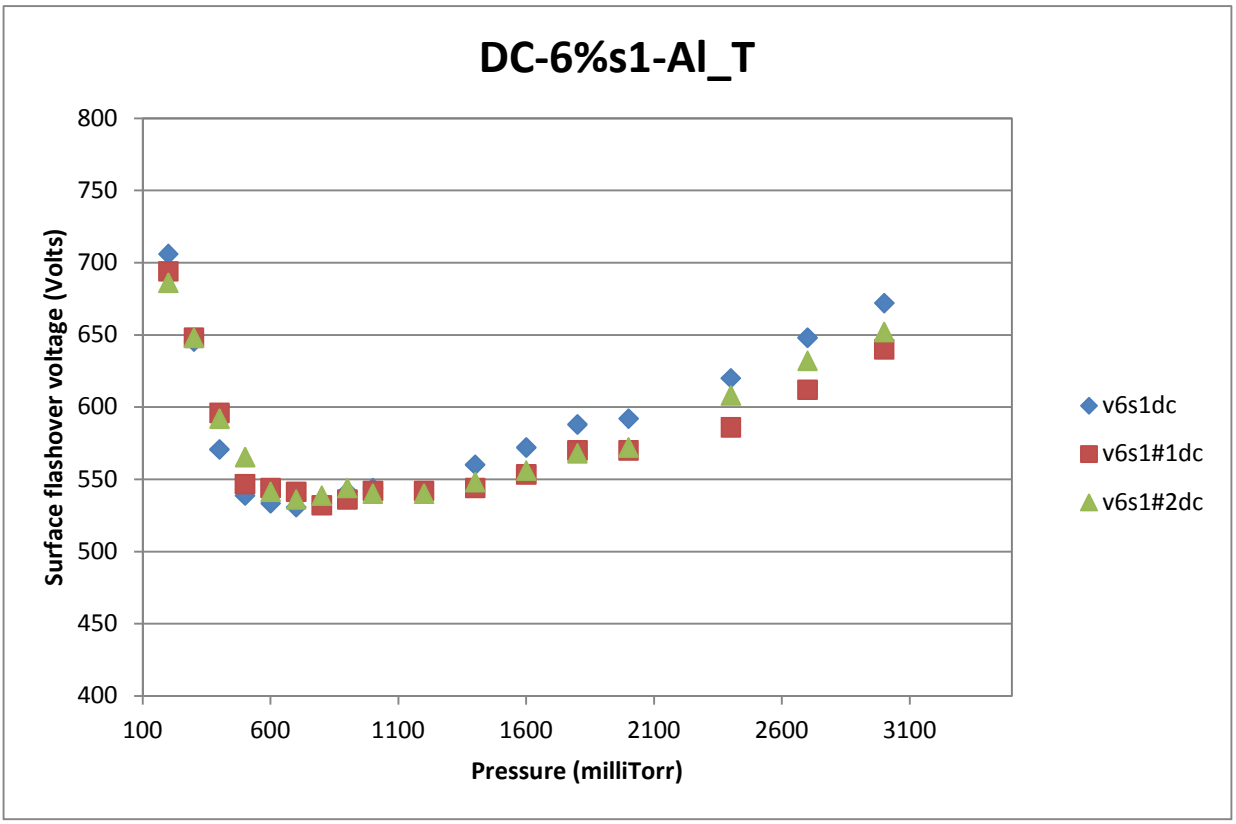

Figure B-4

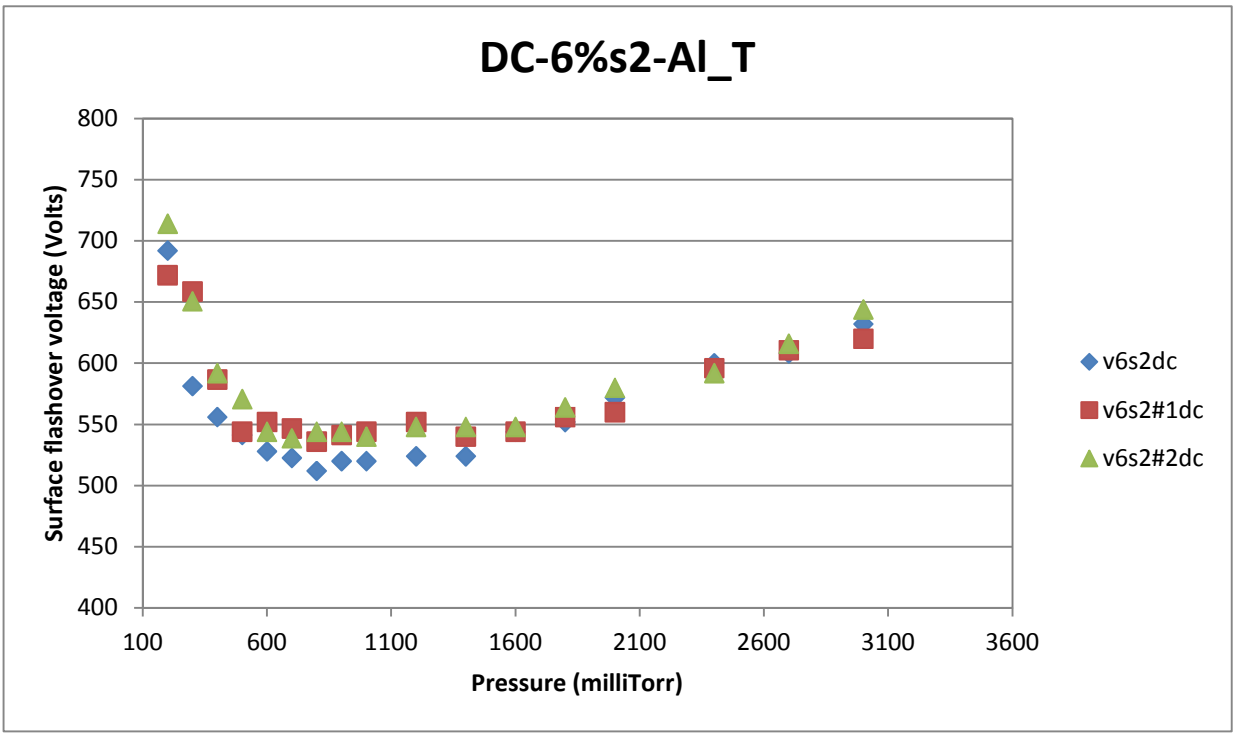

Figure B-5

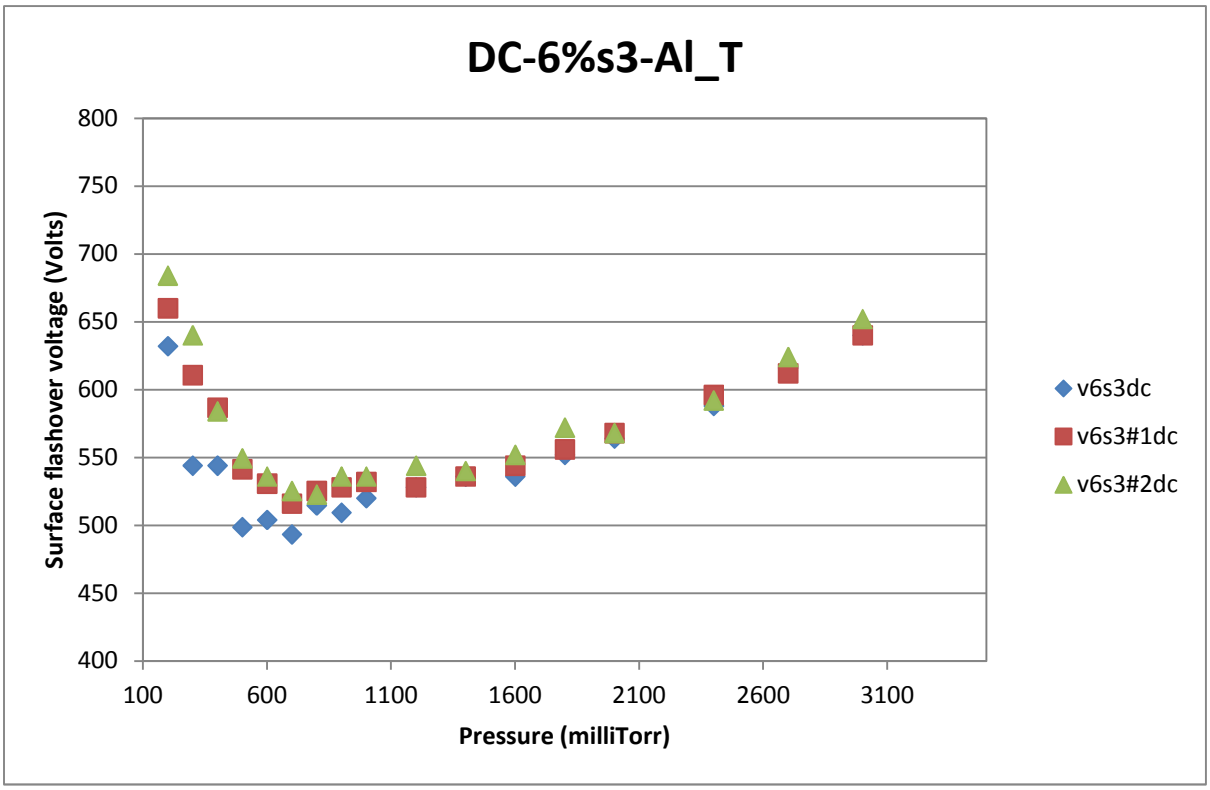

Figure B-6

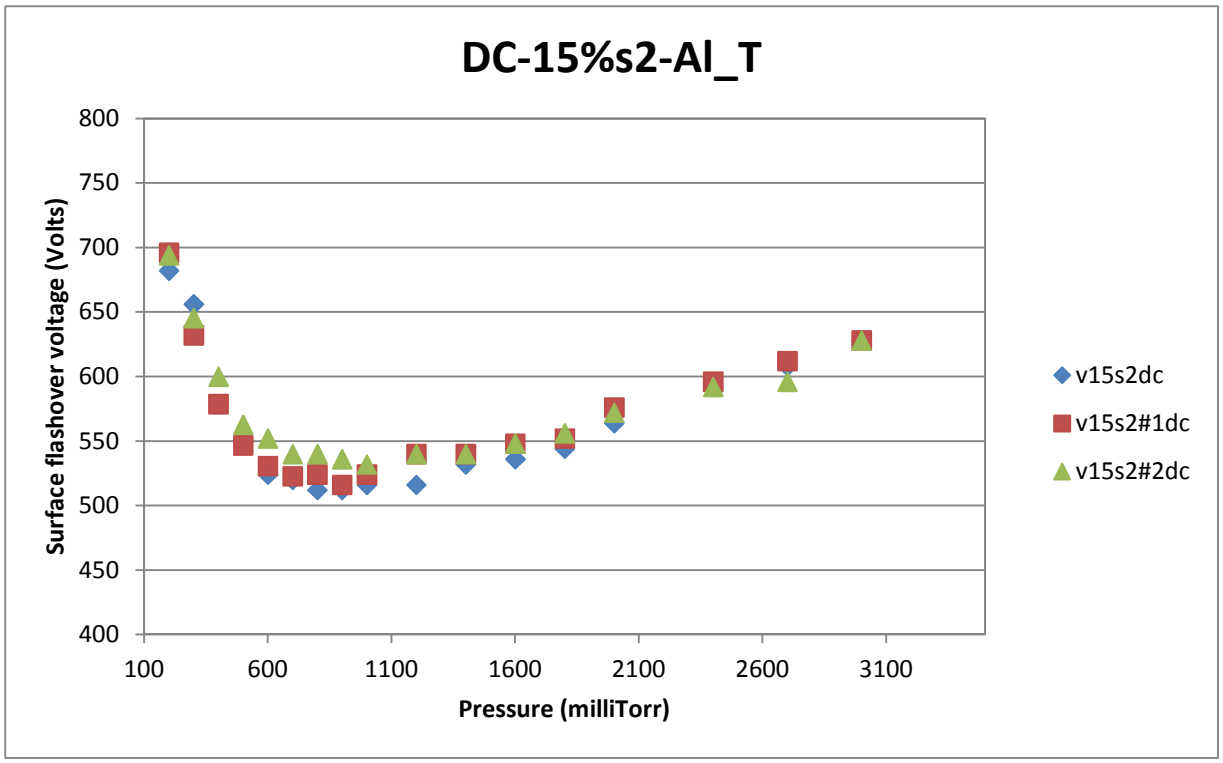

Figure B-7

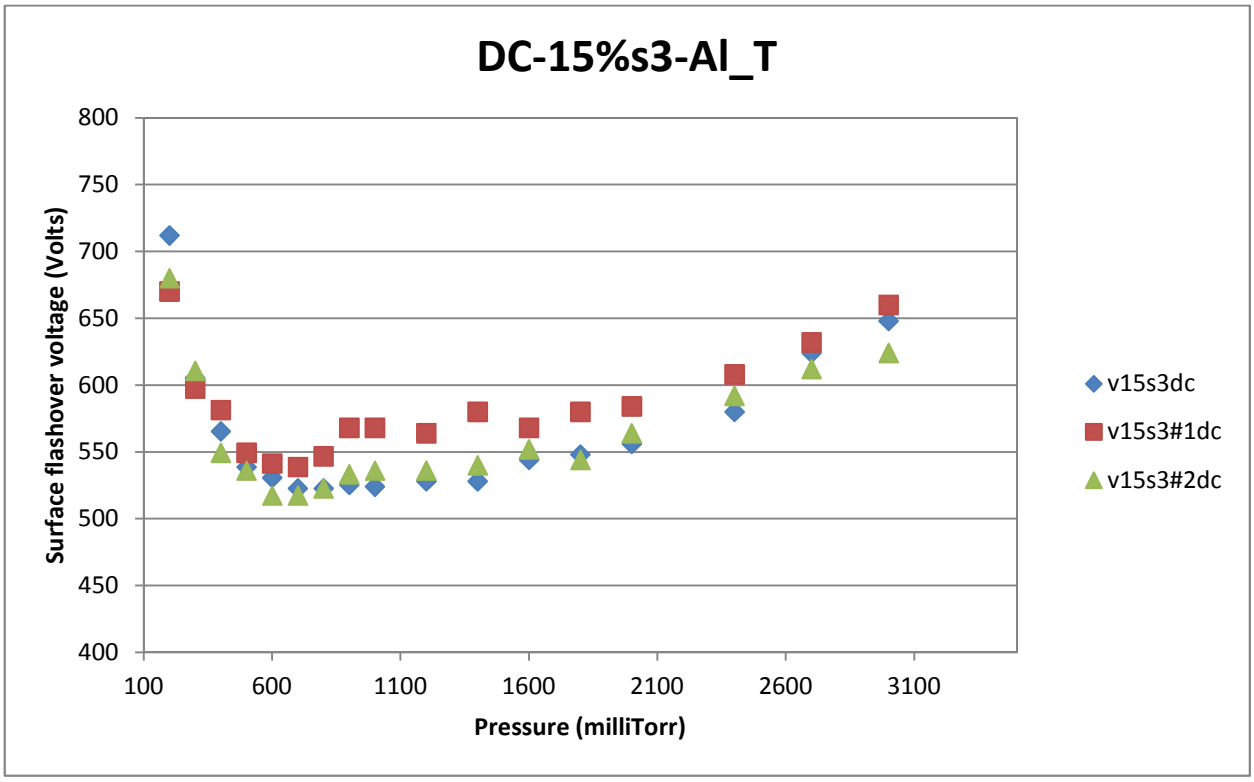

Figure B-8

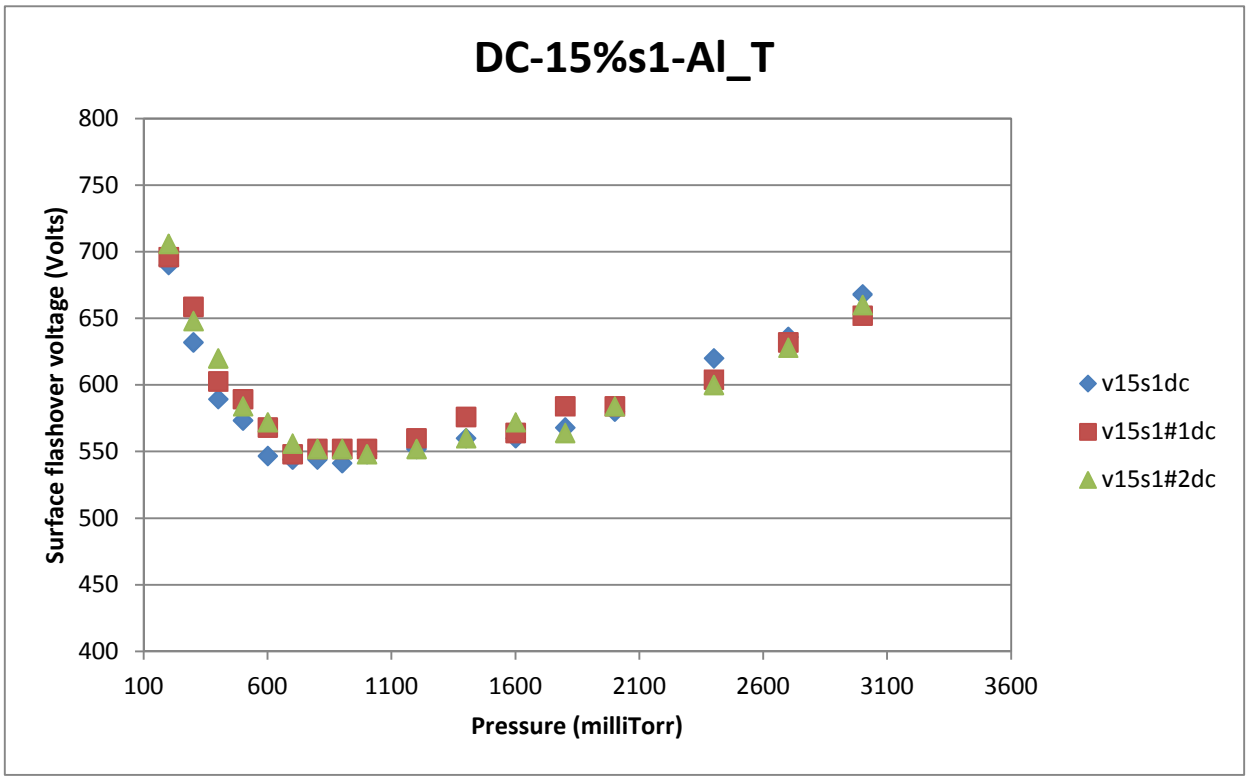

Figure B-9

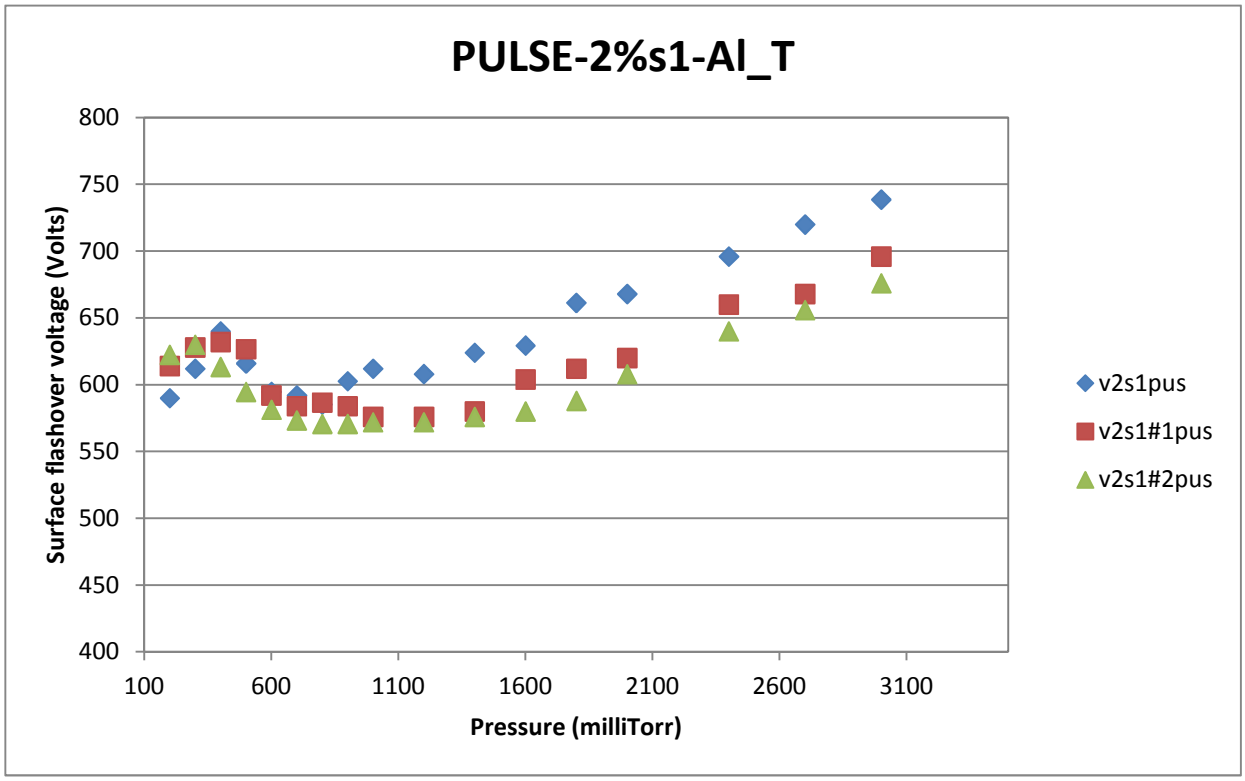

Figure B-10

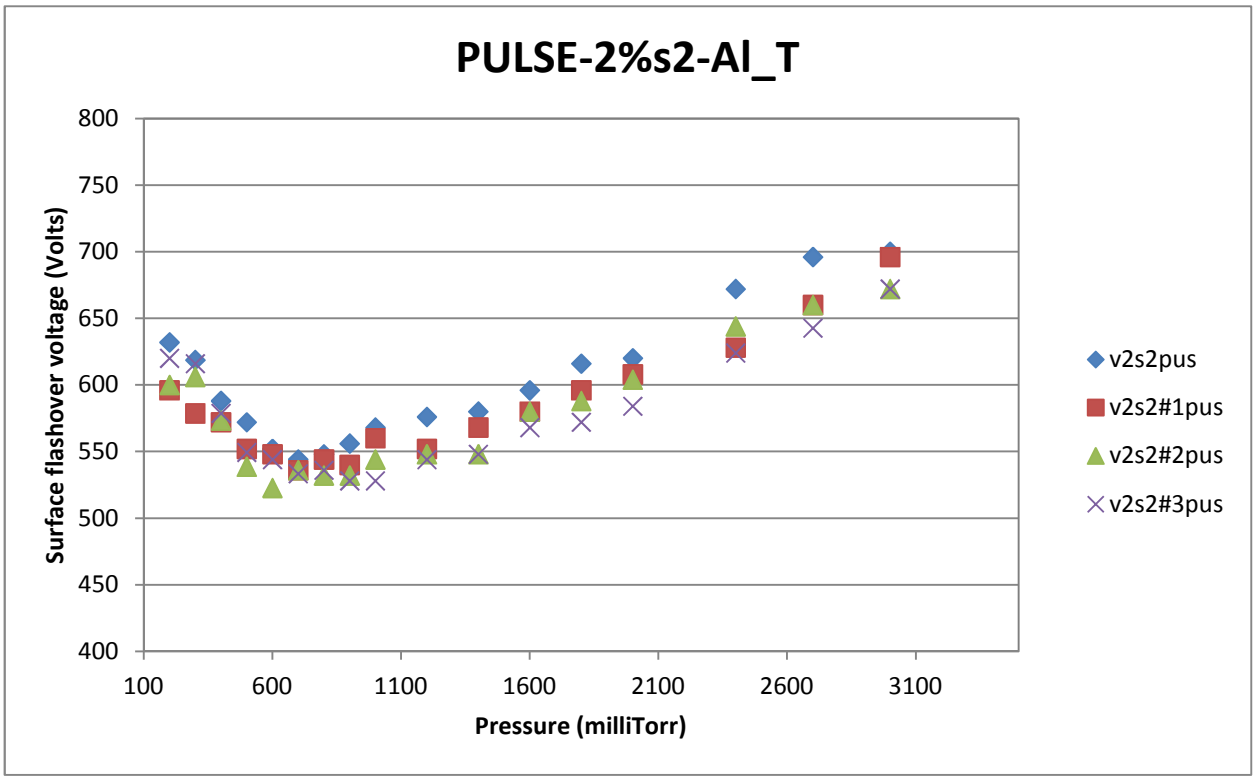

Figure B-11

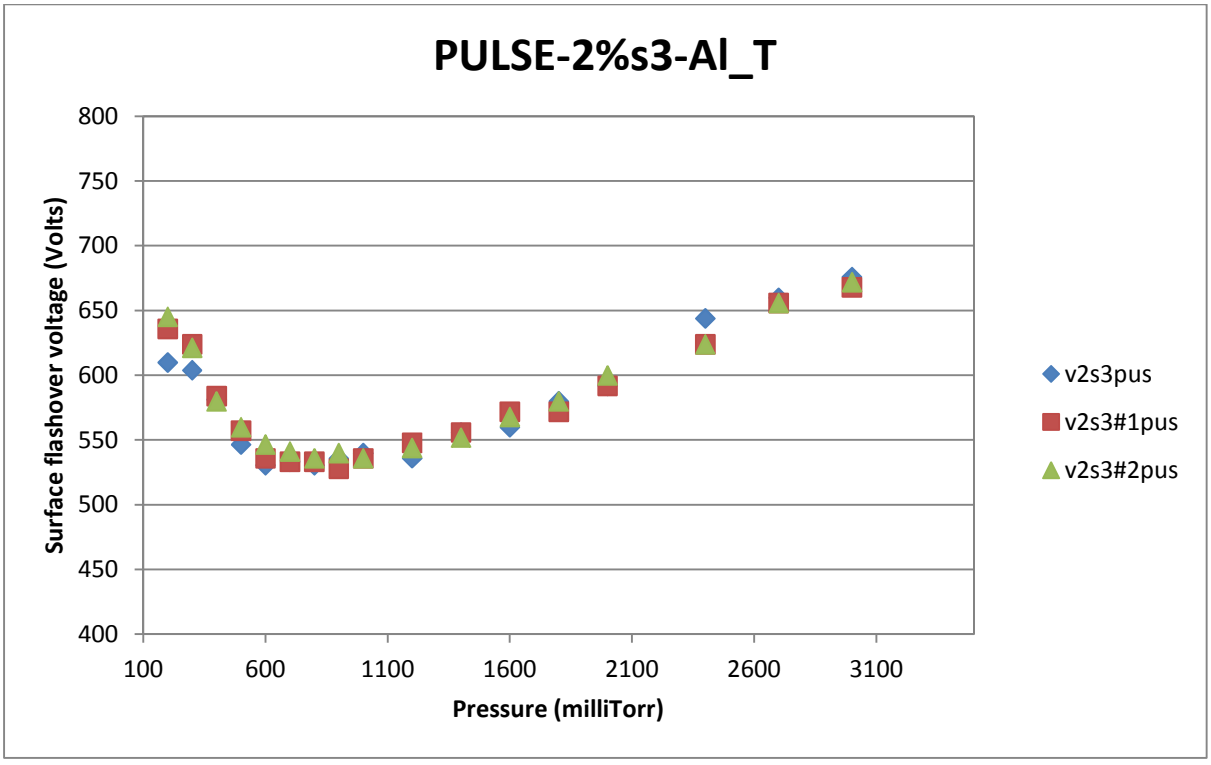

Figure B-12

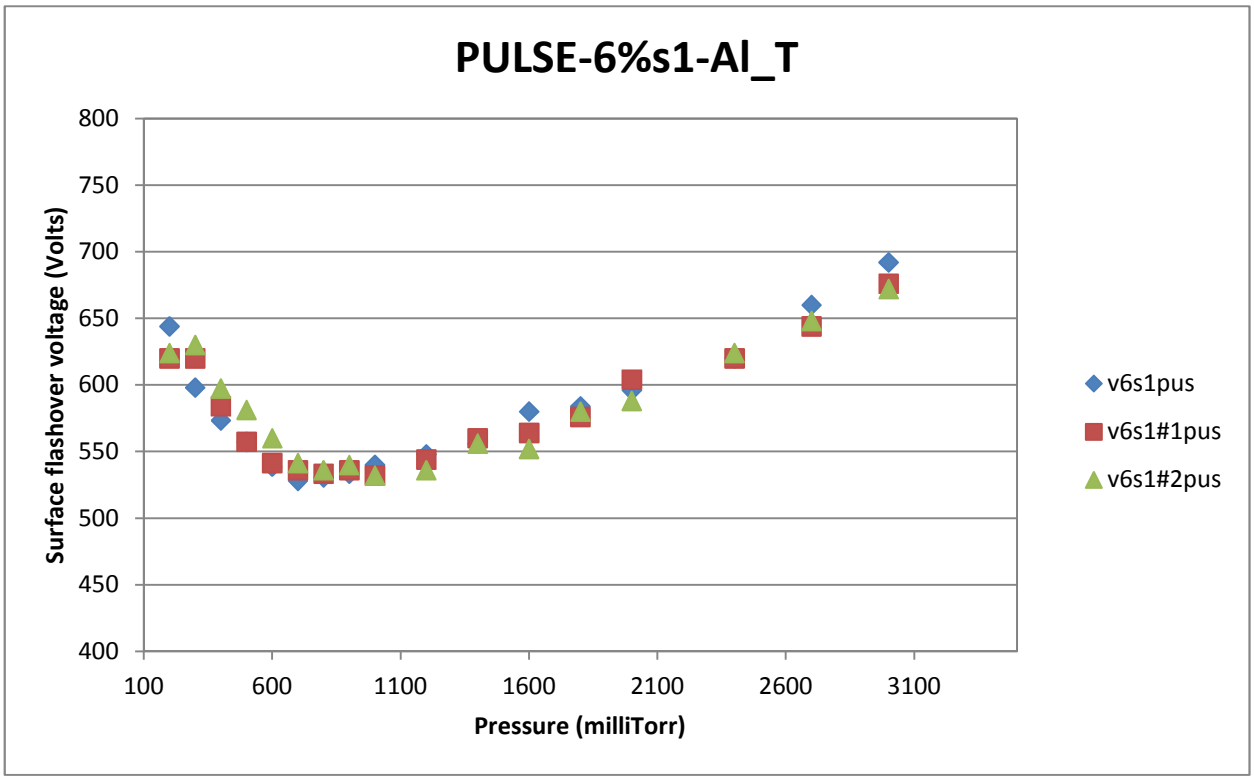

Figure B-13

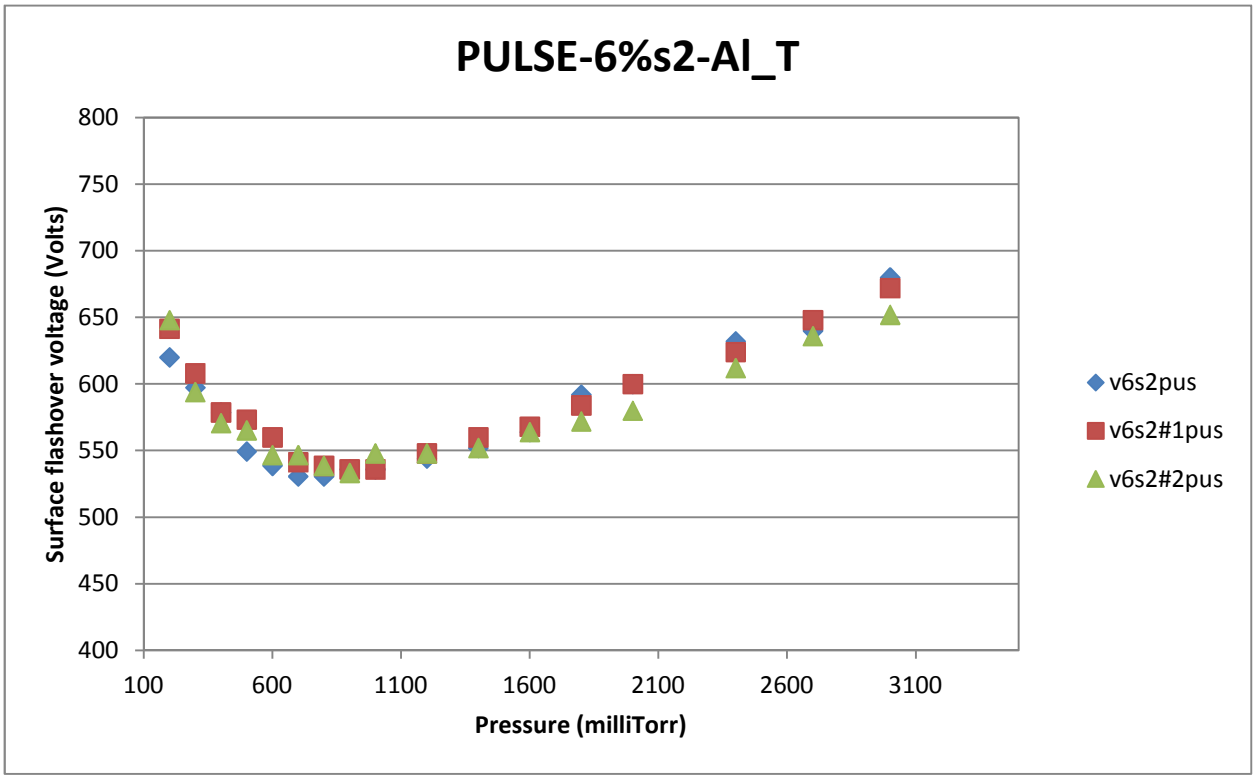

Figure B-14

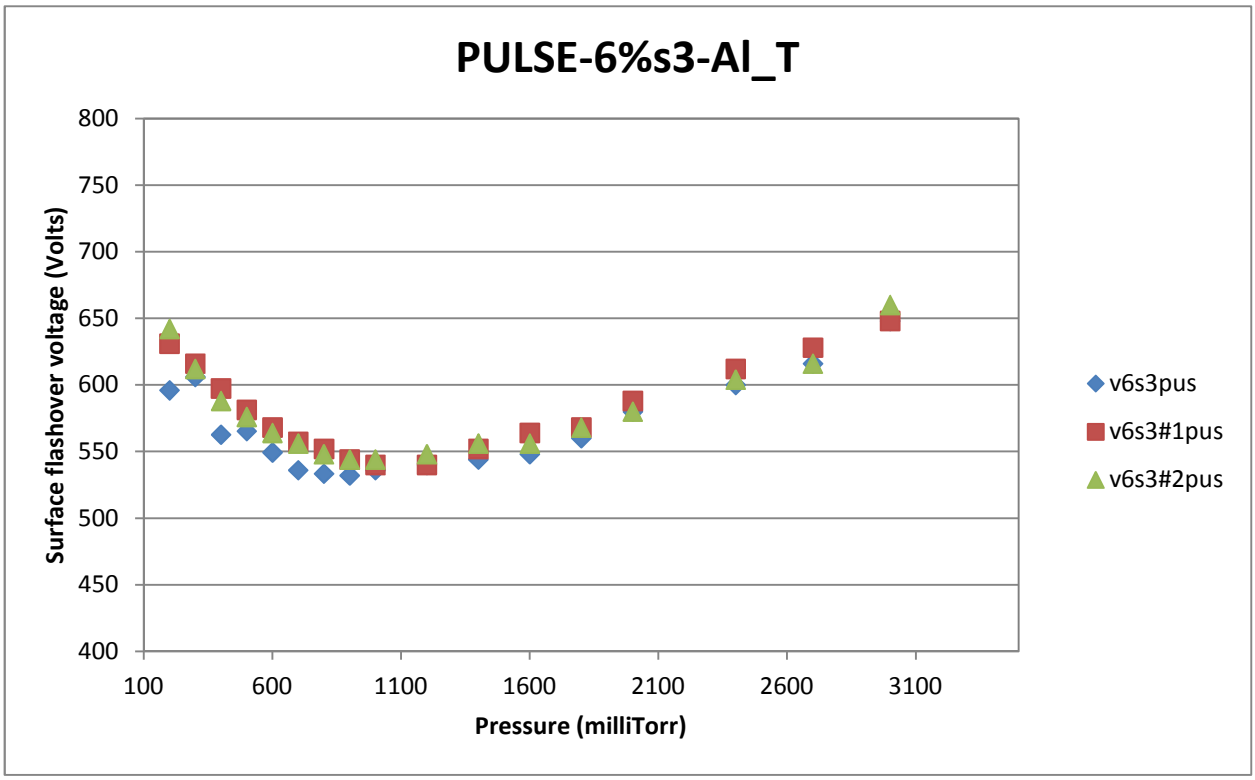

Figure B-15

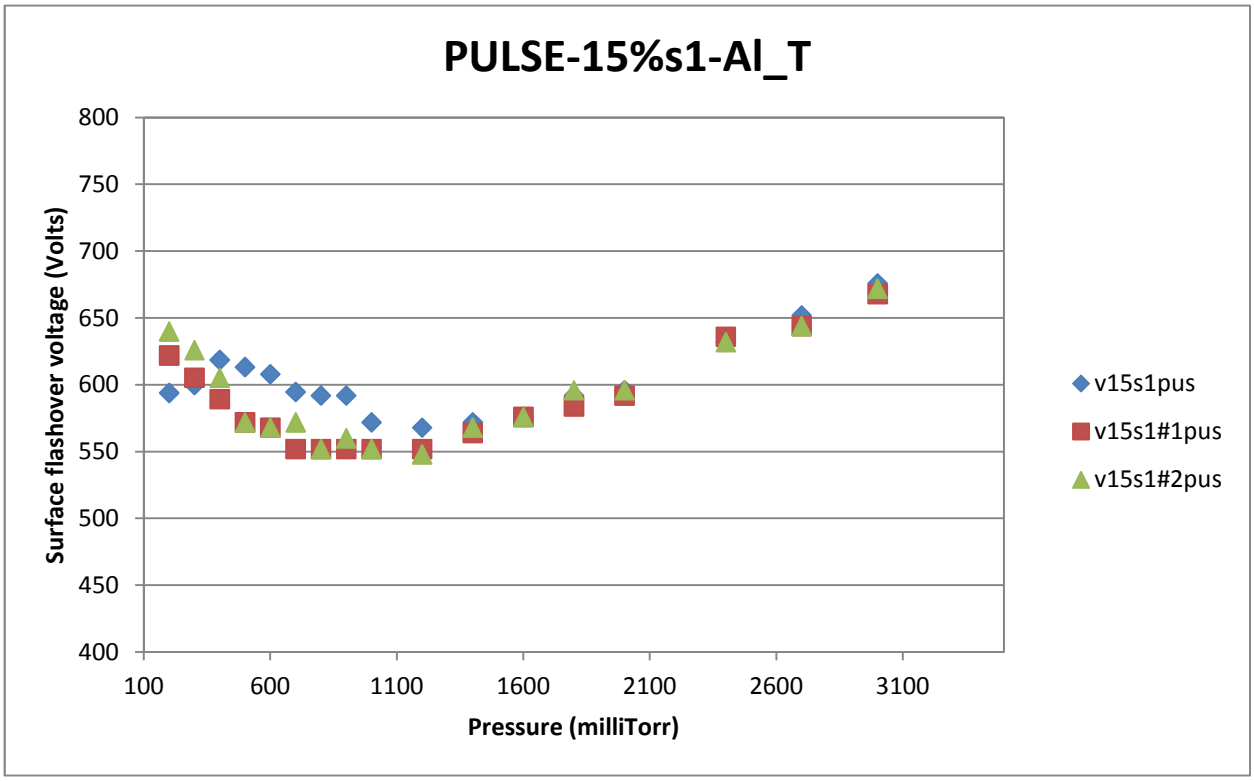

Figure B-16

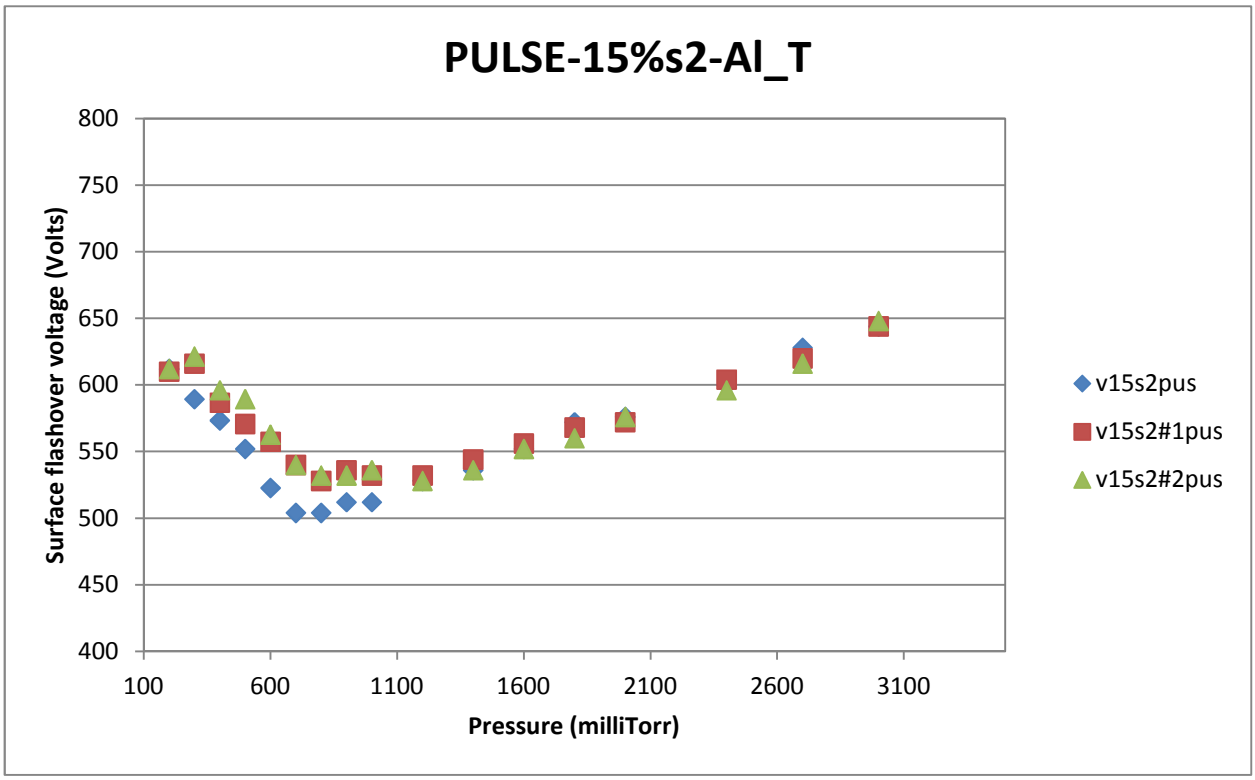

Figure B-17

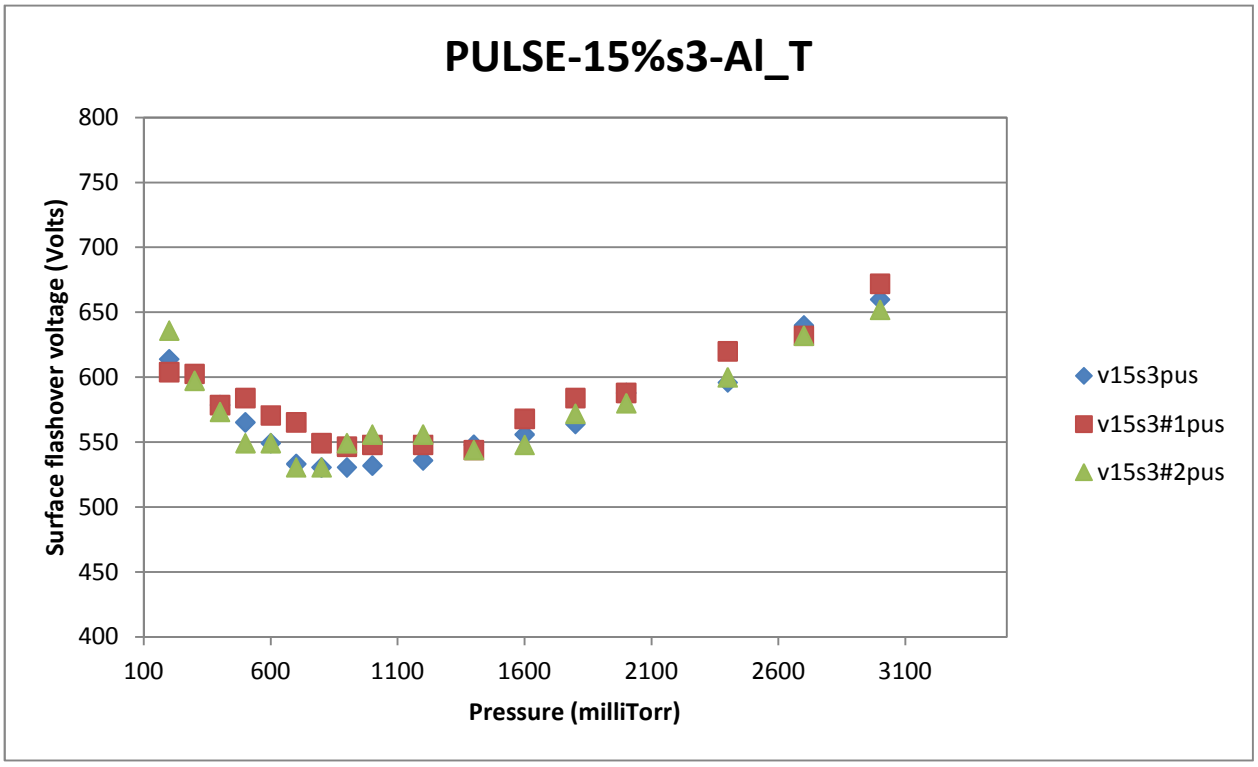

Figure B-18

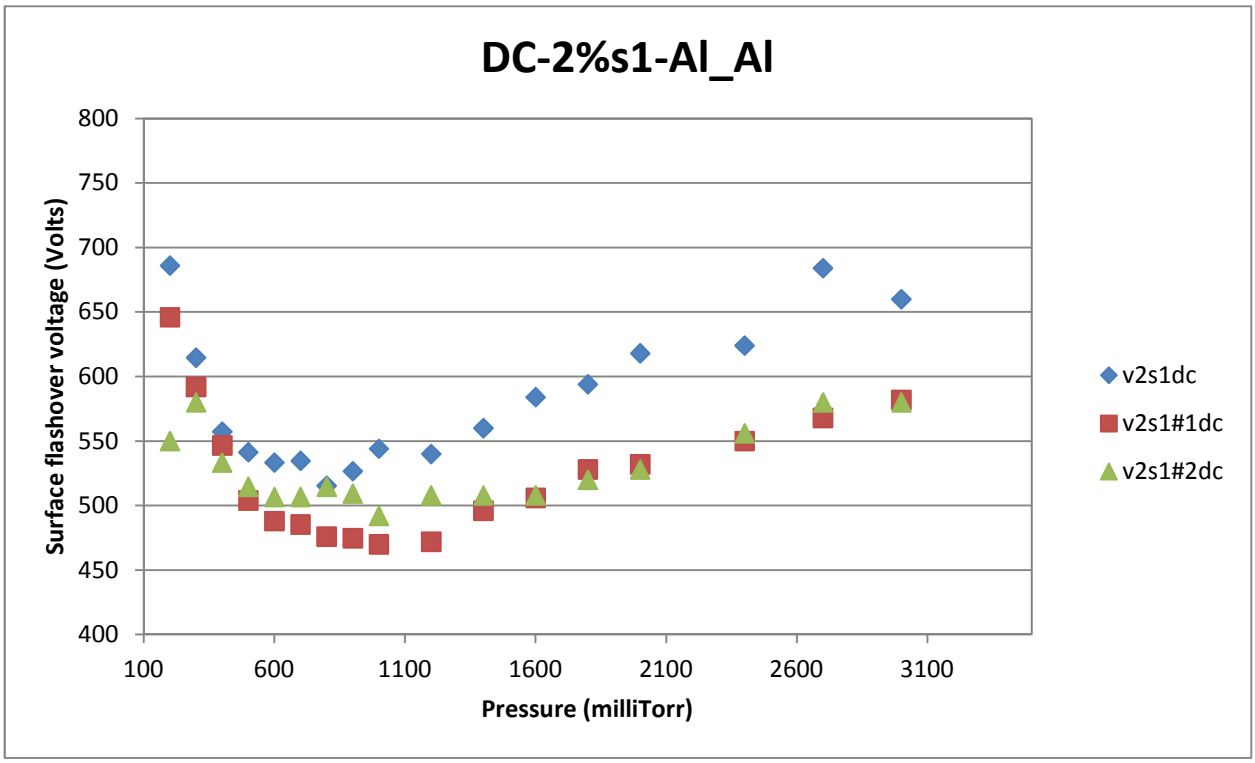

Figure B-19

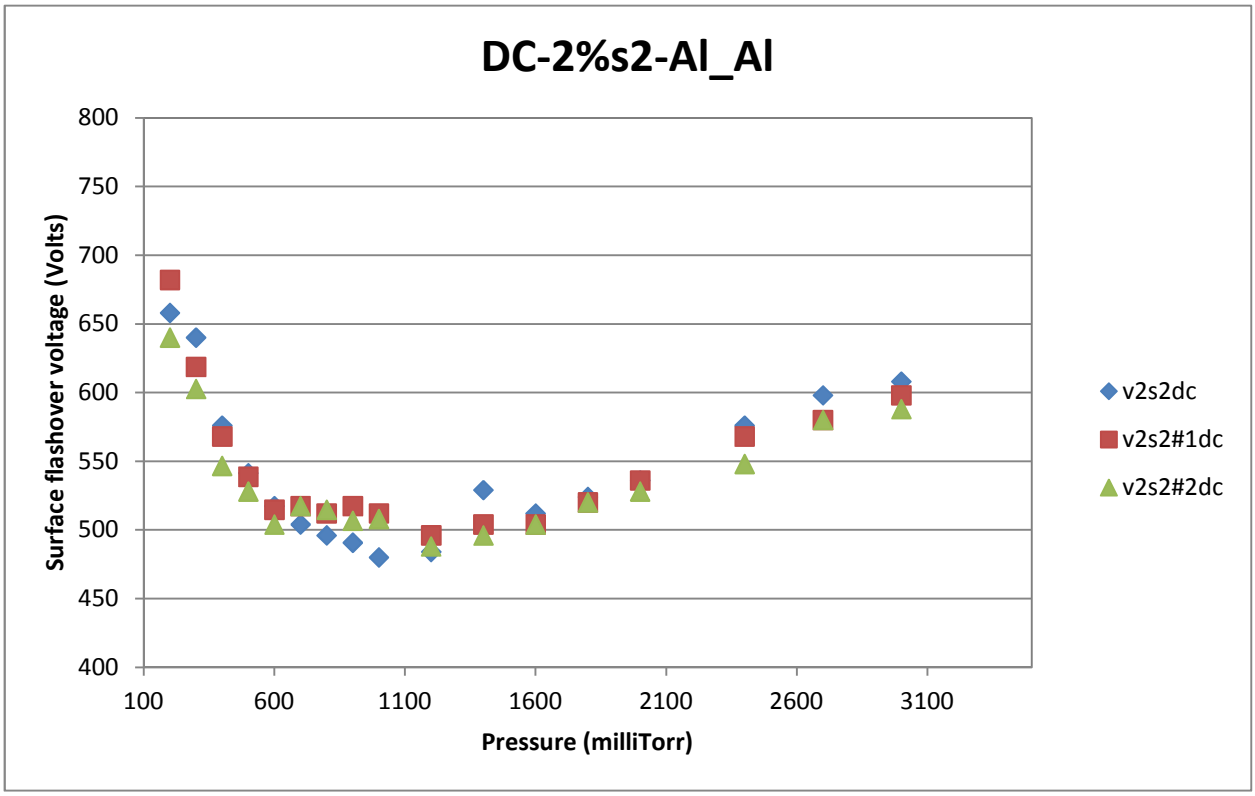

Figure B-20

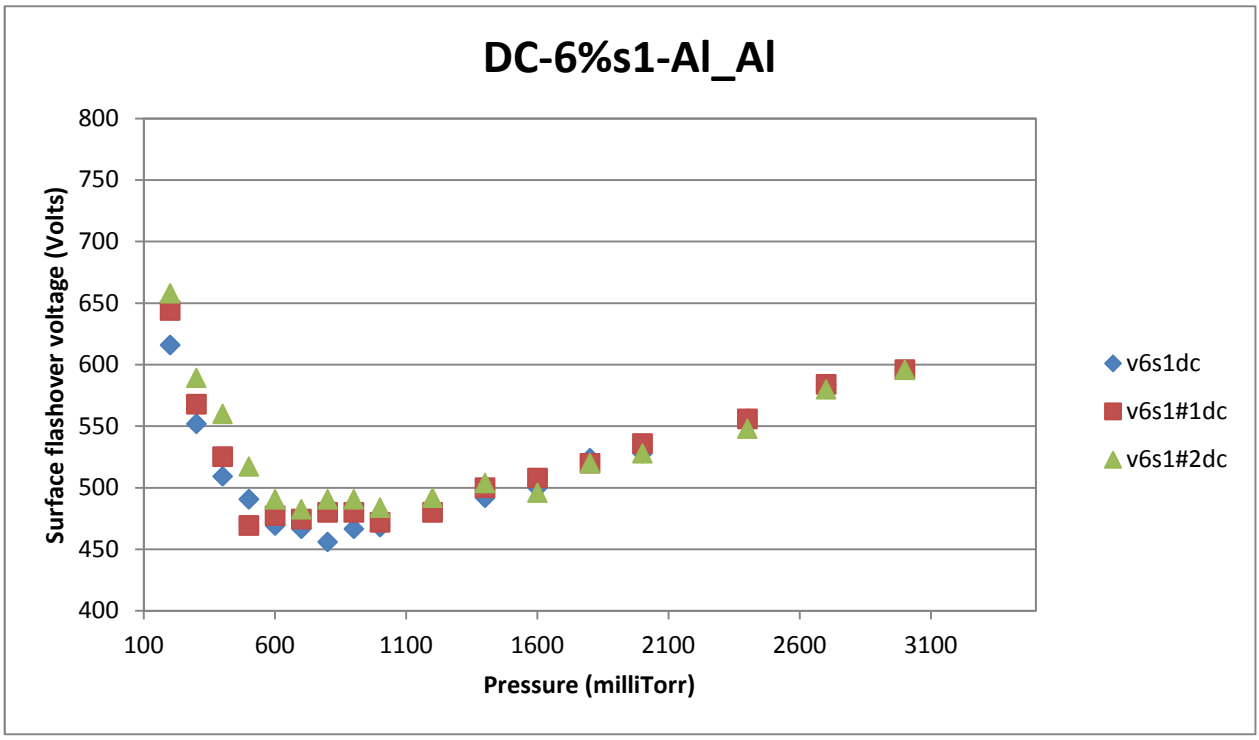

Figure B-21

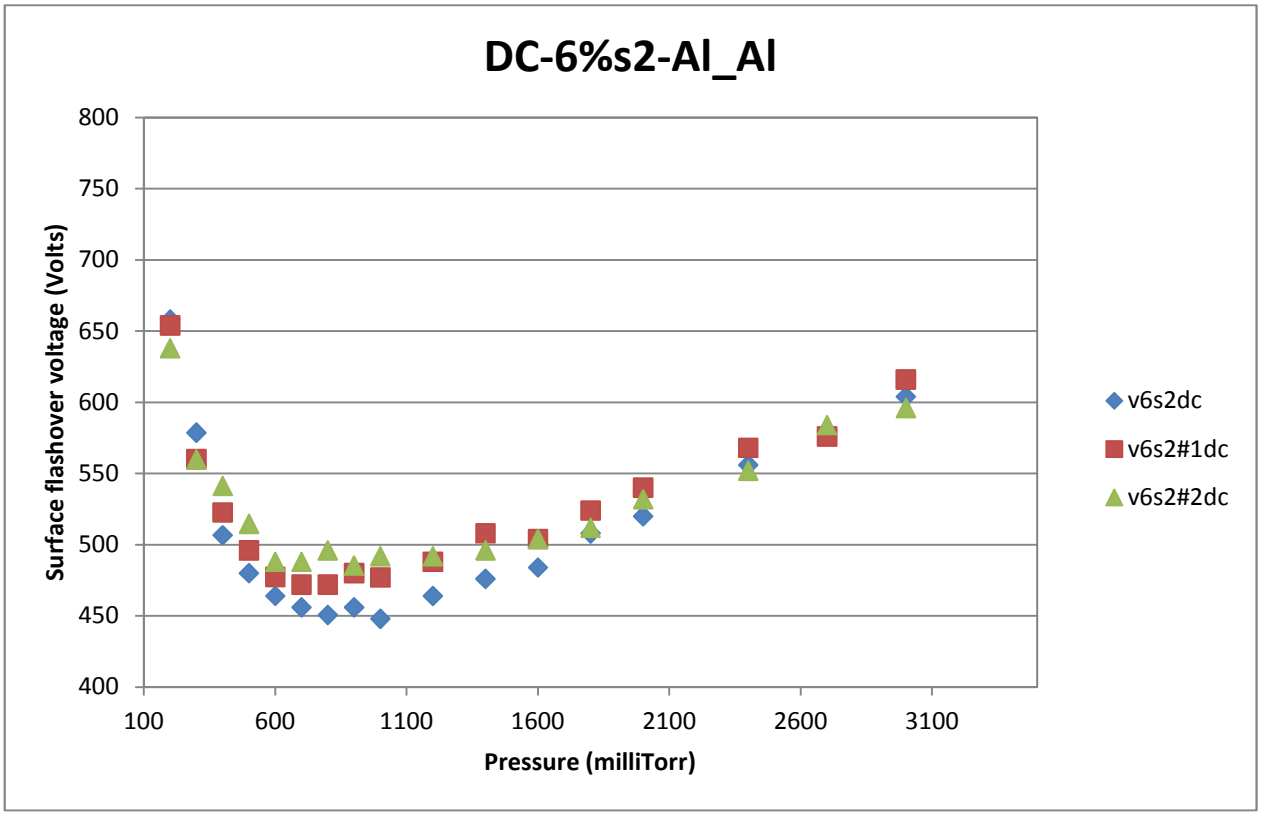

Figure B-22

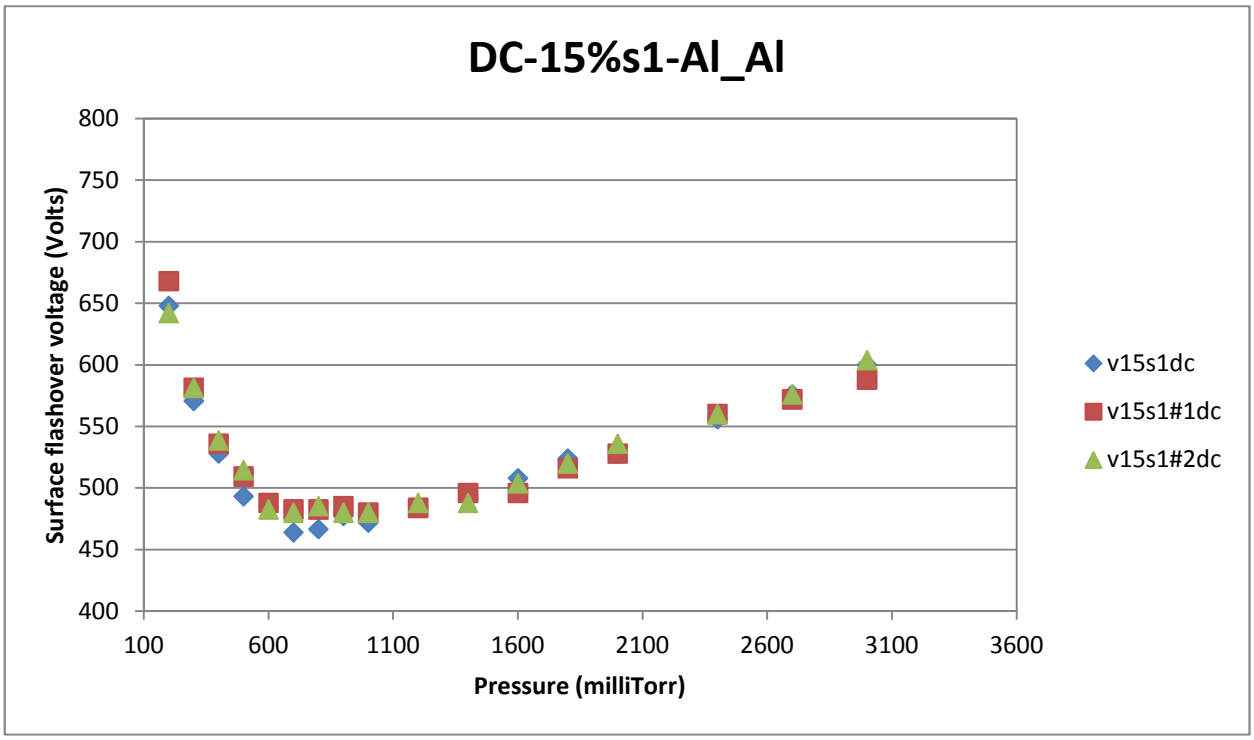

Figure B-23

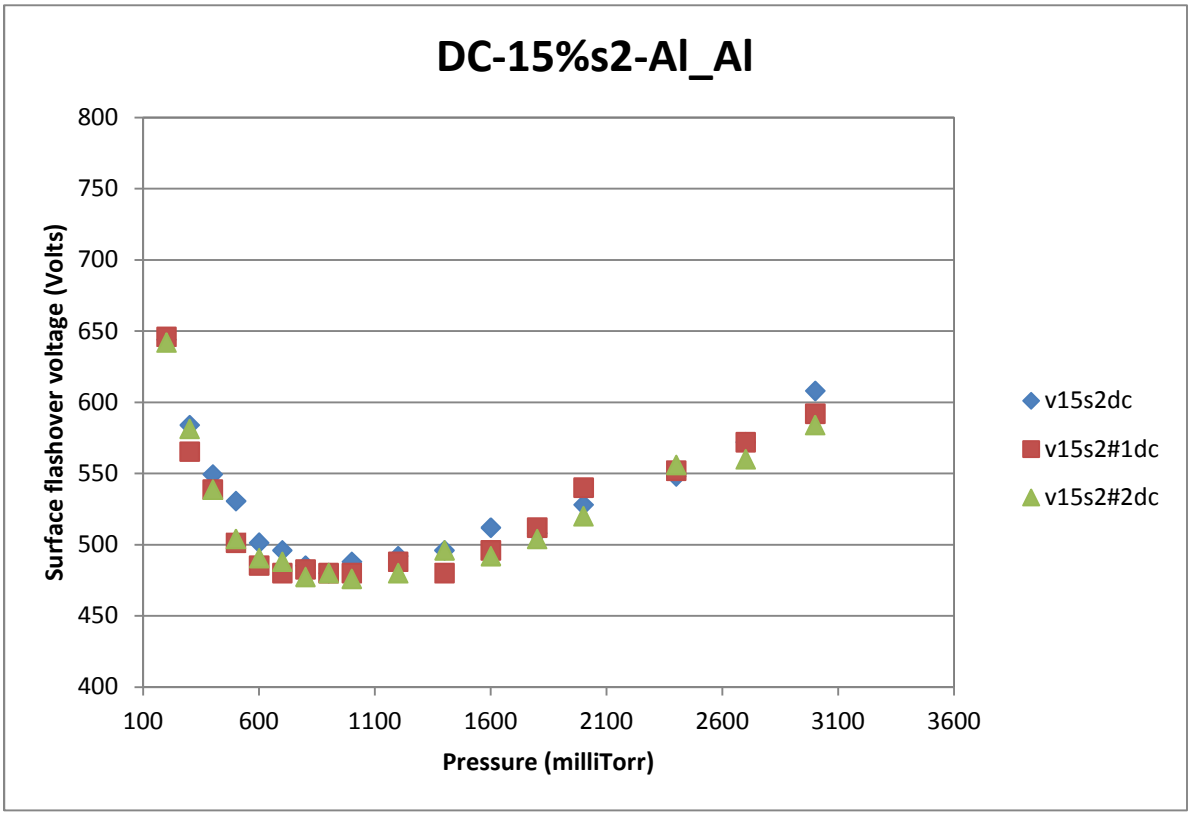

Figure B-24

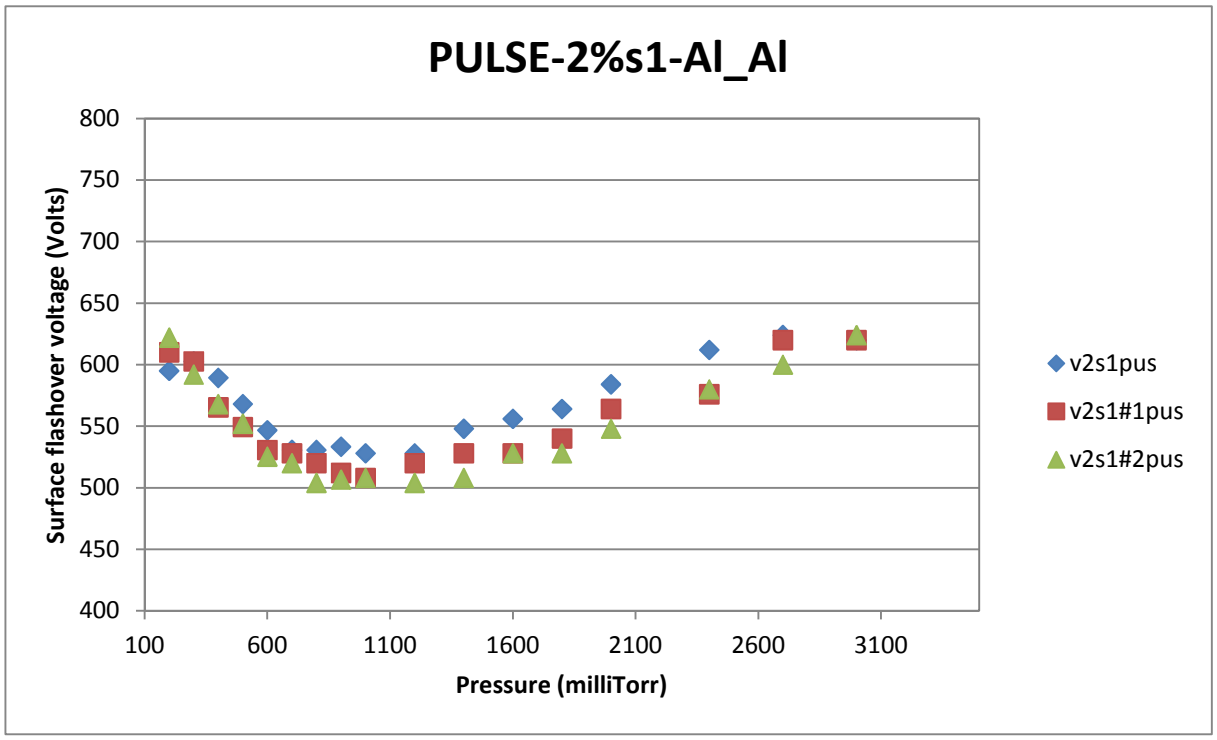

Figure B-25

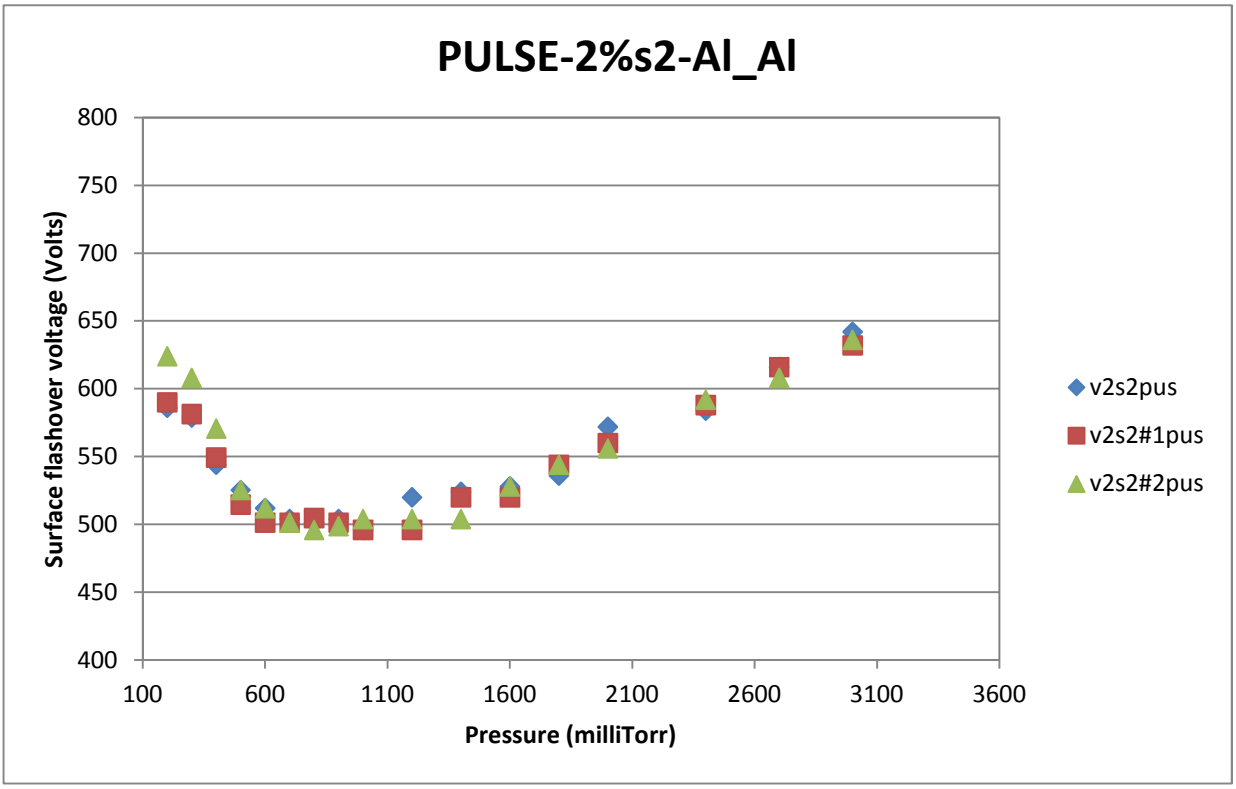

Figure B-26

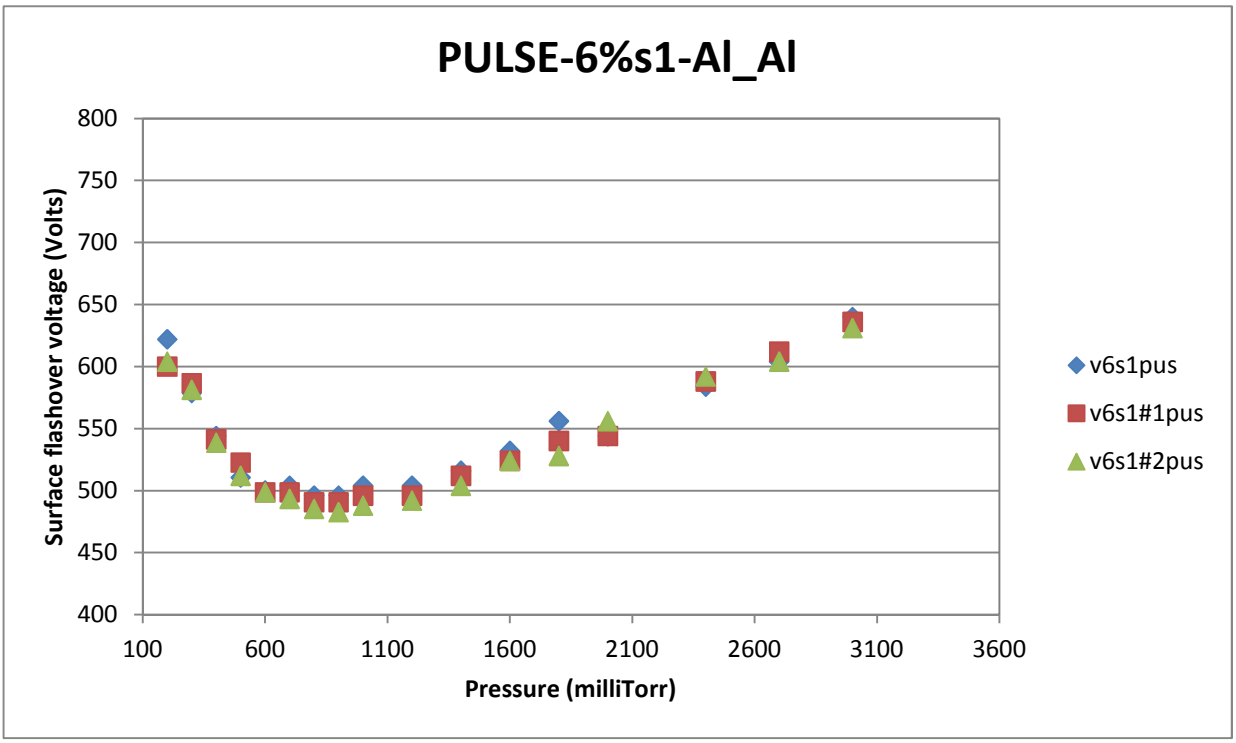

Figure B-27

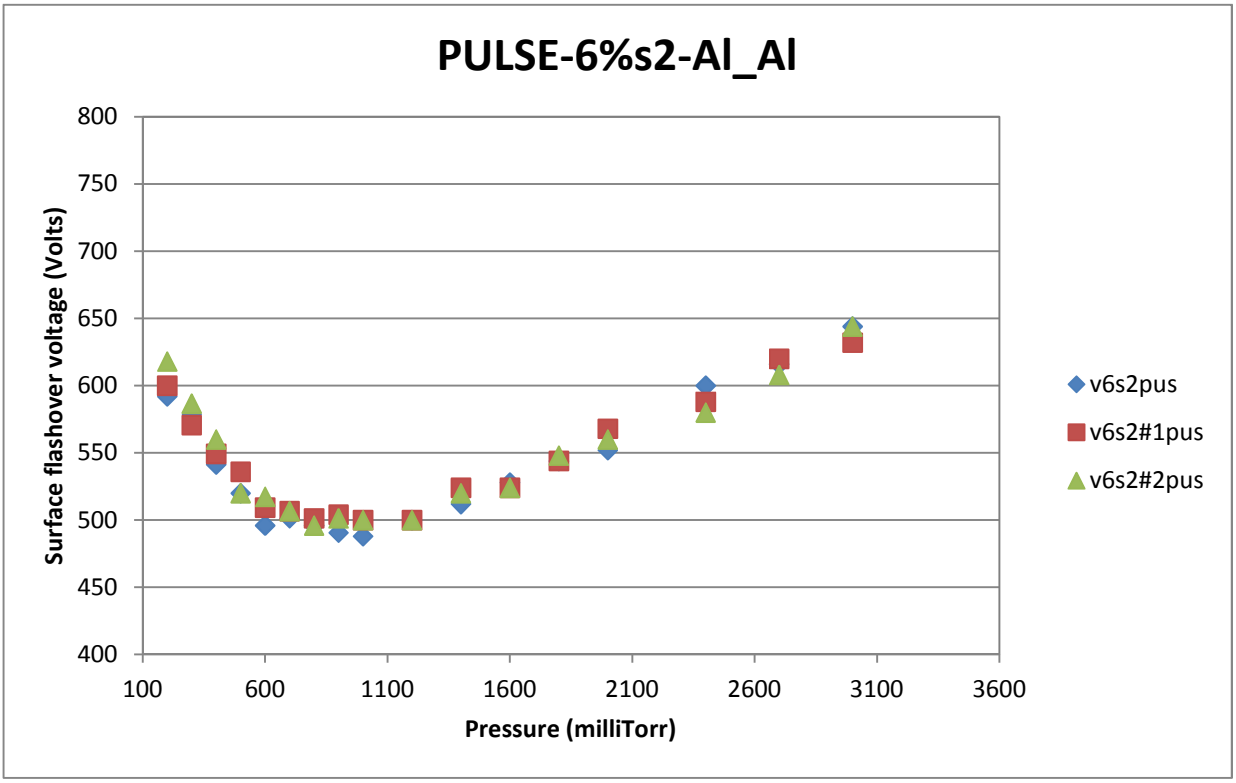

Figure B-28

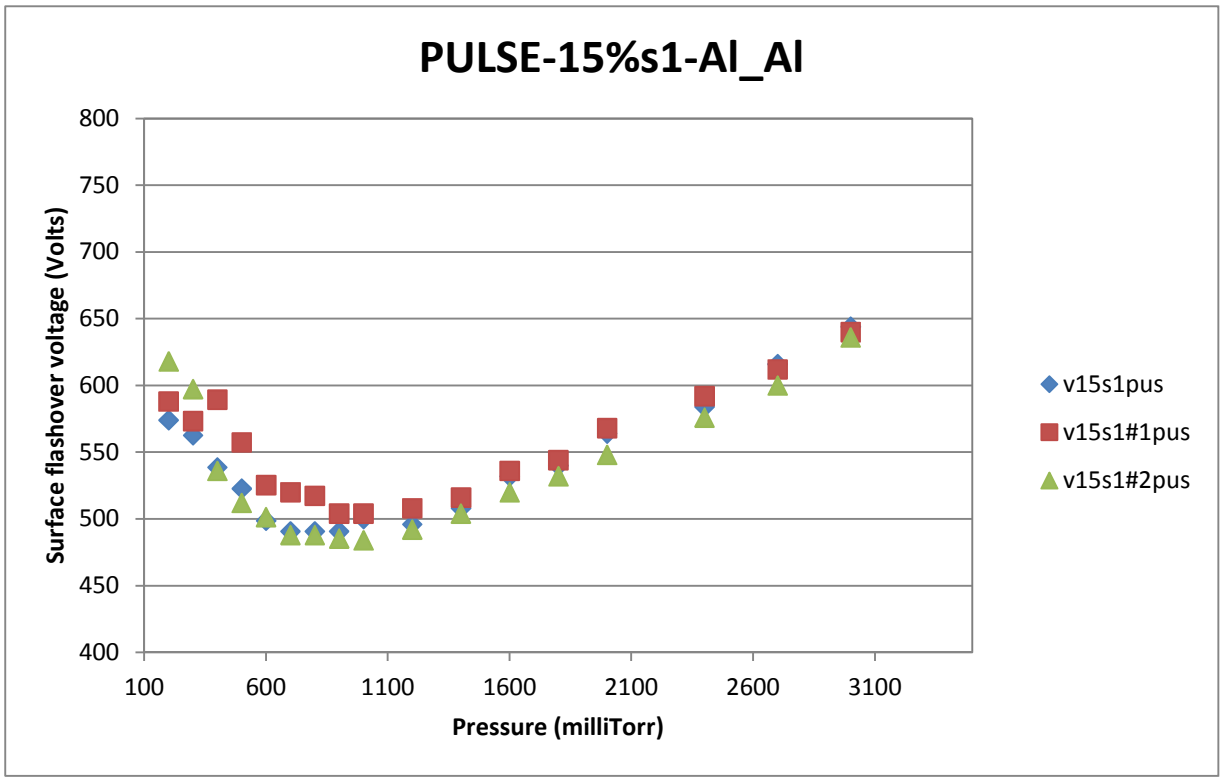

Figure B-29

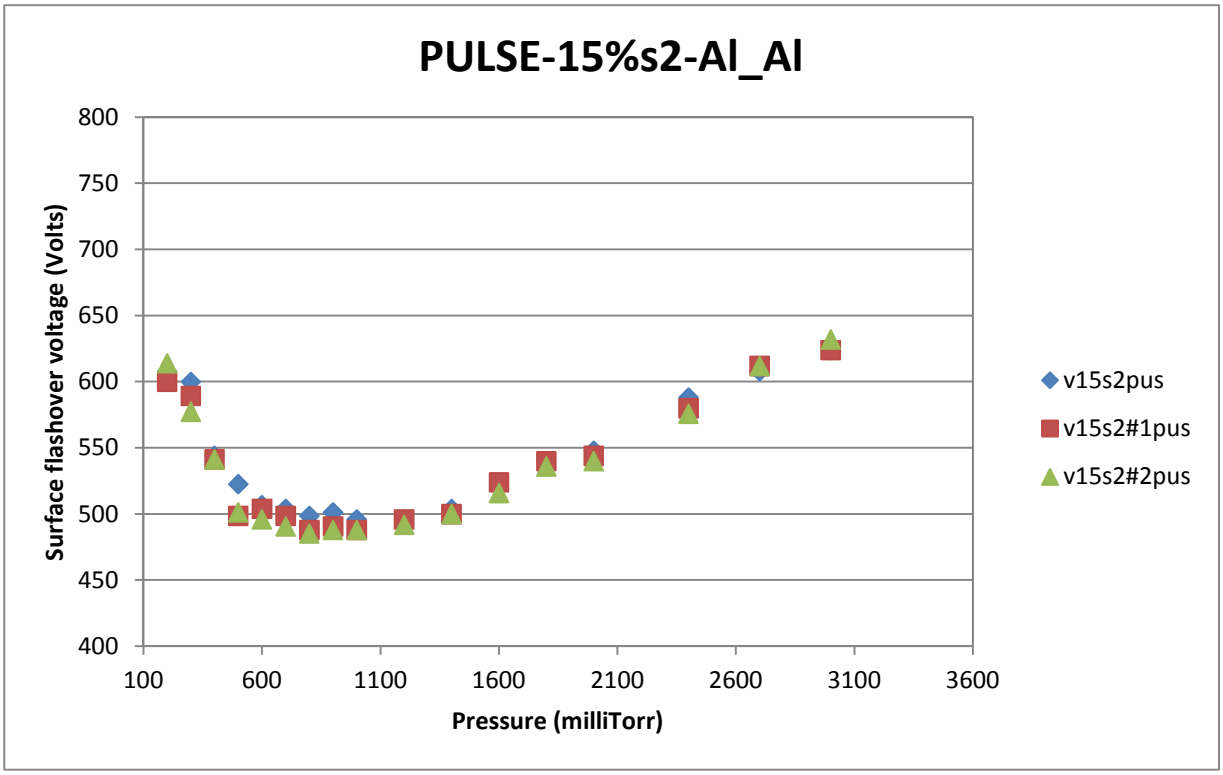

Figure B-30

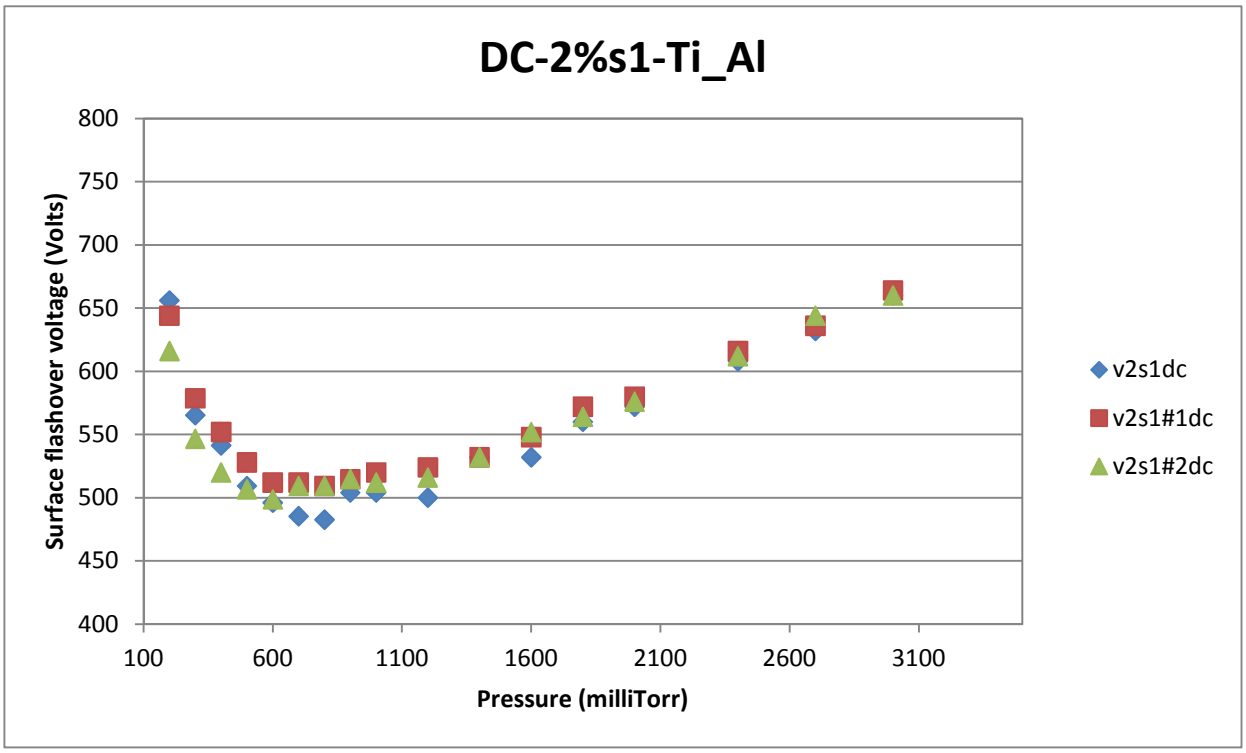

Figure B-31

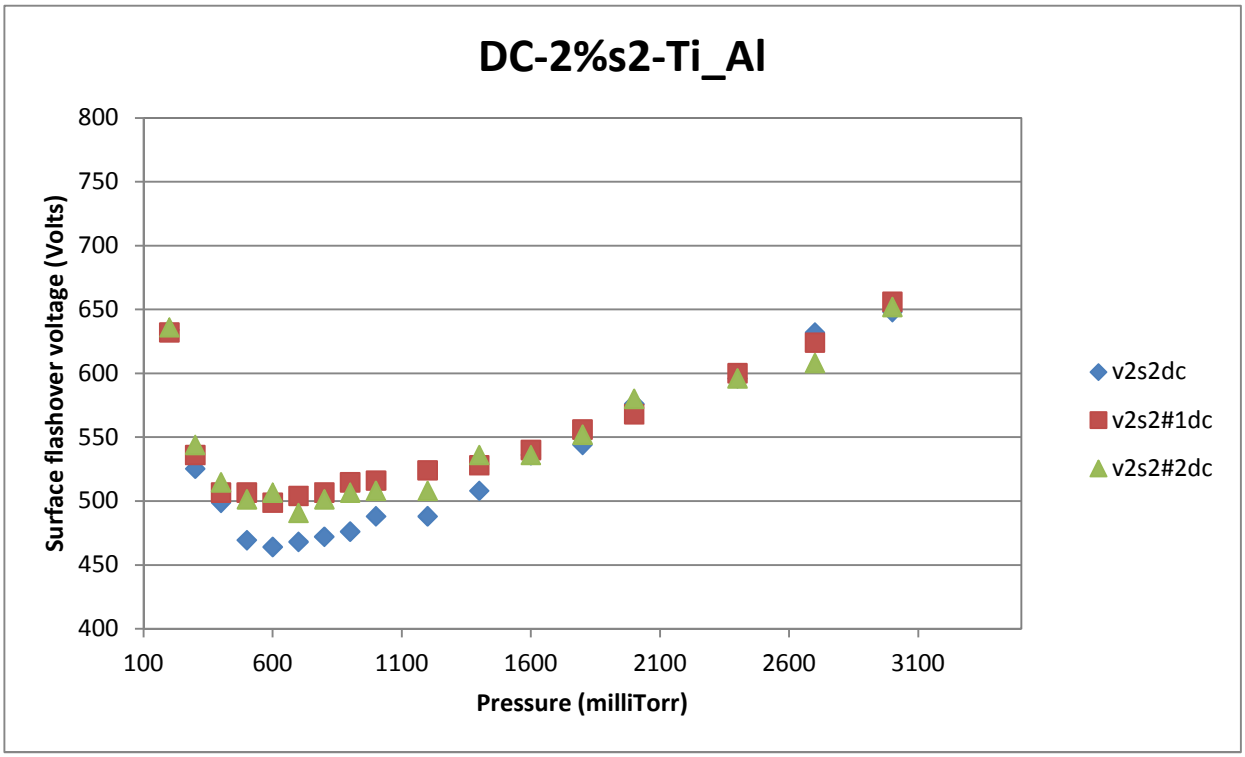

Figure B-32

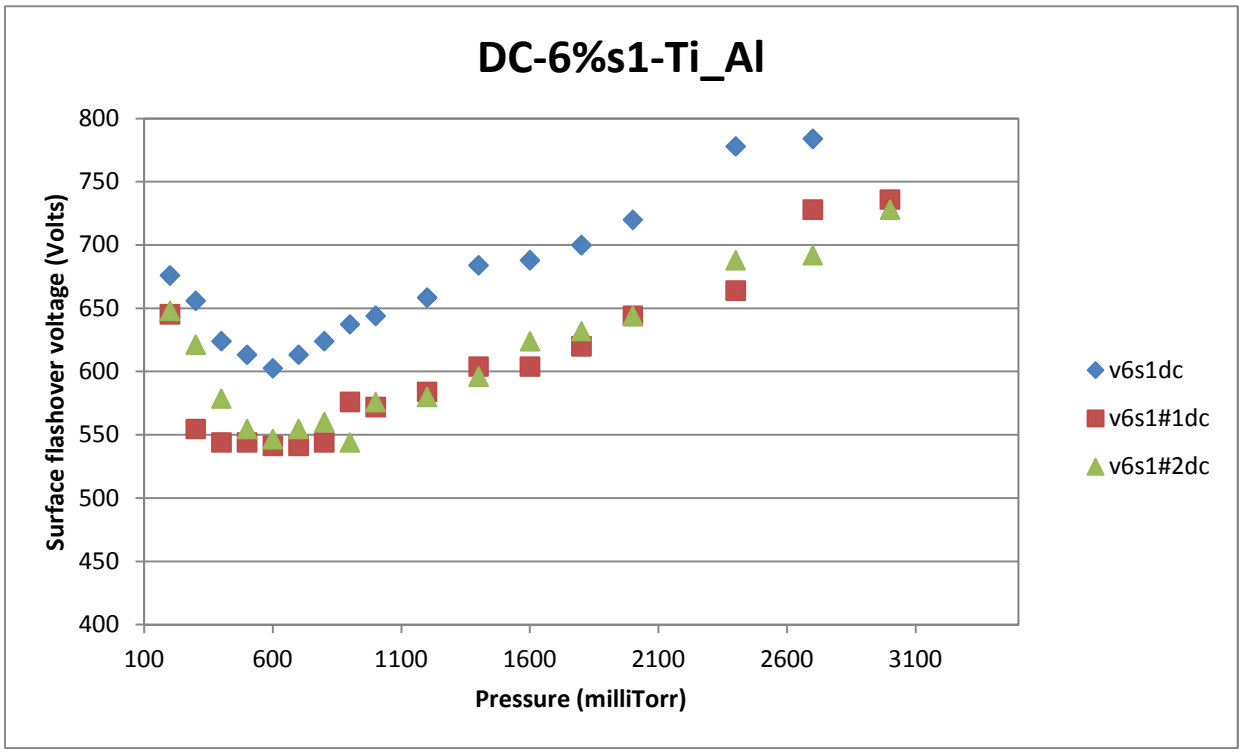

Figure B-33

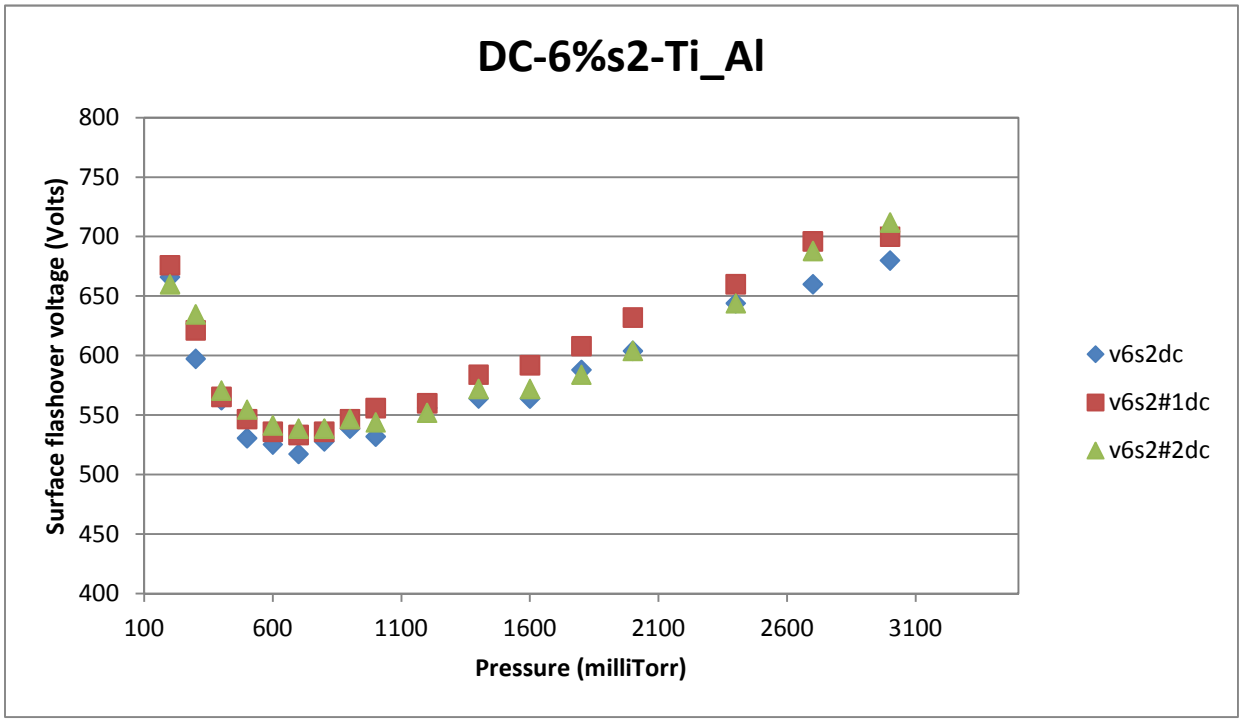

Figure B-34

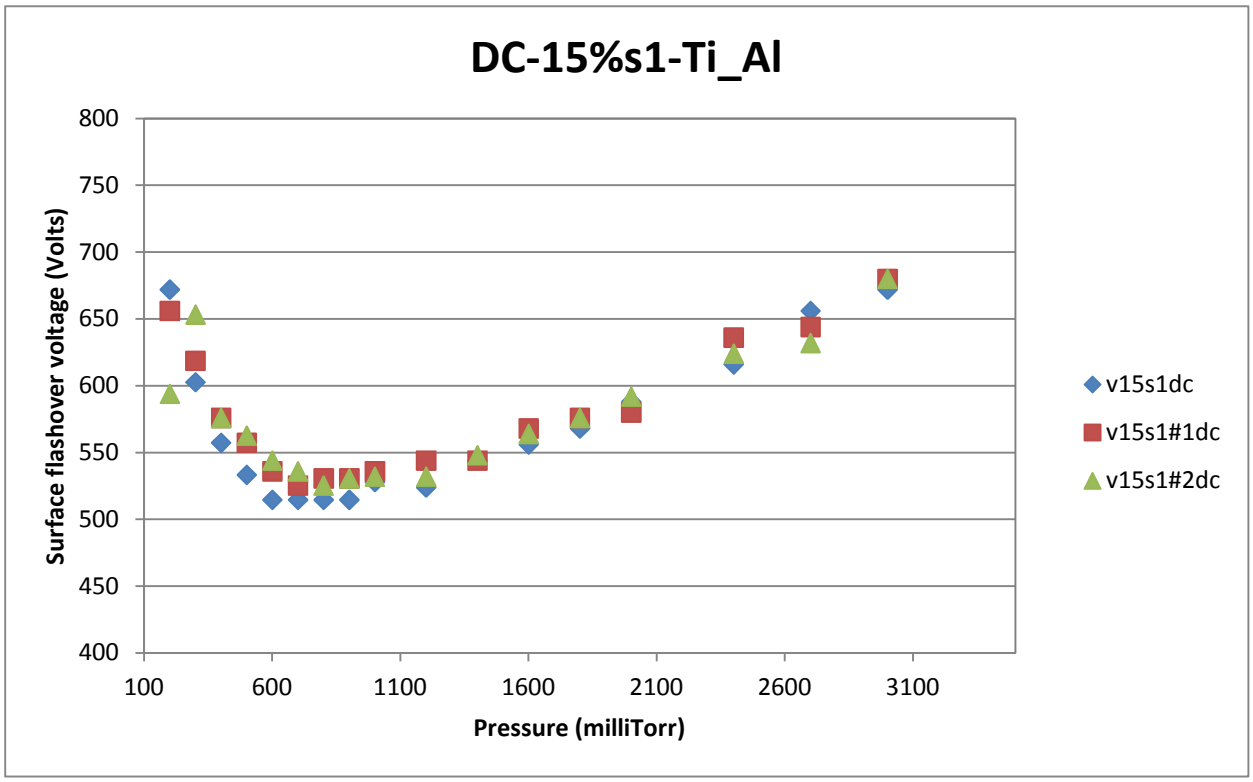

Figure B-35

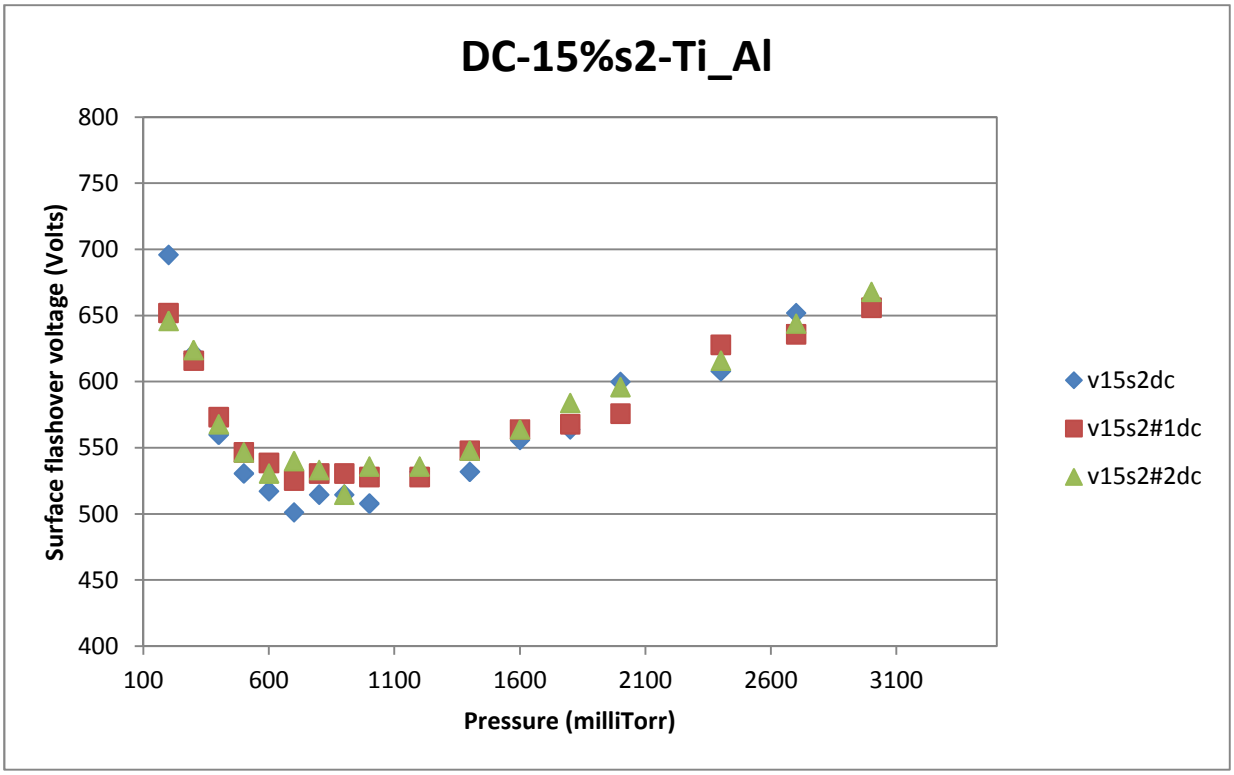

Figure B-36

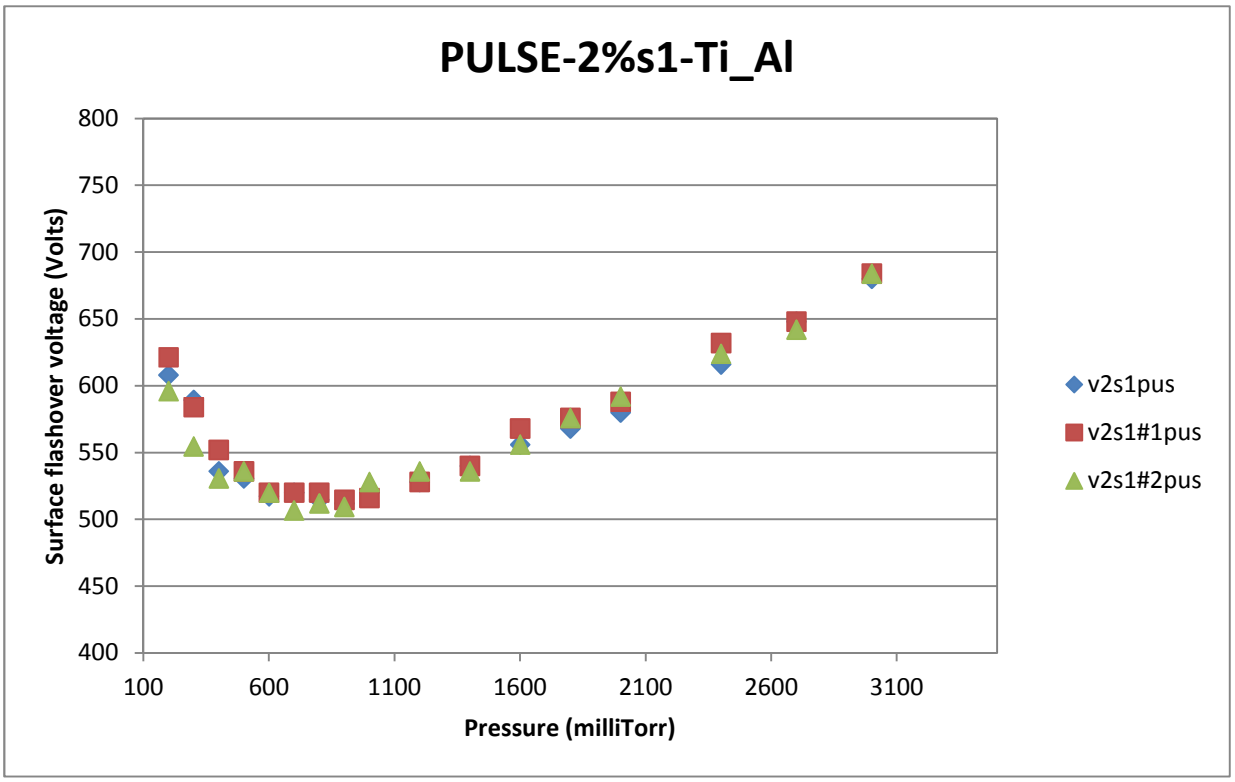

Figure B-37

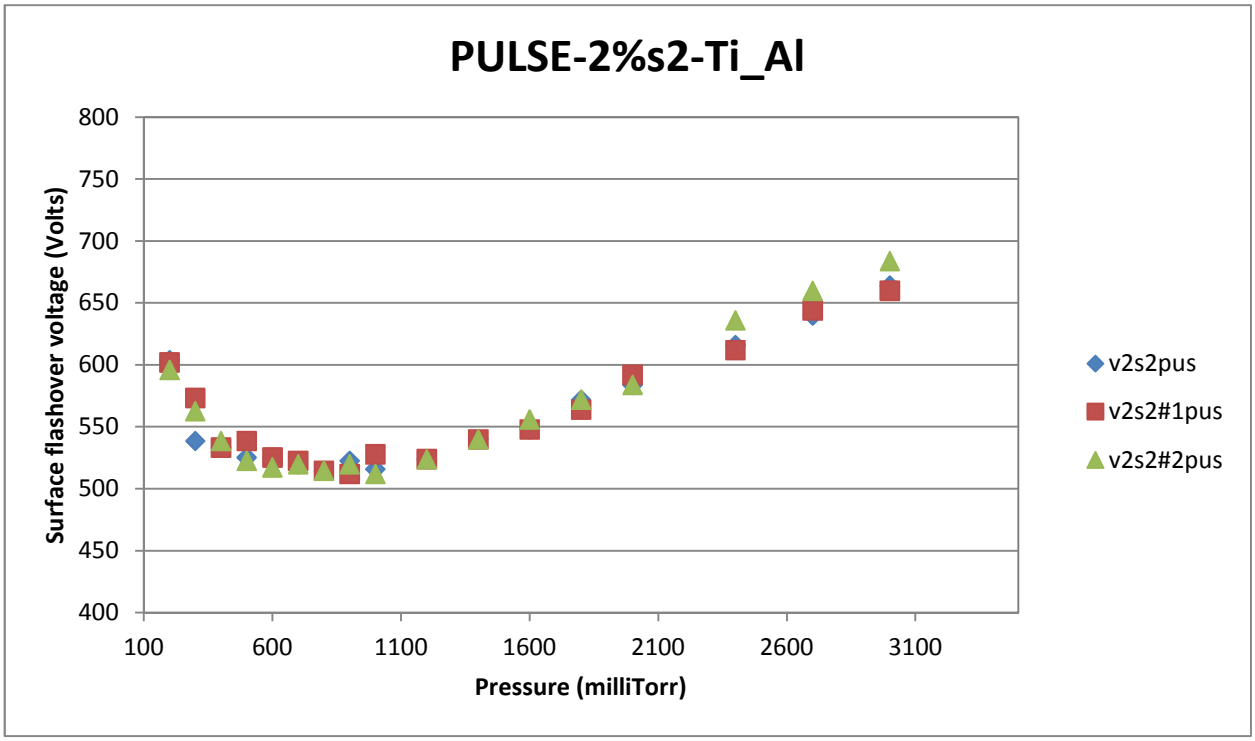

Figure B-38

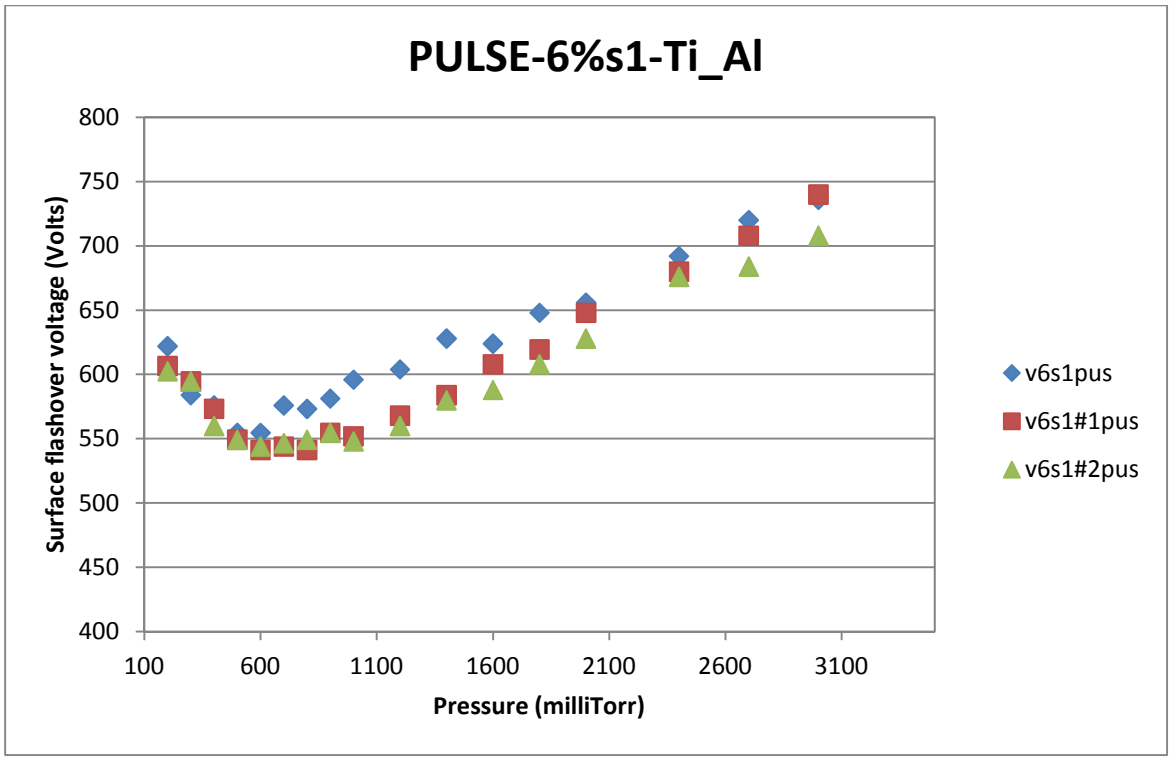

Figure B-39

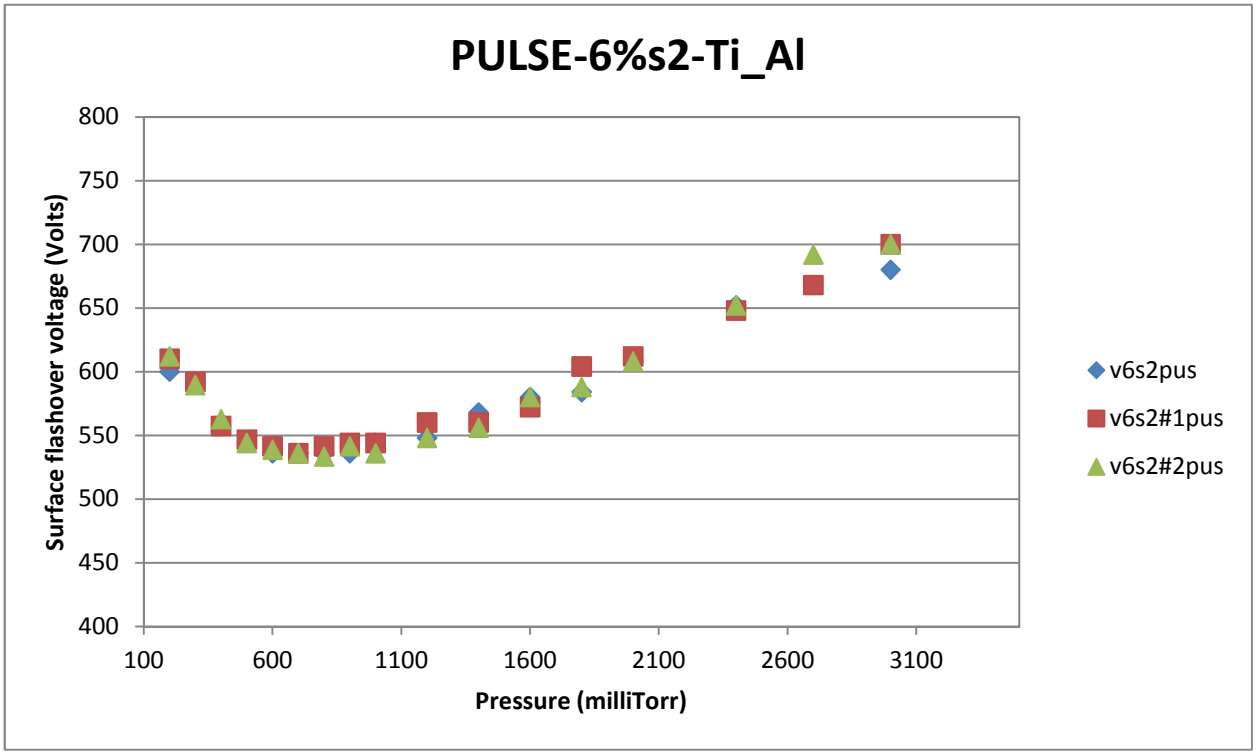

Figure B-40

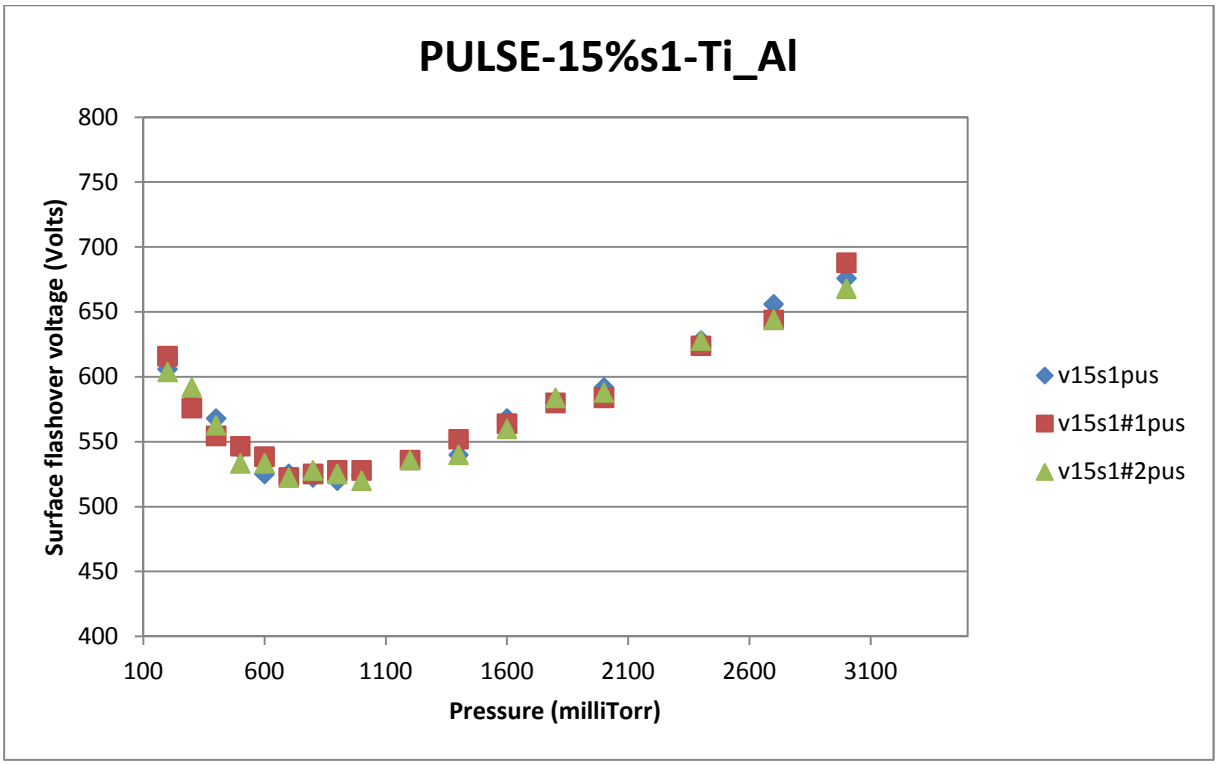

Figure B-41

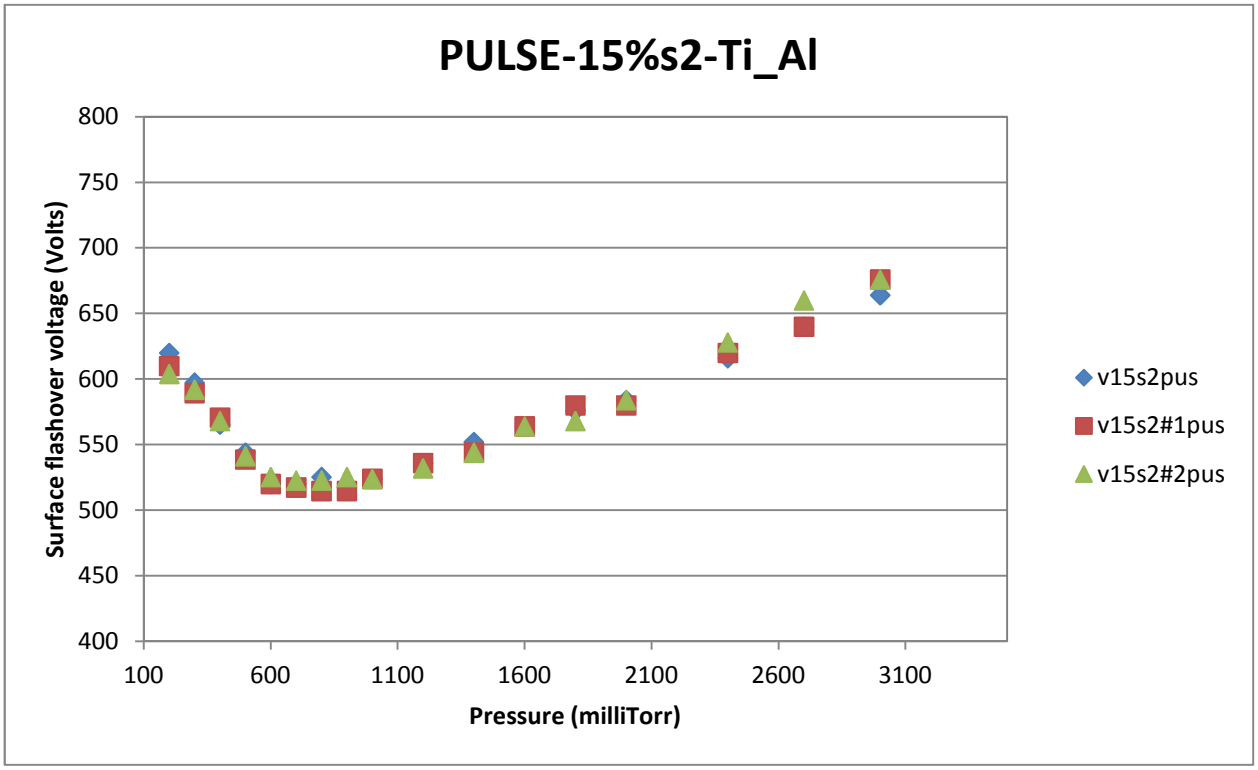

Figure B- 42

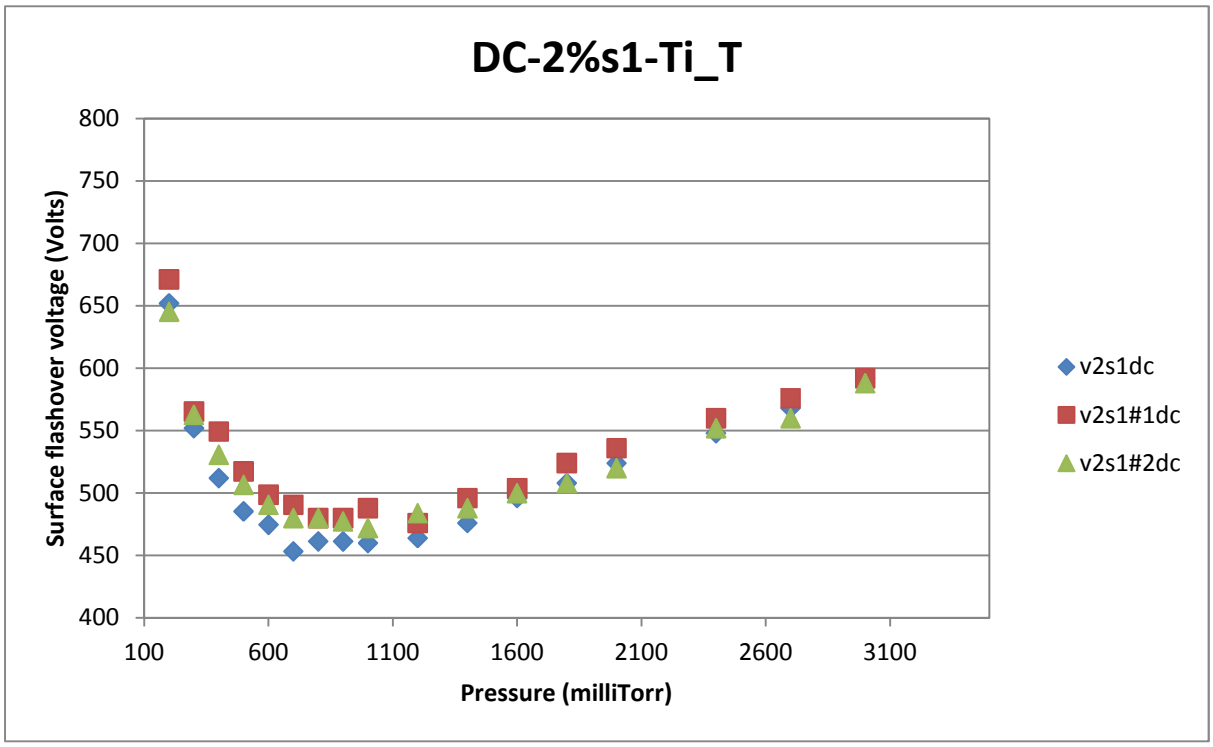

Figure B-43

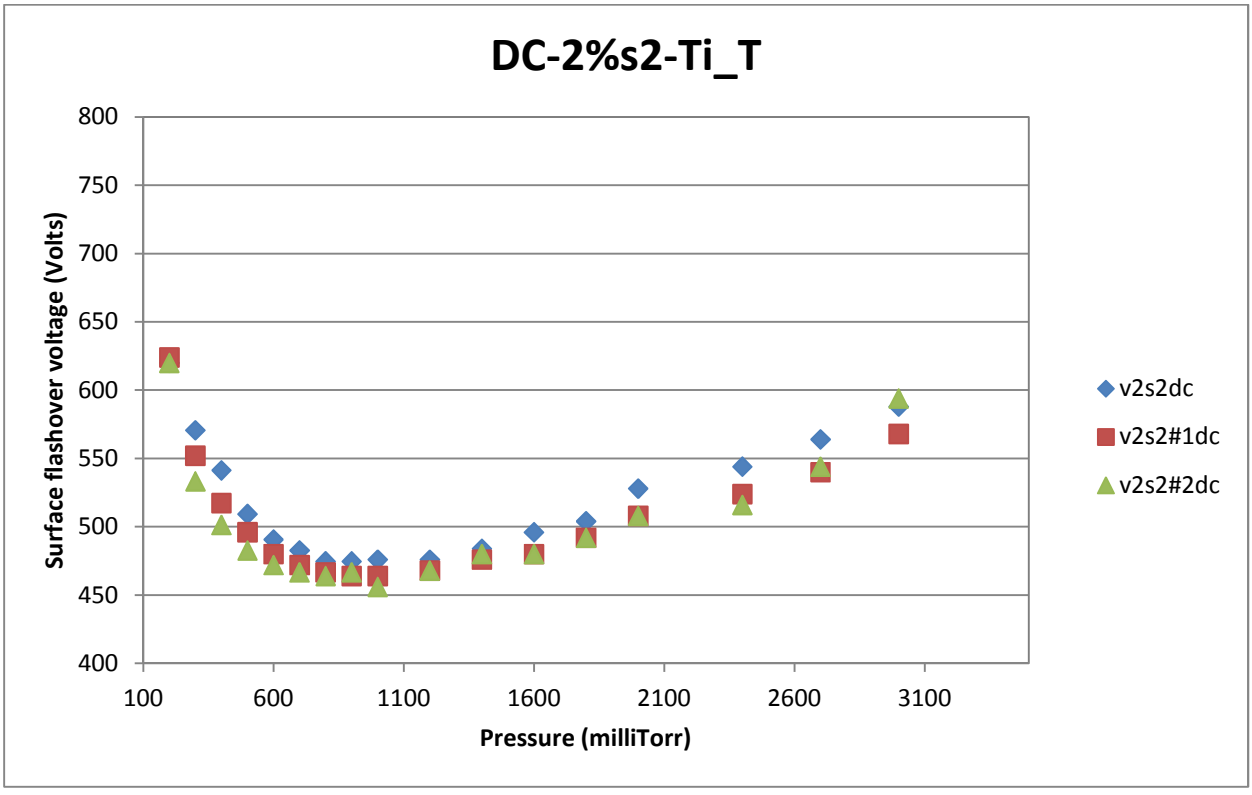

Figure B-44

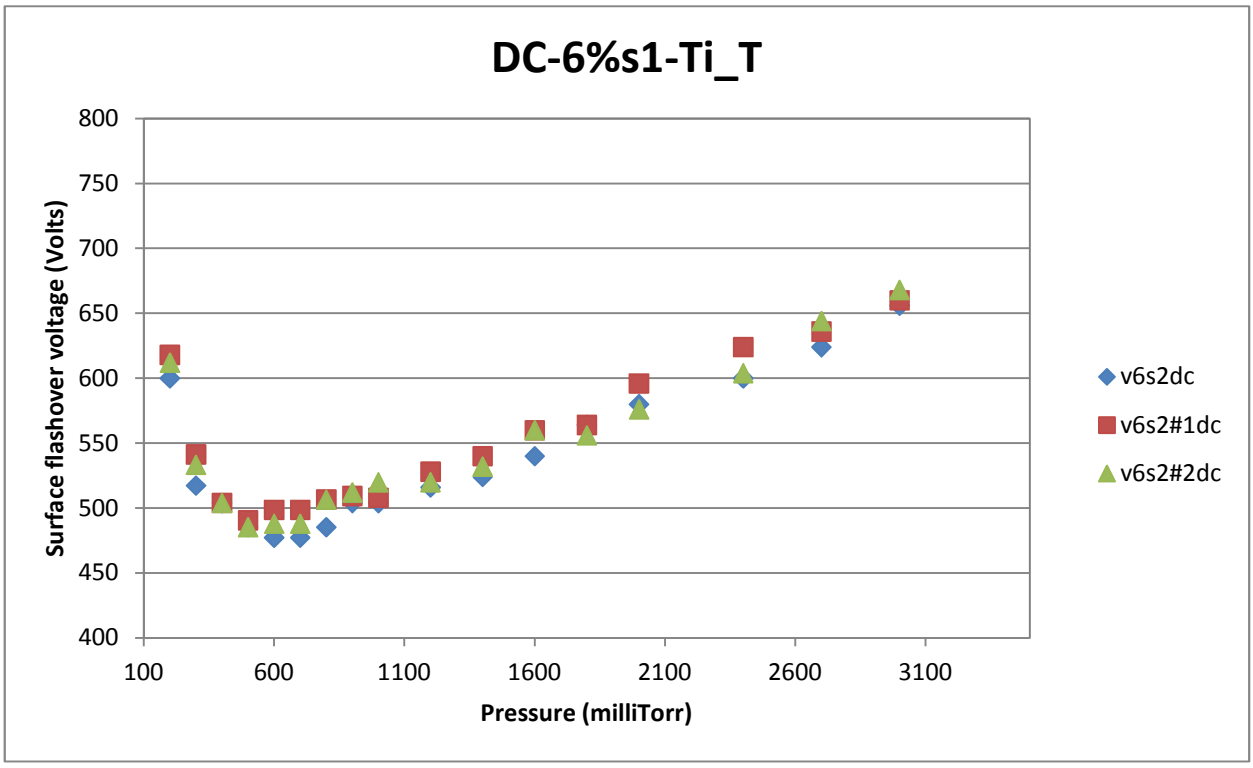

Figure B-45

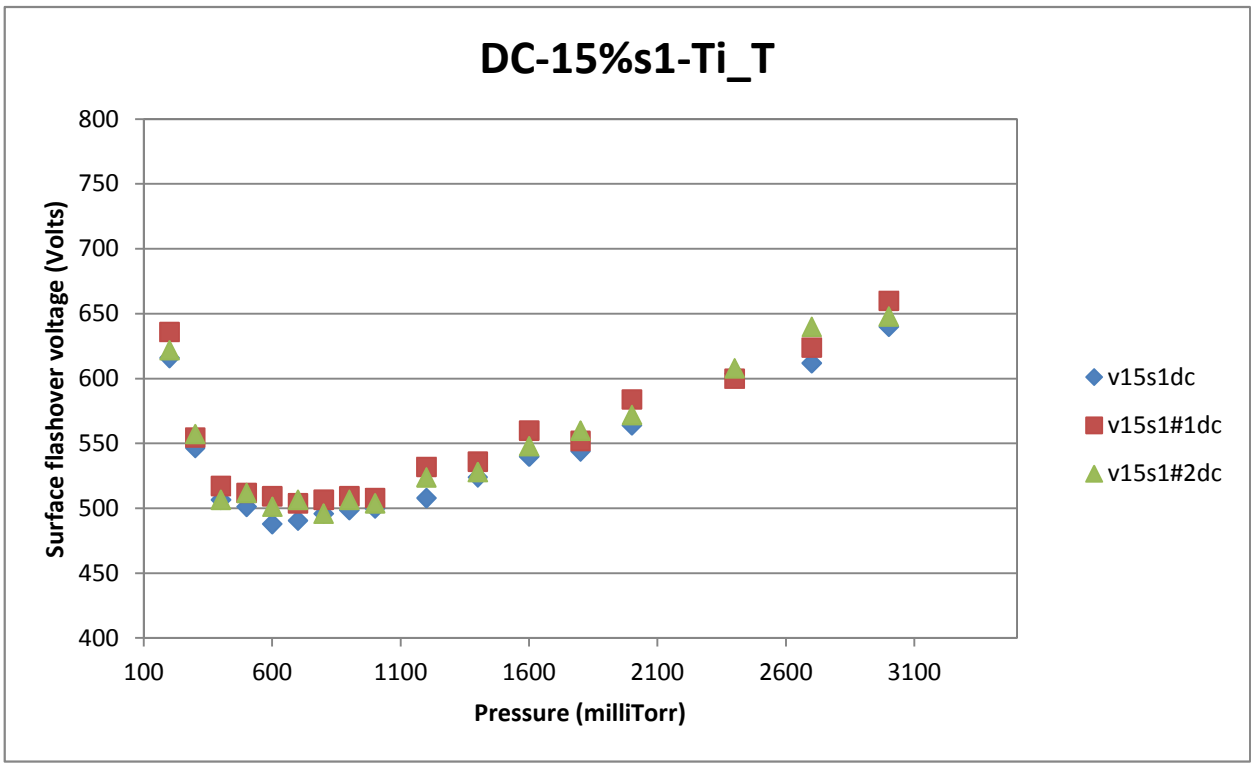

Figure B-46

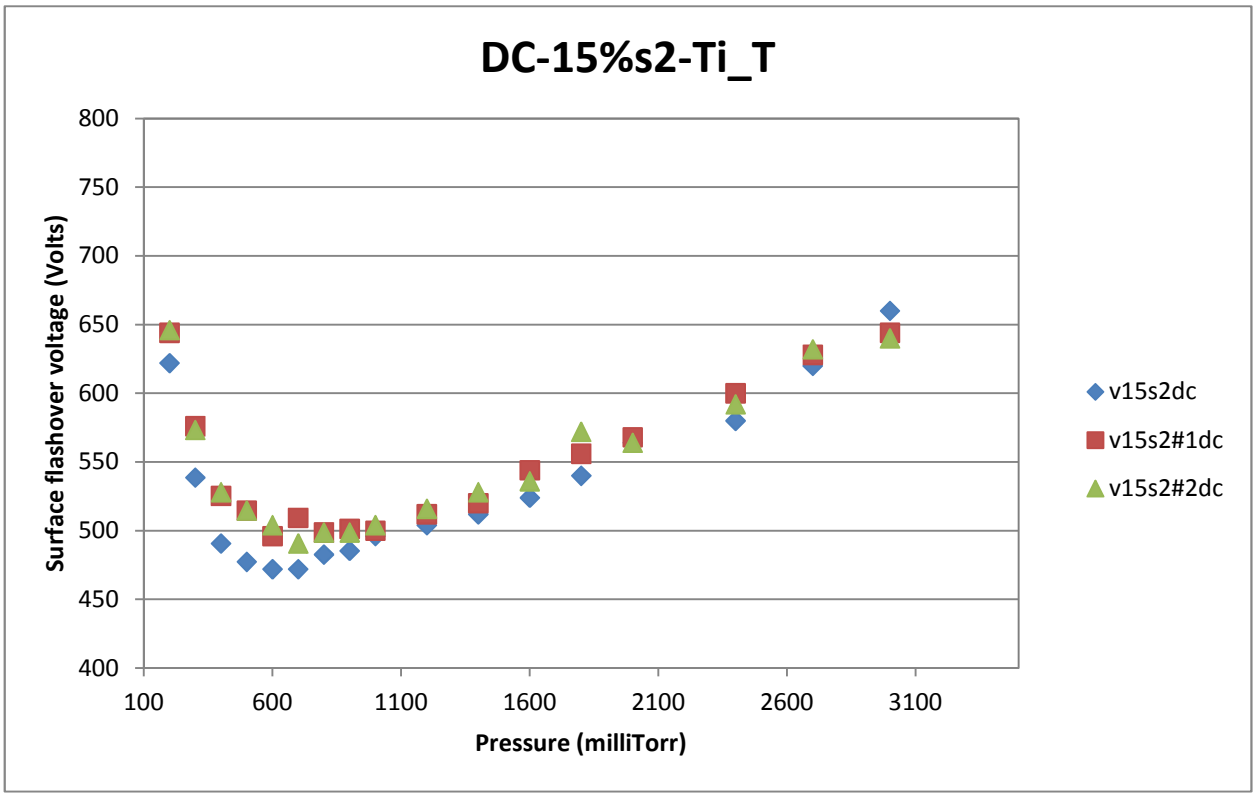

Figure B-47

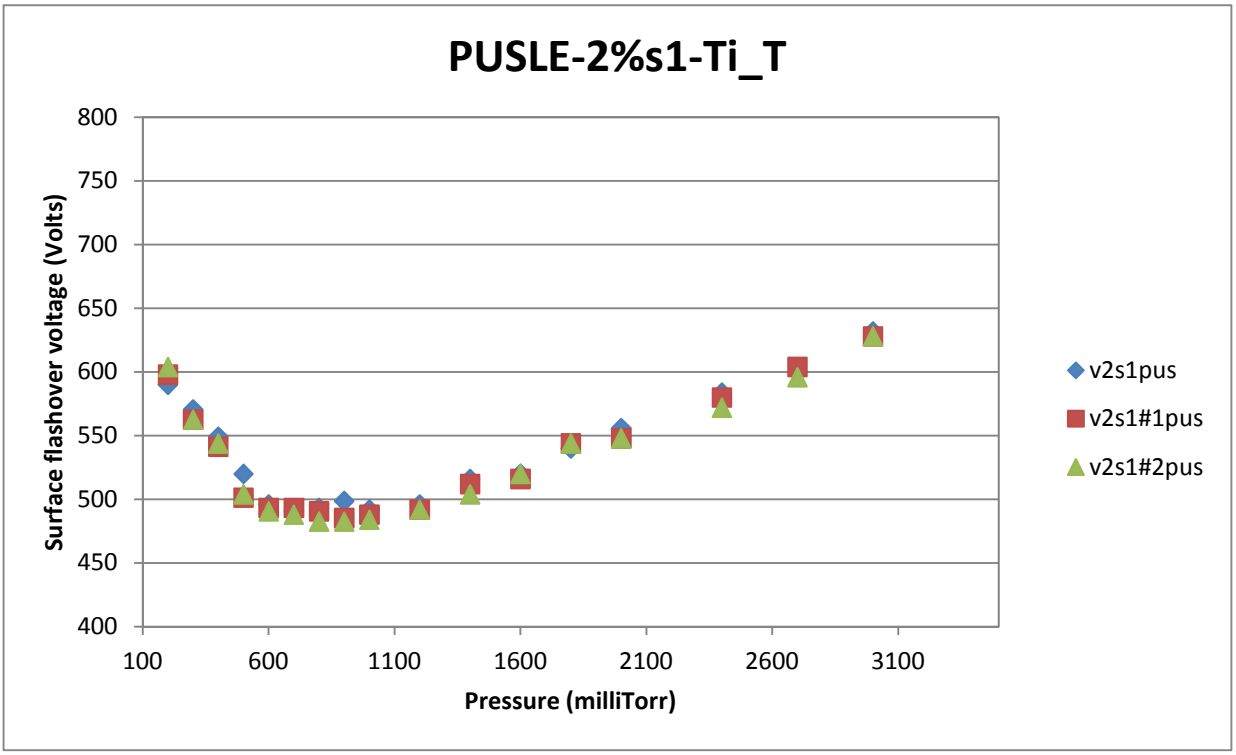

Figure B-48

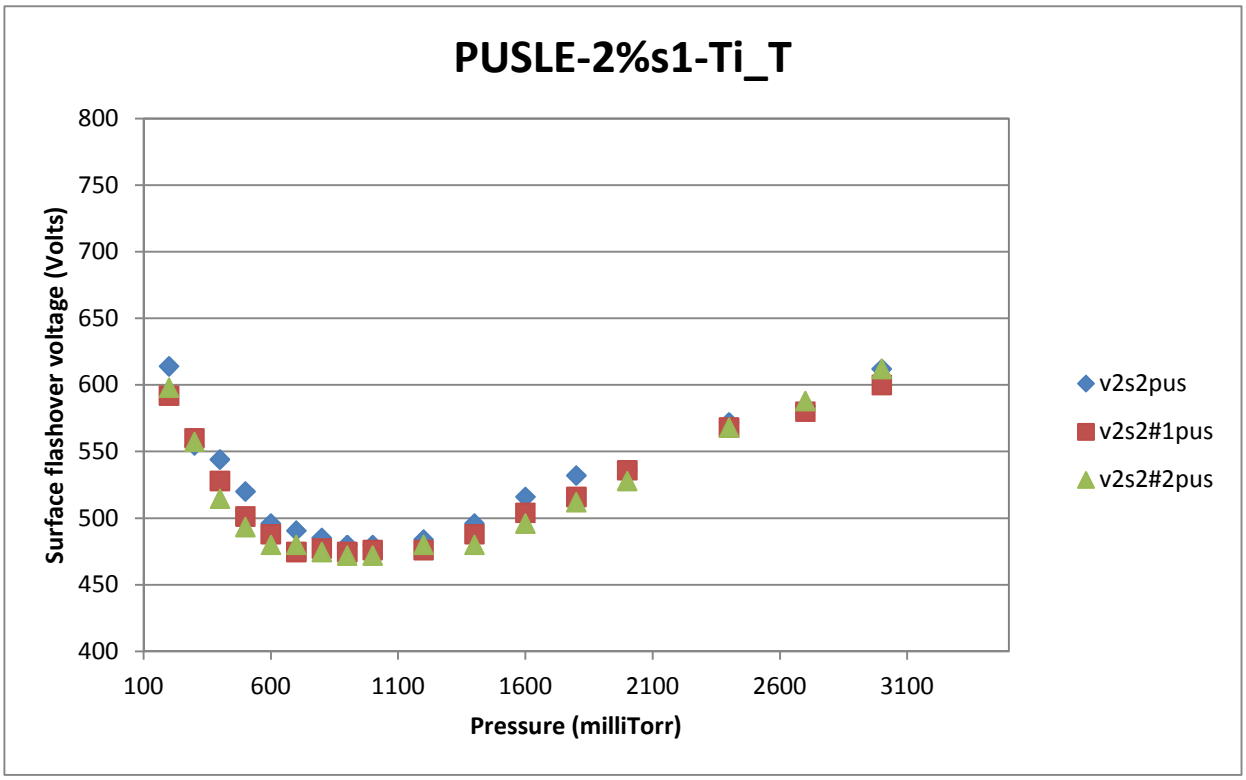

Figure B-49

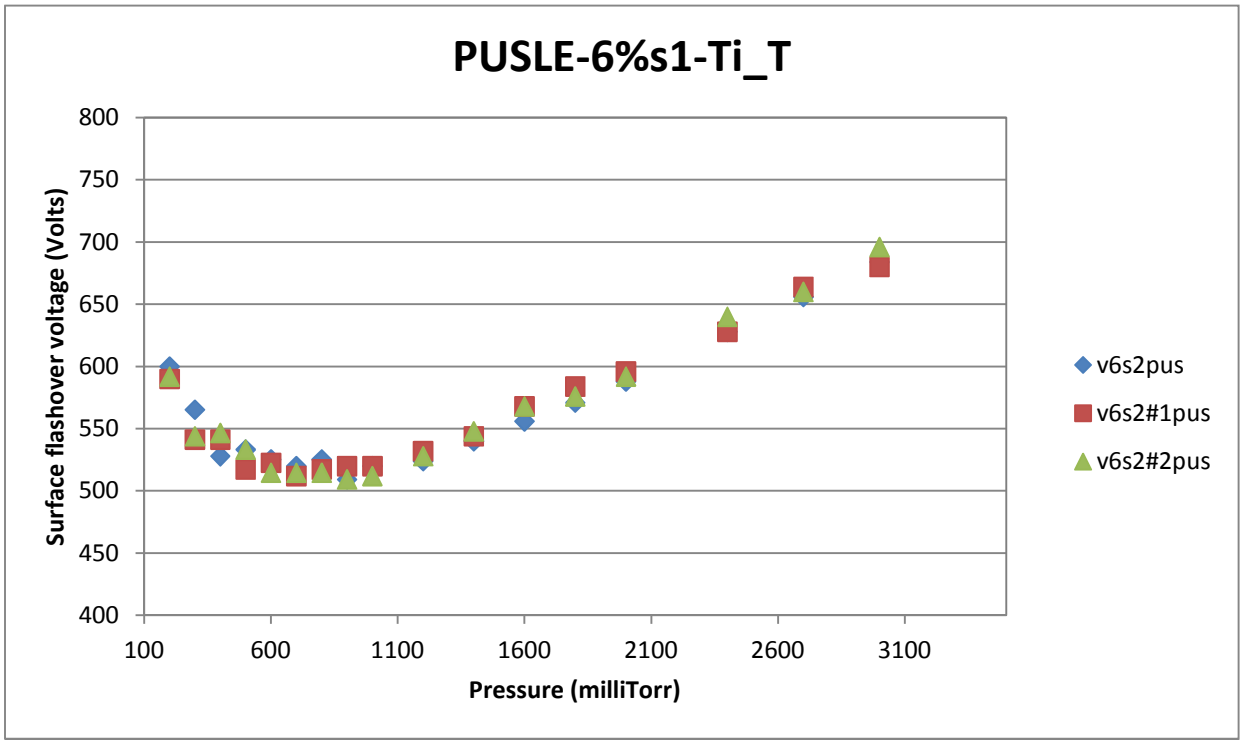

Figure B-50

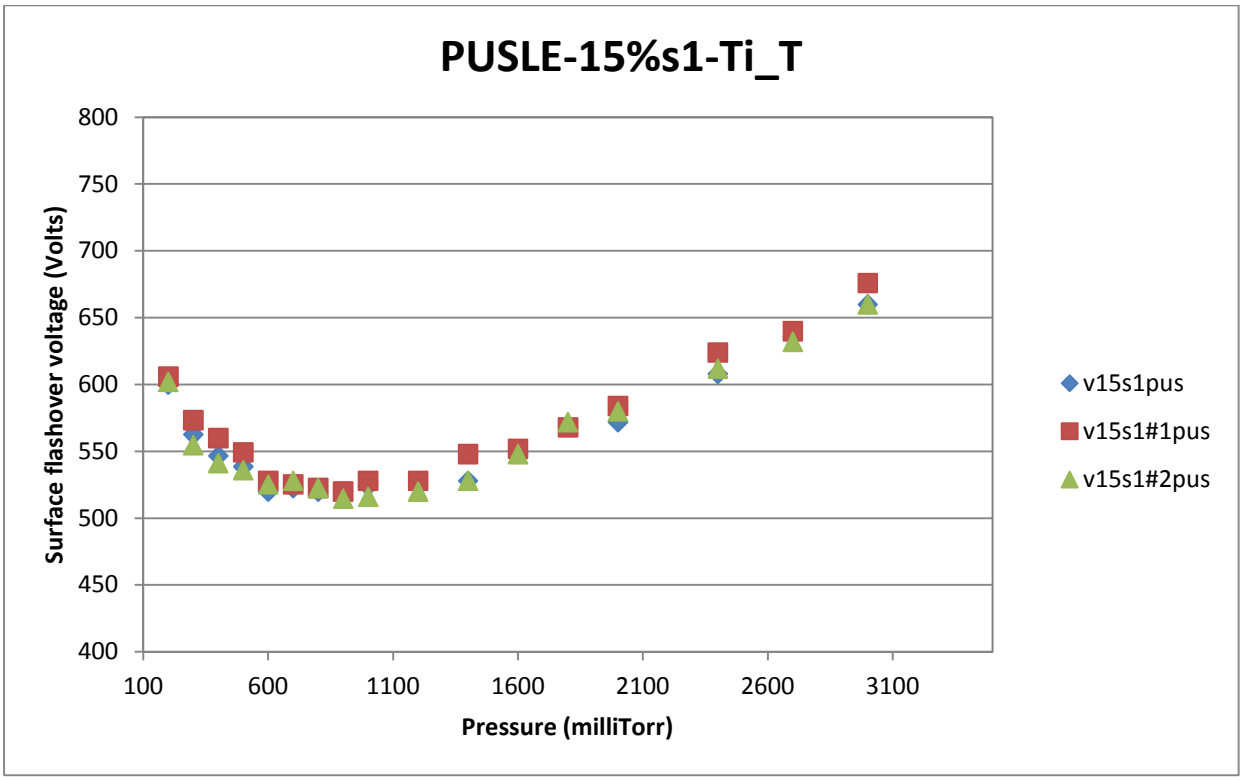

Figure B-51

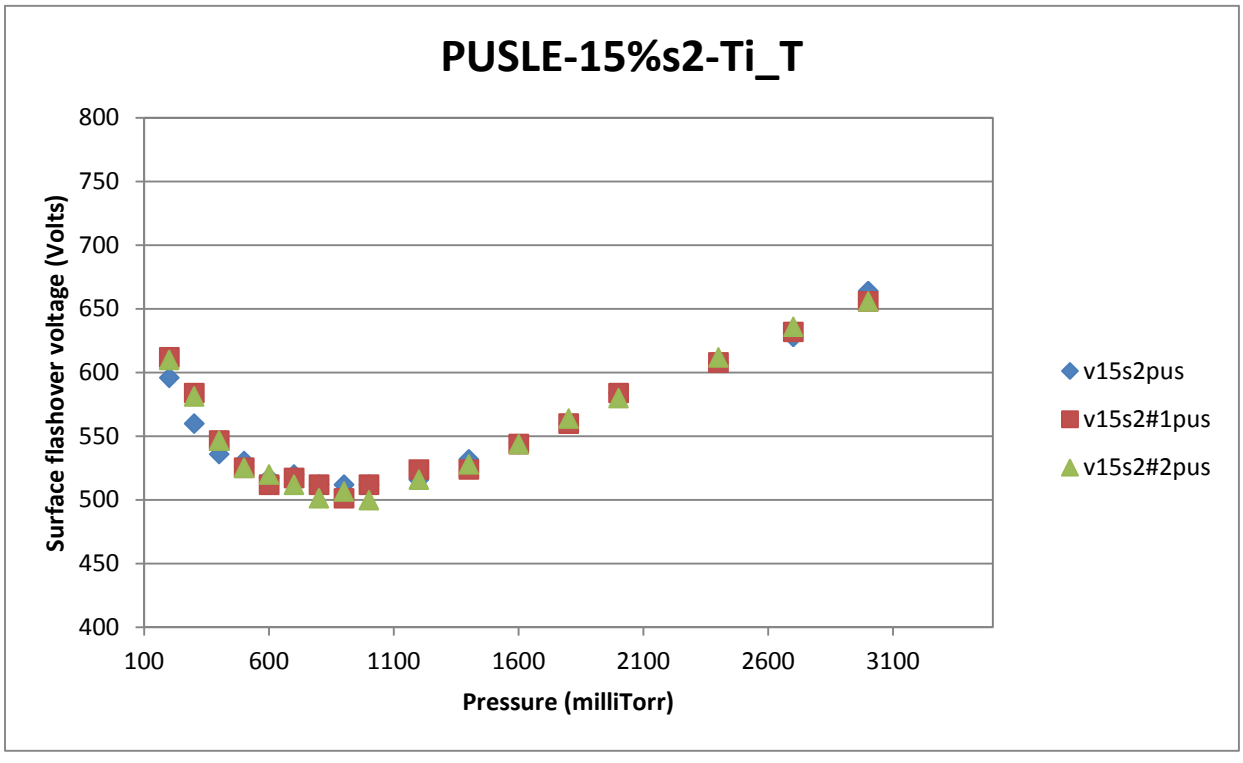

Figure B-52

Appendix C

Complete set of Figures for breakdown voltage under changing frequency. Breakdown voltages are plotted as the frequency of unipolar pulse increased. For one sample, pressure are set at 800 and 1200 millitorr, duty cycle of the pulse signal is 50%. Title of each Figure follows the same pattern, firstly, the type of the loading ratio, then filler substrate configuration, then sample number and repeated number.

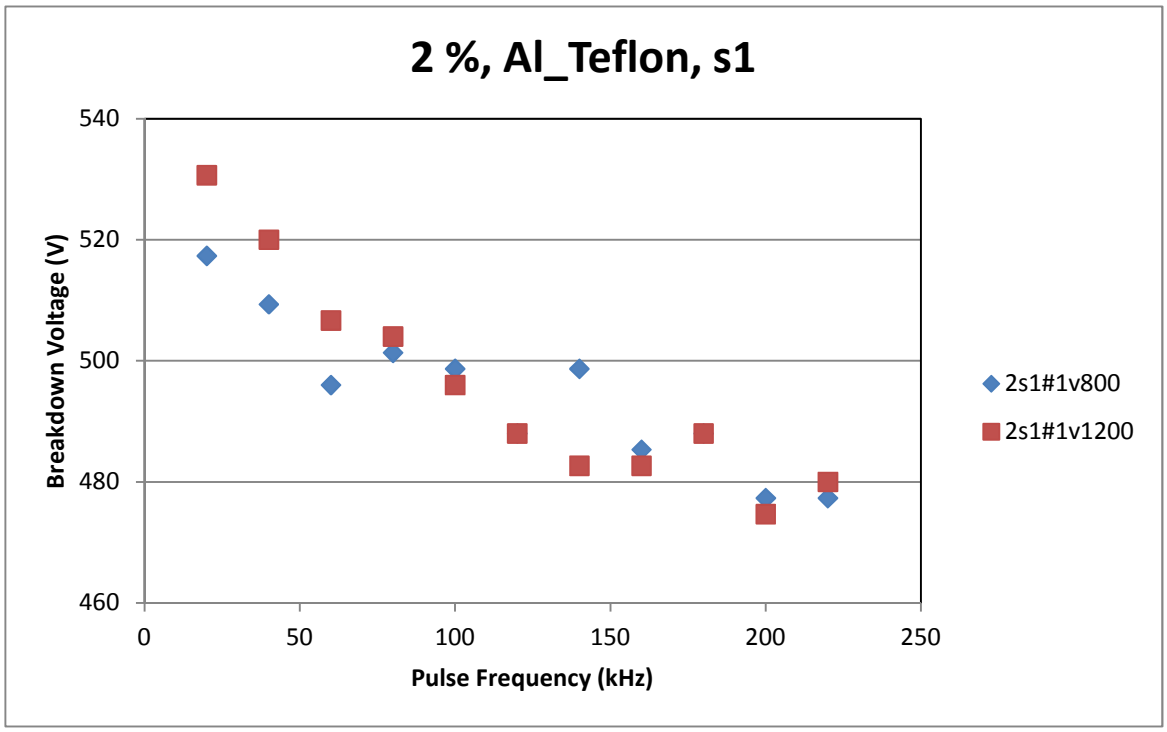

Figure C-1

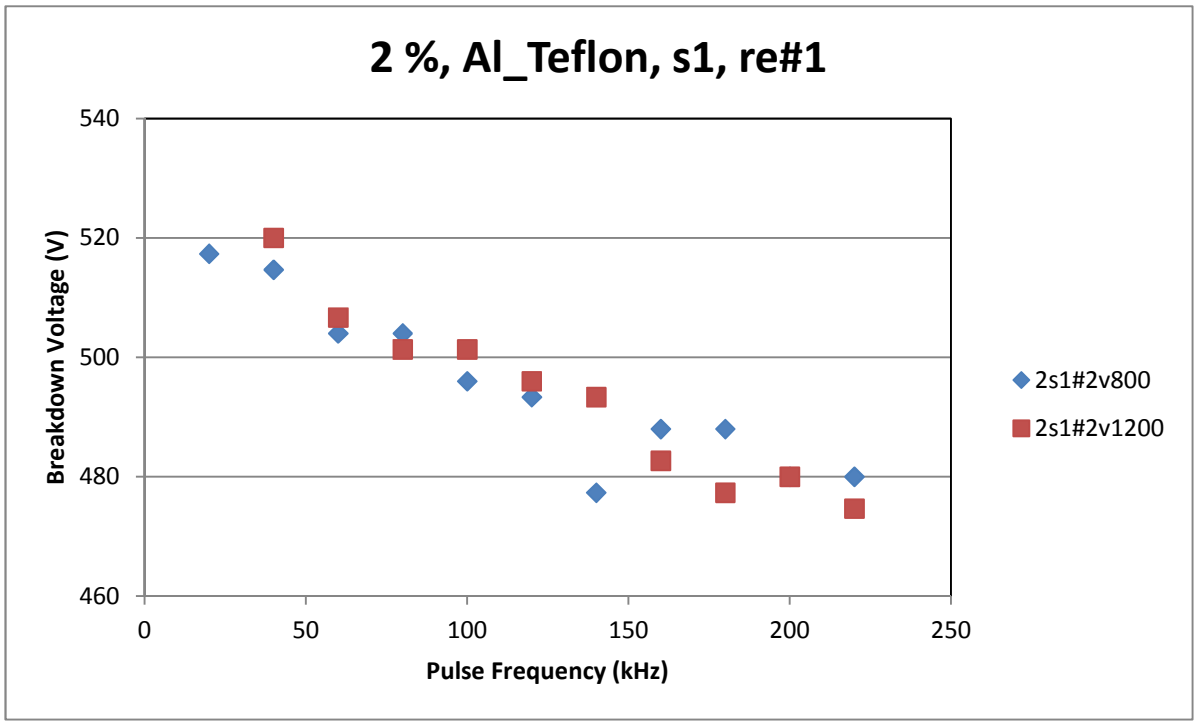

Figure C-2

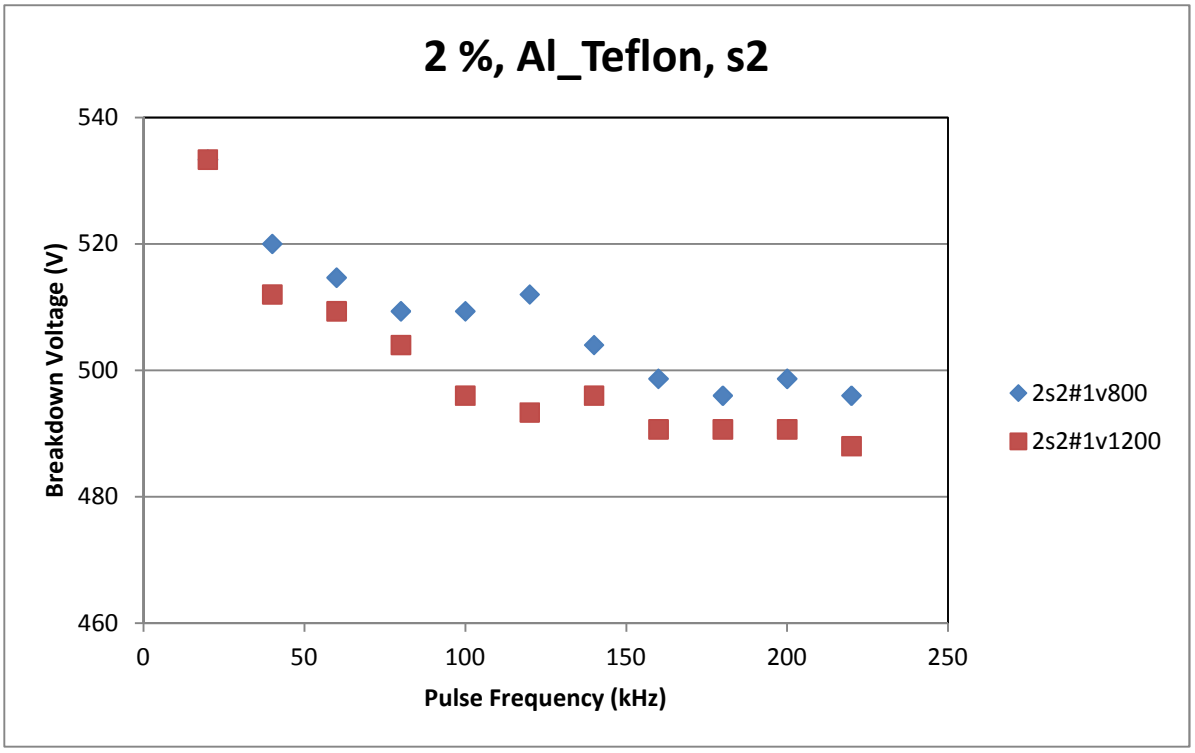

Figure C-3

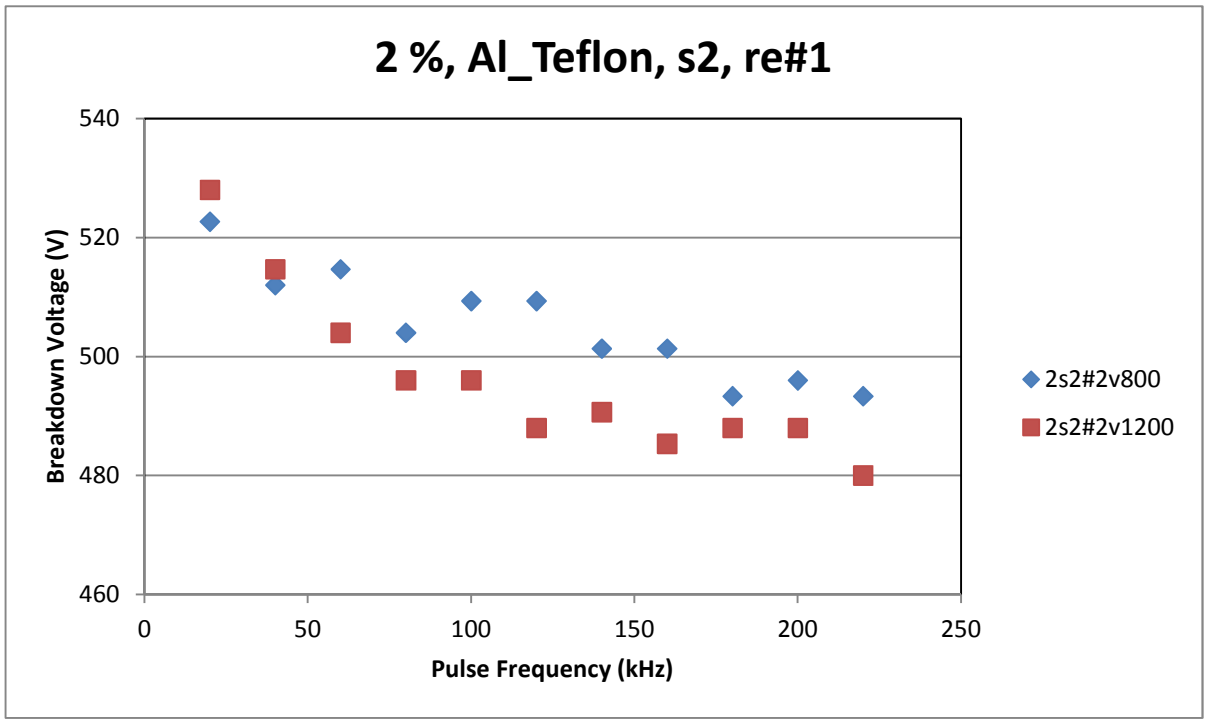

Figure C-4

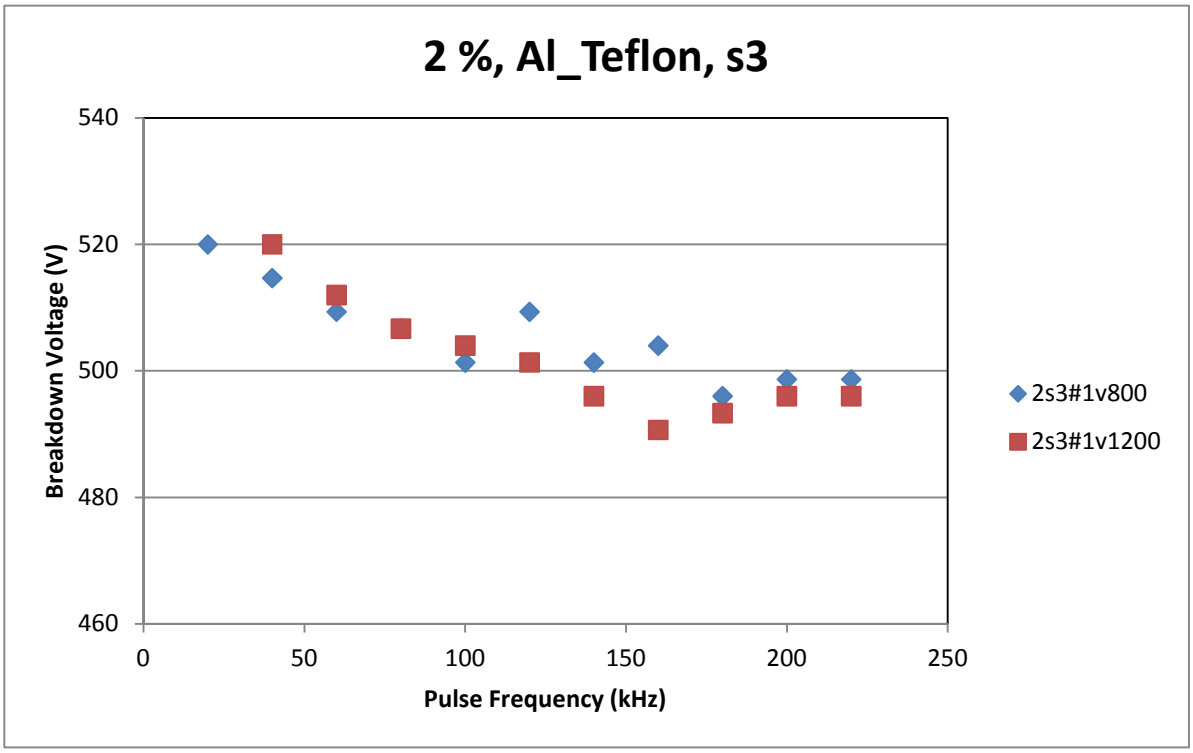

Figure C-5

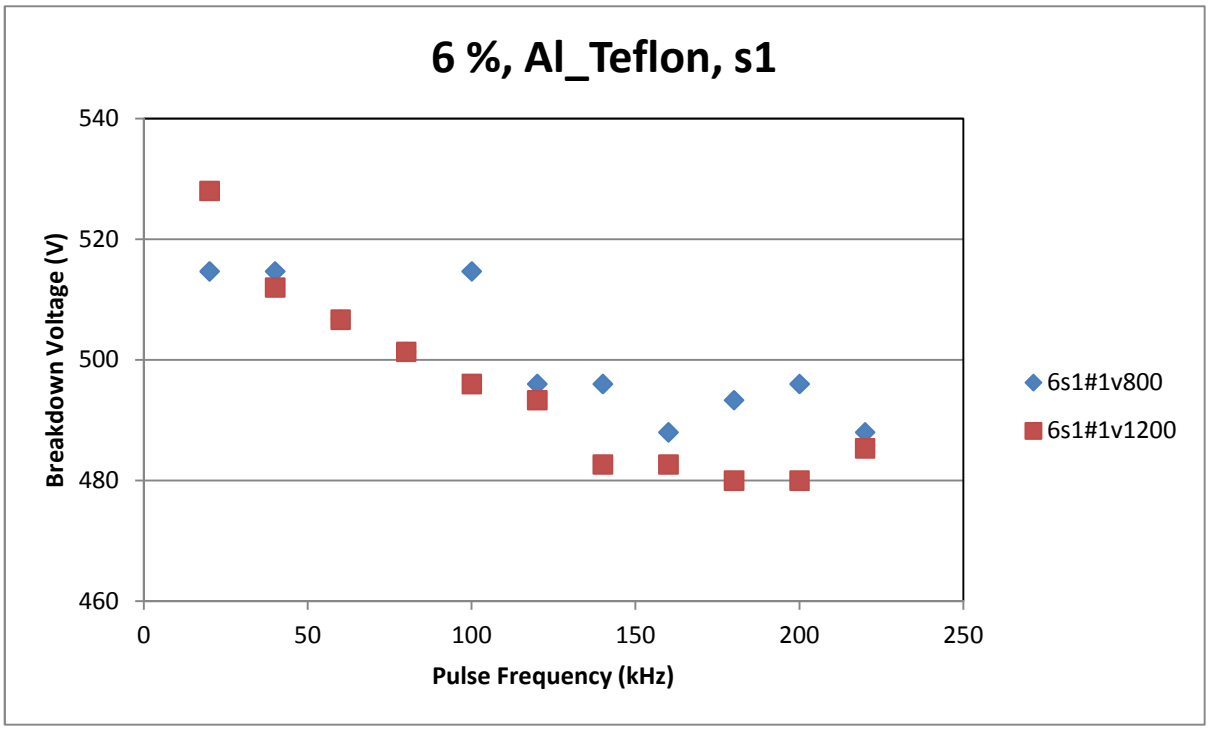

Figure C-6

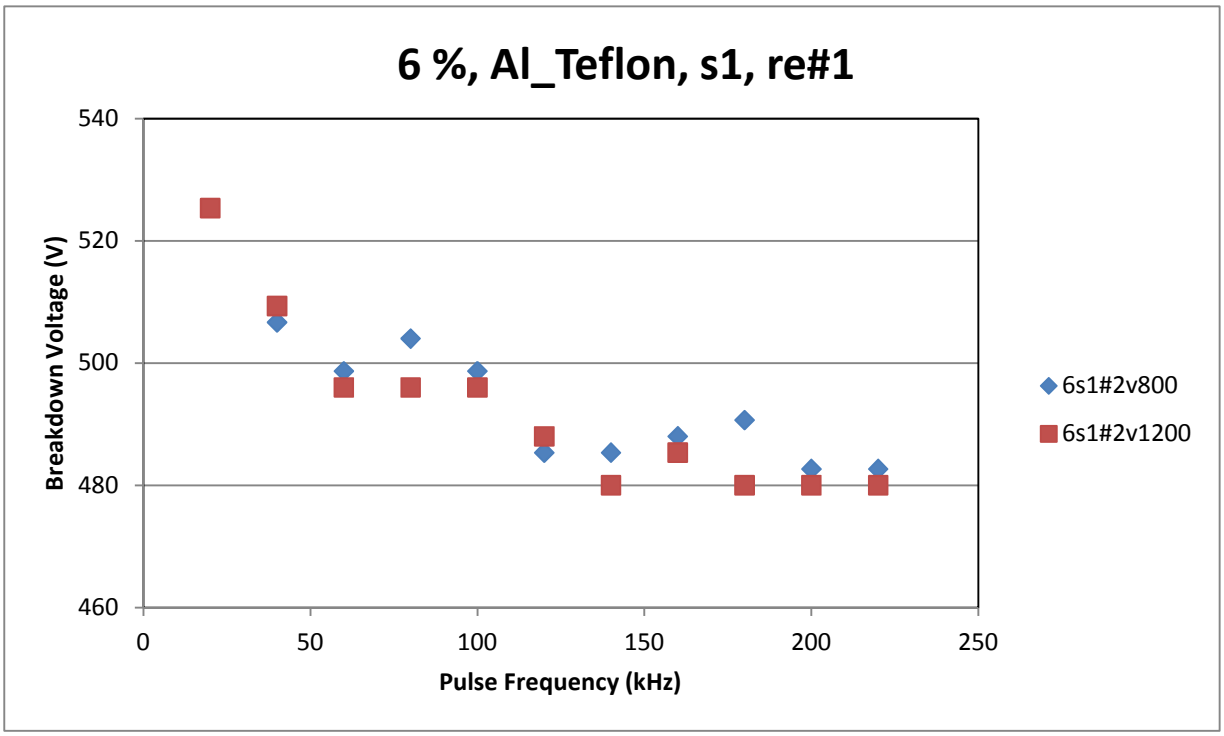

Figure C-7

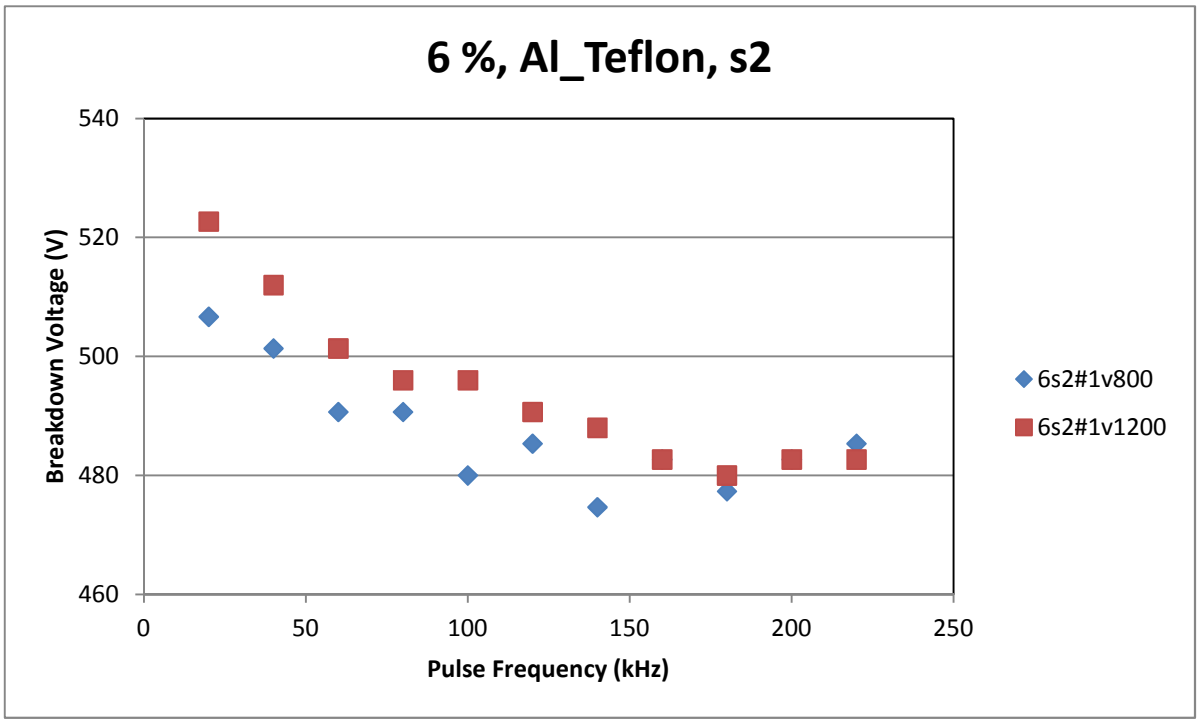

Figure C-8

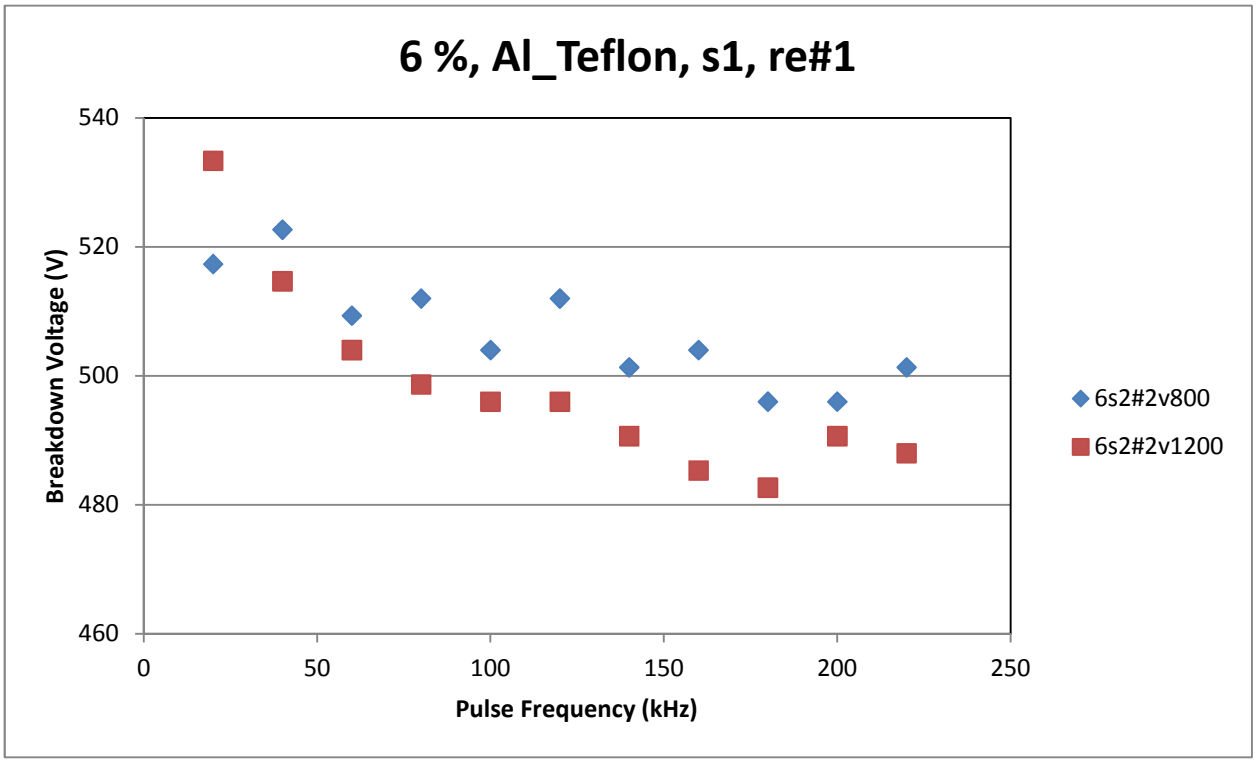

Figure C-9

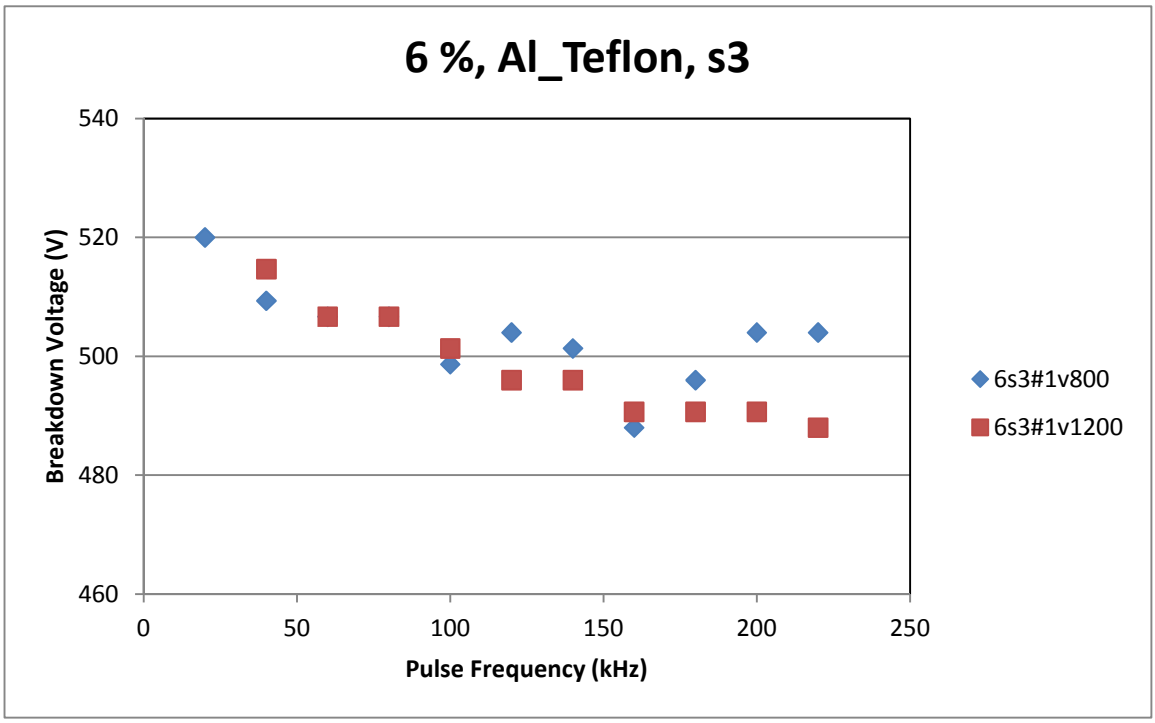

Figure C-10

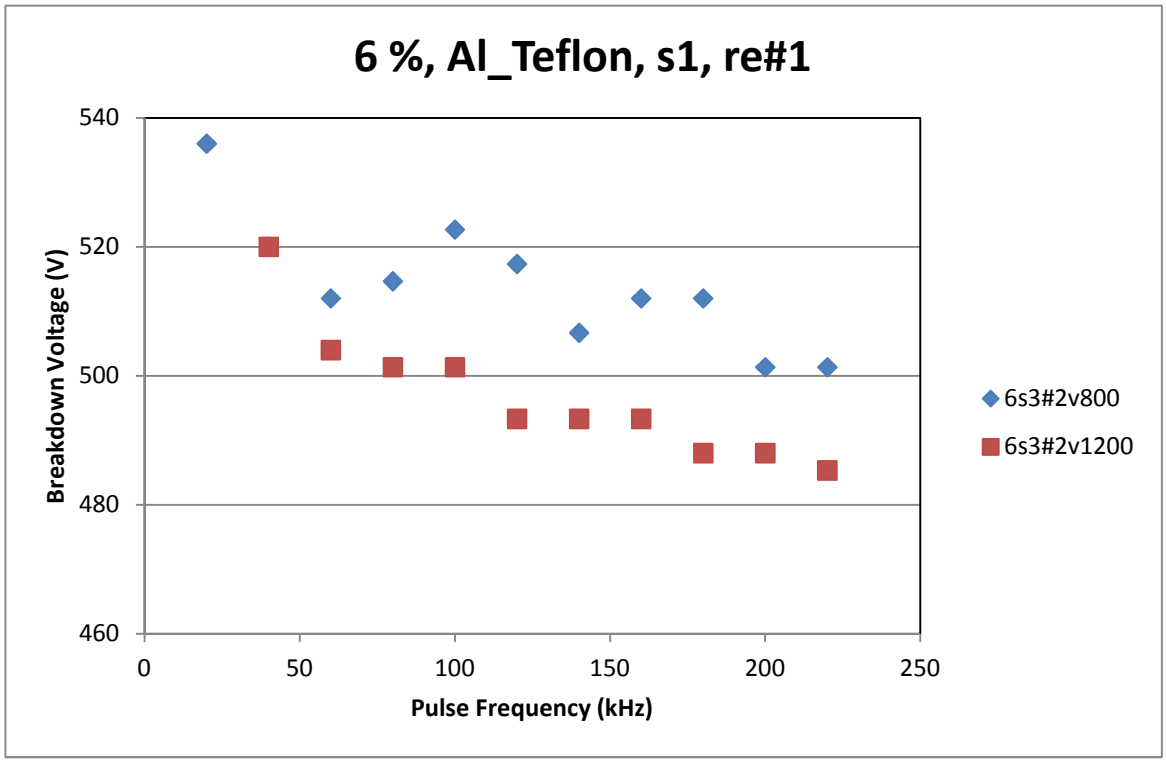

Figure C-11

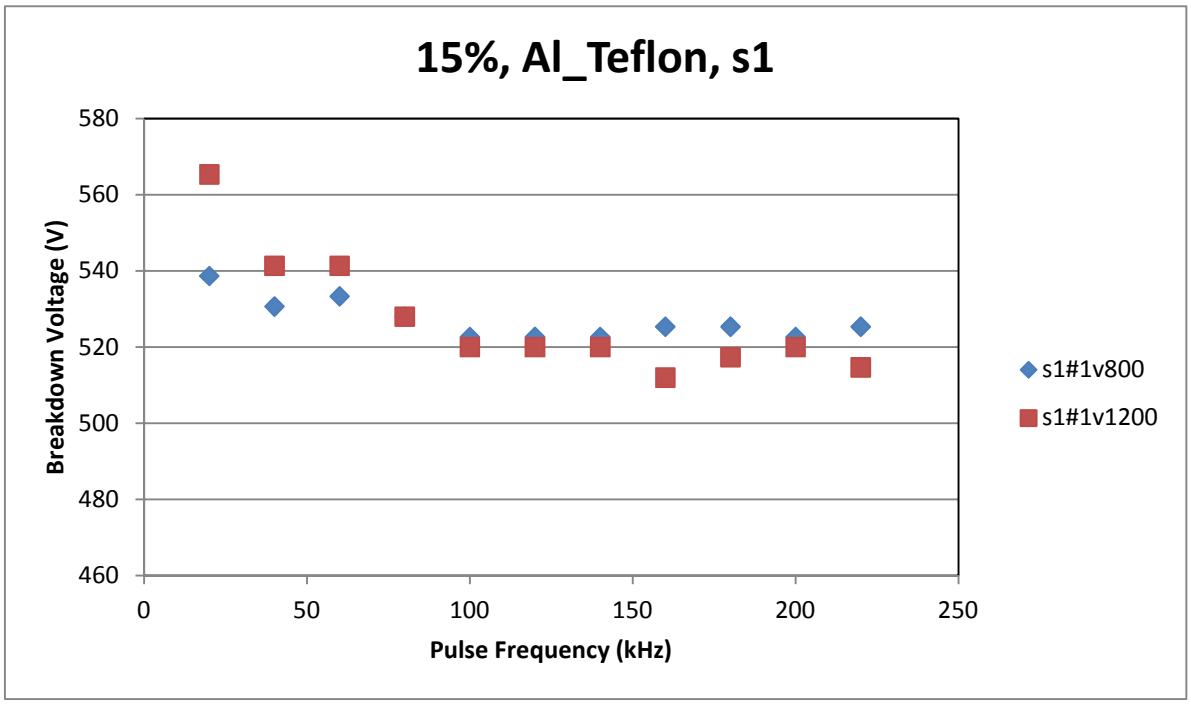

Figure C-12

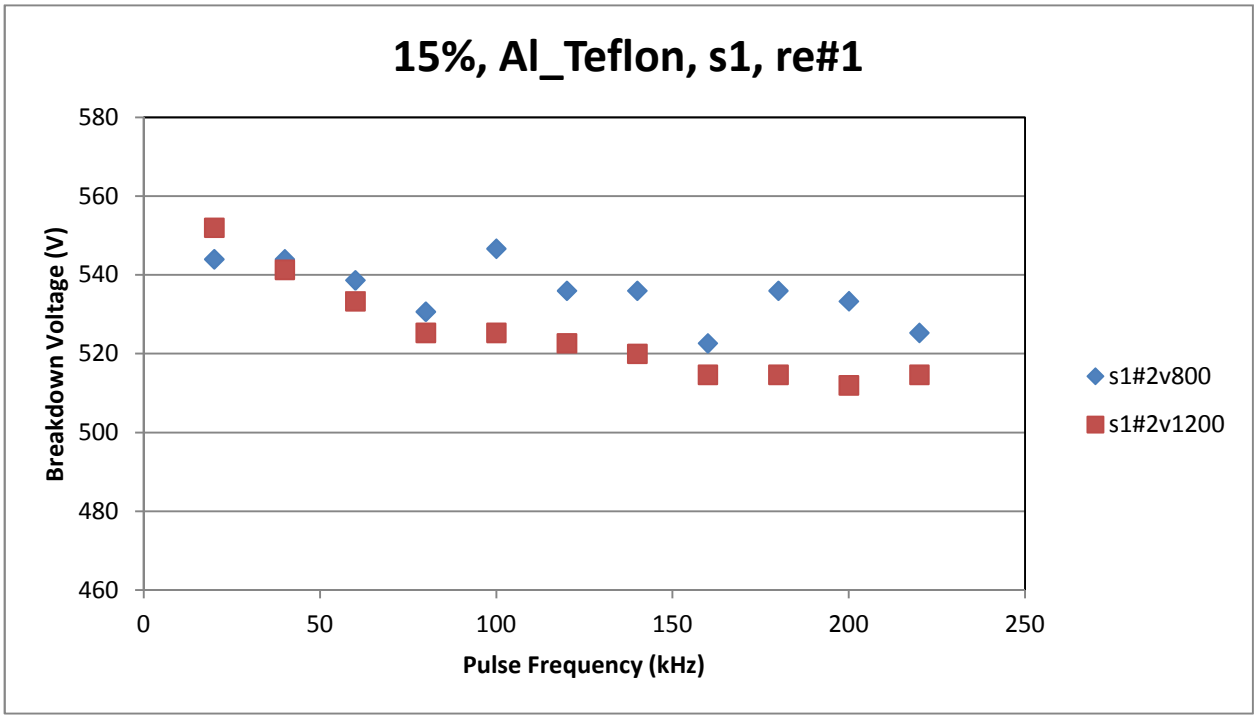

Figure C-13

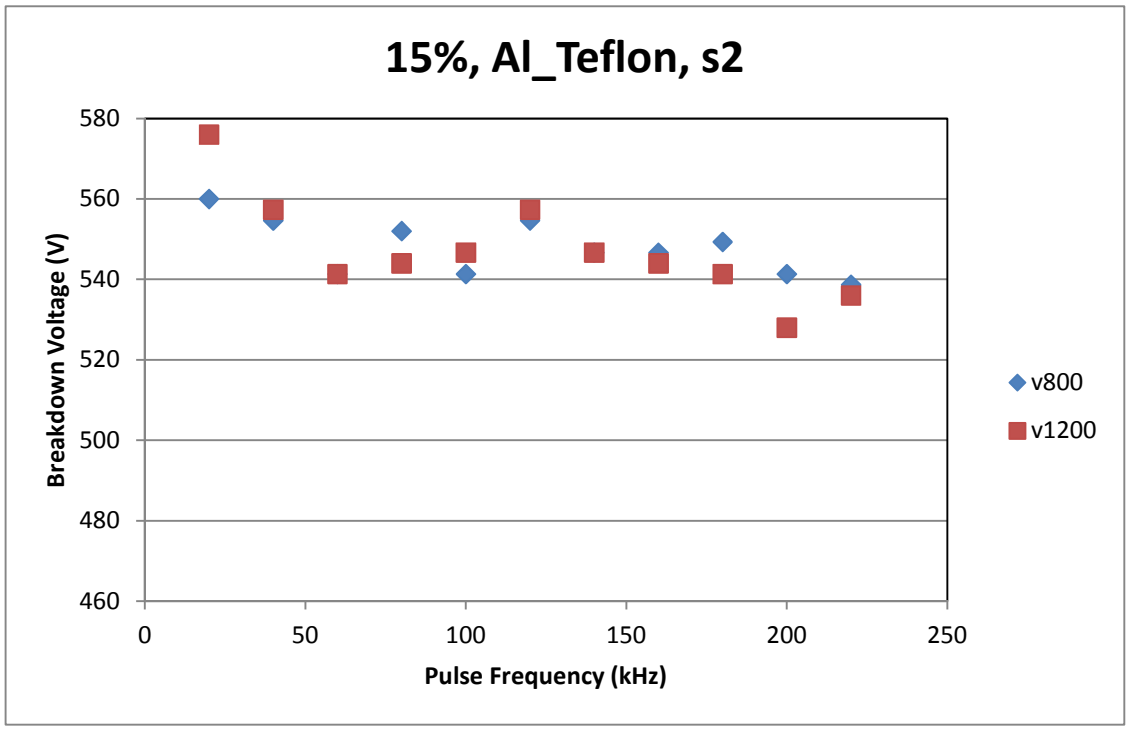

Figure C-14

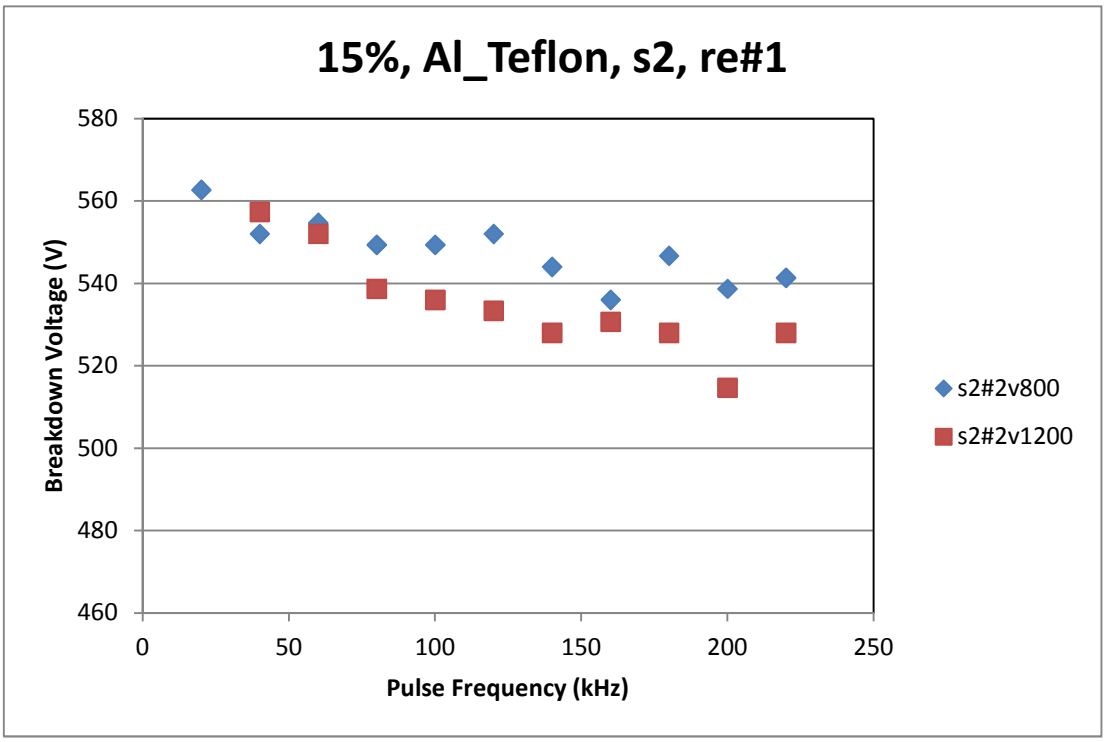

Figure C-15

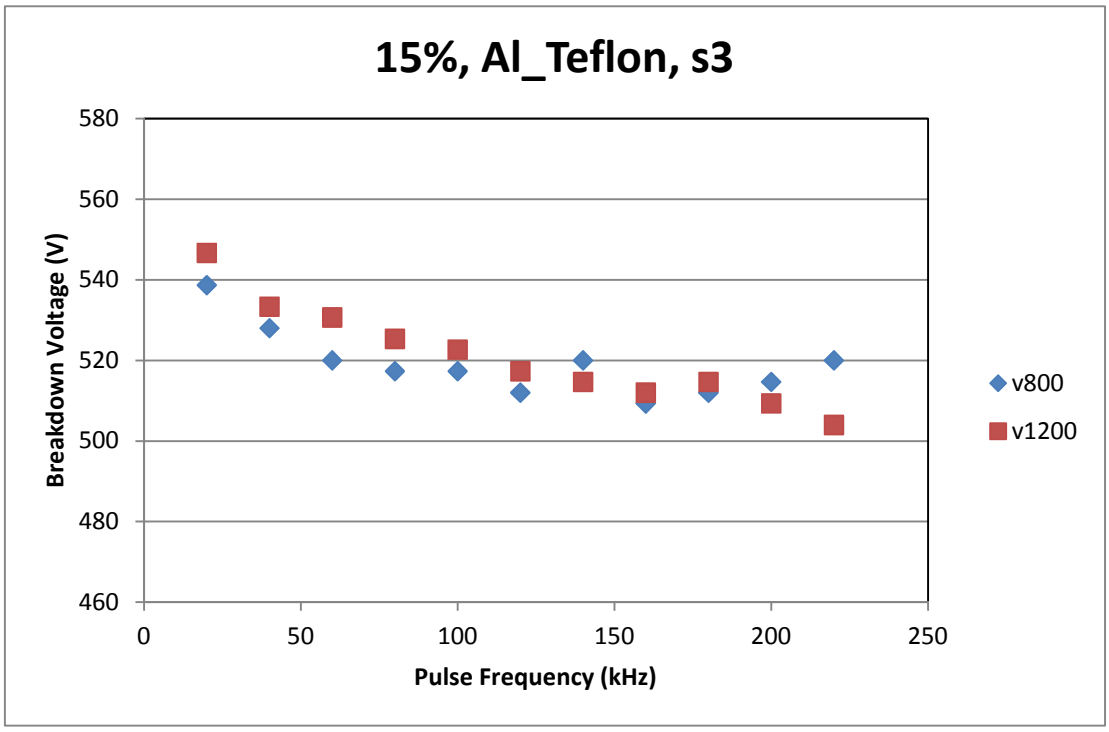

Figure C-16

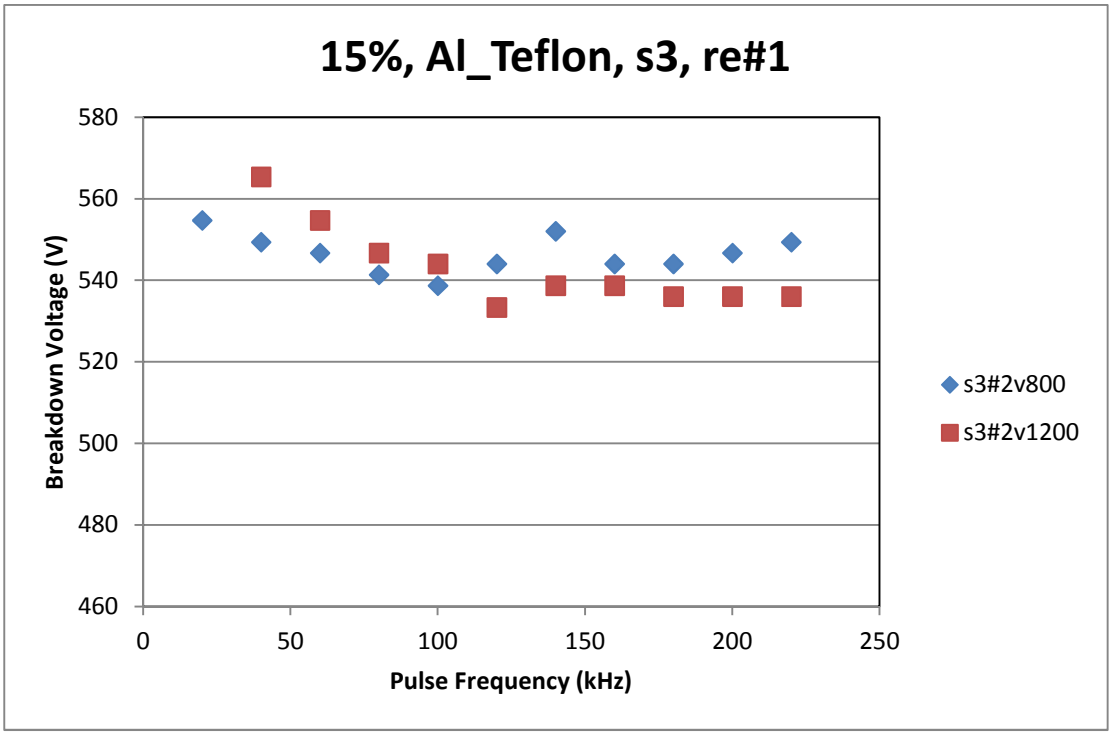

Figure C-17